Dissertation
submitted to the Combined Faculties for the Natural Sciences and
for Mathematics of the
Ruperto-Carola University of Heidelberg, Germany
for the degree of
Doctor of Natural Sciences

presented by
Cornelia Andrea Klein, M.Sc.
born in: Heilbronn, Germany
Oral-examination: 11.06.14

The role of ZC3H32 in *Trypanosoma brucei*

Referees:
Prof. Dr. Christine Clayton
Prof. Dr. Luise-Krauth-Siegel

Thanks to…

Christine Clayton
The AG Clayton (both current and former members) for support and help throughout these years. You are the best.
Luise Krauth-Siegel and her working group
The entire first floor of the ZMBH
HBIGS for offering great courses
and, of course, my friends and family

Table of contents

Summary

In the protozoan parasite *Trypanosoma brucei* gene expression is mostly regulated on the post-transcriptional level. C3H zinc fingers have shown to play an important role in this process. So far, all described C3H zinc finger in *Trypanosoma brucei* have shown to stabilize their targets.

This work focuses on the zinc finger protein ZC3H32. A large-scale isolation of free and membrane-bound polyribosomes from proyclic and bloodstream trypanosomes, which is also described in this thesis, suggested that this protein associates with polyribosomes. However, small-scale polyribosome isolations followed by Western blotting revealed that only a minor fraction of it is actually associated with polyribosomes.

Immunofluorescence showed that ZC3H32 localizes to the cytoplasm. A yeast-two-hybrid screen identified it as a putative binding partner of MKT1. This interaction was confirmed by co-immunoprecipitation.

RNAi, as well as knock-out studies, showed that ZC3H32 is essential in the bloodstream form. Northern blotting, as well as a SILAC screen by Urbaniak et al. indicate that it is also enriched in this life-cycle stage as compared to procyclics.

Artificial tethering of ZC3H32 to a reporter RNA lead to the RNA's degradation, suggesting that this protein has a destabilizing effect. Tethering of ZC3H32 fragments revealed that both its N-terminal, as well as its C-terminal region are able to generate this destabilization effect, while the middle region, containing the zinc finger domains, can't. RNA isolation from polyribosomal fractions showed that tethering of ZC3H32 also decreases the translation of the reporter RNA.

High-throughput sequencing of poly-A+ RNA from a ZC3H32-RNAi cell line revealed 20 RNAs that were up-regulated upon ZC3H32 knock-down and thus might be putative targets. The upregulation was confirmed for three of these candidate RNAs. The majority of the putative ZC3H32 targets play a role in the trypanosome's energy metabolism and 15 of them are up-regulated in procyclics. These results suggest that ZC3H32 might be involved in the stage-specific regulation of these RNAs in the bloodstream form.

Zusammenfassung

Der protozoische Parasit *Trypanosoma brucei* reguliert die Expression seiner Gene zum größten Teil auf der post-transkriptionellen Ebene. Es ist bekannt, dass C3H Zink Finger Proteine dabei eine wichtige Rolle spielen. Für alle bis zu diesem Zeitpunkt untersuchten C3H Zink Finger Proteine in *Trypanosoma brucei* wurde nachgewiesen, dass sie ihre RNA-targets stabilisieren.
Diese Arbeit konzentriert sich auf das Zink Finger Protein ZC3H32. Die Ergebnisse einer großtechnischen Isolation von freien und membrangebundenen Polyribosomen in prozyklischen und Blutstromtrypanosomen, welche ebenfalls in dieser Arbeit beschrieben werden, deuteten darauf hin, dass dieses Protein mit den Polyribosomen verknüpft ist. Eine kleinmaßstäbliche Polyribosomen Isolierung, gefolgt von Western Blotting, zeigte jedoch, dass nur ein kleiner Bruchteil der ZC3H32 Proteinmenge mit den Polyribosomen verknüpft ist.
Durch Immunofluoreszenz wurde gezeigt, dass ZC3H32 sich im Zytoplasma befindet.
Ein Hefe-2-Hybrid Assay identifizierte ZC3H32 als möglichen Ligand von MKT1. Diese Interaktion wurde durch Co-Immunoprezipitation bestätigt.
RNA Interferenz, zusammen mit Knock-out Experimenten, zeigten, dass ZC3H32 in der Blutstromform essentiell ist. Sowohl Northern Blots als auch das SILAC Screening von Urbaniak et al. weisen darauf hin, dass dieses Protein, im Vergleich zu prozyklischen Trypanosomen, in dieser Lebenszyklusphase angereichert ist.
Künstliches Anbinden von ZC3H32 an eine Reporter RNA führte zu deren Abbau, was nahelegt, dass dieses Protein eine destabilisierende Wirkung hat. Das Anbinden von ZC3H32 Fragmenten zeigte, dass sowohl die N-terminale als auch die C-terminale Domäne dieses Proteins eine destabilisierende Wirkung hat, aber die mittlere Domäne, welche die Zink Finger enthält, nicht. RNA Isolation aus einem Polysomengradienten zeigte, dass das Anbinden von ZC3H32 auch die Translation der Reporter RNA einschränkt.
Die Hochdurchsatzsequenzierung von poly-A+ RNA einer ZC3H32 RNAi Zelllinie zeigte zwanzig RNAs, deren Menge zunahm, wenn die ZC3H32 Proteinmenge reduziert wurde. Dieser Effekt wurde für drei dieser RNAs bestätigt. Die Mehrheit dieser mutmaßlichen ZC3H32 Targets spielt eine Rolle im Energiemetabolismus und fünfzehn von ihnen sind in der prozyklischen Form hochgeregelt. Diese Ergebnisse weisen darauf hin, dass ZC3H32 eine Rolle in der phasenabhängigen Regulierung dieser RNAs in der Blutstromform spielt.

1. Introduction

1.1 Kinetoplastids

Trypanosoma brucei are protozoan parasites of the order Kinetoplastida. This order, named after the kinetoplast, a granule containing the mitochondrial genome, diverged early from the eukaryotic lineage (Sogin, Gunderson et al. 1989).
Trypanosoma brucei are transmitted by tsetse flies (*Glossina* genus). Parasites of the subspecies *T. b. rhodesiense* and *T. b. gambiense* can infect humans, while the subspecies *T. b. brucei* causes an illness in cattle known as *nagana.* Other parasitic trypanosomatids include *Trypanosoma cruzi*, which causes Chagas disease (or American trypanosomiasis) and the parasites of the *Leishmania* genus.

1.2 The life cycle of *Trypanosoma brucei*

In order to adapt to the different environments in the mammalian hosts and in the tsetse fly, trypanosomes undergo many changes during their life cycle.
In the mammalian bloodstream, two major forms can be found, the proliferative bloodstream slender and the non-proliferative stumpy form (Robertson 1912, Vickerman 1985).
Both are characterized by a dense coat of variant surface glycoproteins (VSGs), which is used for the evasion of the immune system.
Once the stumpy form is taken up by the tsetse fly, it differentiates into the procyclic form in the fly's midgut. The VSG coat is shed; the procyclics are covered in different surface proteins (procyclins). From the midgut, the procyclic cells migrate to the salivary glands, where they differentiate into epimastigotes. The epimastigotes attach themselves to the salivary glands with their flagellum. (reviewed by (Fenn and Matthews 2007)).
Sexual exchange probably takes place in the salivary gland (Gibson, Peacock et al. 2008), as meiosis-specific genes are expressed and promastigote-like haploid cells can be found there (Peacock, Bailey et al. 2013).
Epimastigotes differentiate into metacyclic trypomastigotes, which detach themselves from the salivary glands and can infect mammals.

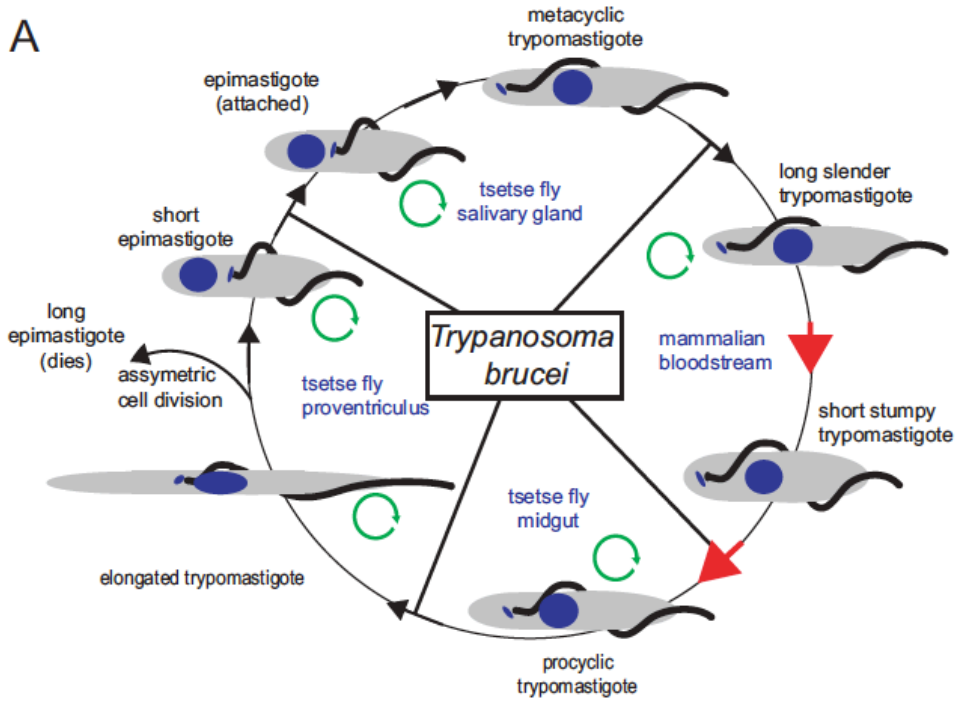

Fig. 1: **Life cycle of *Trypanosoma brucei***, taken from (Kramer 2012)

1.3 Antigenic variation in the bloodstream form

In the bloodstream of the mammalian host, trypanosomes are shielded by a dense coat of variant surface glycoproteins (VSGs), approximately 10 million per cell (Rudenko 2011). Because of this high density, VSG represents about 7-10% of the cells total protein.
Trypanosomes possess about 1000 VSG variants, of which about 5% are fully functional. The remaining genes are pseudogenes (Marcello and Barry 2007). There are ten to twenty VSG expression sites, each containing one *VSG* gene as well as several expression site associated genes (reviewed by (Rudenko 2011)). These expression sites are located at telomeres.
The other *VSG* genes are either localized at the subtelomeric regions (150-250 genes) or at the telomeres of minichromosomes (1250-1400 genes) (De Lange and Borst 1982, Van der Ploeg, Cornelissen et al. 1984, Weiden, Osheim et al. 1991).
Opposite to the majority of the protein coding genes of *Trypanosoma brucei,* the *VSG* genes, as well as the procyclin genes, are transcribed by Polymerase I (Rudenko, Bishop et al. 1989).
Only one *VSG* gene is transcribed at a time, the other expression sites are silenced. The expression of the active VSG site takes place in an extranucleolar locus, the expression site body (ESB) (Navarro and Gull 2001). The monoallellic expression of VSG is controlled at the epigenetic level (reviewed by (Horn and McCulloch 2010)): the active expression site is depleted of nucleosomes (Figueiredo and Cross 2010), while the silenced ones are not.

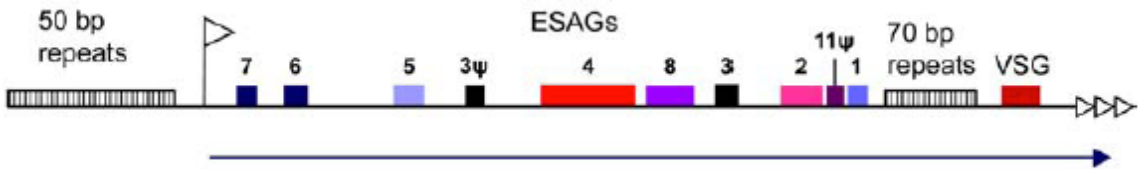

Fig. 2: Schematic representation of a typical VSG expression site. Taken from (Rudenko 2011).
The open flag represents the Polymerase I promoter, the filled boxes the expression site associated genes (ESAGs). The black arrow shows the polycistronic transcription unit, the three triangles at the end represent the telomeric repeats.

The VSG variant is exchanged periodically. In pleomorphic cells, approximately 10^{-2} to 10^{-3} trypanosomes switch per generation (Turner and Barry 1989, Robinson, Burman et al. 1999). In other words, 0.1-1% of "newborn" trypanosomes express a different VSG.
In monomorphic cell lines, like the ones used in the experiments described in this thesis, these switches occur less frequent (10^{-6} to 10^{-7} switch/trypanosome/generation) (Lamont, Tucker et al. 1986, Robinson, Burman et al. 1999).

There are several switching mechanisms, the most common are shown in figure 3.
There are two principle mechanisms: recombinant switching and transcription switching. Transcription switching means that the current expression site is silenced and another one is activated (see fig. 3, panel D).
Recombinant switching, as shown in fig. 3 (panel A, B and C) means that a new *VSG* gene is inserted in the expression site. This can happen by three different mechanisms: Duplicative gene conversion (A), where a gene is copied into the expression site, segmental gene conversion (B), were different parts of different *VSG*s are used to make a new "mosaic VSG" (Marcello and Barry 2007, Hall, Wang et al. 2013) or telomere exchange (C), which means that, due to a crossover with another telomere, the active *VSG* changes place with another *VSG* variant. Opposite to the other two recombination mechanisms, the gene copy of the original *VSG* is kept with this mechanism.

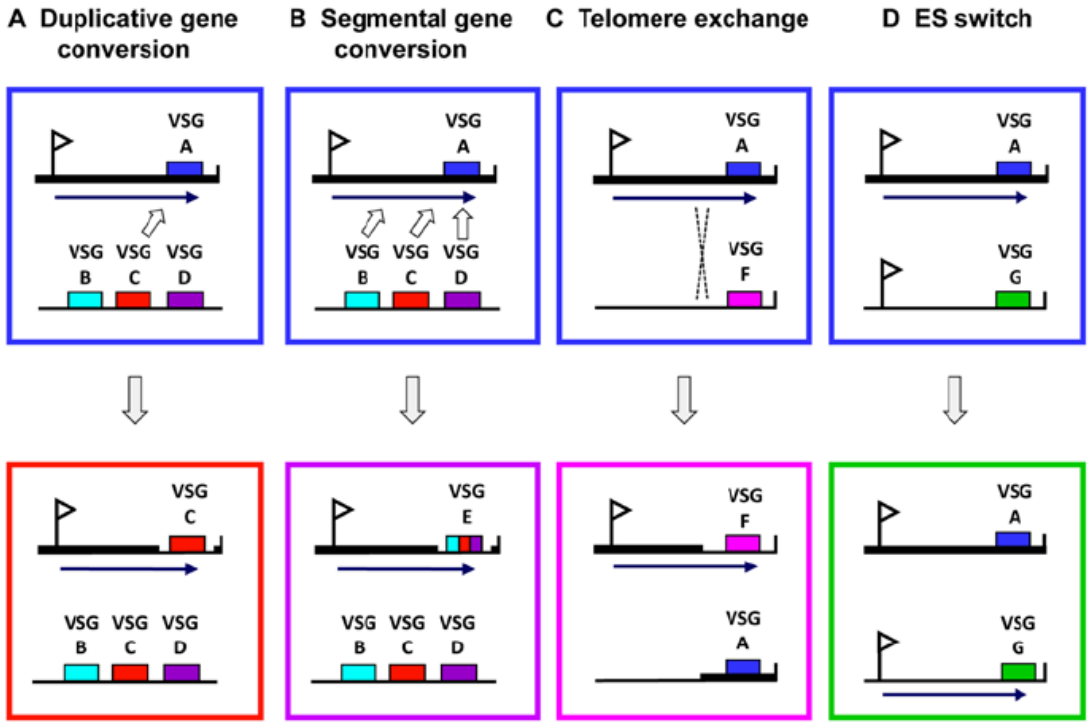

Fig 3: Most important mechanisms for *VSG* switching in *Trypanosoma brucei.* Taken from (Rudenko 2011).

Upon differentiation, the VSG coat is replaced by a procyclin coat. This process is regulated at several levels: transcription elongation is stopped (Vanhamme, Berberof et al. 1995) and the VSG proteins on the surface are cleaved by a glycosylphosphatidylinositol-specific phospholipase C (GPI-PLC) and a zinc metalloprotease (MSP-B) (Gruszynski, van Deursen et al. 2006).
The process is also controlled on the RNA level. The half-life of the *VSG* mRNA decreases from approximately 4.5h to 1.2h when differentiation is induced *in vitro* by the addition of *cis*-aconitate and a temperature reduction from 37°C to 27°C (Ehlers, Czichos et al.

1987). Regulation of VSG mRNA levels is probably controlled by a 97nt element at the 3'end of the RNA, which is found next to the polyadenylation site. Addition of this element to the 3'UTR of a reporter RNA has lead to its stabilization in the bloodstream form and to its degradation in the procyclic form (Berberof, Vanhamme et al. 1995). That indicates that there are specific proteins interacting with the *VSG* RNA, however, these binding partners are unknown.

1.4 Energy metabolism in trypanosomes

In the bloodstream form, glucose is the main energy source. It is mainly degraded to pyruvate (Flynn and Bowman 1973, Hannaert, Bringaud et al. 2003), but also acetyl-CoA is produced, probably as a starting product for the synthesis of lipids (Mazet, Morand et al. 2013). Glycolysis mainly takes place in a specialized peroxisome-like organelle, the glycosome (Hannaert and Michels 1994).

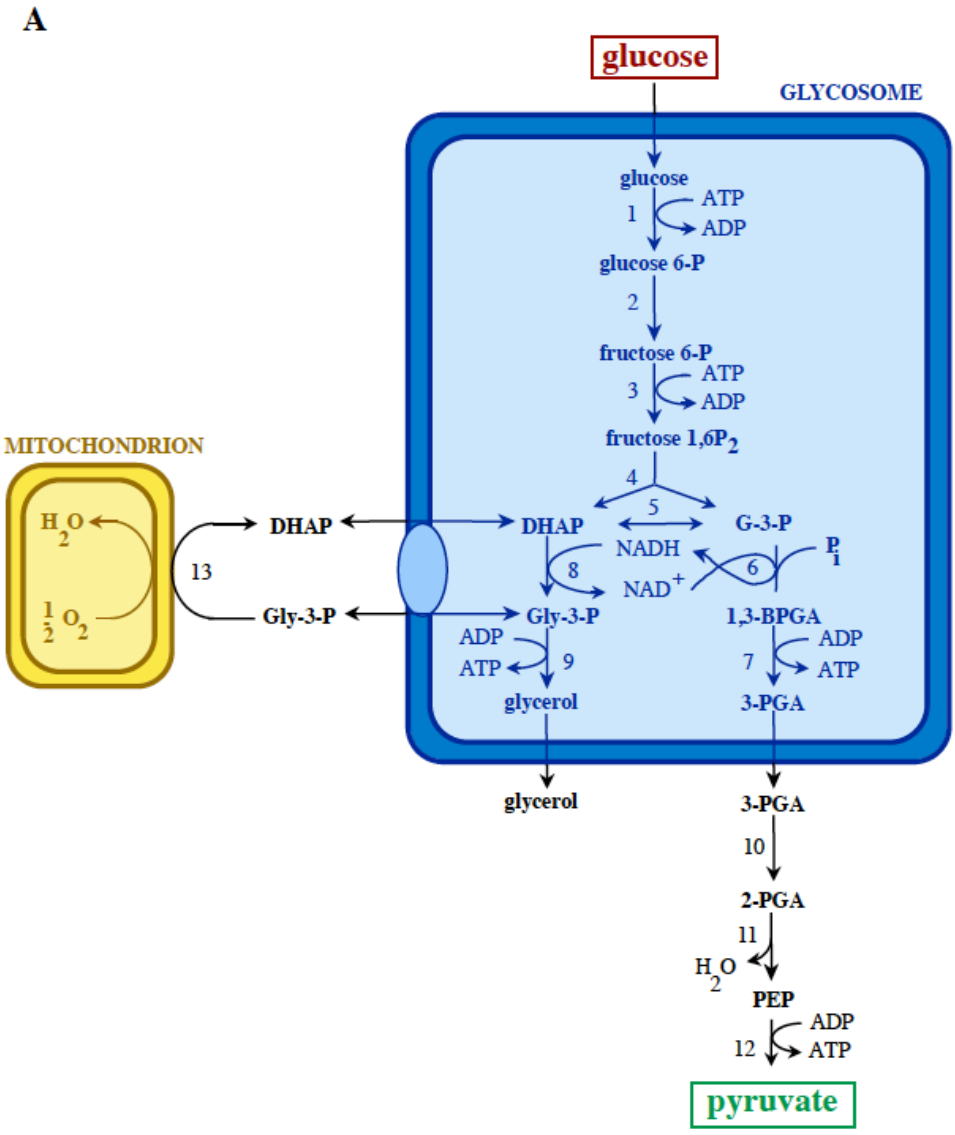

Fig. 4: Glucose metabolism in the bloodstream form trypanosome. Taken from (Hannaert, Bringaud et al. 2003).
Enzymes: 1: Hexokinase, 2: Glucose-6-phosphate-isomerase, 3: Phosphofructokinase, 4: Aldolase, 5: Triosephosphate-isomerase, 6: Glyceraldehyde-3-phosphate dehydrogenase 7: Phosphoglycerate kinase 8: Glycerol-3-phosphate dehydrogenase, 9: Glycerol kinase 10: Phosphoglycerate mutase 11: Enolase 12: Pyruvate kinase 13: Glycerol-3-phosphate oxidase

In the procyclic form, the main energy sources are amino acids like proline and threonine (Evans and Brown 1972, Cross, Klein et al. 1975). However, when glucose is present, procyclics prefer it to proline (Lamour, Rivière et al. 2005). Unlike as in the bloodstream form, the TCA cycle is present in this life cycle stage (see fig. 5) but it does not operate as a full cycle, and does not contribute much to ATP production (van Weelden, Fast et al. 2003).

Threonine is first oxidized by threonine-3-dehydrogenase (TDH) and then split into glycine and Acetyl-CoA by 2,2-amino-3-ketobutyrate-coenzyme-A-ligase. Acetyl-CoA is then converted to acetate, by acetate:succinate CoA-transferase, leading to the production of Succinyl-CoA, which is converted to Succinate by the TCA enzyme Succinate dehydrogenase in an ATP generating reaction.

While not being a great ATP source, threonine is the main source for acetyl-CoA, which is used for the synthesis of fatty acid synthesis (Millerioux, Ebikeme et al. 2013).

Proline is converted to α-Ketoglutarate, which is also converted into Succinyl-CoA. This yields either three reaction equivalents or, when glutamate:oxoglutrate aminotransferase is used for the last step of the pathway (conversion of Glutamate into α-Ketoglutarate), this process yields two reaction equivalents and one oxoacid gets converted into an amino acid (see fig. 5).

Opposite to the bloodstream form, the respiratory chain is present in procyclics. This respiratory chain is similar to that of other eukaryotes, however, additionally to complex I and II, there are two other enzymes donating electrons to the ubiquinone pool: glycerol-3-dehydrogenase and a rotenone-insensitive NADH-oxidoreductase (Fang and Beattie 2002). This kind of NADH-oxidoreductase can also be found in *Archaea*, *Bacteria*, plants and fungi (Kerscher 2000).

Both bloodstream and procyclic cells contain a plant-like alternative oxidase (also called trypanosoma alternative oxidase, short TAO or AOX), which receives electrons from ubiquinole and converts oxygen into water (Clarkson, Bienen et al. 1989, Chaudhuri, Ajayi et al. 1995). In the bloodstream form, it receives the electrons from the oxidation of glycerol-3-phosphate to DHAP. A possible function of this alternative oxidase might be to prevent the creation of reactive oxygen species (ROS) (Fang and Beattie 2003) by superfluous reduction equivalents.

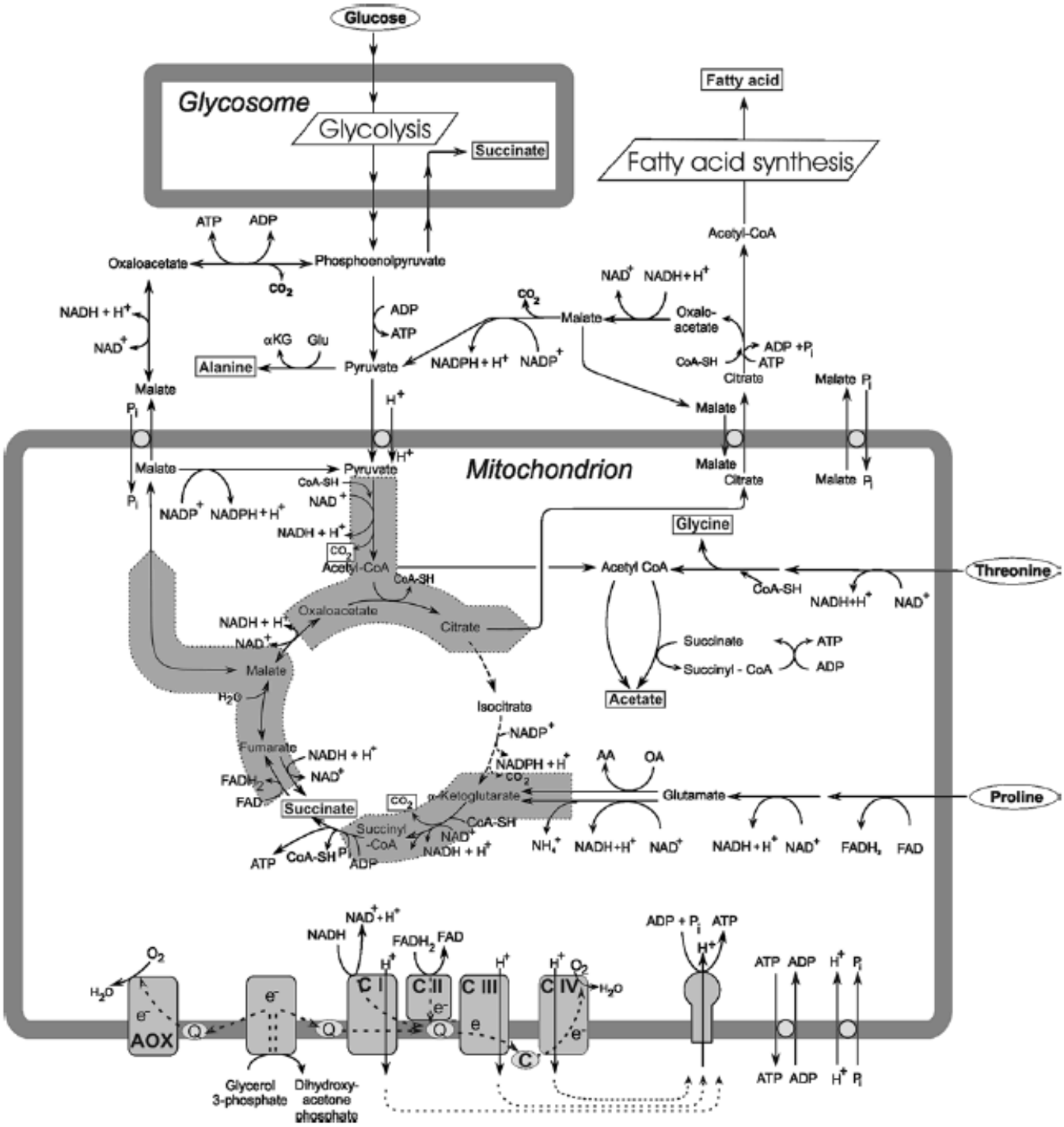

Fig. 5: Energy metabolism in the procyclic trypanosome. Taken from (van Hellemond, Opperdoes et al. 2005), modified from(van Weelden, van Hellemond et al. 2005).
Ovals: substrates, Boxes: end products.
Broad arrows in the citric acid cycle indicate the parts of the citric acid cycle that are active in procyclics.
Note: Acetate, not citrate, is shuttled out of the mitochondrion in trypanosomes (Riviere, Moreau et al. 2009).

1.5 RNA transcription in trypanosomes

The majority of protein coding genes in trypanosomes is transcribed in large polycistronic transcription units. The transcription of these units seems to be mostly unregulated. There is only one described RNA Polymerase II promoter, the promoter of the spliced leader RNA (Gilinger and Bellofatto 2001).
The polycistronic units are separated by *trans*-splicing. In this process a 5' capped, 39 nucleotide RNA, the spliced leader (SL), is attached to the mRNA (Boothroyd and Cross 1982). *Trans*-splicing is coupled to polyadenylation (Sather and Agabian 1985, Hug, Hotz et al. 1994, Vassella, Braun et al. 1994).
As the transcription of most genes is not regulated in trypanosomes, post-transcriptional regulation, especially the control of mRNA levels, plays an important role in these parasites, which makes them a model organism to study these processes.

1.6 Regulation of RNA stability in trypanosomes

While transcription regulation is mostly absent in trypanosomes, mRNA levels vary a lot. While most of the transcripts are present with only three copies per cell or less, others, especially RNAs encoding the tubulins, histones, and ribosomal proteins are quite abundant, for example 600 copies of the alpha tubulin mRNA are present per cell and about a hundred of the mRNA of the ribosomal protein L28 (Manful, Fadda et al. 2011). Although some genes are present with more than one copy (e.g. tubulin, actin), this difference is mostly due to the regulation of RNA stability.
Most mRNAs in trypanosomes are rather unstable, the median half life of an mRNA in the bloodstream form is 13 min and only 5% of the RNAs have a half life of more than 1h (Manful, Fadda et al. 2011). In comparison, in mammalian cells the half-life on mRNAs has been shown to range from 4 to 10 hours (Yang, van Nimwegen et al. 2003, Sharova, Sharov et al. 2009, t Hoen, Hirsch et al. 2011, Clayton 2013).
Also, RNA patterns in trypanosomes change in answer to different environmental conditions (Najafabadi, Lu et al. 2013) and between the different life cycle stages: 5% to 25% of all mRNAs are developmentally regulated between bloodstream and procyclic trypanosomes. (Brems, Guilbride et al. 2005, Jensen, Sivam et al. 2009, Kabani, Fenn et al. 2009, Queiroz, Benz et al. 2009, Siegel, Hekstra et al. 2010, Kramer and Carrington 2011).
The stability of an mRNA is mainly determined by the proteins binding to it. These proteins are also called *trans*-acting factors. The *trans*-acting factors and the mRNA form messenger ribonucleoprotein complexes, short mRNPs. While some of the RNA binding proteins, e.g. the poly-A binding proteins (PABP1 and 2), bind to the majority of mRNAs, others are more specific (Clayton 2013). It is thought that most regulating RNA binding proteins in eukaryotes bind to a specific subset of functionally related RNAs (Keene 2007). This has already been observed in trypanosomes, for example knock-down of the

RRM domain protein DRBD3 (also called PTB1) influences mainly RNAs encoding transmembrane proteins (Stern, Gupta et al. 2009). Another example is the pumilio protein Puf9, which has been shown to bind to a subset of mRNAs which is enriched in the late G0 phase (Archer, Luu et al. 2009). Most Puf9 targets contained a consensus sequence in their 3'UTR (UUGUAC). Puf9 and PTB1 both stabilize their target RNAs, PTB1 is also involved in splicing (Stern, Gupta et al. 2009).

The binding site of RNA binding proteins is mostly found in the untranslated regions, especially the 3'UTR, of their target RNAs. However, there are exceptions, for example, the RNA binding protein RBP42 binds preferably to the coding region of its targets (Das, Morales et al. 2012).

It has been shown that mRNAs with similar functions share common motifs in their 3'UTRs, for example, a uridine-rich sequence (UAUUUUUU) has been found to be enriched in the 3'UTR of procyclic specific genes (Mayho, Fenn et al. 2006). Common regulatory domains, which are found in the 3'UTR of many RNAs, are AU-rich elements, short AREs.

RBP binding sites can be quite short, as the binding sites of most RNA binding proteins bind only to a few nucleotides: The most common RNA binding domain, the RRM domain in eukaroytes, normally binds two to eight nucleotides. The RRM domain is a 90 amino acid long motif and normally folds into a βαββαββ structure (Clery, Blatter et al. 2008, Kramer and Carrington 2011). Another RNA binding domain is the Puf domain, which consists of 40 amino acid repeats and forms an arc-like structure (Wickens, Bernstein et al. 2002). Each Puf repeat binds to one nucleotide (Wang, McLachlan et al. 2002). Usually, Puf domains consist of eight Puf repeats. *Trypanosoma brucei* encodes 10 Puf proteins (Caro, Bercovich et al. 2006) with eight Puf repeats or less. Puf9, for example, has six Puf repeats. Thus, the binding sites of these proteins are probably no longer than eight nucleotides or, in the case of Puf9, shorter.

mRNAs can have multiple RBP binding sites in their sequence, therefore they can bind to different RNA binding proteins and form different mRNPs. The mRNP composition can in turn decide the fate of the RNA: whether it is translated, degraded or stored in stress granules or P-bodies. This allows flexible regulation of the mRNA (Keene and Tenenbaum 2002).

The fact that one mRNA can have several regulatory elements and is usually regulated by multiple factors makes the dissection of regulatory UTRs difficult.

An example is the 3'UTR of the procyclin gene *EP1*. Procyclin genes are expressed specifically in the procyclic form. Transcription is down-regulated in the bloodstream form to 5-15% (Berberof, Pays et al. 1991, Vanhamme, Berberof et al. 1995) and the transcribed procyclin RNA is unstable (Berberof, Vanhamme et al. 1995, Furger, Schürch et al. 1997, Hotz, Hartmann et al. 1997).

Three regulatory elements have been found in this UTR: two stabilizing stem loops (LI and LIII) and a destabilizing stem loop (LII) (Hehl, Vassella et al. 1994, Furger, Schürch et al. 1997, Hotz, Hartmann et al. 1997, Schürch, Furger et al. 1997). These structures

are conserved in the UTRs of different *EP* genes, the rest of the 3'UTR sequences varies. The destabilizing LII domain contains a conserved 26mer, while the LIII domain contains a conserved 16mer.

The main method used to functionally map the *EP1* 3'UTRs was to add the 3'UTR to a reporter RNA and check the reporter's expression. Deletions of different parts of the UTR served to map the regions responsible for positive and negative regulations. The results, however, were difficult to interpret, for several reasons:

mRNA regulation can occur on more than one level (*trans*-splicing, nuclear transport, mRNA stability, mRNA localization, translation etc.). For example, deletion of the conserved 16mer in the LIII domain leads to a decrease in reporter protein levels, but not mRNA levels. This suggests an effect on translation, however, it could have also been caused by rapid protein degradation (Hehl, Vassella et al. 1994).

Different deletions can have different effects even if they affect the same domain. The regulation of the *EP1* RNA is stage-specific, it is down-regulated in the bloodstream and up-regulated in the procyclic form. However, deletions of LII and LIII had the same effects in bloodstream and procyclics. LII deletion lead to an increase, LIII deletion to a decrease of reporter mRNA and protein levels. The effect on the protein levels were higher, which suggests translational regulation (Furger, Schürch et al. 1997, Schürch, Furger et al. 1997). While deletion of the entire LII domain did not show a stage-specific effect, the effect of deletion of a part of this domain was stage specific. This part was the conserved 26mer. In the bloodstream form, a *CAT* reporter RNA carrying the *EP1* 3'UTR without the 26mer deleted was ten times more abundant than a reporter mRNA with a complete *EP1* 3'UTR. However, deleting the 26mer had no effect on the expression of the reporter RNA in procyclic forms. (Hotz, Hartmann et al. 1997). Thus, it can be concluded that sequences within a regulatory domain (in this case LII) can influence the regulation of the entire domain. As RNA binding proteins bind only to a few nucleotides, these sequences can be quite short.

The open reading frame can have an effect on mRNA levels: while reporter RNAs carrying the *EP1* 3'UTR could still be detected, the *EP1* RNA could not. Also, deletion of the destabilizing domain had a greater effect on the *EP1* RNA than on the reporter constructs (Schürch, Furger et al. 1997).

The surrounding sequences of a regulatory element might be important. For example, the 26mer did not show an effect when being inserted into another part of the 3'UTR (Hotz, Hartmann et al. 1997). This can either be due to the three dimensional structure of the RNA: a regulatory element might not be functional if it is in the wrong conformation. It can also be due to the crosstalk between different regulatory elements: For example, deletion of the conserved 16mer in the LIII domain decreases the reporter's expression in both bloodstream and procyclics. However, if the destabilizing LII domain is deleted as well, the deletion of the 16mer had no effect. This indicates that proteins binding to the 16mer counteract the destabilizing effect of the LII domain. A possible candidate protein, which could regulate this effect is the C3H zinc finger ZFP3,

which binds to the *EP1* and *GPEET* mRNAs (Walrad, Paterou et al. 2009). The binding of ZFP3 is dependent on LII and LIII, which indicates that it binds to one of this regions. It might be possible that ZFP3 either induces translation or prevents a negative regulator from binding (Walrad, Paterou et al. 2009). Another finding that supports this is that ZFP3 is associated with polyribosomes in the procyclic, but not in the bloodstream form (Paterou, Walrad et al. 2006).

It can be concluded that the effect of regular domains in RNA sequences depends on many factors; for example the cellular environment (e.g. different life cycle stages, environmental stresses etc), the surrounding sequences in the 3'UTR and also the open reading frame of the gene itself.

There are many ways in which an RNA binding protein can influence its target mRNA. For most RNA binding proteins in trypanosomes, however, the mechanism is not known. Stabilizing factors can, for example, be involved in *trans*-splicing, like DRBD3 and DRBD4 (also called PTB1 and PTB2)(Stern, Gupta et al. 2009). They also can prevent destabilizing factors from binding, either by competing with them for the same binding site or by changing the mRNA's confirmation.

Destabilizing factors can also act on different stages. An example for the different ways in which a protein can influence RNAs is the yeast protein DHH1 (DEAD box helicase 1). DHH1 can induce decapping by interacting with both deadenylases and the decapping enzyme (Coller, Tucker et al. 2001, Fischer and Weis 2002). This protein is also involved in the formation of P-bodies (Coller and Parker 2005). P-bodies are RNA-protein aggregates were translationally repressed RNAs can both be stored and degraded (reviewed by (Kulkarni, Ozgur et al. 2010)). DHH1 also inhibits translation by slowing down ribosome movement (Sweet, Kovalak et al. 2012). In *T. brucei*, it has been shown that DHH1 destabilizes and represses the translation of developmentally regulated mRNAs in procyclics (Kramer, Queiroz et al. 2010).

1.7 mRNA degradation in trypanosomes

mRNA degradation starts usually with deadenylation. This step is mostly catalyzed by the CAF1/NOT complex (Schwede, Ellis et al. 2008), the Pan2/Pan3 complex (Schwede, Manful et al. 2009) or by one of the three PARN deadenylases (Utter, Garcia et al. 2011). This step is normally followed by decapping, however, a general decapping enzyme has, so far, not been found in trypanosomes. The deadenylated mRNA can be degraded from the 3' end by the exosome complex (Estevez, Kempf et al. 2001, Estevez, Lehner et al. 2003) and from the 5' end by the exoribonuclease XRNA (Li, Irmer et al. 2006).

RNA regulation by micro RNAs does not play a role in *Trypanosoma brucei*: While the RNAi machinery is present in *Trypanosoma brucei*, it serves mainly for the degradation of retroposon transcripts but does not seem to process micro RNAs, as an affinity purification of *Tb*Ago1 revealed none (Tschudi, Shi et al. 2012). The fact that *Tb*Ago1 is not essential in trypanosomes also indicates that RNAi does not play a major role in the

regulation of mRNA stability (Janzen, van Deursen et al. 2006).

1.8 Regulation of protein synthesis in trypanosomes

While regulation of RNA stability seems to be more important trypanosomes, regulation of translation plays a role as well.

For example, changes in protein levels during the differentiation of *T. b. brucei* correlate with RNA level changes (van Deursen, Thornton et al. 2003, Jensen, Sivam et al. 2009, Fernandez-Moya and Estevez 2010), suggesting that for differentiation RNA stability is more important than translational regulation and protein stability. However, translational control also plays a role: Global translation, which can be observed by making polyribosome profiles, vary in the different life cycle stages (Brecht and Parsons 1998). Translational efficiency does not correlate with RNA stability, which indicates that it is regulated independently. Also, the translational efficiency with which different mRNAs are translated can vary over two orders of magnitude in the same condition (Vasquez, Hon et al. 2014). This means that, in one cell, some mRNAs are translated more than others, which shows that translation is regulated.

The translational machinery seems to be conserved in trypanosomes (Fernandez-Moya and Estevez 2010) although the structure of the ribosome differs. The most notably difference is that the ribosomal RNA is cleaved into six pieces, two large ones and four smaller ones (Campbell, Kubo et al. 1987).

Translation initiation is regulated in trypanosomes. There are four different eIF4E isoforms that seem to have different importance in different life cycle stages: while eIF4E1, 3 and 4 are essential in the bloodstream form, only eIF4E3 is essential in procyclics. Also, they interact differentially with the eIF4G homologues: while eIF4E3 interacted with both eIF4G3 and G4, eIF4E4 interacts only with G4. No interaction was observed between eIF4G homologues and eIF4E1 and 2 (Freire, Dhalia et al. 2011). This suggests that there might be different initiation complexes with different functions. It has also been shown that eIF4E3 and 4, as well as eIF4G4, are highly phosphorylated. This phosphorylation has most likely a function in the regulation of translation; it has been shown that eIF4E4 is phosphorylated in procyclics in the logarithmic grow phase, but not when the growth is arrested due to higher density (Pereira, Malvezzi et al. 2013).

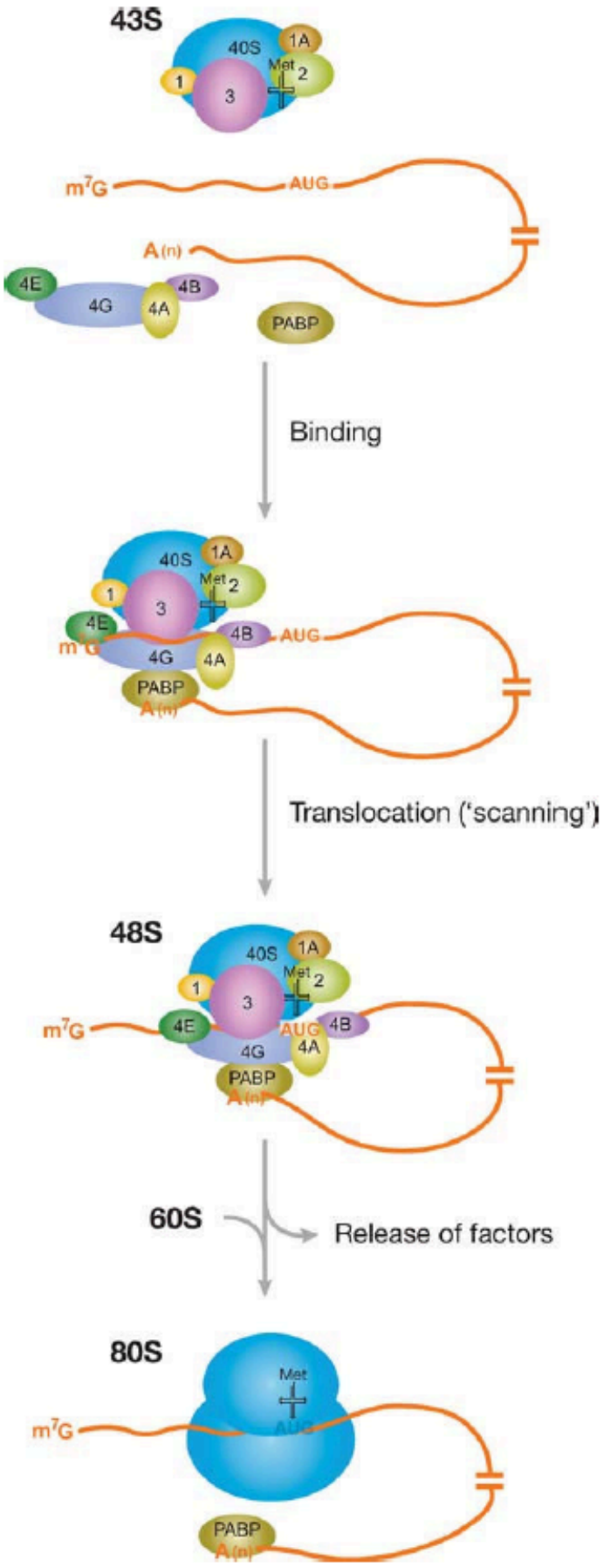

Fig. 6: Translation initiation in eucaryotes
Taken from (Kindler, Wang et al. 2005).
The 43S complex, consisting of the small ribosomal subunit, the aminoacyl-tRNA and the initiation factors eIF1, 1A, 2 and 3 gets recruited to the mRNA. This is mediated by the eIF4 complex, consisting of eIF4A and B, the cap-binding protein eIF4E and eIF4G, which binds to the poly-A protein, which leads to a circulation of the mRNA.
In *Leishmania*, however, the eIF4E homologue, not the eIF4G homologue, seems to bind to PABP (Zinoviev and Shapira 2012).
After recruiting the 43S complex to the mRNA, the complex "scans" the mRNA for the initiation codon. The scanning is promoted by eIF4A and B. Then, the 60S subunit joins and the initiation factors are released.

1.9 CCCH zinc finger proteins

One group of RNA binding proteins are the CCCH zinc finger proteins, which bind RNA with a zinc finger, a small protein motif, which is stabilized by its interaction with a zinc ion. The CCCH zinc finger consensus sequence is defined as C-X(4-15)-C-X(4-6)-C-X3-H (Wang, Guo et al. 2008) (C: cysteine, H: histidine, X: any amino acid), the most common variations are the C-X7-C-X5-CX3-H and the C-X8-C-X5-C-X3-H motif (Kramer, Kimblin et al. 2010).
The best-described CCCH protein is tristetraproline (TTP), the founding protein of the Tis11 family. Proteins of the Tis11 family bind to AU-rich elements (AREs) in the 3'UTR of their target RNAs. Most Tis11 family members destabilize their targets by interacting with the RNA degradation machinery (Sanduja, Blanco et al. 2011) (see fig. 7).

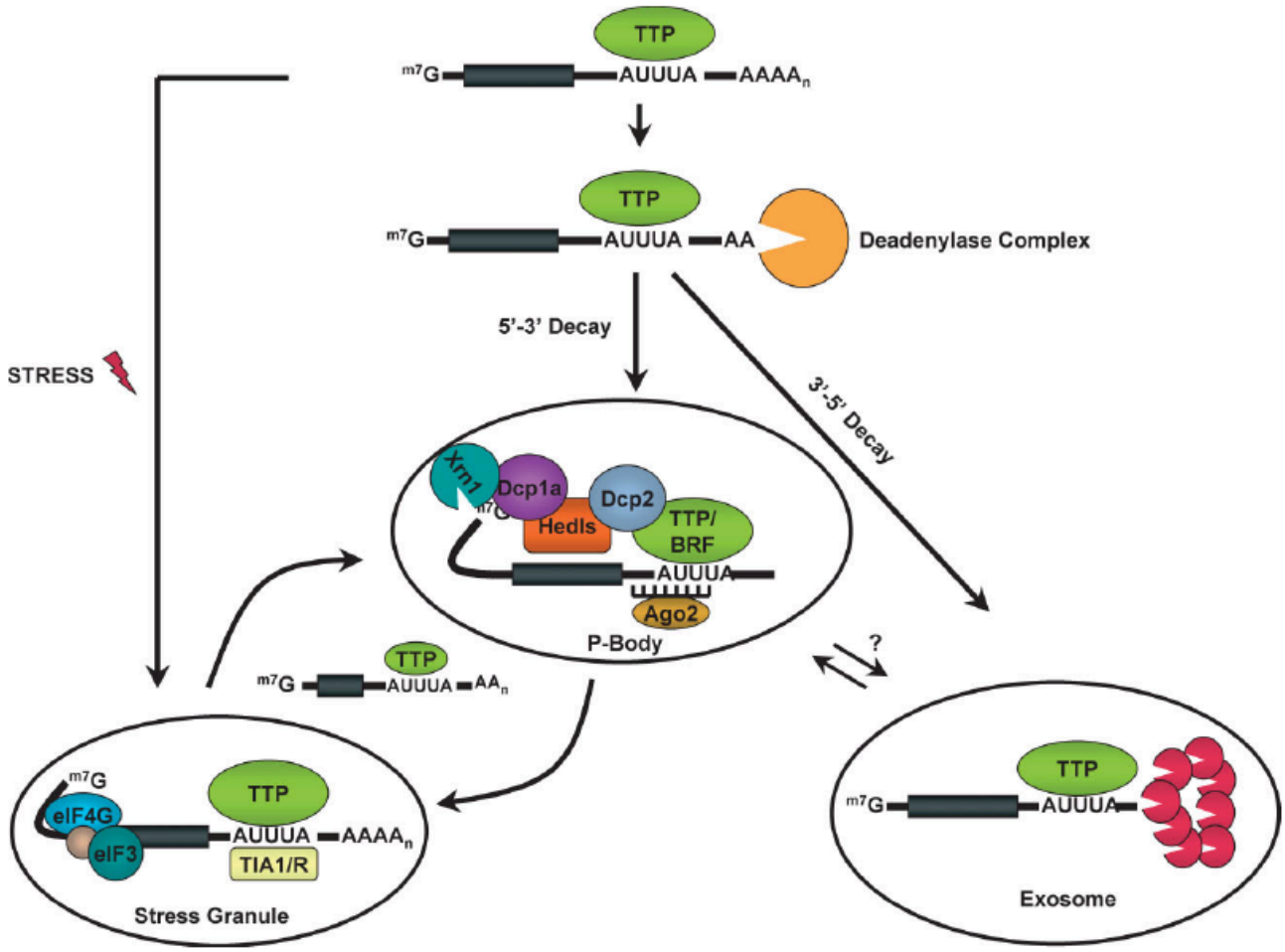

Fig. 7: ARE mediated mRNA decay by the Tis11 family CCCH zinc finger proteins TTP and Brf1 and 2. Taken from (Sanduja, Blanco et al. 2011).
TTP can induce deadenylation by recruiting the CCR4/CAF1/NOT deadenylation complex by direct interaction with CCR4 and the central region of the scaffold protein NOT1(Sandler, Kreth et al. 2011). They can also recruit the PARN deadenylase complex via an indirect interaction. TTP can interact with components of the exosome complex, which catalyses 3'-5' mRNA decay.

TTP and BRF proteins can also mediate the localization of the deadenylated RNAs to P-bodies, where TTP can interact with the decapping complex, as well as the exonuclease XRN1, which leads to 5'-3' exonucleotic decay.
TTP mediate the interaction between its target RNA and Argonaute proteins (AGO), which can promote microRNA dependent decay.
TTP and BRF are also associated with stress granules. It is thought that these proteins facilitate the transport of RNAs from stress granules to P-bodies. The ARE binding proteins TIA1 and TIAR have been shown, among other functions, to be important for stress granule formation (Kedersha, Gupta et al. 1999). An immunoprecipitation of myc-TTP followed by mass spectrometry suggested that TTP interacts with TIAR.

Trypanosoma brucei possess 48 putative zinc finger proteins, most of them are unique to kinetoplastids (Kramer, Kimblin et al. 2010).
One third of these proteins possess one zinc finger. It was thought that, as TTP requires both its CCCH domains to bind to RNA, that two zinc fingers are required for RNA binding (Lai, Carballo et al. 1999) but it was shown by (Michel, Guerrerio et al. 2003) that one functional zinc finger can bind RNA specifically. Therefore, these proteins containing a single zinc finger could either act on their own or as homo- or heterodimers.
In Michel at al.'s study, a seven nucleotide sequence was needed for the binding of the C3H domain peptide (UUUAUUU).
The binding site for the two zinc fingers of Tristetraprolin is a nonamer (UUAUUUAUU) (Worthington, Pelo et al. 2002, Blackshear, Lai et al. 2003) and each zinc finger binds to one UAUU site (Hudson, Martinez-Yamout et al. 2004). TTP related proteins are likely to have the same or similar binding sites (Brooks and Blackshear 2013).
Contrary to TTP, the zinc finger proteins described in *Trypanosoma brucei* have so far all shown to have a stabilizing effect on their mRNA targets.
ZFP1, ZFP2 and ZFP3, a group of small proteins (12, 16 and 14kDa respectively) possessing only one C3H zinc finger each, seem to play a role in the differentiation of bloodstream trypanosomes to procyclics.
While ZFP2 knock-down inhibits differentiation (Hendriks, Robinson et al. 2001), knock-out of ZFP1 impairs the repositioning of the kinetoplast during this process (Hendriks and Matthews 2005).
These three proteins have shown to interact with each other *in vivo* (Paterou, Walrad et al. 2006).
ZFP3 binds to *EP1* and *GPEET* procyclin RNA (Paterou, Walrad et al. 2006, Walrad, Paterou et al. 2009), as well as several transcripts that are up-regulated in the stumpy form. *EP1* RNA and other transcripts seem to be stabilized by ZFP3, as their levels increase if ZFP3 is overexpressed (Walrad, Capewell et al. 2012).
ZC3H18 probably plays a role in differentiation as well, as downregulation of this protein, while not stopping this process, does slow it down (Benz, Mulindwa et al. 2011).
ZC3H20 is up-regulated in procyclics, in opposite to the bloodstream form, and has been

shown to stabilize and interact with two RNAs which are also enriched in procyclics (Ling, Trotter et al. 2011).
ZC3H12 has been shown to interact with the exonuclease XRNA, but artificial tethering of this protein to a reporter RNA lead to no decrease in RNA levels (Ouna, Stewart et al. 2012).
ZC3H11 is involved in the heat shock response in trypanosomes. It is up-regulated upon heat shock and its RNA targets include chaperones, e.g. *Hsp70*. It has been shown that this zinc finger binds to the *Hsp70* RNA via an AU-rich element in its UTR (Droll, Minia et al. 2013).
A TAP purification revealed that ZC3H11 binds to MKT1. It was shown that MKT1 (see fig. 8) interacts with PBP1, which in turn interacts with the poly-A-binding protein. It is thought that this mechanism could lead to the stabilization of the target RNA (Singh, Minia et al. 2014).

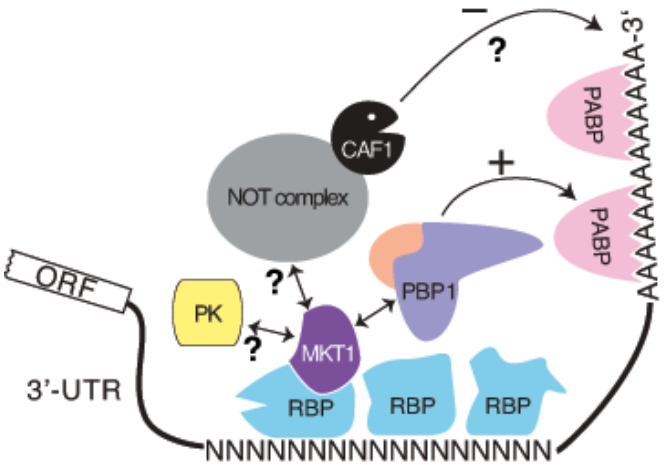

Fig. 8: Putative mechanism of MKT1. Taken from (Singh, Minia et al. 2014).
RBP: RNA binding protein, PK: protein kinase (putative MKT1 interaction partner).

A yeast-two-hybrid screen identified 16 predicted RNA-binding proteins as putative MKT1 binding partners. 10 of these 16 proteins were zinc finger proteins. The screen also identified a putative MKT1 binding motif, the "HNPY" consensus motif ((H/N)(D/E/N/Q)PY).
Another binding partner found in the yeast-two-hybrid screen is the protein Not2, which is a part of the CAF1-NOT deadenylation complex. Also, two other components of this complex (CAF40 ant NOT1) were co-purified with MKT1 in a TAP purification. This indicates that MKT1 could, next to RNA stabilization, also mediate RNA deadenylation and thus RNA decay. (Singh, Minia et al. 2014).

1.10 Aims of the thesis

The main aim of my first and second project (described in section 3.1 and 3.2) was to find *trans*-acting factors of the *VSG* mRNA. Although there is evidence that VSG expressing is regulated on the mRNA level (Ehlers, Czichos et al. 1987), so far no *trans*-acting factors of the VSG mRNA have been found.
The first step was to find proteins associated with free and membrane-bound polyribosomes in procyclic and bloodstream cells. In order to do that, free and membrane-bound polyribosomes were separated by ultracentrifugation at 30 000g and the polyribosomes were subsequently purified by separation on a sucrose-gradient. The isolated polyribosomes were concentrated and sent for mass spectrometry analysis.
As VSG is the major surface protein in trypanosomes, a large percentage of membrane-bound polyribosomes should translate VSG. Thus, proteins with RNA binding domains that are found exclusively in the membrane-bound polyribosomes of the bloodstream form might be candidates for *VSG* mRNA binding proteins.
The large-scale purifications should also be helpful in order to identify other RNA binding proteins that associate with polyribosomes. Knowing whether a putative RNA binding protein is associated with polyribosomes is quite useful; not only does polyribosome association point towards a function in translation regulation, it also indicates that this protein is indeed binding to RNA.
The second method that was used to try to identify *VSG* mRNA binding proteins was polyribosome purification followed by immunoprecipitation with a polyclonal VSG antibody (described in section 3.2).
The third project described in this thesis (section 3.3) was about identifying the role of a C3H zinc finger protein, ZC3H32. ZC3H32 was identified in the mass spectrometry results of the purification of the membrane-bound polyribosomes of the bloodstream form. It was also identified as a putative binding partner of MKT1 in a yeast-two-hybrid screen (Singh, Minia et al. 2014). The main aims of this project were to find out whether this protein is essential, how it influences the mRNA metabolism of the cell and to find its RNA targets and protein binding partners.

2. Materials and Methods

2.1 General cloning methods

2.1.1 PCR

PCR was performed in a Thermocycler using GoTaq (promega) polymerase. The usual settings were:
DNA denaturation at 95°C for 5 min, 24-30 cycles with 30-45 seconds denaturation at 95°C, 30-45 seconds annealing at 52-55°C and 1min elongation at 72°C.

PCR reaction mix:
1x Taq polymerase buffer
100 pM fw primer
100 pM reversed primer
20mM DMSO (optionally)
0.4 mM of each dNTP
100 ng genomic DNA
0.5U Taq polymerase

For long open reading frames, as well as for the testing of the knock-out cell lines, the Q5 Polymerase (NEB) was used. The PCR protocol was adusted according the manufacturers instructions.

The PCR product was analysed on a 1% agarose gel containing 0.7μg/ml ethidiumbromide and purified either by PCR-clean up or the whole sample was separated by electrophoresis and purified from the agarose gel. For both methods the Nucleospin ExtractII kit (Macherey-Nagel) was used.

2.1.2 Isolation of trypanosome genomic DNA

About 10^8 trypanosome cells were harvested by centrifugation (2000rpm, 10min, RT). Genomic DNA was isolated using the illustra GenomicPrep cells and tissue DNA isolation kit (GE Healthcare). The isolated DNA was stored at –20°C.

2.1.3 Agarose gel electrophoresis

1% agarose Gels were prepared by dissolving 1g ultrapure agarose in 100ml TAE buffer in a microwave. After cooling down, 10μl ethidiumbromide (70μg) were added and the gel mix was poured in a tray. 6x DNA loading dye was added to a final concentration of

1x and the DNA was separated at 100-170V. Visualisation was done using a UV Transilluminator.

TAE buffer:
40mM Tris-HCl
1mM EDTA (pH 8.0)
0.11% Acetic acid

DNA loading dye:
10mM Tris·HCl (pH=7.6)
60mM EDTA
0.09% Bromphenolblue
0.09% Xylenecyanole FF
60% glycerin

2.1.4 Restriction endonuclease digest

The reaction was performed in the buffer recommended by the manufacturer (NEB). In case of a double digest, which means that two enzymes were used simultaneously, the buffer which resulted in the highest activity of both enzymes was used. BSA was added if recommended. 2-5U of enzyme was used to digest 1µg DNA. Usually, 15µl purified PCR product or 5µl plasmid preparation were digested with 1µl restriction enzyme solution. The reaction was incubated for at least 2h at the recommended temperature. If two temperatures were recommended, the digest was incubated for 1h at the first, then for 1h at the second temperature.
After digestion, the DNA was purified either by PCR clean-up or by gel extraction, as described before. Digested vectors were dephosphorylated first (see below).

2.1.5 Dephosphorylation of 5'ends

Dephosphorylation was performed to prevent self-ligation of a digested vector. The reaction was performed by adding 1U alkaline phosphatase (Roche, 1U/µl) and 1µl of the respective buffer to the restriction digest and incubating for 10-15min at 37°C.

2.1.6 Klenow cleavage of DNA

In order to get blunt ends after a restriction endonuclease digest the plasmid or the DNA fragment was treated with Klenow, Large Fragment of DNA Polymerase I (USB). 2 - 4µg DNA were blunted with 1µl (5U) Klenow in a reaction including one volume of 10x Klenow buffer and 0.5mM of each dNTP.

2.1.7 Ligation of DNA fragments

PCR fragments or inserts excised from plasmids were ligated into digested vectors using 1U DNA ligase (NEB, 1U/µl) in a 10µl reaction in the appropriate buffer. Insert and

vector were ligated in a molar ratio of approximately 1:5. The reaction was incubated for 2-16h at 16°C.

2.1.8 Transformation of competent cells

50µl DH5α or BL21 cells were thawed on ice and incubated on ice for 5-20min with 10µl of the ligation reaction mix. Then the bacteria were heat-shocked for 90 seconds at 42°C, chilled for two minutes on ice and grown in 200µl LB medium (without antibiotics) at 37°C for 30 minutes. The transformation was plated out on LB plates with ampicillin and incubated at 37°C over night.

Luria Bertani (LB) Medium:
10 g/l Tryptone
5 g/l Yeast extract
10 g/l NaCl

LB Medium + Agar (LB-Agar)+ Ampicillin
LB Medium
15 g/l Bacto-Agar
100 µg/ml ampicillin

Ampicillin stock solution:
10mg/ml ampicillin
50% ethanol

2.1.9 Screening of transformed bacteria by colony PCR

A PCR mastermix was prepared as described in 2.2.1 (without DMSO).
10-20 colonies of one transformation were picked from an ampicillin plate using a yellow pipette tip, resuspended partially in 10µl water and mixed with 15µl PCR mastermix. The rest of the culture was used to inoculate 2ml LB medium with ampicillin. 10µl of pure water was used as a negative control. Alternatively, 10-20 cultures were picked the day before and grown over night in 2ml LB medium with ampicillin. 2µl of each bacteria culture were added to 23µl PCR mastermix.
PCR was performed as described before. The PCR products were analyzed on an agarose gel. Positive clones were grown over night, or respectively the liquid culture was used directly for a plasmid preparation.

2.1.10 Plasmid preparation

2-4ml LB media with ampicillin was inoculated with bacteria and grown over night. The plasmid preparation was done using the NucleoSpinPlasmid kit (Macherey-Nagel) according to the manufacturers instructions. The plasmid preparation was screened for the desired vector by restriction digest. The vector was then checked by sequencing performed by GATC Biotech.

For higher plasmid concentrations, which are needed for the transformation of trypanosomes, a 12ml culture was inoculated and grown over night. 6ml of this culture were spun down in an eppendorf tube and the cell pellet was used for a plasmid preperation. After elution of the plasmid DNA, the column was reused for the preparation of the rest of the culture. The two eluates were pooled and the plasmid concentration was measured using a nanodrop.

2.1.11 Ethanol precipitation of DNA

The DNA was mixed with 1/10 volume of 3M sodium acetate and 2.5 volumes of ethanol. The mixture was incubated for at least 45min at -20°C. The precipitate was spun down in a microfuge at top speed for 15min at 4°C. The supernatant was discarded and the pellet air-dried. If the DNA was used for the transformation of trypanosomes, the drying was done in a laminar flow hood.

2.2. Cell culture methods

2.2.1 Cultivation of bloodstream trypanosomes

Bloodstream trypanosomes were cultivated in HMI-9 medium at 37°C in a humid athmosphere with 5% CO_2 in a Heraeus incubator. In order to allow gaseous exchange, the caps of the flasks were loosely tied. Bloodstream cells were kept at concentrations around
$5 \cdot 10^5$ cells/ml and not exceeeding $2 \cdot 10^6$ cells/ml.

HMI-9 medium

Iscove's modified Dulbecco's medium	17.66 g/l
$NaHCO_3$	3.024 g/l
Hypoxanthine	136 mg/l
Sodium pyruvate	110 mg/l
Thymidine	39 mg/l
Bathocuprono disulfonic acid disodium salt	28 mg/l

pH = 6.3
The media was filter-sterilized and stored at –20°C in 450ml aliquots.

Additional components (added prior to use):

Heat-inactivated FCS* (Biochrom)	10% (v/v)
Penicillin/Streptomycin (Sigma)	50U/ml (5ml of a 5000U/ml stock solution
L-Cysteine-HCL· H_2O	1.5mM
β-Mercaptoethanol (Sigma)	0.14% (7μl)

*Heat inactivation of FCS was done for 30min at 55°C

For cryopreservation 500µl of cells in a logarithmic state of growth (5-10·10^5 cells/ml) were transferred to cryovials and mixed with 500µl of HMI-9 medium containing 20% glycerol. To freeze the cells gradually, the cryovials were wrapped in a thick layer of paper, left at
-80°C for at least one day and then transferred to cryoboxes in a liquid N_2 tank.
To restart the culture, the cells were thawed at 4°C or at room temperature, washed once with HMI-9 and then resuspended in 10-20ml HMI-9 containing the appropriate antibiotics.

2.2.2 Stable transfection of bloodstream trypanosomes

1-2·10^7 cells in a logarithmic state of growth (5-10·10^5 cells/ml) were spun down at 2000rpm for 8 min at room temperature. The cell pellet was suspended in 10ml ice-cold cytomix and centrifuged as before. Then the cells were resuspended in 500µl cytomix, transferred to a BTX electroporation cuvette and mixed with 10µg linearised plasmid DNA. Electroporation was done with a single 1.5kV pulse at a resistance of 24 Ohm using a BTX electroporator. The cells were transferred to 20ml prewarmed HMI-9 medium containing the appropriate antibiotics for the used cell line and diluted until the concentration was lower than 5·10^5 cells/ml. The next day, the cells were diluted to a concentration of 2·10^5 cells/ml and the appropriate selective antibiotic was added (for concentration see 2.3.3). The cells were distributed into a 24-well plate (1ml per well). Stable clones, which could be collected after a minimum of 4 days, were diluted and grown for further analysation.

Cytomix (1l):
0.76g EGTA
9g KCl
0.022g $CaCl_2 \cdot 2H_2O$
8.66ml K_2HPO_4 (1M)
1.34ml KH_2PO_4 (1M)
pH=7.6 (adjust with KCl)

2.2.3 Stable transfection of bloodstream trypanosomes – Amaxa system

1-2·10^7 cells in a logarithmic state of growth (5-10·10^5 cells/ml) were spun down at 2000rpm for 8 min at room temperature. The cell pellet was resuspended in 200µl Amaxa buffer, transferred to a BTX electroporation cuvette and mixed with 10µl linearised plasmid DNA solution (conc. appr. 1µg/µl). The transfection was done according to (Schumann Burkard, Jutzi et al. 2011), using program X-001 of the Amaxa Nucleofector. The antibiotic selection was done as described in 2.3.2.

Amaxa buffer:
90mM sodium phosphate
5mM potassium chloride
0.15mM calcium chloride
50mM HEPES, pH 7.3

2.2.4 Antibiotics used for selection

		Bloodstream		**procyclics**	
Antibiotic	Stock	added vol./ 100ml media	final conc.	added vol./ 100ml media	Final conc.
Phleomycin	5mg/ml	4µl	0.2µg/ml	4µl	0.2µg/ml
G148 (Neomycin)	50mg/ml	10µl	5µg/ml	30µl	15µg/ml
Hygromycin B	50mg/ml	30µl	15µg/ml	100µl	50µg/ml
Blasticidin	5mg/ml	100µl	5µg/ml	200µl	10µg/ml
Puromycin	1mg/ml	20µl	0,2µg/ml	100µl	1µg/ml

Table 1: Concentration of stock solutions and final concentration in the media of antibiotics used for selection

2.2.5 Cultivation of procyclic trypanosomes

Procyclic trypanosomes were cultivated in MEM-Pros medium in a climatised room at 27°C. Cells were diluted to a concentration no lower than $5 \cdot 10^5$ cells/ml and grown up to $5 \cdot 10^6$ cells/ml.

Mem-PROS *(Minimum essential medium* for procyclic trypanosomes):

$CaCl_2 \cdot 2H_2O$	265mg/l
Kcl	400mg/l
$MgSO_4 \cdot 7H_2O$	200mg/l
NaCl	6.8g/l
$NaH_2PO_4 \cdot H_2O$	140g/l
HEPES	7.14g/l
L-Arg-HCl	126mg/l
L-Cys-Cys	240mg/l
L-Gln	292mg/l
L-His-HCl·H_2O	42mg/l
L-Ile	52mg/l
L-Leu	52mg/l
L-Lys	73mg/l
L-Met	15mg/l

L-Phe	100mg/l
L-Thr	48mg/l
L-Trp	10mg/l
L-Tyr	100mg/l
L-Val	46mg/l
L-Pro	600mg/l
Adenosine	12mg/l
Ornithine·HCl	10mg/l

Table 2: contents of MEM-Pros

1l of a 10x MEM-PROS mixture (Biochrom) containing the mentioned components was mixed with 4l water. The pH was adjusted to 7.4 using NaOH. Then, 4l water, 100ml MEM non-essential amino acids, 100ml MEM vitamins (SIGMA) and 100mg phenol red were added. The pH was again adjusted to 7.4, the media was sterilized by filtration and stored in 450ml aliquots at –20°C.

Additional components which were added prior to use:
Heat-inactivated FCS* (Biochrom) 10% (v/v)
Hemin 7.5mg/l (1.5ml of a 2.5 g/l stock solution)
Penicillin/Streptomycin (Sigma) 50U/ml (5ml of a 5000U/ml stock solution)
*Heat inactivation of FCS was done for 30min at 55°C

For cryopreservation, approximately 2ml of cells in the logarithmic state of growth (1-2·10^6 cells/ml) were spun down and resuspended in 500µl media. The cells were transferred to cryovials and mixed with Mem-Pros medium containing 20% glycerol. Freezing and thawing was identical to bloodstream trypanosomes. Thawed procyclic trypanosomes were washed once with Mem-Pros medium and transferred to conditioned Mem-Pros medium. Conditioned Mem-Pros medium was obtained by spinning down a culture of procyclic 1313 cells and supplying the supernatant with the appropriate antibiotics.

2.2.6 Stable transfection of procyclic trypanosomes

1-2·10^7 cells in a logarithmic state of growth (1-2·10^6 cells/ml) were spun down at 2000rpm for 8min at room temperature. The supernatant was kept as conditioned medium. The cell pellet was suspended in 10ml cold ZFPM (Zimmerman post-fusion medium) and spun down as before. The cells were resuspended in 500µl ZFPM and mixed with 10µg linearised plasmid DNA. Electroporation was performed as described for bloodstream cells (see 2.3.2). The cells were transferred to a culture flask with 5ml Mem-Pros medium, containing the appropriate antibiotics for the cell line used and grown over night. The next day, the cells were diluted to a concentration of 2·10^5

cells/ml using the conditioned medium and the appropriate selective antibiotic was added. The cells were transferred to a 24wells plate. Stable clones were obtained approximately 7 days later.

5xZFPM:
38.57 g NaCl
2.98g KCl
7.12g $Na_2HPO_4 \cdot 2H_2O$
1.02g KH_2PO_4
0.536g magnesiumacetate ($C_4H_6O_4Mg \cdot 4H_2O$)
0.066 $CaCl \cdot 2H_2O$

2.2.7 Induction of RNAi constructs with tetracycline

The *Tn10 tet* repressor gene is integrated in the genome of the1313 514 cell lines (procyclic and bloodstream) and expressed constitutively. The Tet repressor binds to promoter regions containing the two appropriate operation sites and blocks the expression of the respective gene. When tetracycline is added, it binds to the repressor, which detaches itself from the promoter, thus allowing gene expression. This system is used for induced gene expression in trypanosomes.
Here, the $p2T7^{TA}$blue vector was used, which contains two Tet-inducible promoters on each side of the inserted gene. Upon adding of tetracycline, this leads to the expression of two complementary RNA strands, which form a double-stranded RNA. The presence of this double-stranded RNA complementary to the target gene leads RNA interference and thus inhibits its expression.
In order to observe the effects of the knockdown of the target gene, cell growth was monitored up to 7 days. Bloodstream cells were diluted to a starting concentration of 5.104 cells/ml, procyclics to 5.105. Induction of the Tet promoter was done by adding tetracycline to a final concentration of 0.1µg/ml (0.02µl/ml of a 5µg/µl stock solution or 1µl/ml of a 1:50 dilution). After one day, the cells were counted, re-diluted to this concentration and the cell number and the dilution ratio were documented.

2.3 General methods for protein analysis

2.3.1 Extraction of total protein

0.2 - $1 \cdot 10^7$ cells were harvested at 2000rpm for 8min at room temperature. The cell pellet was resuspended in 2xLaemmli buffer and boiled for 5min at 95°C.

2.3.2 SDS-PAGE

The samples were loaded on a 10% or a 15% PAA gel and run at 80-150V. A mini protean electrophoresis apparatus (BioRad) was used to make and run the PAA gels.

2x Laemmli-buffer:
125 mM Tris-Cl pH=6.8
4% SDS
15mM EDTA
10% β-Mercaptoethanol
20% glycerol
0.1% bromphenolblue

seperation gel
10-15% polyacrylamide
25% 1.5M Tris-Hcl, pH 8.8
1% SDS (10% stock solution)
1% APS (10% stock solution)
0.05% TEMED

stacking gel
4% polyacrylamide
25% 1M Tris-HCl, pH 6.8
1% SDS (10% stock solution)
1% APS (10% stock solution)
0.1% TEMED

Running buffer:
3.03g Tris
14.42g glycine
1g SDS
+ millipore water until volume equals 1l

2.3.3 Western blotting

The proteins were transferred to a nitrocellulose transfer membrane (Whatman, Schleicher & Schuell) using a biorad apparatus. Blotting was done in 1x blotting buffer, which was stirred using a magnetic stirrer, at 4°C at 100V for 1-3 hours.
The blot was washed once with water, stained with ponçeau, destained with PBS and blocked for at least 1h with 5% skimmed milk powder in TBS-T. All incubations and washing steps were performed with gentle agitation at room temperature, except incubations over night, which were done at 4°C.
The blot was incubated with the primary antibody for at least 1 hour. Antibodies were

dissolved in 5% milk in an appropriate ratio. To remove the unbound primary antibodies, the blots were washed 3 times for 5 min with 1xTBS-T. Then the blot was incubated for at least an additional hour with a horseradish-peroxidase conjugated secondary antibody. Before detection, the blot was washed three times for 10 min with 1xTBS-T.
The protein bands were detected using the Western lightning Plus or Ultra ECL™ detection reagents (Perkin Elmer). The blots were either exposed on ECL films for 1-30min or analysed using the LSA-4000 (usual settings: increment, 10sec exposure time, standard exposure).
If necessary, the antibodies were removed using stripping buffer and new antibodies were applied.

Blotting Buffer:
3.03g Tris
14.4g glycine
200ml methanol
millipore water until volume equals 1l

TBS-T:
50 mM Tris
150 mM NaCl
0.05% Tween 20

Stripping buffer:
25mM glycine
1%SDS
adjusted to pH:2 with HCl

2.3.4 Gel staining methods

Colloidal Coomassie:

The gel was fixed for at least 1h in fixing solution. Then it was stained for at least 15min in colloidal coomassie stain. After staining, the gel was washed in bi-distilled water until the bands were visible.

Coomassie brilliant blue stock:
5g Coomassie
100ml millipore water

Colloidal coomassie dye stock (500ml):
50g ammoniumsulfat
6 ml phosphoric acid (85%)
10ml Coomassie brilliant blue stock

Colloidal coomassie dye:
100ml Colloidal coomassie dye stock
25ml methanol

2.3.5 TCA precipitation

1/5 volume of 100% TCA was added to the protein solution. The mixture was vortexed and incubated at -20°C overnight. The precipitate was spun down for 15min at room temperature. The pellet was washed by adding 3 volumes of the original sample volume of acetone, incubating the mixture for 10min at room temperature and then spinning down as before. The supernatant was removed and the pellet was dried for 10min and then either stored at -20°C or dissolved in 1x Laemmli buffer.

2.4 Co-Immunoprecipitations

2.4.1 Preparation of cell lysate for Immunoprecipitation

1-2·10^8 bloodstream cells were harvested at a density of approximately 1·10^6cells/ml. The cells were spun down at 2300g at 4°C for 10min and washed twice with ice-cold PBS. The cell pellets were snap-frozen in liquid nitrogen and stored at -80°C. The cell pellet was thawed on ice and dissolved in 300µl lysis buffer.
If needed, 0.5µg/µl RNAseA or 6µl RNAseIN (RNase Inhibitor, promega) were added to the lysis buffer.
Cell breakage was performed by passing the cells approximately 50 times through a 21 gauge needle. The lysate was spun at 13.000g for 5min at 4°C to remove the cell debris. Before the IP, the NaCl concentration of the cleared lysate was increased to 100-150mM.

2.4.2 Immunoprecipitation

30-50µl α-V5, α-myc (both from abgene) or GBP beads were washed three times with IP buffer. The cleared lysate was added to the beads and incubated for 2h on a rotary shaker at 4°C. The supernatant was removed by spinning the beads at 2000rpm at 4°C. Then the beads were washed three to five times with IP buffer. The beads were boiled with 10µl 4x Laemmli.
The samples were then analysed on a Western blot.

Lysis buffer:
10mM Tris-Cl
10mM NaCl
0.2% IGEPAL
2mM DTT
complete protease inhibitor (Roche)
pH=7.4

Wash buffer:
10mM Tris-Cl
100-150mM NaCl
0.1% IGEPAL
pH=7.4

2.5 Preparation of total RNA and Northern blotting

2.5.1 Preparation of total RNA

Total RNA was isolated from 2-10·10^7 cells. Bloodstream cells were harvested at a density of 0.5-1·10^6 cells/ml, procyclic cells at a density of 1-6·10^6cells/ml. The cells were pelleted by centrifugation (10min, 2000rpm) and the cell pellet was resuspended in 1ml pegGOLD TriFast™ (Peqlab, GmbH) and incubated for 5 min at room temperature. 0.2ml of chloroform was added to the samples. The tubes were shaken for 15 seconds, incubated at room temperature for 2-3minutes and centrifuged in a microfuge at 4°C for 10min at full speed. The mixture separates into a lower organic phase, an interphase and an upper aqueous phase, which contains the RNA. The aqueous phase is transferred into a fresh tube and the RNA is precipitated by adding 0.5ml isopropyl alcohol. The samples are incubated for 10min at room temperature and then centrifuged at 4°C for 20min at 12.000rpm. The supernatant was removed and the cell pellet washed with 75% ethanol. After the wash, the RNA was pelleted by centrifugation at 4°C for 5min at 10.000rpm. The pellet was air-dried for 5-10min and dissolved in 10µl sterile water.

2.5.2 Northern blotting of total RNA

Before loading, 10µg RNA was mixed with RNA loading mic (50% formamid, 6.5% formaldehyde, 1xMOPS buffer, total volume: 20-30µl) and denaturated by incubation at 65°C for 15min. After denaturation, 6x sample dye (15% ficoll) and 1µl ethidium bromide solution (1mg/ml) were added and the RNA was loaded on a 1% agarose/ formaldehyde gel (0,5M Formaldehyde, 1% Agarose, 1xMOPS). The gel was run at 15-20mV over night or for approximately 4 hours at 60mV using 1x MOPS as running buffer. The gel was washed 2 times with water (10min) and once with 10xSSC (15min).
The RNA was transferred to a Nytran N membrane using the Turbo blotter system and 10xSSC as blotting buffer. Blotting was either done over night or for at least 4 hours.
After blotting, the RNA was cross-linked to the membrane using a UV Stratalinker 1800.
The membrane was then washed for 15min in 5% acetic acid and stained with methylen blue stain (0.04% methylen blue, 0.5M sodium acetate, pH: 5.2). The blot was pre-hybridized for at least 2h at 65°C in a hybridization tube using approximately 10ml hybridization solution (5xSSC, 0,5% SDS, 1% Denhard's, 0.1mg/ml salmon sperm).
The ^{32}P-dCTP-labeled probe was made using the Prime-It ® RmT Random Primer Labeling Kit (Stratagene). The probe was purified using the Quiagen nucleotide removal kit and added to 10ml hybridization mix. Hybridization was performed at 65°C overnight on a spinning wheel. The blot was washed 1 time for 10min with 2x SSC+ 0.1%SDS and two times for 10-20min with 1xSSC+ 0.1%SDS at 65°C.
The blot was then exposed to a phosphoimager screen for at least one hour.
Non-radioactive detection (used only for VSG) was done using the DIG RNA labeling kit, as well as the DIG RNA detection kit from Roche, according to the manufacturers' instructions. The hybridization temperature was 60°C.

2.6 Tethering assay

(PhD Thesis, Dorothea Droll, modified).
To determine the effect of different ZC3H32 protein construct, two chloramphenicol acetyl transferase (CAT) reporter constructs were used. One contained the BoxB domain from phage lambda in its 3'UTR, the other one did not. The BoxB is bound by the λN peptide, which was fused to the myc-tagged ZC3H32 protein constructs (see 2.14 for plasmids). Thus, the λN-ZC3H32-myc construct was tethered to the reporter RNA.
CAT was chosen as reporter as the CAT transcript can easily be detected on Northern Blot and the protein expression can be assayed with an enzymatic reaction in the CAT assay.
CAT transfers an acetyl group from radioactively labeled ^{14}C butryl CoA to chloramphenicol. After uptake of an acetyl group, chloramphenicol will become water insoluble and move from the aqueous phase of the reaction solution to the upper non-aqueous phase of the scintillation solution (Econofluor-2, Perkin Elmer). With time, more and more acetyl-chloramphenicol (and therefore radioactive ^{14}C) will move to the upper phase, which will be measured by the scintillation counter.

2.6.1 Sample preparation and determination of protein concentration

The expression of the λN-ZC3H32-myc construct was induced 24hours prior to harvesting by adding tetracycline.
For one sample ≥10^7 cells were taken and spun down at 2,000 rpm for 10 minutes.
Pellets were transferred to a microfuge tube, centrifuged at 3,000 rpm for 2 minutes and washed using cold 1x PBS. The cell pellet can be frozen in liquid nitrogen and stored at -80°C. For lysis 300 µl of CAT assay buffer was added followed by freeze-thawing three times in liquid nitrogen. After centrifugation at 13,000 rpm at 4°C for 3 minutes, the supernatant was transferred to a new tube and can be stored at - 80°C until use.
The Bradford assay is used to determine the total protein concentration of a sample. The assay is based on the proportional binding of the Coomassie Blue dye to proteins. Coomassie bound to protein has an absorption maximum at 595 nm. The higher the protein concentration, the higher the absorption at 595 nm will be.
Bradford: 0, 5, 10, 15, 20µg of BSA (0.5 µg/µl stock) in 800µl for standard curve 50 µl of each protein sample +750µl water all + 200µl Bradford reagent (Biorad), mix, incubate ca. 5 min and measure absorption at 595nm in photometer.

2.6.2 The CAT Assay

For this assay, equal amounts of protein were taken for each sample and scaled up to 50µl using 100 mM Tris-HCl, pH 7.8. After addition of 200 µl 100 mM Tris-HCl, pH7.8, 2 µl chloramphenicol (40 mg/ml), 10 µl ^{14}C-butryl CoA (box 21C in -80°C) and finally 4 ml

scintillation cocktail (in fume hood, Econofluor-2), the samples were measured in a scintillation counter (Beckman LS6000IC) using program #7, measuring ^{14}C. Samples were measured at appropriate time intervals, every 12 to 16 minutes or as required. The increase of ^{14}C signal in the scintillation fluid is proportional to the amount of enzyme present in the sample. Therefore after blotting the data the slope in the linear range (before saturation) can be compared between the different samples and the relative CAT protein amount calculated.

2.7 CLIP (Crosslinking and Immuoprecipitation)

Protocol from Bhaskar Anand Jha, (Jha, Fadda et al. 2014) a combination of the PAR-CLIP (Hafner, Landthaler et al. 2010, Hafner, Landthaler et al. 2010) and the CLIP protocol (Ule, Jensen et al. 2005) with slight modifications.

2.7.1 Crosslinking

The cells were spun down at room temperature at 2000rpm for 10min, resuspended in 25ml medium and put on big petri disk. The cells were crosslinked twice, on a metal plate (for reflection) with a Stratalinker 2400 (Strategene, Germany) at 4000 x 100 microjoule/cm^2, spun down at 3000rpm at 4°C, washed twice with PBS, frozen in liquid nitrogen and stored at -80°C.

Cells lines used:
bs 1313 514, density appr. $1 \cdot 10^6$ cells/ml, 250-300ml “WT”
bs 1313 2332 2487 2488, density appr. $1 \cdot 10^6$ cells/ml, 250-300ml “Z32”
pc 1313 myc-UBP1 from B. Jha as positive control “UBP1”

2.7.2. Cell lysis

The cell pellets were dissolved in 250µl lysis buffer and incubated on ice for 10min. The cell lysis was checked under the microscope.
The lysate was cleared twice in order to remove the cell debris for 5min at 13000rpm.

2.7.3. RNAse T1 treatment

RNAse T1 was added to the sample (2U/µl) and the sample was incubated 22°C for 10min, shaking at 800rpm and then kept on ice for 5min.

2.7.4 Immunprecipitation

75 or 100µl myc beads were used per IP (75µl for 250ml cells, 100µl for 300ml).
The beads were washed 5x with PBS (1000rpm) and once with IP wash buffer. The lysate was added and the IP was rotated for 1-2h at 4°C (program F5, 10rpm)

Then the supernatant was removed and the IP was washed 3x with IP Wash buffer and 2x with High Salt Wash buffer (1000rpm, 4°C)

2.7.5 Phosphatase treatment

The beads were resuspended in 1 bead volume of 2xNEB3 (1:5 dilution of original NEB3) supplied with 2µl (80U) RNAsIN. Calf intestinal phosphatase was added to a final conc of 0.5U/µl (conc. stock solution: 10U/µl). The beads were incubated for 10min at 37°C, shaking at 800rpm and then washed twice with 1ml phosphatase wash buffer.

2.7.6 Phosphonucelotidekinase (PNK) treatment

The beads were washed twice with cold PNK buffer.
The following steps were done in the isotope lab with appropriate shielding.
1 bead volume of PNK buffer was added to beads, together with 1/10 bead volume PNK and 3.3-5µl yATP (33-50µCi). The reaction was incubated for 20min at 37°C and then washed three times with PNK buffer.
The beads were resuspended in 20µl 4x NuPAGE LSD sample buffer (Invitrogen), with 500mM DTT and boiled for 5min at 95°C. This elution step was done twice.
The eluates were loaded on a on a 4-12% NuPAGE Bis-Tris gel together with 5µl prestained protein marker.
For the first CLIP experiment, the two elutions were loaded in separate wells, for the following two experiments the two elutions (of each bead sample) were loaded in one well.
The gel was run at 200V for 50min in 1x NuPAGE MOPS SDS running buffer (Invitrogen).
Then the gel was wrapped in saran wrap and exposed to a phosphoimager screen for at least one hour.

2.7.7 Buffers

Lysis buffer

HEPES pH 7.5	50mM
KCl	150mM
EDTA	2mM
NaF	1mM
NP-40	0.50%
DTT	0.5mM
RNASIN	4000U
compl. Inhibitor, Roche	0.5 tablet/ml

IP wash buffer

HEPES pH 7.5	50mM
KCl	150mM
NP-40	0.05%
DTT	0.5mM
RNASIN	1600U
compl. Inhibitor, Roche	1 tablet/10ml

High salt wash buffer

HEPES pH 7.5	50mM
KCl	500mM
NP-40	0.05%
DTT	0.5mM
RNASIN	1600U
compl. Inhibitor, Roche	1 tablet/10ml

Phosphatase wash buffer

Tris HCl pH 7.5	50mM
EGTA	20mM
NP40	0.05%
RNAsIN	1600U

polynucelotide kinase buffer

Tris HCl pH 7.5	50mM
NaCl	50mM
MgCl2	10mM
RNAsIN	1600U

2.8 Web resources

Kinetoplastid databases with expression data and user comments: TriTrypDB http://tritrypdb.org GeneDB; www.genedb.org
NCBI databases, e.g. BLAST NCBI
http://blast.ncbi.nlm.nih.gov/Blast.cgi

2.9 Polyribosome isolation

2.9.1 Cycloheximide treatment

Bloodstream cells:
Bloodstream cells (d=$1 \cdot 10^6$ cells/ml) cells were given into centrifuge flasks and cycloheximide was added to a concentration of 25 μg/ml. The cells were incubated for 1min at room temperature and then chilled in a dry ice ethanol bath. The cells were then spun down (4°C, 2,300g, 20min), transferred to Eppendorf tubes and spun down again at 2,300g for 2min. The pellet was either used immediately or resuspended in freezing buffer, wrapped in cold paper and kept at -70°C.

Procyclic cells:
Procyclic cells (d=$4 \cdot 10^6$ cells/ml) were spun down (RT, 2,300rpm, 10min) and resuspended in 20-50ml of medium (app. 1/20 of the former volume). Cycloheximide was added to a concentration of 100 μg/ml, the cells were incubated for 5min at room temperature, chilled on ice and spun down (4°C, 2,300rpm, 8min). The cell pellet was either used immediately or resuspended in freezing buffer, wrapped in cold paper and kept at -70°C.

Before preparation of cell lysates, the pellets were thawed on ice and washed twice (4°C, 2min, 3000rpm) with wash buffer.
Then the cells were lysed, either by the method described in 2.9.2 (total cell lysate) or 2.9.3 (separation of cytosolic and membrane-bound fractions). The used buffer was taken from (Hanas, Linden et al. 1975, Brecht and Parsons 1998)

2.9.2 Preparation of total cell lysate

Cell lysates were prepared on ice.
The cell pellet was resuspended in lysis buffer containing 0,2% NP-40 and lysed using a gauge needle at 4°C (put at least 50 times through the gauge needle). The lysate was cleared by centrifugation (4°C, 4,500rpm, 5min) and given on the sucrose gradient.

2.9.3 Separation of free and membrane-associated fractions

Cell lysates were prepared at 4°C.

Acid ethanol-washed glass beads (300μg/ml lysis buffer) were washed twice with wash buffer. The cell pellet was resuspended in lysis buffer **(without NP-40/IGEPAL)** and added to the beads. Cell lysis was accomplished by vortexing in intervals of 30sec following 10 sec chilling on ice (total vortexing time: 20min).
Lysis was checked under a glass slide. The lysate was cleared twice by centrifugation (4°C, 4,500rpm, 5min). Then the membrane fraction was separated by ultracentrifugation (4°C, 30000g, 20min, Rotor: S45A). The supernatant ("free" fraction) was taken and the pellet ("membrane-bound" fraction) resuspended in lysis buffer containing 0,2% Triton-X (detergent to lyse the membranes). Triton-X (use 10% Triton-X stock solution) was added to a final concentration of 0,2% to the supernatant ("free" fraction).
The "free" fraction was given on a sucrose gradient. The membranes in the membrane-bound fraction were dissolved by pulling the pellet through a gauge needle followed by short vortexing. The membrane fraction was cleared by ultracentrifugation (4°C, 30000g, 20min, Rotor: S45A). The supernatant was given on a sucrose gradient.

2.9.4 Preparation of sucrose gradients

The lighter sucrose fraction (15%) was underlayed with the heavier sucrose solution (50-55%) and rotated in the gradient maker (Gradient Master, Biocomp) for 2min at an angle of 45°.
Alternatively, the gradients were sealed with parafilm and turned horizontally for two hours.
Gradients were prepared in Beckmann polyallomer tubes with a volume of 14x89mm (12ml gradient, 1ml lysate) or 11x60cm (4,8ml gradient, 0,2 ml lysate).
15%-50% sucrose gradients were made for optimal resolution of fractions. 15%-55% sucrose gradients were used for a higher concentrated polyribosome fractions.
Gradients were frozen at -70°C and thawed approximately 1h prior to use at 4°C.

2.9.5 Sucrose gradient centrifugation and separation of fractions

Sucrose gradient centrifugation was done at 4°C, either at 36000rpm for 2,5h or at 40,000rpm for 2h. For 14x89mm tubes the SW41 rotor, for 11x60mm tubes the SW60 rotor was used.
The fractions were collected and the OD_{260} profile measured using an ISCO 160 gradient former.
Fractions can be collected every minute (volume app. 1,2ml), every 30 sec (volume app. 0,6ml), every 22 seconds (for Western blots, resulted in appr. 10 fractions with a volume of appr. 0.4ml) or every 15 seconds (for Northern blots, appr. 14 fractions, volume appr. 0.3ml).

2.9.6 Concentration (for mass spectrometry samples)

The samples were diluted 1:4 with gradient buffer without sucrose and concentrated using Centricon tubes (Molecular cut-off: 100kDa). After the desired volume was reached the samples were precipitated with TCA.
For direct TCA precipitation, the samples were also diluted 1:4 with gradient buffer.

2.9.7 Sample preparation for Western and Northern blotting

For a Western blot, 300-400ml bloodstream cells (density approximately $1 \cdot 10^6$) were used for total polyribosomes and the double/triple amount for separated free and membrane bound polyribosomes. 5-15 times less was loaded in the first three fractions, as these contained a lot of proteins. For the rest of the fractions, 30-50µl were loaded on the gel. In order to prevent the samples from solidification (due to the high sucrose content), the samples were kept warm during the loading of the Western blot.
For RNA isolation, the samples were mixed with 3 parts peqGOLD TriFastFL and processed according to the manufacturer's description.

2.9.8 Solutions

Stock solutions:

2xPolyribosome buffer:
20mM Tris (pH: 7,4-7,5)
20mM $MgCl_2$
600mM KCl

200mg/ml Heparin (dissolved in water, stored at -20°C)

1M DTT (dissolved in water, stored at -20°C)

5mg/ml Leupeptin (dissolved in water, stored at -20°C)

100mg/ml Cycloheximide (dissolved in ethanol, stored at -20°C)

Buffers:

Freezing buffer (1ml):
1x Polyribosome buffer
200mM Sucrose (0,0684g)
10% Glycerol (100µl)
100 µg Cycloheximide (1 µl)

Lysis buffer:
1x Polyribosome buffer (10mM Tris (pH: 7,4-7,5), 10mM $MgCl_2$, 300mM KCl)
200mM Sucrose
1 tablet/5ml complete protease inhibitor (Roche, without EDTA)
2mM/ml DTT
0,4mg/ml Heparin
10μg/ml Leupeptine
100μg/ml Cycloheximide
for total lysate only: 0,2% NP-40
ddH_2O until final volume

Wash buffer (5ml):
2,5 ml 2x Polyribosome buffer
0,342g sucrose (final conc.: 200mM)
ddH_2O until final volume

Gradient buffer:
0%, 15%, 50% or 55% sucrose
0,5 volumes 2x Polyribosome buffer
2mM/ml DTT (1:500)
400μg/ml heparin (1:500)
10μg/ml leupeptin (1:500)
ddH_2O until final volume

10% Triton-X
0,5 volume 2x Polyribosome buffer
0,2 volumes 1M sucrose
0,2 volumes ddH_2O
0,1 volume Triton-X

2.10 Polyribosome isolation followed by immunoprecipitation

2.10.1 VSG222 pull-down

VSG222 clonal selection

In order to get a monoclonal population of VSG222 expressing cells, bs1313 cells were diluted to a concentration of 12.5 cells/ml and plated out on a 96well plate. 40µl were given in each well, thus, statistically there were 0.5 cells/well. The cells were left to grow for ten days, then protein samples were collected.
VSG222 expression was tested by Western blotting, the cell line with the strongest VSG222 expression (VSG222 WT11) was used for the following experiment.

Antibody purification (protocol from AG Melchior, ZMBH)

1ml VSG222 polyclonal antibody was mixed with 2ml PBS and supplemented with EDTA-free Protease Inhibitor (Roche, 1 tablet in 3.5 ml PBS). The solution was mixed with 2ml ProteinA beads, which were washed with 50ml PBS. The beads and the antibody solution were incubated over night rotating at 4°C.
The following day, the column was washed with 60ml PBS with 500mM NaCl. The antibody was eluted 15x with 1ml elution buffer (200mM acetic acid, 500mM NaCl, pH=2.7, adjusted with NaOH). Each eluate was mixed with 200µl 1M Tris-Cl (pH=11) in order to neutralize the solution. Samples of the eluates were given on a dot blot. The dot blot was stained by ponceau in order to check whether the eluates still contained protein. At the 15^{th} elution, no protein could be detected, thus, the elution was stopped.
The eluates were concentrated using four centricon columns (10kDa cut-off). After concentration, in order to change the buffer, sterile PBS (20ml) was added to the columns. The samples were concentrated until the volume was 1ml. In order to store the antibody, it was mixed 1:2 with glycerol. Thus, 1µl of the purified antibody corresponds to 0.5µl of the original antibody.

Polyribosome isolation and immunoprecipitation

Polyribosomes were isolated as described in 2.9. Approximately $8 \cdot 10^8$ bs1313 cells (selected for VSG222 expression) were used. The polyribosome fractions were taken and split into 5 parts. 300µl were used as Input sample, 600µl were used for each IP ($1.7 \cdot 10^8$ cells each).
Two IPs were done with 100µl ProteinA beads mixed with 10µl purified VSG222 antibody. One was incubated (rotating at 4°C) for 1h, the other one for 30min. The other two IPs were done with 200µl Protein A beads, mixed with 10µl and 20µl purified antibody. Both of these IPs were incubated for 1h. After the incubation, the supernatant was removed and 300µl (half of the supernatant, corresponds to $0.85 \cdot 10^8$ cells) were

taken as RNA sample. In order to elute the RNA, the pellets were mixed with 750µl Trifast.

2.10.2 VSG118 pull-down

Antibody purification

75µl VSG118 antibody was purified as described before (2.10.1). In order to determine how much of the original antibody corresponds to the purified antibody, a dot blot was made, probed with anti-rabbit and the signal was quantified. The quantification showed that 2.5µl of the purified antibody corresponded to 1µl unpurified antibody.

Polyribosome isolation and immunoprecipitation

$6 \cdot 10^8$ bloodstream wild type cells expressing VSG118 were used for this experiment.
Polyribosomes were isolated was described in 2.9. 600µl polyribosomes were used for each IP. 300µl of the polyribosomes were used as polyribosome sample for the Northern blot, 30µl were used as protein sample.
3 aliquots of 100µl ProteinA beads were mixed with 2.5µl, 5µl and 12.5µl purified VSG118 antibody (corresponding to 1µl, 2µl and 5µl unpurified antibody). To each IP, 8µl VRCs, 12µl RNAsIN (promega) and 0.6µl cycloheximide were added. The IPS were rotated for 2 hours at 4°C and then washed 1x with Wash buffer and 2x with polyribosome buffer. 300µl of the flow-through was taken as RNA and 30µl as protein sample.
1/20 of the pellet was taken as a protein sample, the rest mixed with Trifast in order to elute the RNA.
The protein samples were analysed by Western, the RNA samples by Northern blotting.

2.11 Peptide antibody against VSG118

The following sequence was chosen for the production of a peptide antibody against VSG118 (by the manufacturers of the antibody):

CKMS KELK ATAM RAAN DAKL KITE

The protein sequence is 24 amino acids long and starts at position 47 of the VSG118 protein.
The antibodies were raised in two rabbits, with an immunization of 90days, by Pierce custom antibodies (Thermo scientific)

2.12 VSG118 Immunoprecipitation with cells *in vivo* labeled with ^{35}S methionine

2.12.1 Preparation of protein-A beads

1st experiment: six aliquots of 100µl Protein A beads were incubated with 1µl, 5µl or 10µl VSG118 antibody (received from J. Banks) or the peptide antibody (see 2.11). The beads were incubated with the antibody in 1xPolyribosome wash buffer (see 2.10) overnight, rotating at 4°C.
Prior to the immunoprecipitation, the beads were washed 3x with 500µl wash buffer.
2nd experiment: five aliquots of ProteinA beads were used. 1µl, 4µl and 8µl VSG118 antibody were mixed with 200µl, 200 µl and 300µl ProteinA beads. 10µl and 20µl VSG118 peptide antibody were mixed with 300µl ProteinA beads each. The beads and antibodies were incubated with 500µl PSB wash buffer for 4 hours at room temperature and washed 4x with 1ml wash buffer prior to the experiment.

2.12.2 *In vivo* labeling of cells

All centrifugations were done at room temperature. All steps after the adding of ^{35}S methionine were performed with appropriate shielding.
1st experiment: $3 \cdot 10^7$ bs1313 3850 cells were spun down at 2500rpm, transferred to a 1.5ml Eppendorf tube and washed twice with 1xPBS. Then the cells were resuspended in 400µl labeling medium. 6µl ^{35}S methionine solution, with an activity of about 60µCi, was added. The cells were incubated for 1h at 37°C. Then the cells were pelleted and washed three times with 1x polyribosome wash buffer (see 2.9.9).
2nd experiment: $2.5 \cdot 10^7$ VSG118 expression cells were used. The labeling was done like in the first experiment, using 60µCi of ^{35}S methionine, despite the lower amount of cells.

2.12.3 Immunoprecipitation and gel electrophoresis

1st experiment: The cell pellet was dissolved in 500µl lysis buffer and incubated on ice for 30min, with occasional vortexing. Then the cell debris was spun down at room temperature (5 min, 5.000rpm). A 10µl sample was taken (input) and 80µl of the lysate was given on each of the six bead aliquots.

The IPs were rotated for 2 hours at 4°C. Then the beads were spun down at 2000rpm for 2min at room temperature and the supernatant was removed. The beads were washed once with 1ml wash buffer and then mixed with 15µl 4x Laemmli.
A 15µl sample from the supernatant was also mixed with 4x Laemmli. The samples were kept at -20°C and separated on a 12% PAA gel the next day.
2nd experiment: The cells were lysed in 200µl lysis buffer for 30min on ice with occasional vortexing. The lysate was cleared for 10min at 10,000rpm, a 5µl input sample was taken. For each IP, 40µl of the lysate was mixed with 60µl 60% sucrose (in order to mimic the sucrose concentration in the polyribosome samples) and mixed with one bead aliquot.
The IPs were rotated for 1 hour at 4°C. The beads were spun down and a 20µl supernatant sample was taken and mixed with 7µl 4x Laemmli. The pellets were washed with 500µl wash buffer and mixed with 4x Laemmli. The samples were kept at 4°C and separated on a 12% PAA gel the next day.

The PAA gels were fixed for 1 hour in a mix of 60% water, 30% methanol and 10% acetic acid and then incubated with enhance solution (Perkin Elmer) for another hour. The gels were washed with water and dried for 3 hours at 65°C using a vacuum dryer. Then the gels were exposed to an x-ray film for at least 3 hours.

2.13 Indirect Immunofluorescence

The immunofluorescence was performed according to the EMBO/TDR protocol. The anti-myc and the anti-V5 antibody from abgene (mouse, 1:500) were used.
The Olympus CellR microscope was used for image acquisition.

2.14 Plasmids and Primers

2.14.1 Plasmids

pHd number	description	provided by	Result section
1781	pHD1744 +PUF3 ORF (TAP-tag-HYG)	Dr. S. Archer	3.1.4
1783	pHD1744 +PUF6 ORF (TAP-tag-HYG)	Dr. S. Archer	3.1.4
2161	Bla V5 + RBP29 ORF + UTR		3.1.4
2162	Bla V5 + ZC3H29 ORF+ UTR		3.1.4
2332	pHd1700 + ZC3H32 ORF		3.3
2343	Bla-V5 Z32 ORF +UTR		3.3
2375	P2T7TABlue ZC3H32		3.3.3
2437	pHd2412 + ZC3H32 ORF from AA 83-655		3.3.6
2438	pHd2412 + ZC3H32 ORF from AA 211-655		3.3.6
2439	pHd2412 + ZC3H32 ORF from AA 1-158		3.3.6
2482	pHd2412 + ZC3H32 ORF AA 1-253		3.3.6
2483	pHd2412 + ZC3H32 ORF AA 1-274		3.3.6
2484	pHd2412 + ZC3H32 ORF AA 1-362		3.3.6
2485	pHd2412 + ZC3H32 ORF AA 274-655		3.3.6
2486	pHd2412 + ZC3H32 ORF AA 362-655		3.3.6
2487	ZC3H32 KO - in 1748 (BLA resistance)		3.3.4
2488	ZC3H32 KO - in 1747 (PURO resistance)		3.3.4
2527	Bla-v5+ Not2 ORF + UTR		3.3.9
2573	pHd1701 + Tb927.7.2780		3.3.10
2575	phd1701 + DRBD2		3.3.10
2579	pHd1912 + ZC3H28 fragment (N-term. YFP-tag)		3.3.10
2580	pHd2412 + ZC3H32 AA 362-538		3.3.6
2581	pHd2412 + ZC3H32 AA 1-253		3.3.6
2582	pHd2412 + ZC3H32 AA 1-145		3.3.6
2594	pHd2412 + ZC3H32 AA 146-362		3.3.6
2595	pHd2412 + ZC3H32 AA 146-538		3.3.6
1995	pHD1912+MKT1 fragment (N-term. YFP-tag)	Dr. D. Droll	3.3.2
2413	pHd2412 + ZC3H32 ORF		3.3.6
2606	integrates in front of *VSG121* in the VSG121 (MITat1.6) expression site. After integration you get the following: ESAG1 -VSG118 ORF with VSG221 intergenic regions - blasticidin resistance cassette with tubulin intergenic regions –	Dr. A. Schwede, from Mark Carrington's lab	3.2.2

	VSG121 The vector is linearised for transfection with KpnI and SacI		
2605	p2676 (Kelly, Reed et al. 2007) Puro resistance replaced with Bla stuffer + tag cut out, VSG222 inserted		3.2.1
2607	P2T7 VSG118, for non radioactive probe		3.2.2

Table 3: Plasmids used for the work described in this Thesis.

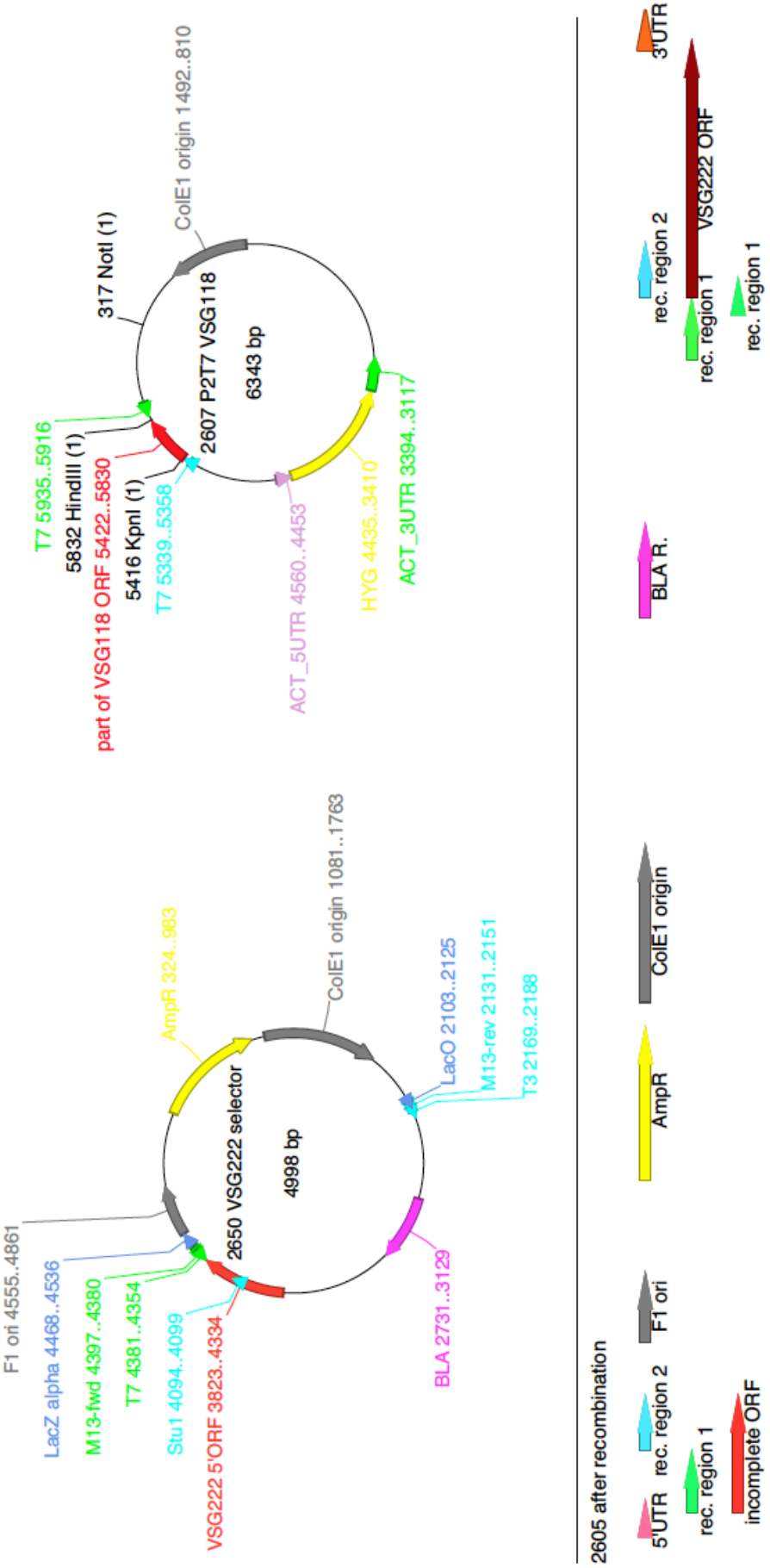
317 NotI (1)
ColE1 origin 1492..810
2607 P2T7 VSG118
6343 bp
T7 5935..5916
5832 HindIII (1)
part of VSG118 ORF 5422..5830
5416 KpnI (1)
T7 5339..5358
ACT_5UTR 4560..4453
HYG 4435..3410
ACT_3UTR 3394..3117
2650 VSG222 selector
4998 bp
AmpR 324..983
ColE1 origin 1081..1763
LacO 2103..2125
M13-rev 2131..2151
T3 2169..2188
BLA 2731..3129
F1 ori 4555..4861
LacZ alpha 4468..4536
M13-fwd 4397..4380
T7 4381..4354
Stu1 4094..4099
VSG222 5'ORF 3823..4334
3'UTR
rec. region 2
VSG222 ORF
rec. region 1
rec. region 1
BLA R.
ColE1 origin
AmpR
F1 ori
2605 after recombination
5'UTR
rec. region 2
rec. region 1
incomplete ORF

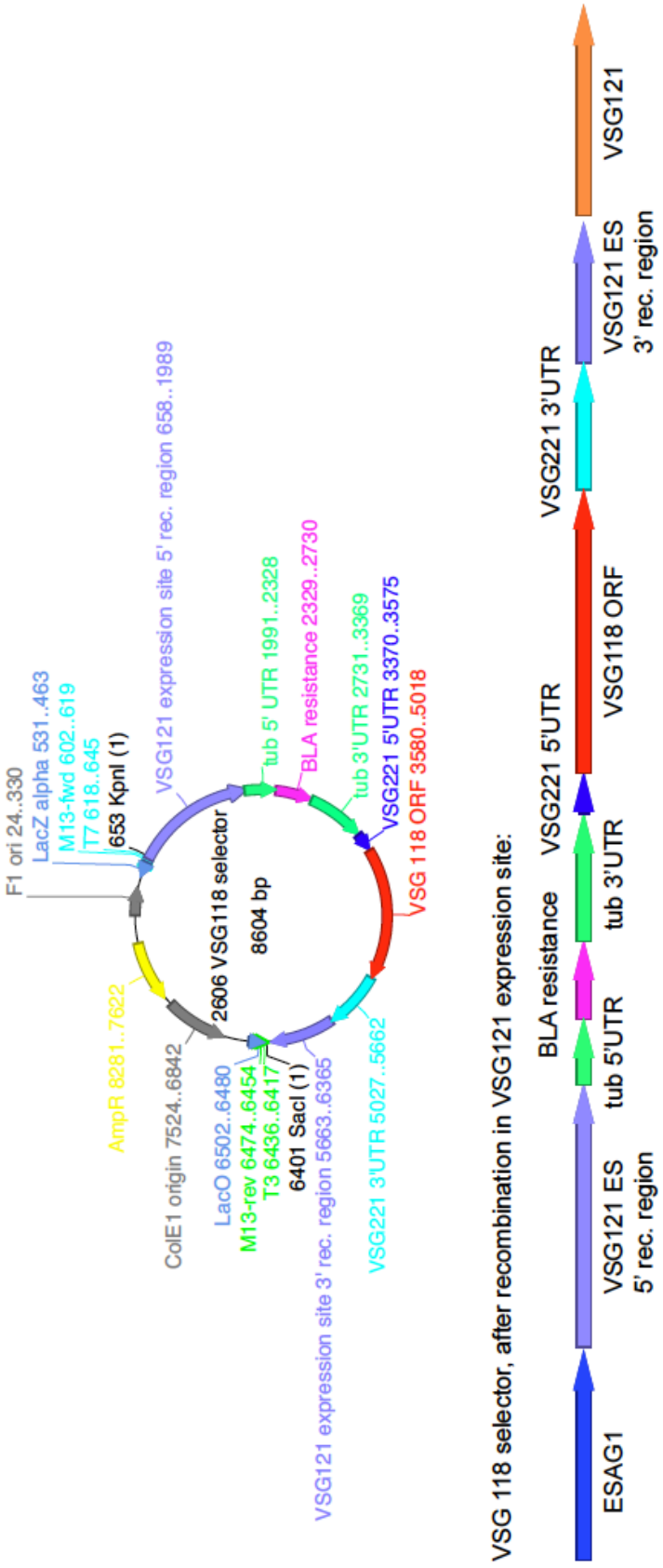

Fig. 9: Maps of plasmids used for VSG project (Result section 3.2)

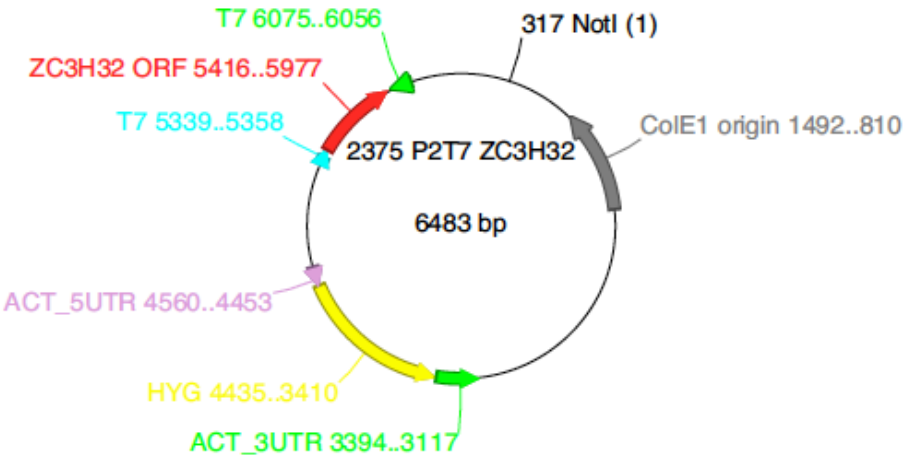
T7 6075..6056
317 NotI (1)
ZC3H32 ORF 5416..5977
T7 5339..5358
ColE1 origin 1492..810
2375 P2T7 ZC3H32
6483 bp
ACT_5UTR 4560..4453
HYG 4435..3410
ACT_3UTR 3394..3117

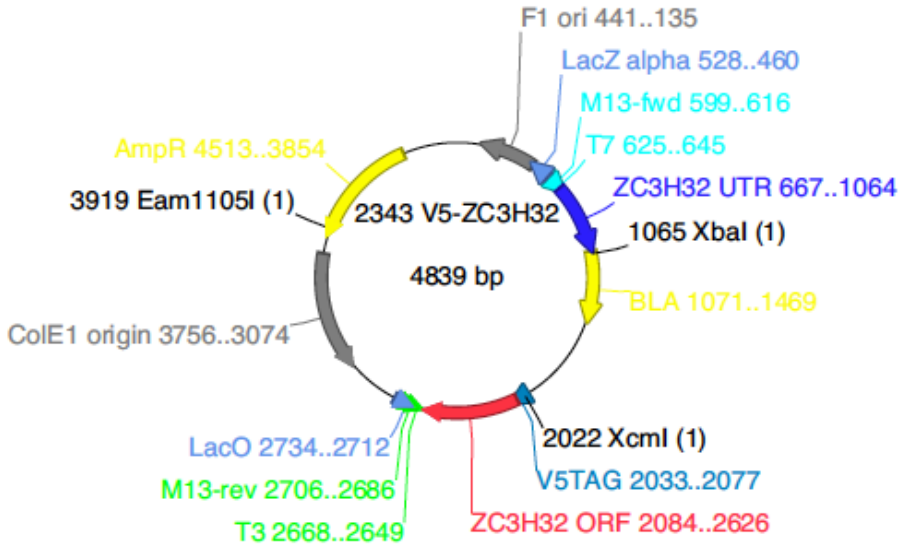
F1 ori 441..135
LacZ alpha 528..460
M13-fwd 599..616
AmpR 4513..3854
T7 625..645
ZC3H32 UTR 667..1064
3919 Eam1105I (1)
2343 V5-ZC3H32
1065 XbaI (1)
4839 bp
BLA 1071..1469
ColE1 origin 3756..3074
LacO 2734..2712
2022 XcmI (1)
M13-rev 2706..2686
V5TAG 2033..2077
T3 2668..2649
ZC3H32 ORF 2084..2626

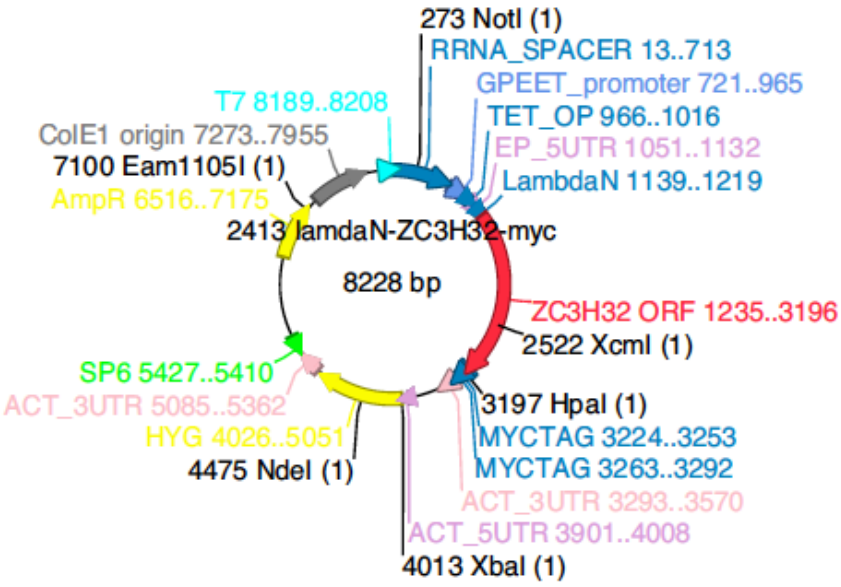
273 NotI (1)
RRNA_SPACER 13..713
GPEET_promoter 721..965
T7 8189..8208
TET_OP 966..1016
ColE1 origin 7273..7955
EP_5UTR 1051..1132
7100 Eam1105I (1)
LambdaN 1139..1219
AmpR 6516..7175
2413 lamdaN-ZC3H32-myc
8228 bp
ZC3H32 ORF 1235..3196
2522 XcmI (1)
SP6 5427..5410
3197 HpaI (1)
ACT_3UTR 5085..5362
MYCTAG 3224..3253
HYG 4026..5051
MYCTAG 3263..3292
4475 NdeI (1)
ACT_3UTR 3293..3570
ACT_5UTR 3901..4008
4013 XbaI (1)

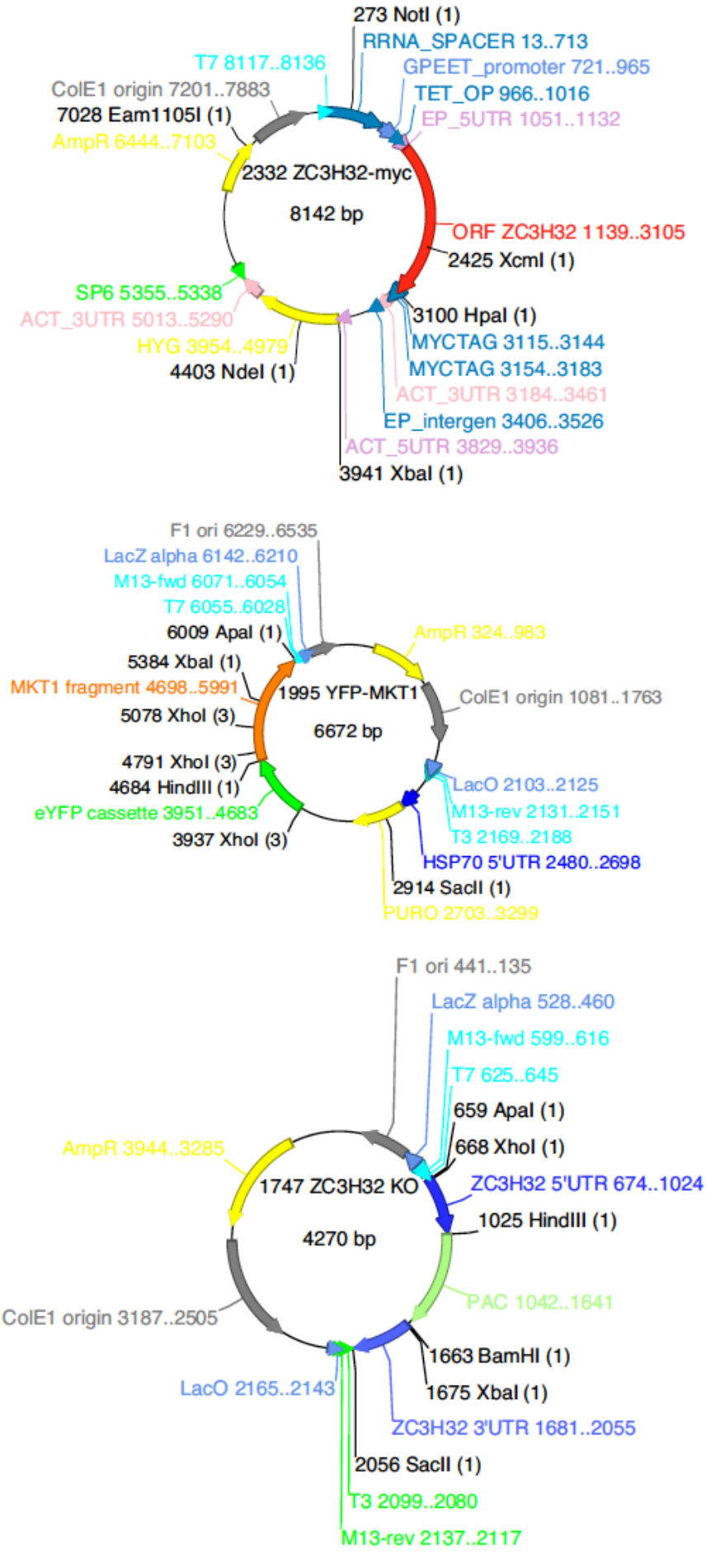
273 NotI (1)
RRNA_SPACER 13..713
GPEET_promoter 721..965
TET_OP 966..1016
EP_5UTR 1051..1132
T7 8117..8136
ColE1 origin 7201..7883
7028 Eam1105I (1)
AmpR 6444..7103
2332 ZC3H32-myc
8142 bp
ORF ZC3H32 1139..3105
2425 XcmI (1)
SP6 5355..5338
ACT_3UTR 5013..5290
HYG 3954..4979
4403 NdeI (1)
3100 HpaI (1)
MYCTAG 3115..3144
MYCTAG 3154..3183
ACT_3UTR 3184..3461
EP_intergen 3406..3526
ACT_5UTR 3829..3936
3941 XbaI (1)
F1 ori 6229..6535
LacZ alpha 6142..6210
M13-fwd 6071..6054
T7 6055..6028
6009 ApaI (1)
AmpR 324..983
5384 XbaI (1)
MKT1 fragment 4698..5991
1995 YFP-MKT1
6672 bp
ColE1 origin 1081..1763
5078 XhoI (3)
4791 XhoI (3)
4684 HindIII (1)
eYFP cassette 3951..4683
3937 XhoI (3)
LacO 2103..2125
M13-rev 2131..2151
T3 2169..2188
HSP70 5'UTR 2480..2698
2914 SacII (1)
PURO 2703..3299
F1 ori 441..135
LacZ alpha 528..460
M13-fwd 599..616
T7 625..645
659 ApaI (1)
668 XhoI (1)
AmpR 3944..3285
1747 ZC3H32 KO
4270 bp
ZC3H32 5'UTR 674..1024
1025 HindIII (1)
PAC 1042..1641
ColE1 origin 3187..2505
1663 BamHI (1)
1675 XbaI (1)
LacO 2165..2143
ZC3H32 3'UTR 1681..2055
2056 SacII (1)
T3 2099..2080
M13-rev 2137..2117

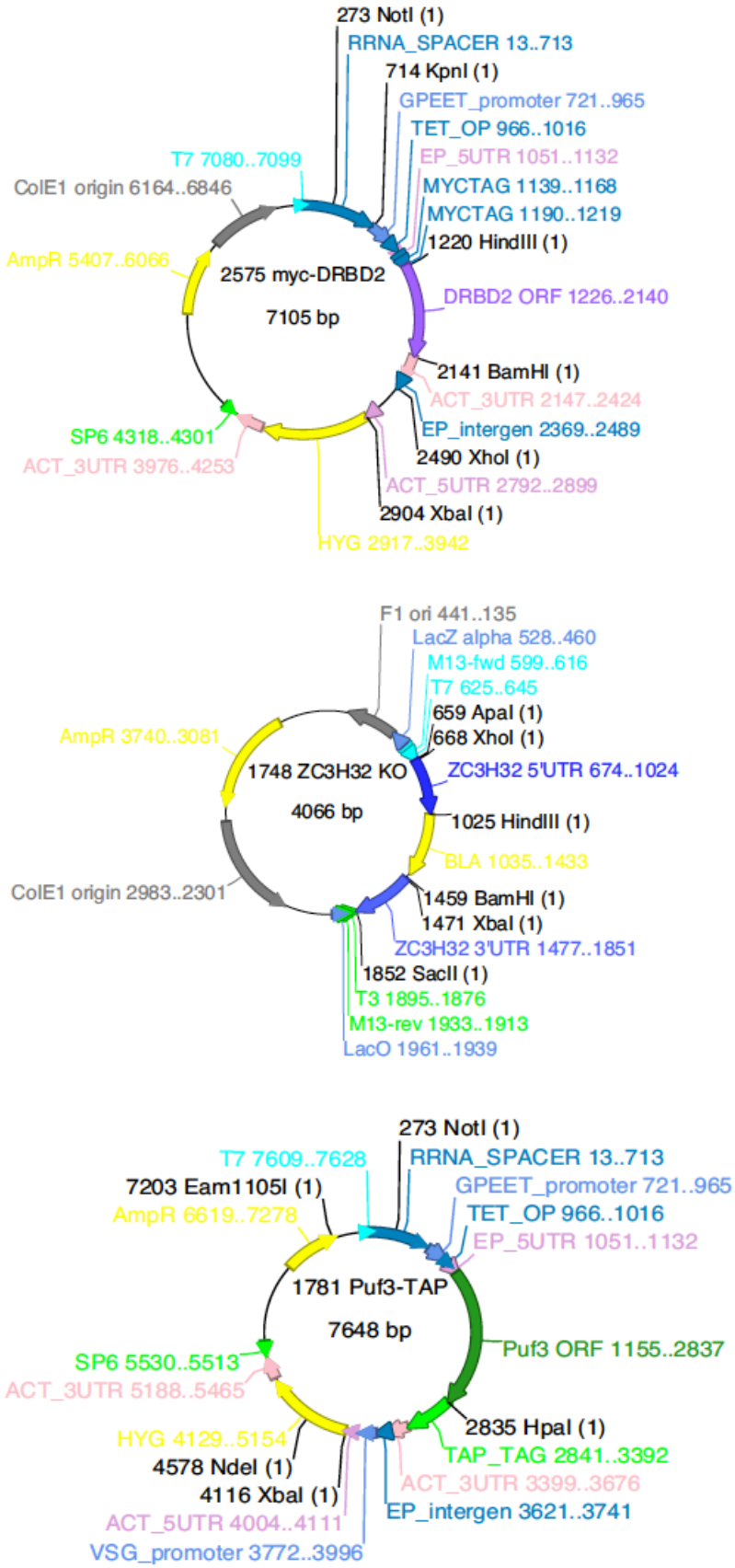

Fig. 10: Vector maps of plasmids used for the ZC3H32 project (Result section 3.3), as well as for tagging proteins found in the mass spectrometry results (Result section 3.1)

2.14.2 Primer

CZ number	name	sequence	used for pHD
3819	rvORFZC3H29Apa1	ATAgggcccGATAGCAACCGTGGAATA	2162
3820	fwORFZC3H29Xho1	CAGctcgagATGACACAGGTCATCACG	2162
3821	fwUTRZC3H29Sac2	CACccgcggATGTATTTGTTAAACGAG	2162
3822	rvUTRZC3H29Xba1	CACtctagaGTTAATGGGCAATAACTA	2162
3823	fwORFrbp29Xho1	GAGctcgagATGGCGCATGTTGGACAG	2161
3824	rvORFrbp29Apa1	ATAgggcccTGCTCGCAGTATTGCTGG	2161
3825	fwUTRrbp29Sac2	CACccgcggGAGCCTAGAAAATAGATA	2161
3826	rvUTRrbp29Xba1	ATAtctagaCCGTTCGGCGCTTGCCTT	2161
4350	VSG118hind3revshort	ATCaagcttCTAGTTCTGTGTGTGTT	2607
4414	vsg118wosskpn1fw	TatggtaccACAAACAATCACGGC	2607
3854	VSG rev 2nd Apa1	AGCgggcccTCTGATTTGTTGTATCCGAAC	2606
3855	VSG fw 2nd Xho1	atactcgagATGCAGATGCGGCTGTGG	2606
4087	ZC3H32Hpa1rvb	TATgttaacTCTCTGTTTCTGCGTGGC	2332 2413 2437 2438 2485 2486
4501	ZC3H32Hind3fw	GCGaagcttATGTCTGGCACTAATCAC	2332
4678	Z32UTRRvXbaI	GCGtctagaGATGTTTTCCTTCCCCTT	2343
4679	Z32UTRfwSac2	CATccgcggACTCACTCATACATCTAA	2343
4681	Z32ORFrvApa1	ATAgggcccAAGCCAGAATATCATCT	2343
4682	Z32ORFfwXho1	CATctcgagATGTCTGGCACTAATCAC	2343
4747	ZC3H32 RNAi fw	GAAGAAGAGGACGCTGATGG	2375
4748	ZC3H32 primer rv	ACTGCGAAGGGTTGCTAAGA	2375
4978	Z32.83.fw.asc1	TATGGCGCGCCtaTCTTTTGAGGTTCAC	2437
4979	Z32.211.fw.asc1	TATGGCGCGCCtaGTGGAAGTTCCGATT	2438
4980	Z32-538-rvHpa1	CATgttaacGCAACTGCGACTAGCCTGACT	2439 2580 2595
5069	Z32 KO rv Sac2 3'UTR	ataCCGCGGtcctgacttggttcgtta	2487 2488
5070	Z32 KO fw Xho1 5'UTR	tatCTCGAGttcaggaaattgtgtcgt	2487 2488
5071	Z32 KO rv hind 3 5'UTR	ataAAGCTTgatgttttccttccccttc	2487 2488
5072	Z32 KO fw Xba1 3'UTR	cgcTCTAGAttgtgcctcgttaccatggt	2487 2488
5073	Z32.274.fw.asc1	TATGGCGCGCCtaGTCGACTTCACATGG	2485
5074	Z32.274.rvHpa1	GAGgttaacCTGCATCCATGTGAAGTCGAC	2483
5075	Z32teth253rvHpa1	GAGgttaacGGCAGTTGGTAACTGCGA	2581
5076	Z32teth362rvHpa1	GAGgttaacAGCTAAGTACCGCGGTATCAC	2484 2594

5077	Z32teth362fwAsc1	TATGGCGCGCCtaGTGATACCGCGGTAC	2486 2580
5148	Z32gatewayfw	AAAGCAGGCTCCATGtctggcactaatcac	2507
5149	Z32 gateway rv	GTACAAGAAAGCTGGGTTtcatctctgtttctgcgt	2507
5245	PDH E1 fw	TCATCTGCTGCACTTGGTTC	probe
5244	PDH E1 rv	AGCATAACGACGGGATTGTC	probe
5243	PPDK fw	GCGGACGGTAACAAGAACAT	probe
5242	PPDK rv	AGCTCCTTTAGGTCCGAAGC	probe
5241	IDH fw	AAGACGGAGGATCGTGTGAC	probe
5240	IDH rv	CTTGAAACGCCCATCGTAAT	probe
5239	MCP 9 fw	CAAGGCAACAAAGGGGAATA	probe
5238	MCP 9 rv	CTTGATTCCGTGCTCACTCA	probe
5269	Not2 UTR fw Sac2	tatccgcggacagtaaatgaagaagtg	2527
5454	DRBD2 fw Hind3	TATaagcttCAAGGAGGAAATATGTTCGAC	2575
5455	DRBD2 rv BamH1	ATAggatccTCATGAAGTGGATTTATTGTC	2575
5436	Tb927.7.2780 fw Hind3	gctaagcttTCTAAAGCTCCTTCGCAACCAGCC	2573
5435	Tb927.7.2780 rv BamH1	ATAggatccCTATGCCGCCGCTGC	2573
5438	ZC3H28 fw Mlu1	GCGacgcgttaTATTCTAGCGAAAAGGAGAAG	2579
5437	ZC3H28 rv Hpa1	TATgttaacTCACGAACGACCCGGATGCTT	2579
5460	Z32teth145rvHpa1	CTCgttaacAATTCGCGCGAAACTTTTCCC	2582
5491	Z32tethfw146ASC1	TATGGCGCGCCtaTGTGACGCCCATCCC	2595 2594
4906	Z32ASC1tethfw	tat ggc gcg cct atc tgg cac taa tca	2413 2439 2483 2484 2581 2582
3854	VSG rev 2nd Apa1	AGCgggcccTCTGATTTGTTGTATCCGAAC	2605
3855	VSG fw 2nd Xho1	atactcgagATGCAGATGCGGCTGTGG	2605

Table 4: Primers used for the work described in this thesis.

3. Results

3.1 Mass Spectrometry of free and membrane bound polyribosomes

The aim of this project was to identify proteins associating with polyribosomes in the bloodstream and the procyclic form of *Trypanosoma brucei.*
This was done for two reasons:
Polyribosome association of a candidate protein can give a hint towards its role in the RNA metabolism of the parasite. There are many putative RNA binding proteins in *Trypanosoma brucei.* If a candidate protein, e.g. a protein with an RRM or a zinc finger domain, is found on the polyribosomes, this would indicate that this protein can indeed bind to RNA. Also, polyribosome association points towards a stabilizing role, instead of a role in RNA degradation.
The second aim was to find proteins binding to the *VSG* mRNA.
As VSG is the major surface protein and makes out about 10% of the cell's total protein, the polyribosomes at the ER should be enriched with VSG mRNPs. Thus, it was concluded that RNA binding proteins found exclusively in the membrane-bound polyribosome of the bloodstream form were likely candidates for *VSG* mRNA binding proteins.
Therefore, the polyribosomes of the bloodstream, as well as the procyclic form, were separated into free and membrane-bound polyribosomes.
To obtain the membrane-bound fraction, the lysis was done without detergent, using glass beads and vortexing. The membrane fraction was separated from the cytosolic fraction by centrifugation at 30,000g. Subsequently, the pellet (membrane fraction) and the supernatant (free fraction) were treated with Triton-X in order to lyse the membranes (for a more precise description see 2.9).
The polyribosomes were isolated by sucrose gradient centrifugation. The two fractions were loaded on two different sucrose gradients, thus, membrane-bound polyribosomes and free polyribosomes were isolated separately. Using an ISCO 160 gradient former, the fractions were collected and the polyribosome profile was recorded by measuring the absorption at 254nm.

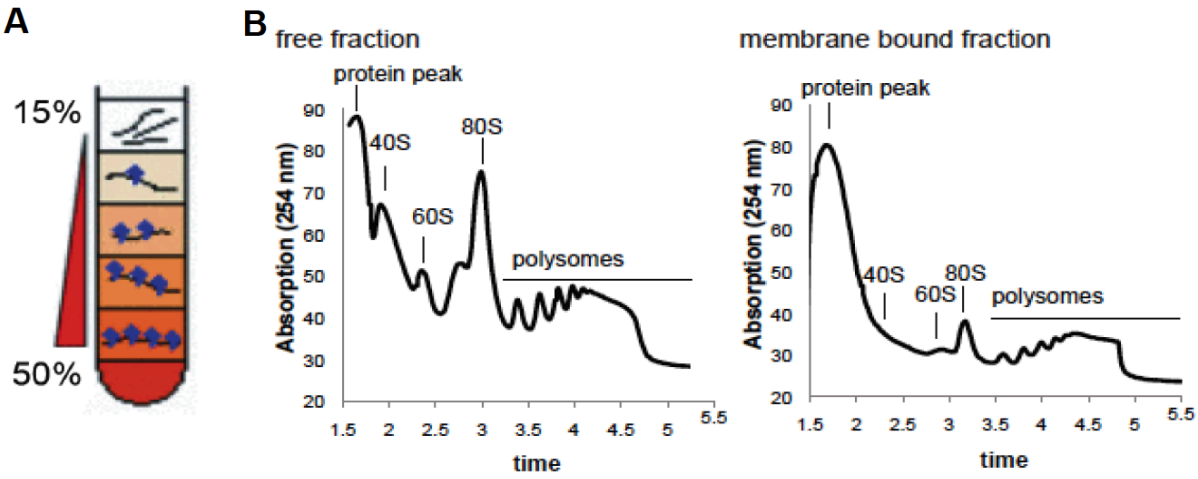

Fig. 11: Scematic representation of a sucrose gradient centrifugation.
A: Taken from (Spriggs, Stoneley et al. 2008)
B: examples for polyribosome gradients of free polyribosomes (made from the cytosolic fraction) and membrane-bound polyribosomes (made from the membrane fraction). Note that the preribosomal subunits (40S and 60S) are almost exclusively found in the cytosolic fraction.

3.1.1 Methods and pre-trials

The first polyribosome isolation, followed by mass spectrometry of the polyribosome fractions, was done as a pre-trial, in order to see how much sample is needed in order to see RNA-binding proteins. $1.8 \cdot 10^9$ procyclic cells were used. The polyribosomes were concentrated using centricon columns.
The concentration of the polyribosomal fractions using centricon columns turned out to take more time than expected (approximately 5 hours), due to the high sucrose concentration of the samples.
The amount of protein was measured using the Bradford assay. The total amount of protein was 384µg for the free polyribosomes and 128µg were loaded on the gel. For the membrane bound polyribosomes, the total amount of protein was 83,3µg and 52µg were loaded on the gel.

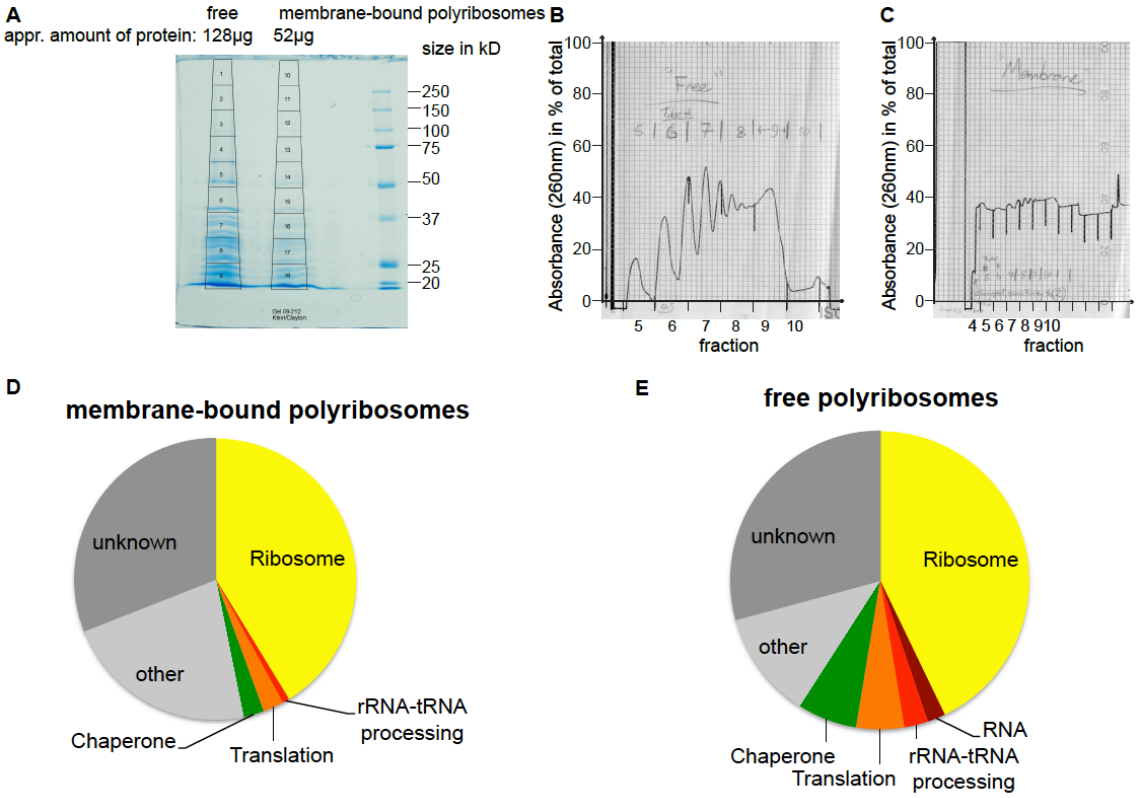

Fig. 12: Results of first mass spectrometry of free and membrane bound polyribosomes from procyclics A: Coomassie-stained gel for mass spectrometry B: Polyribosome profile for free polyribosomes C: Polyribosome profile for membrane-bound polyribosomes. Note: Before fraction 5 (free polyribosomes) and 4 (membrane-bound polyribosomes) the sensitivity of the machine was set too high (1 instead of 2), therefore, the absorption for the protein peak, as well as the 40S, 60S and 80S peak, was to high to be measured.
D: mass spectrometry results for the membrane-bound polyribosomes. 126 proteins were identified in total. E: mass spectrometry results for the free polyribosomes. 155 different proteins were identified.
The proteins labeled as contaminants include cytosceletal and mitochondrial proteins, proteins which have a function in the glucose metabolism and the citric acid cycle, in the cell cycle, in vesicular transport, in lipid and fatty acid synthesis as well as in the synthesis of purines and pyrimidines (for a complete list: see Suppl. 6.1)

The mass spectrometry (see fig. 12) results contained a lot of ribosomal proteins, proteins involved in translation but only very few RNA binding proteins.
In the free polyribosomes, the cap-binding initiation factor, eIF4E4, was found. As this protein should be present only once on each polyribosome, we concluded that, for the free polyribosomes, we loaded enough material to see proteins binding to mRNAs with only a single copy.
In order to see RNA binding proteins, however, which are, opposite to translation initiation factors, not found on every RNA, we would need more material. As one third of the material for free polyribosomes was loaded on a gel and $1{,}8 \cdot 10^9$ cells were used, this would correspond to $6 \cdot 10^8$ cells.

A protein that would bind the VSG RNA would bind to approximately 10% of the total RNA, but probably to 50% of the RNA transcribed on the membrane-bound polyribosomes.
Comparison of the gradients from the free and membrane bound polyribosomes in bloodstream cells (see fig. 14 A and C, the height of the polyribosome peak was compared) showed that there are approximately three times more free polyribosomes than membrane bound ones.
Therefore, in order to, theoretically, be able to see a protein binding to the VSG mRNA, we need at least 6 times more material, which would correspond to $3{,}6 \cdot 10^9$ cells for the membrane bound polyribosome isolation.
In order to have enough material, for the first mass spectrometry for the free polyribosomes, I used $5{,}6 \cdot 10^9$ bloodstream cells (see fig. 14, A and B).
For the preparation of the membrane bound polyribosomes double as many cells were used ($1{,}06 \cdot 10^{10}$ cells) (result see fig. 15).
In this second large-scale preparation, the cytosolic fraction (free polyribosomes) was distributed over three different gradients, two 15-50% and one 15-55% gradient, in order to avoid overloading of the gradient (see fig. 15, C-E).
The membrane fraction was loaded on 15-55% gradient (see fig. 15, A).

However, after reviewing the results of the free and the membrane-bound polyribosomes, it was seen that much less proteins were obtained in the free polyribosomes than in the results from the membrane-bound ones (112 proteins as compared to 394). Therefore, the mass spectrometry of the bloodstream free polyribosomes was repeated using the free polyribosomal fractions from the larger polyribosome preparation (see fig. 15 C-E).

As already mentioned, the concentration of the samples using centricon columns took quite a long time, due to the high sucrose concentration. Also TCA precipitation works badly with polyribosome samples, because the pellets did not dissolve well in the Laemmli buffer, as compared to “normal” protein samples (e.g. the Flow-through of an immunoprecipitations), and were larger due to the sucrose.
As can be seen in fig. 13, however, even though the centricon concentration takes time and even if the samples are frozen in between, the majority of polyribosomes stays intact, although some seem to fall apart into monosomes.
Also, due to the molecular cut-off of 100kDa, this method serves as an additional purification step. However, material also gets lost during this step, this can be seen by the fact that the peaks in gradient B are not as high as expected.
As the samples concentrate slower due to the sucrose content, I tried shortening the spin time by diluting the samples with sucrose-free polyribosome buffer. Although leading to a larger volume, a 1:4 dilution did reduce the concentration time. Also, the diluted concentrate could be TCA precipitated. Thus, for the large-scale preparation for the bloodstream-form polyribosomes, a combination of both methods was chosen. The

samples were diluted 1:4, with sucrose-free polyribosome buffer (see Materials and Methods), then concentrated using centricon columns. The concentrate was then precipitated with TCA.

For the procyclic preparation $1{,}35 \cdot 10^{10}$ cells were used. Again four gradients were made. The membrane fraction was given on a 15-55% gradient (see fig.16, A), as well as half of the cytosolic fraction (see fig. 16, C). The polyribosome fractions from these two gradients were concentrated with centricons directly after fractionation and the concentrate was sent for mass spectrometry. The other half of the cytosolic fraction was split on two 15-50% gradients (not shown), these were not used for mass spectrometry. As the final volume of both the free and the membrane-bound polyribosomes was small enough to be loaded on a gel, no TCA precipitation was done after the centricon concentration. However, the remaining sucrose in the sample destroyed the chromatograph's column, therefore this method is not recommendable.

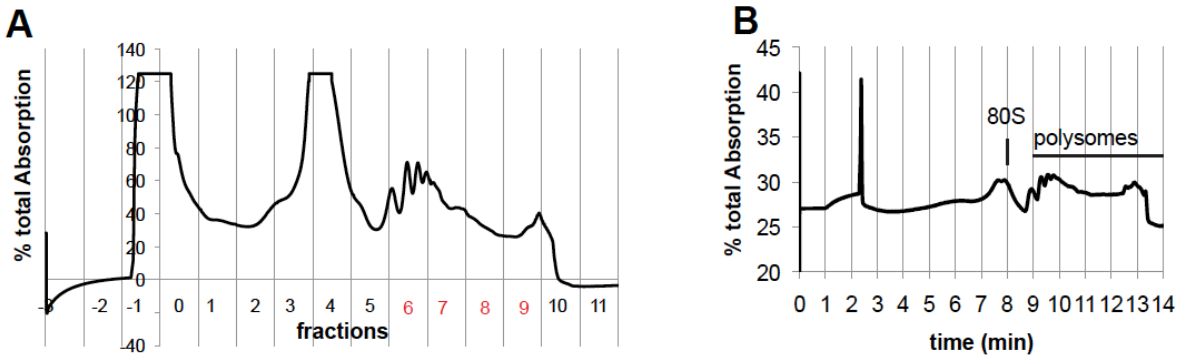

Fig. 13: Concentration of polyribosome fractions with Centricon A: polyribosome gradient (15-50%), with free poyribosomes, made with $2.4 \cdot 10^9$ procyclic cells. Fractions 6,7,8 and 9 (polyribosomes, shown in red) were pooled, 45% of the pooled polyribosomes were frozen over night at 80°C and concentrated with a centricon column the next day. The concentracte was given on a new gradient, which is seen in B: Polyribosome gradient with sample after concentration with centricon column (MW:100kDa).

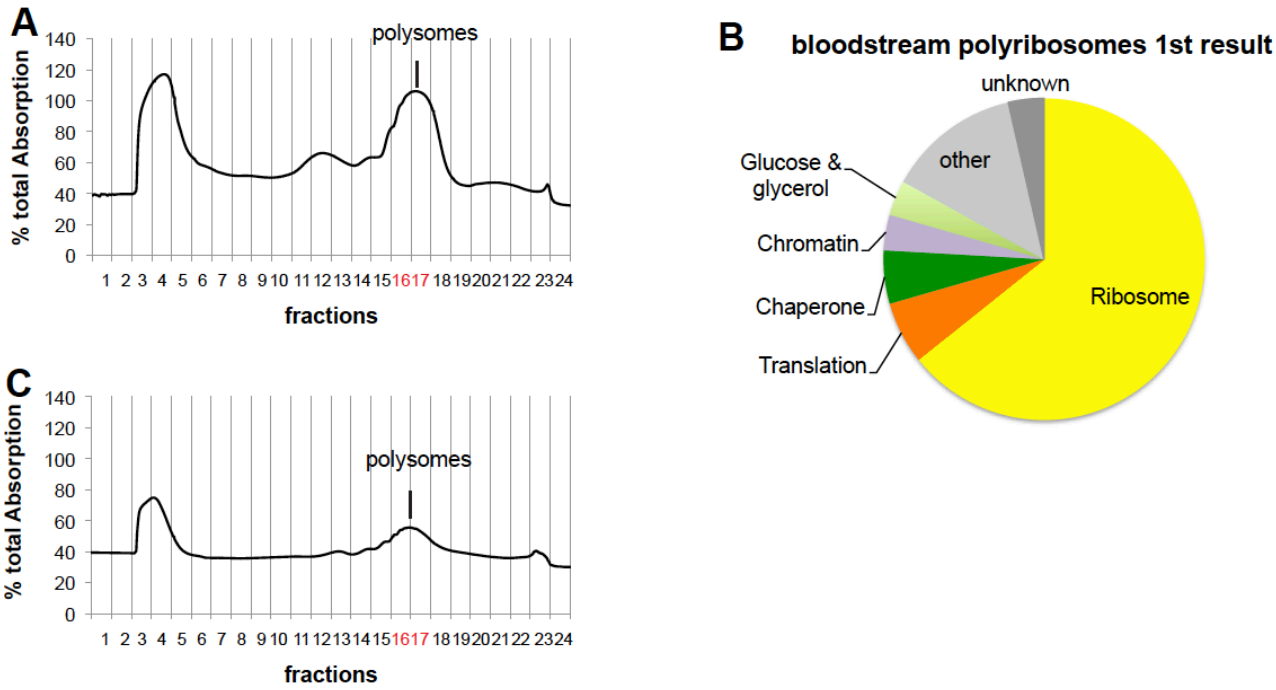

Fig. 14: **Results of first mass spectrometry of free polyribosomes from bloodstream trypanosomes** A: polyribosome gradient, free polyribosomes (profile membrane bound polyribosomes, see C.). Made with $5{,}6 \cdot 10^9$ bloodstream cells. Fraction 16 and 17 were diluted 1:4 and concentrated using a centricon column (time needed: ca. 150min). The final volume (about 345µl) was TCA precipitated, washed with Ethanol, run on a PAA gel, coomassie stained and sent for mass spectrometry. B: Overview of Mass Spectrometry results from concentrated polyribosomes C: membrane bound polyribosomes from same cell lysate as used in A (not analysed by mass spectrometry, too little material).

3.1.2 Mass spectrometry results from the large scale polyribosome isolations

1507 unique peptides were found in the mass spectrometry results of the bloodstream free polyribosomes, done with $1{,}06 \cdot 10^{10}$ cells, and 1859 unique peptides were found in the membrane-bound polyribosomes (for a complete list see suppl. 6.1). This shows that, despite the use of additional material for the free polyribosomes, there was still a smaller yield than for the membrane-bound ones.

For procyclics ($1{,}34 \cdot 10^{10}$ cells used), 2123 peptides were found in the membrane-bound, but only 423 in the free polyribosomes. This shows that, for the free polyribosomes, the yield is very low, therefore, the data used from this preparation should be used with some caution, meaning, if a protein is found only with the procyclic membrane-bound polyribosome data set, it does not necessarily mean that it cannot be present in the free polyribosomes.

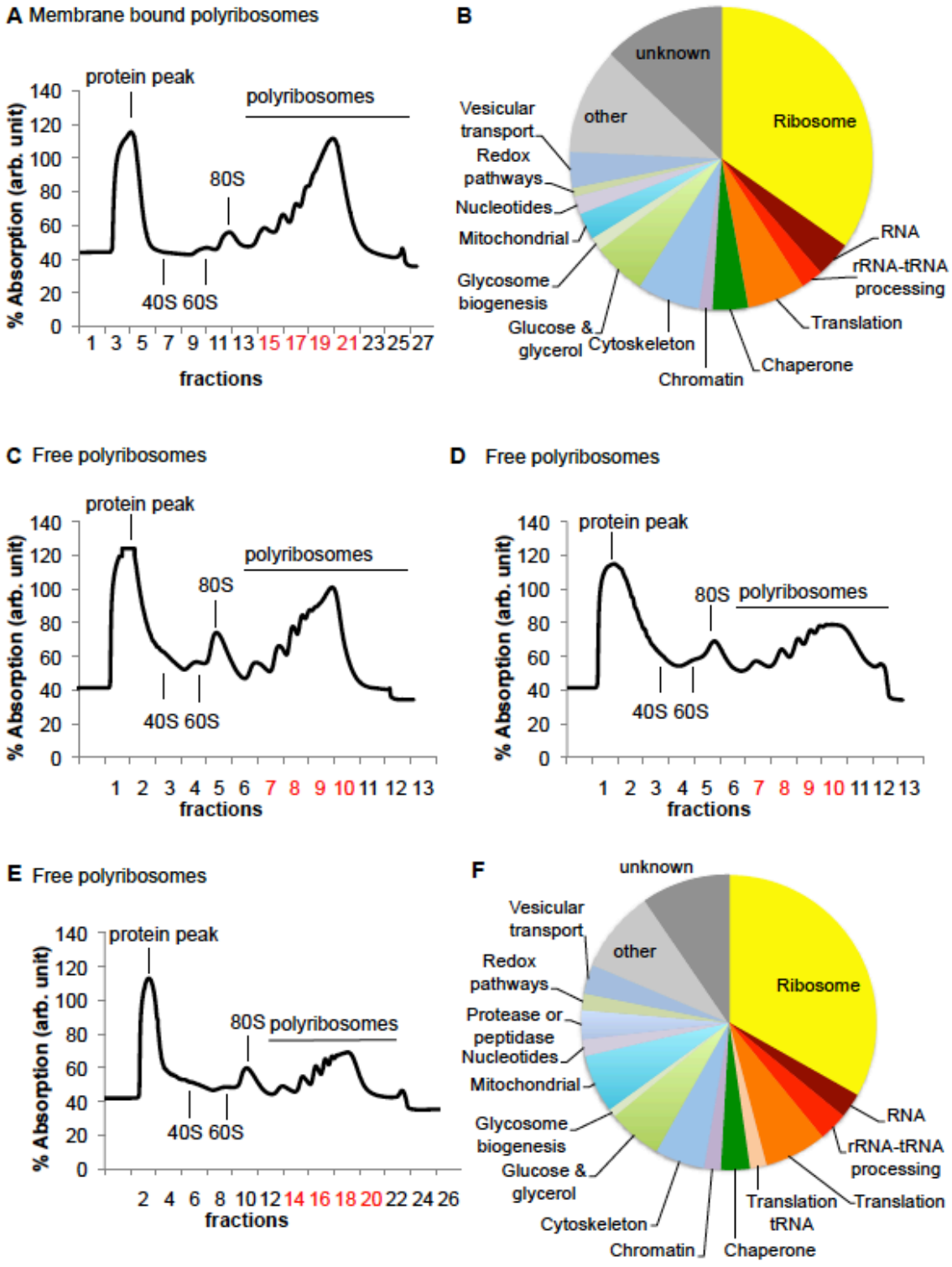

Fig.15: Large scale isolation of bloodstream free and membrane-bound polyribosomes

A: polyribosome profile of the membrane bound polyribosomes. Fractions shown in red were concentrated with a centricon column, then TCA precipitated and sent for mass spectrometry.

B: Overview of proteins found by mass spectrometry (bloodstream membrane-bound polyribosomes). C, D, E: polyribosome profiles for free polyribosomes. Fractions shown in red were concentrated with a centricon column, then TCA precipitated and sent for mass spectrometry. F: Overview of proteins found by mass spectrometry (bloodstream free polyribosomes) .

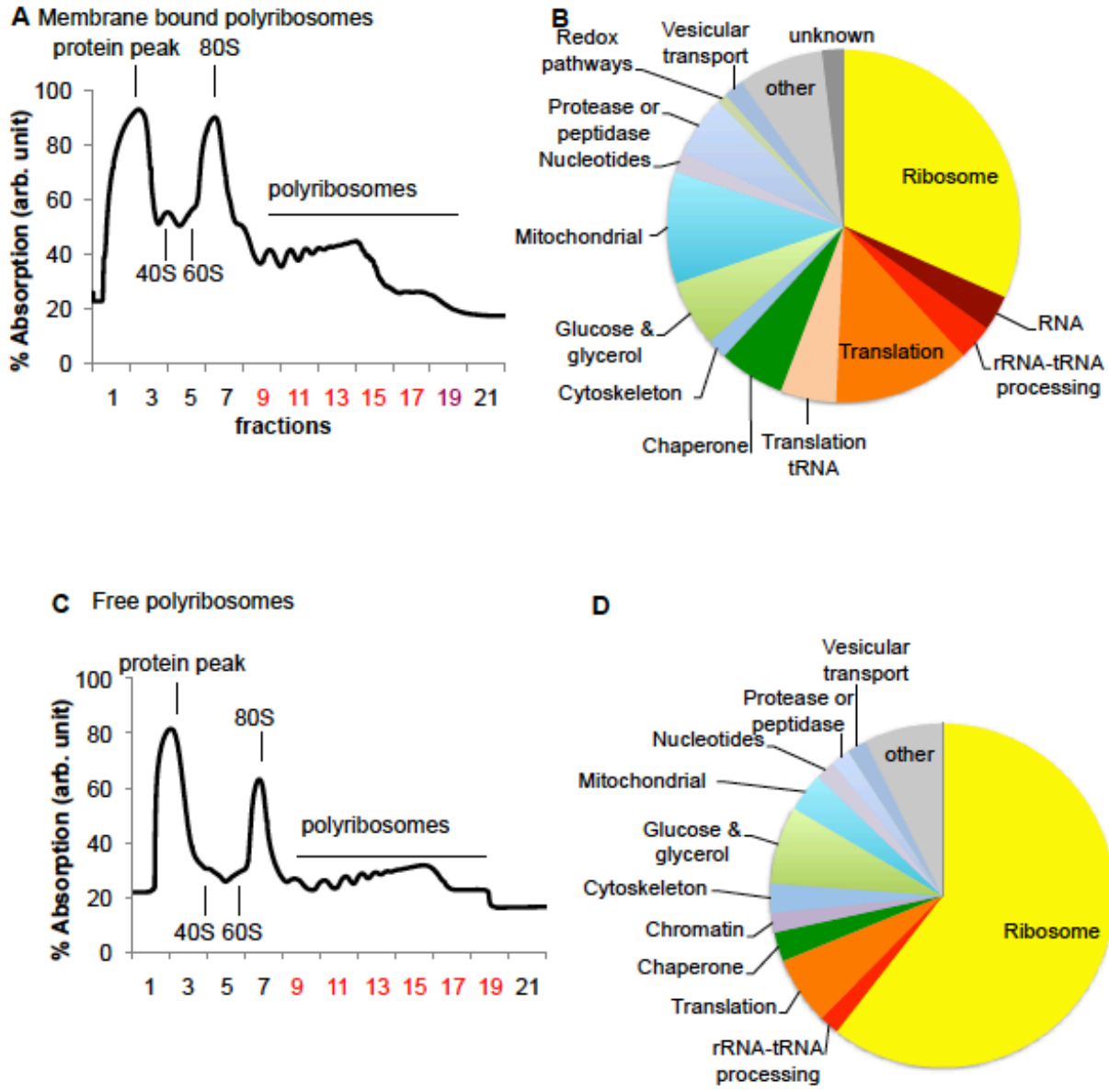

Fig.16: Large scale isolation of procyclic free and membrane-bound polyribosomes

A: Polyribosome profile of the membrane bound polyribosomes. Fractions shown in red were concentrated with a centricon column and sent for mass spectrometry.

B: Overview of proteins found by mass spectrometry (procyclic membrane-bound polyribosomes)

C: polyribosome profile of the free polyribosomes. Fractions shown in red were concentrated with a centricon column and sent for mass spectrometry.

D: Overview of proteins found by mass spectrometry (procyclic free polyribosomes) .

3.1.3 Mass spectrometry results – Proteins involved in translation

In the mass spectrometry results of the isolated polyribosomes, 3% to 9% of the found proteins have already been shown to have a function in translation or are homologues of proteins having a function in translation in other organisms (see fig. 15 and 16). These proteins are summarized in table 5.
The poly-A binding proteins were found in all isolations, as well as elongation factor 1 gamma and TbRACK1, a WD-repeat protein that binds to eEF1A and has already been shown to be associated with polyribosomes (Regmi, Rothberg et al. 2008). All eight TCP proteins, the subunits of the TRiC complex, were found in the bloodstream membrane bound polyribosomes. The TRiC complex is involved in folding of the nascent polypeptides (Frydman, Nimmesgern et al. 1994). Some of the TCP proteins were found in the other purifications as well.
In the samples from the bloodstream form, the trypanosome homologue to Bfr1 was found, a protein which is associated with polyribosomes in yeast (Lang, Li et al. 2001). We also found the *T. brucei* homologues of the DEAD-box helicase DED1, DED1-1 and DED1-2, whose homologues in Leishmania were shown to be associated with translation initiation factors (Zinoviev, Leger et al. 2011, Zinoviev, Akum et al. 2012).

Elongation, initiation and termination factors were found as well, but not to comparable amounts in all purifications, which shows a major flaw in these results. For example, according to the mass spectrometry results, the translation initiation factors eIF4E3, eIF4E4, eIF4G3 and eIF4G4 seem to be differentially distributed between free and membrane-bound polyribosomes in the bloodstream form: while eIF4E3 and G4 are found exclusively, or with more unique peptides, in the mass spectrometry results of the membrane-bound polyribosomes, eIF4E3 and G4 seem to be mainly associated with free polyribosomes. This would have, to a certain extent, matched the results of (Freire, Dhalia et al. 2011), as they showed that E3 binds G3 and G4, while E4 binds only G3, as well as that these initiation factors are associated with polyribosomes.
In order to check whether this difference was genuine, I made Western blots from free and membrane-bound polyribosomes. The polyribosome fractions were pooled and concentrated with centricon columns (see fig. 17). The elongation factors were detected using antibodies from (Freire, Dhalia et al. 2011). However, these Western blots showed that the distribution of these proteins does not differ between free and membrane-bound polyribosomes (see fig. 17), at least not to a detectable extent.

Protein name	Protein accession number	Number of unique peptides				
		bs free	bs mb	pc mb	pc free A	pc free B
Bfr1	Tb927.10.14150	3	6			
DED1-1	Tb927.10.14550	3	9	3		
DED1-2	Tb09.211.3510		9	5		
EF1α	Tb927.10.2100	9	10	9		1

EF1β	Tb927.4.3570	2		3		
EF1γ	Tb11.01.4660	4	1	10	2	1
EF2	Tb927.10.4560	10		45	8	
EIF	Tb11.01.3420			6		
EIF2γ	Tb11.01.4830			3		
eIF2α	Tb927.3.2900			2		
EIF3	Tb11.01.1370			5		
EIF3 subunit 7	Tb927.6.4370			7		
EIF3a	Tb927.7.6090	8		16		
EIF3b	Tb927.5.2570			6		
EIF3c	Tb927.10.8270	1		13		
EIF3c	Tb927.10.8290	1				
EIF3g	Tb927.4.1930	5				
eIF3L	Tb927.10.4640			6		
EIF4A1	Tb09.160.3270	6	6	8		
EIF4E3	**Tb11.01.3630**	**1**	**3**			
EIF4E4	**Tb927.6.1870**	**10**	**3**	**2**		**1**
EIF4G3	**Tb927.8.4820**	**14**		**5**		**1**
EIF4G4	**Tb11.01.2330**		**3**			
EIF5	Tb927.10.2770		5	4		
ERF1	Tb11.22.0012		1	4		
ERF3	Tb11.02.4030			3		
IF2	Tb927.2.3780			2		
PABP1	Tb09.211.0930	24	11	25	4	1
PABP2	Tb09.211.2150	28	21	24	6	1
RBG1	Tb927.10.6800		3			
TbRACK1	Tb11.01.3170	15	14	15	8	1
TCP 1 γ	Tb927.8.3150		2	17		
TCP 1 α	Tb11.01.8510			18		1
TCP 1 β	Tb11.42.0003			16		1
TCP 1 δ	Tb927.10.1060			17	2	
TCP 1 ε	Tb11.01.5860			15		1
TCP 1 η	Tb09.211.2570			11		1
TCP 1 θ	Tb927.10.8190	2		17		1
TCP 1 ζ	Tb11.02.0750	1		14		

Table 5: **Proteins involved in translation found in the mass spectrometry results.**

bs free: bloodstream free polyribosomes (see fig. 15 C,D,E and F), bs mb: bloodstream membrane-bound polyribosomes(see fig. 15 A+B), pc mb: procyclic membrane-bound polyribosomes (see fig. 16 A+B), pc free A: procyclic free polyribosomes, 2nd mass spectrometry results (see fig. 16, B+C), pc free B: procyclic free polyribosomes, 1st mass spectrometry results (see fig. 12 A, B, E).

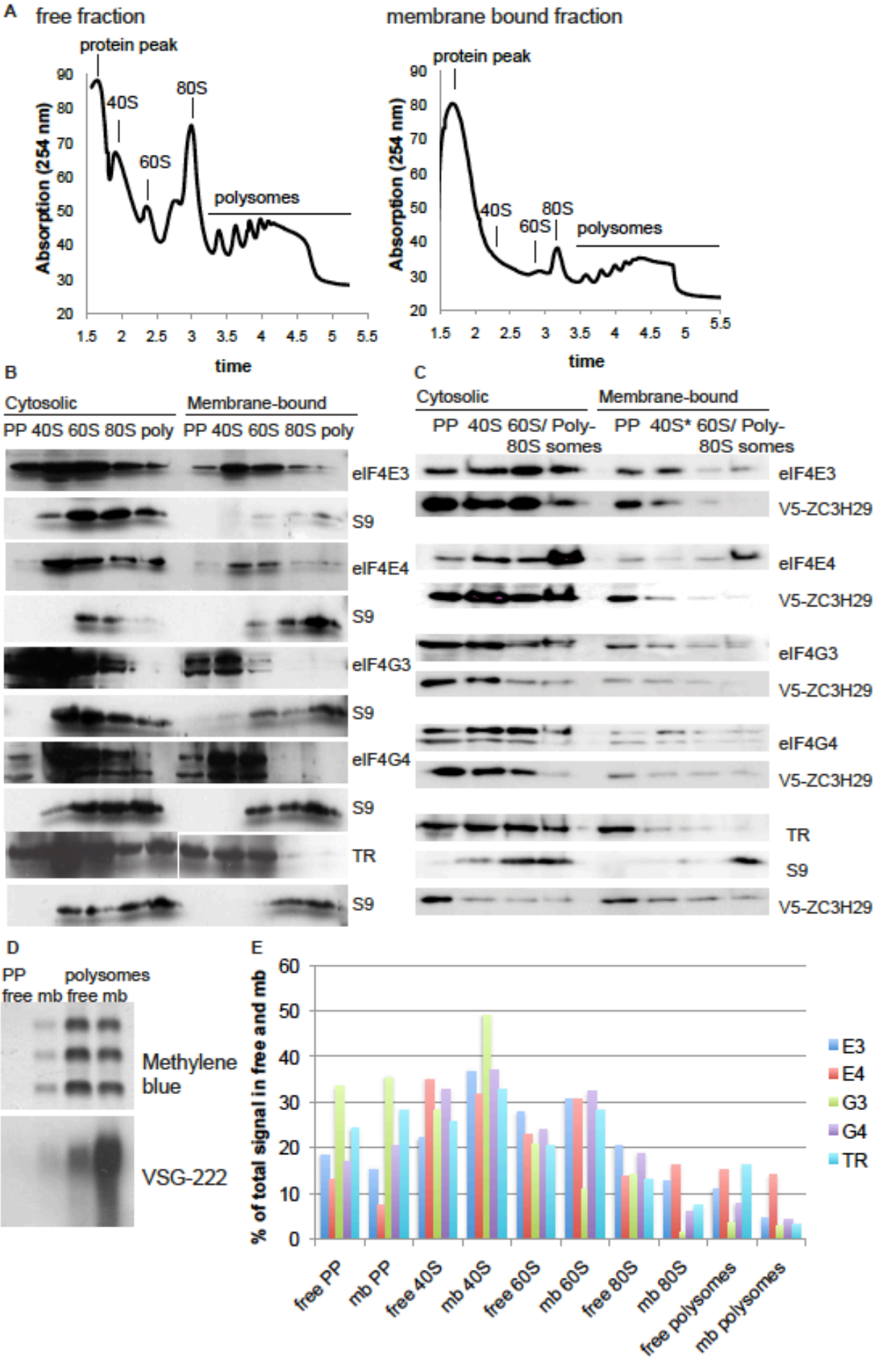
A
free fraction
protein peak
40S
80S
60S
polysomes
Absorption (254 nm)
time
membrane bound fraction
protein peak
40S
60S
80S
polysomes
Absorption (254 nm)
time
B
Cytosolic
Membrane-bound
PP 40S 60S 80S poly PP 40S 60S 80S poly
eIF4E3
S9
eIF4E4
S9
eIF4G3
S9
eIF4G4
S9
TR
S9
C
Cytosolic
Membrane-bound
PP 40S 60S/ Poly- PP 40S* 60S/ Poly-
80S somes 80S somes
eIF4E3
V5-ZC3H29
eIF4E4
V5-ZC3H29
eIF4G3
V5-ZC3H29
eIF4G4
V5-ZC3H29
TR
S9
V5-ZC3H29
D
PP polysomes
free mb free mb
Methylene blue
VSG-222
E
% of total signal in free and mb
E3
E4
G3
G4
TR
free PP
mb PP
free 40S
mb 40S
free 60S
mb 60S
free 80S
mb 80S
free polysomes
mb polysomes

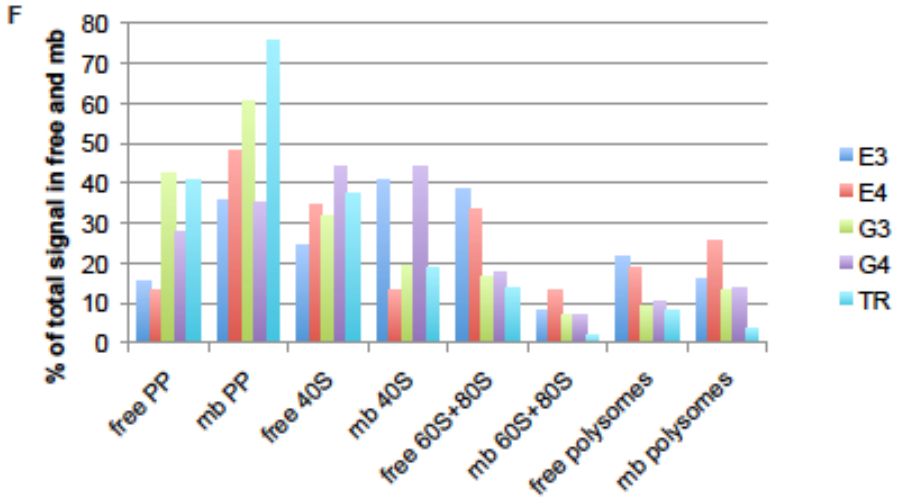

Fig. 17: **eIF4E3 and G4 are not exclusively associated with free and eIF4E4 and G3 are not with membrane bound polyribosomes**

A: Polyribosome profiles, free and membrane bound polyribosomes, from bloodstream trypanosomes B: Western blots made with samples from polyribosome isolation shown in A.

PP: protein peak. Fraction 1 and 2 of each gradient were pooled, 1/100 was used as sample per Western blot.

40S, 60S, 80S: Fraction 3 (40S), fraction 4 (60S) and fraction 5 (80S) were concentrated using a microcon column, 1/10 of the concentrated samples was used per Western blot.

Poly: Polyribosomes, Fractions 6-8 were pooled and concentrated using a centricon column. 1/10 of the concentrate was used per Western blot.

C: Same experiment, different polyribosome isolation. V5-ZC3H29 was used as loading control.

PP: protein peak. 1/100 of the non-concentrated protein peak fractions was loaded.

40S: 1/16 of non-concentrated 40S fraction was loaded,

80S: 60S and 80S fractions were combined and concentrated using a microcon column (peaks were not clearly separated into two fractions in these profiles),

poly: polyribosome fractions were combined and concentrated using two microcon columns. 1/16 of the concentrated sample was loaded on the Western blots.

D: Northern blot probed against the *VSG* mRNA with samples made from the protein peak (PP) and the polyribosomes from both the gradients shown in A, free and membrane-bound (mb), in order to show the proper separation of free and membrane-bound polyribosomes (*VSG* mRNA should localize to the membrane-bound polyribosomes).

E: The signals from the Western blots were quantified. The signal was added up separately for free and membrane-bound polyribosomes. Then the percentage of the total signal was calculated for each fraction (PP, 40S, 60S 80S and polyribosomes).

F: quantification of Western blots shown in C.

3.1.4 Testing of polyribosome association of RNA binding proteins

In the mass spectrometry results of the isolated polyribosomes, 2% to 8% of the found proteins (see fig. 15 and 16) are either shown to bind RNA or have RNA binding domains (see 3.1.5, table 6).
In order to test whether these RNA binding proteins were genuinely associated with polyribosomes and not just contaminants, I used tagged versions of four candidate proteins and tested their movement through a sucrose gradient by Western blot.
As the goal was, initially, to find proteins associated with the *VSG* mRNA, the four chosen candidate proteins were RNA binding proteins exclusively associated with bloodstream membrane-bound polyribosomes. These candidates were the zinc finger protein ZC3H29, which was found with two unique peptides in the membrane-bound polyribosomes, the pumilio-domain proteins Puf3 and Puf6 (2 and 3 unique peptides respectively) and the RRM-domain protein RBP29 (4 unique peptides). ZC3H29 and RBP29 were endogenously V5-tagged, while for Puf3 and Puf6 exogenously TAP-tagged versions were used.
RBP29 was clearly not associated with polyribosomes, as it localizes to the nucleus (see fig. 18).
As was shown by Western blot, the other three proteins were mainly not associated with polyribosomes either but seem to trail down the gradient in a similar fashion as the negative control, trypanothione reductase (see fig. 19 for ZC3H29, fig. 20 for Puf6 and fig. 21 for Puf3).
However, as Puf6 and Puf3 were exogenously expressed, it cannot be ruled out that the expression levels of the tagged protein is higher than the endogenous protein levels and that therefore there is a large pool of superfluous protein, which would not bind to RNA targets and thus not be associated with polyribosomes. This could lead to a larger amount of protein found in the first fractions and thus might cause a false negative result.
Stabilization of the polyribosomes by UV-crosslinking the RNAs to the proteins did not lead to an increase of either ZC3H29 or Puf6 protein levels in the higher fractions (see fig. 22 for ZC3H29 and fig. 23 for Puf6). Also, dissociation of polyribosomes did not lead to a shift of the ZC3H29 and Puf6 signal to the lower fractions. This speaks against a specific association with polyribosomes.
As these proteins were all found in the membrane-bound sample, it was tested for ZC3H29 whether this protein accumulates in the membrane-bound polyribosomes. However, the amount of ZC3H29 found in the membrane-bound polyribosomes is not higher than the amount found in the free polyribosomes (see fig. 24).
In order to check whether any of these proteins binds to the *VSG* mRNA, RNA was pulled down by immunoprecipitation, either with V5-beads (ZC3H29 and RBP29) or IgG beands (Puf6 and Puf3). The RNA level of VSG was then checked by qPCR. However, the results were inconclusive and, as it was discovered later that these proteins were mainly not associated with polyribosomes, the testing was stopped.

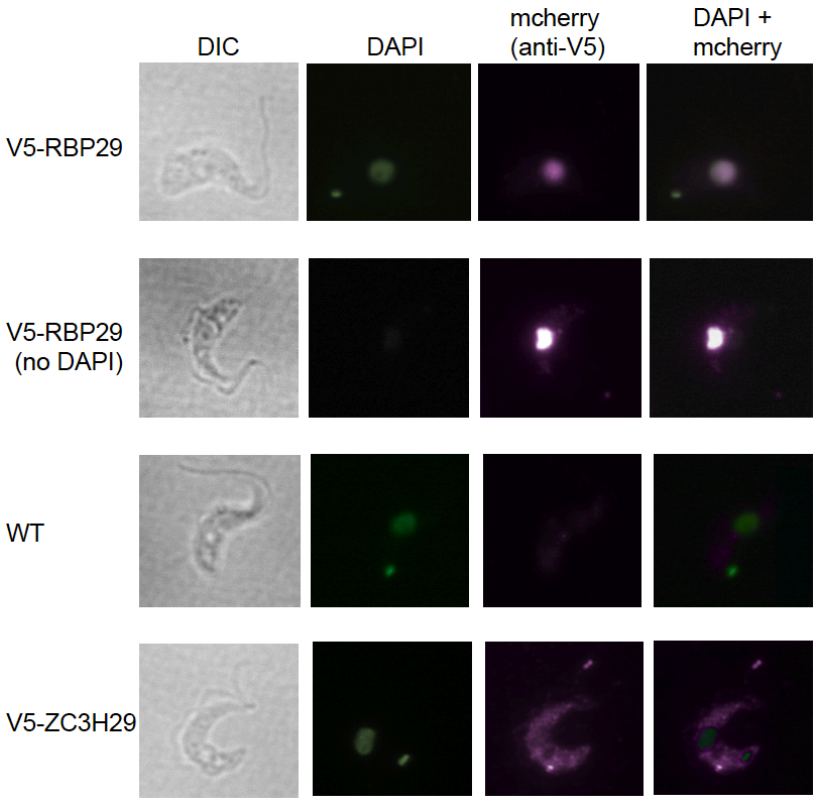

Fig. 18: V5-RBP29 localizes to the nucleus, V5-ZC3H29 to the cytoplasm

Localization of V5-RBP29 and V5-ZC3H29 using immunofluorescence against the V5-tag. DAPI was used to stain the nucleus.

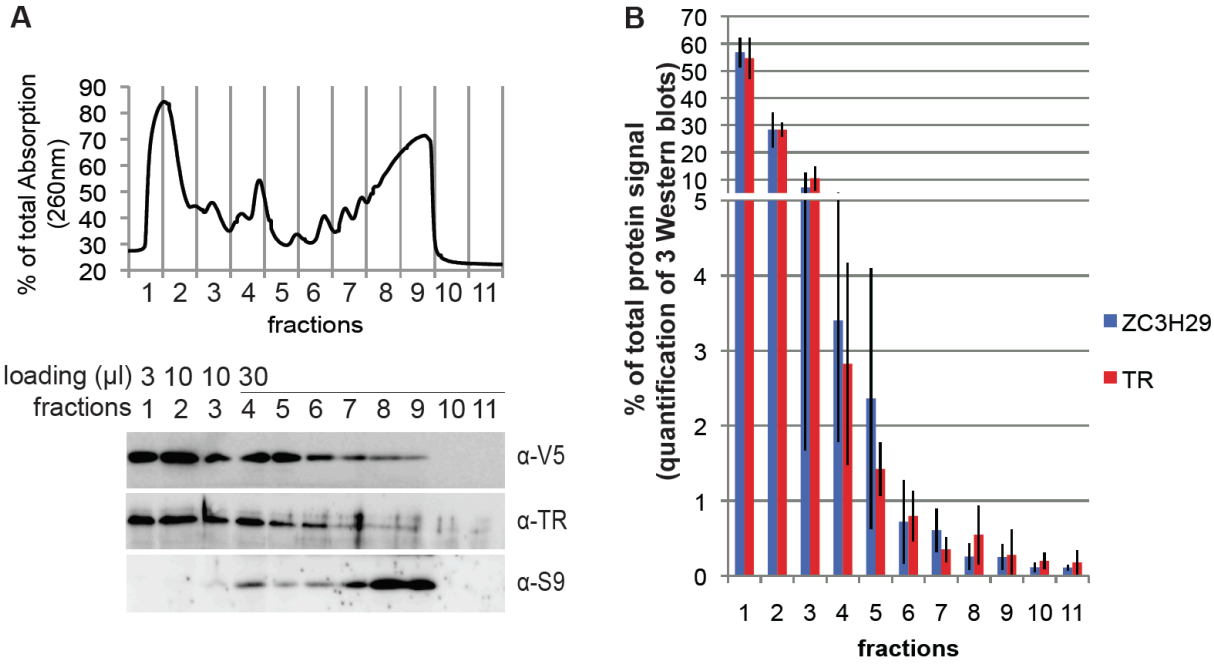

Fig. 19: ZC3H29 is mainly not associated with polyribosomes.

A: Polyribosome profile and Western blot using bloodstream cells expressing V5-ZC3H29. TR: trypanothione reductase, negative control S9: ribosomal protein S9 (small subunit), positive control. B: Summary of the quantified results of three Western blots made with samples from three different gradients (as shown in A, but with different loading order). The quantification was done with respect to the differential loading (3µl in the first, 10µl in the second and third fraction, 30µl of the others).

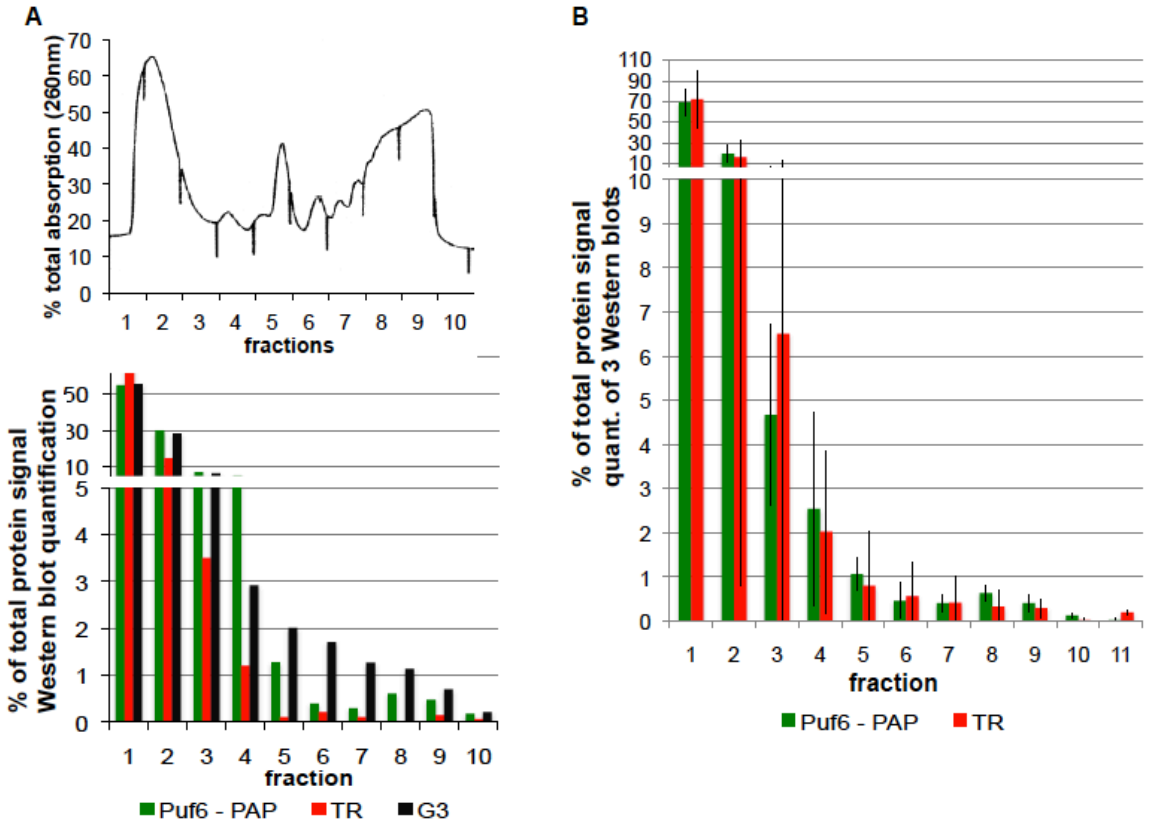

Fig. 20: Puf3 is mainly not associated with polyribosomes. A: Sucrose gradient made with bloodstream cells expressing TAP-tagged Puf6 and quantification results of a Western blot made with samples from this gradient. TR: trypanothione reductase, negative control G3: eIF4G3 (translation initiation factor) positive control. B: Summary of the quantified results of three Western blots made from samples of three different gradients. The quantification was done with respect to the differential loading (2µl in the first and second, 10µl in the third fraction, 30µl of the others).

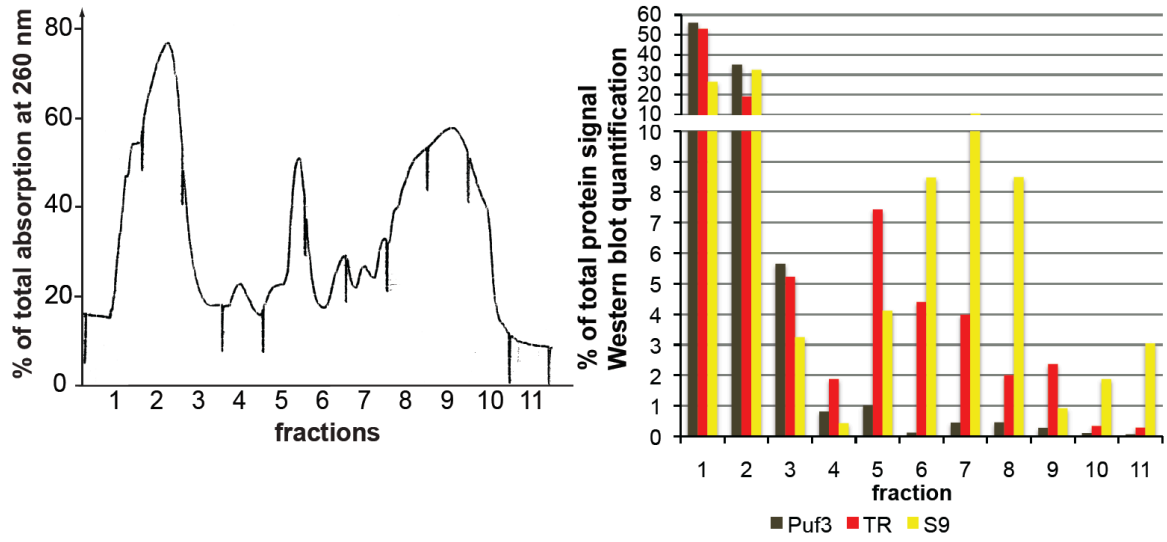

Fig. 21: **Puf3 is mainly not associated with polyribosomes.** A: Sucrose gradient and Western blot quantification using bloodstream cells expressing TAP-tagged Puf3. TR: trypanothione reductase, negative control, S9: ribosomal protein S9 (small subunit), positive control. The quantification was done with respect to the differential loading (1µl in the first and second, 10µl in the third fraction, 30µl of the others).

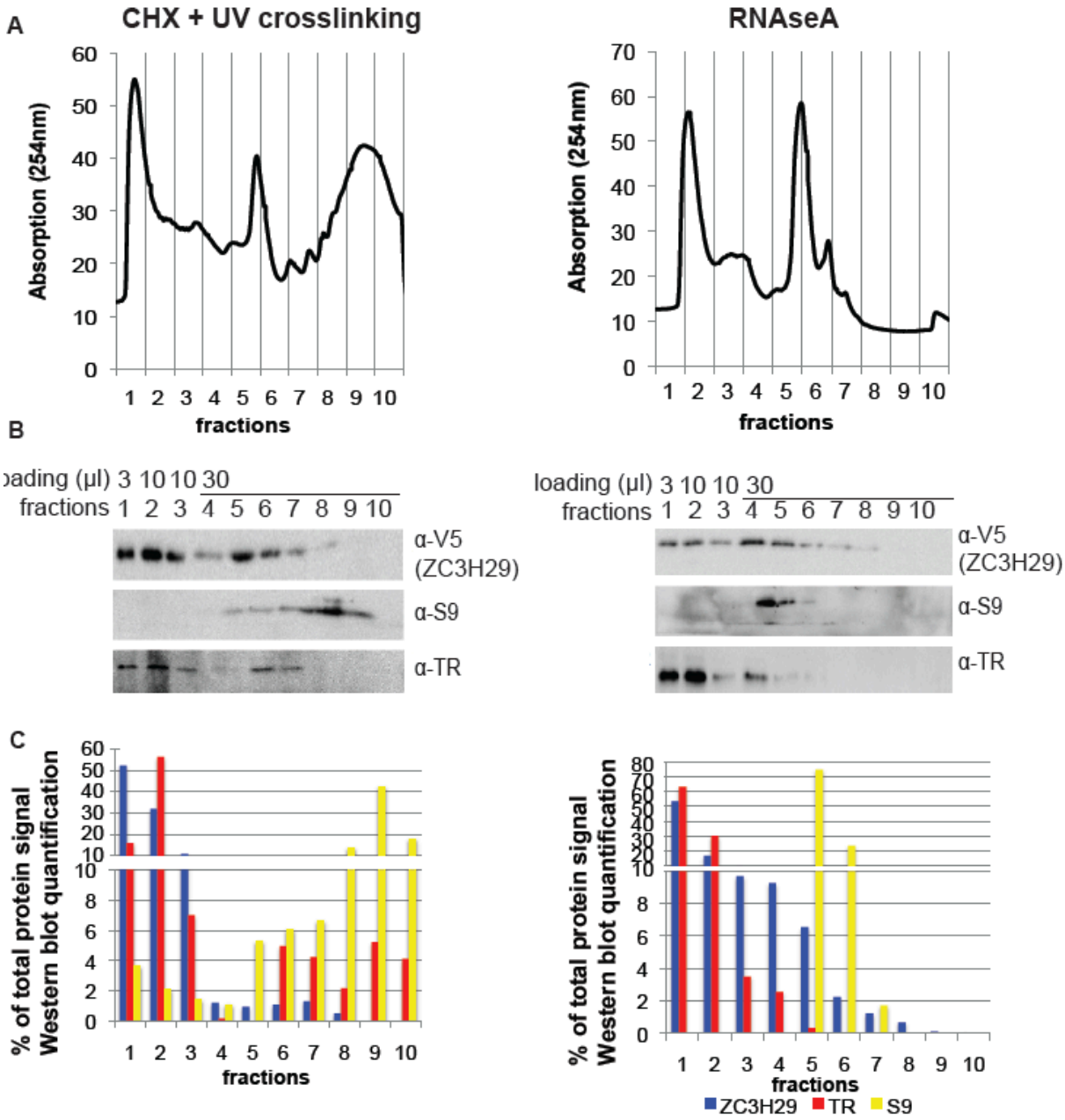

Fig. 22: Polyribosome dissociation has no influence ZC329 migration through the gradient
Sucrose gradients of V5-ZC3H29 cells which were treated with cycloheximide prior to UV crosslinking in comparison to cell lysates treated with RNAseA A: Sucrose gradient profiles of crosslinked and RNAseA treated samples. B: Western blots probed against V5-ZC3H29, TR (trypanothione reductase) and S9 (ribosomal protein S9) C: quantification of Western blots, differential loading was taken into account.

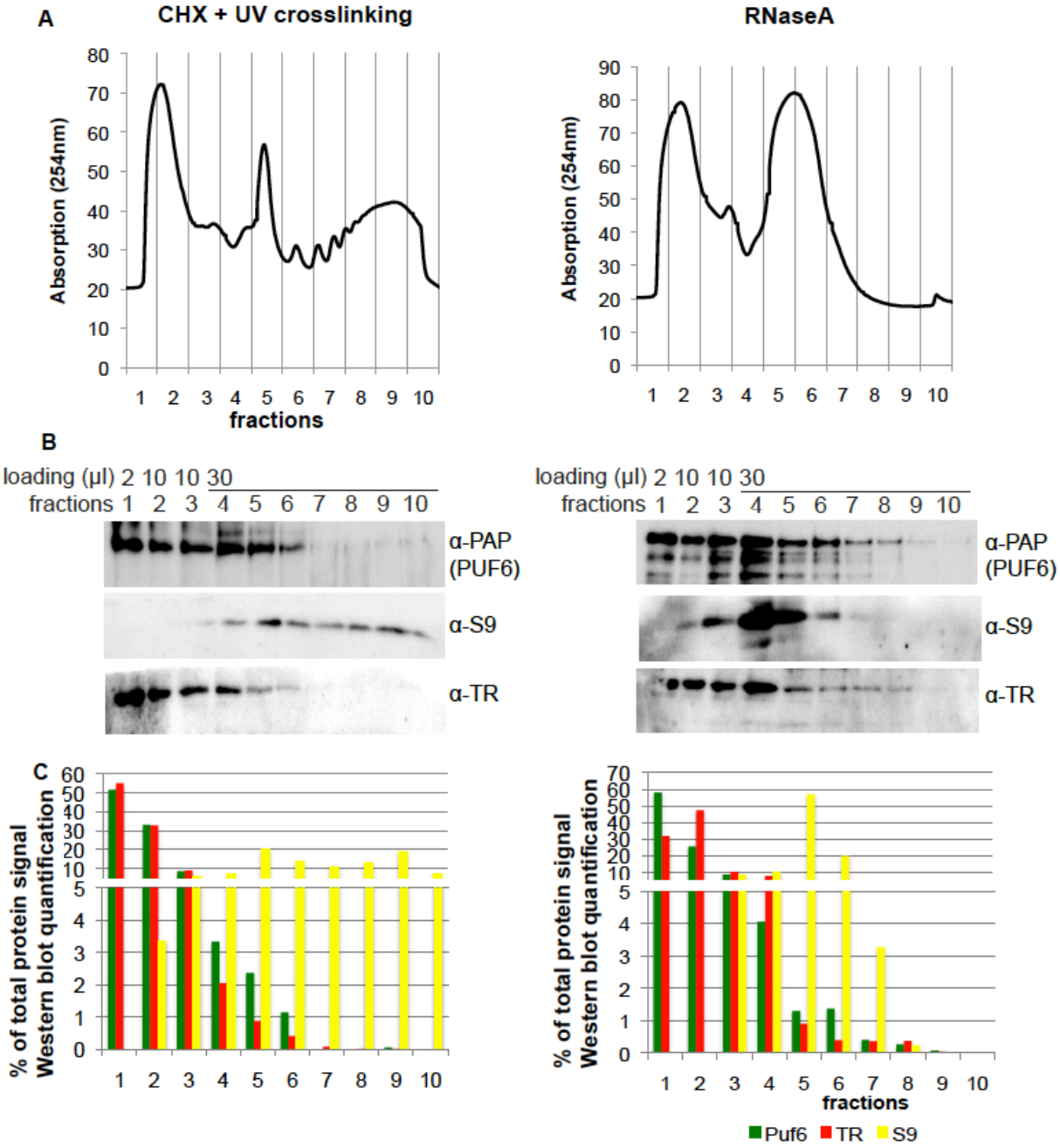

Fig. 23: **Polyribosome dissociation has no influence Puf6 migration through the gradient**
Sucrose gradients of TAP-Puf6 cells which were treated with cycloheximide prior to UV crosslinking in comparison to cell lysates treated with RNAseA
A: Sucrose gradient profiles of crosslinked and RNAseA treated samples. B: Western blots probed against TAP-Puf6 (with anti-PAP), TR (trypanothione reductase) and S9 (ribosomal protein S9) C: quantification of Western blots, differential loading was taken into account.

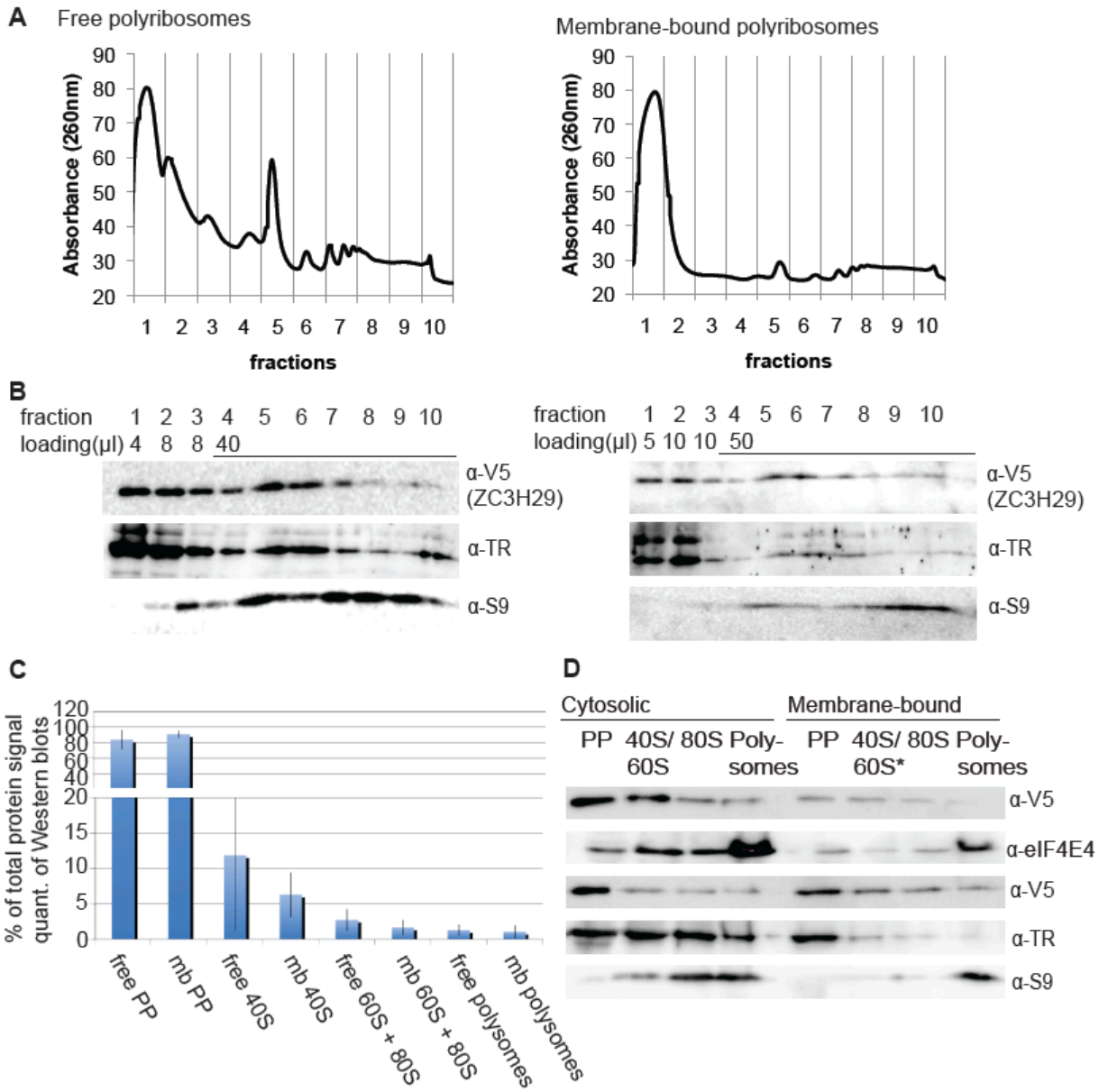

Fig. 24: ZC3H29 is mainly not associated with membrane-bound polyribosomes.
A: Polyribosome profiles of free and membrane-bound polyribosomes B: Western blots made with samples from polyribosome isolation shown in A. Probed against V5-ZC3H29, TR (trypanothione reductase) and S9 (ribosomal protein S9). C: quantification of ZC3H29 signal from Western blots shown in fig. 16 and partially in D.
mb: membrane-bound
PP: protein peak. 1/100 of unconcentrated protein peak fractions was loaded.
40S: 1/16 of unconcentrated 40S fraction was loaded,
80S: 60S and 80S fractions were combined and concentrated using a microcon column
polysomes: polyribosome fractions were combined and concentrated using two microcon columns. 1/16 of the concentrated samples was loaded on the Western blots.
D: Two of the five Western blots (made from the same samples) used for the quantification seen in C.

I also checked the polyribosome association of DHH1, which was found in the mass spectrometry results of the bloodstream free and membrane-bound polyribosomes, as well as in the procyclic membrane-bound polyribosomes (see table 6). DHH1 has been shown to be associated with polyribosomes in yeast (Sweet, Kovalak et al. 2012). It also has been shown that this protein is responsible for the regulation of RNA translation in trypanosomes (Kramer, Queiroz et al. 2010). As a DHH1 antibody was available (Hartmann, Benz et al. 2007), tagging of this protein as well as making new polysome gradients was not necessary. I used protein samples of already existing polysome gradients, made from cells that were crosslinked and treated with cycloheximide prior to harvesting (for profiles see fig. 22, 23 and 34).

As expected, DHH1 is enriched in the polyribosomal fractions, as compared to the negative control, trypanothione reductase (see fig. 25).

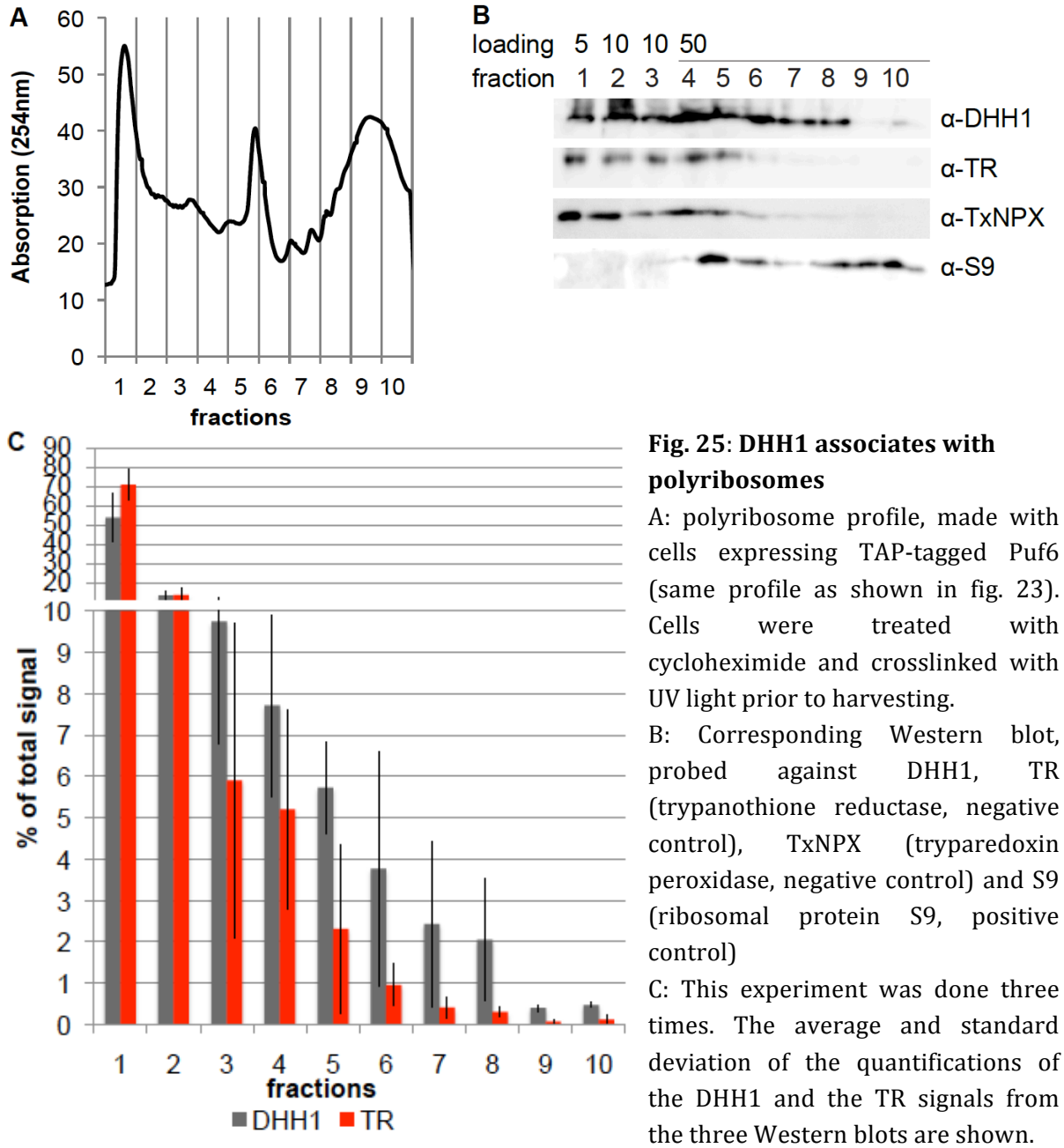

Fig. 25: DHH1 associates with polyribosomes

A: polyribosome profile, made with cells expressing TAP-tagged Puf6 (same profile as shown in fig. 23). Cells were treated with cycloheximide and crosslinked with UV light prior to harvesting.

B: Corresponding Western blot, probed against DHH1, TR (trypanothione reductase, negative control), TxNPX (tryparedoxin peroxidase, negative control) and S9 (ribosomal protein S9, positive control)

C: This experiment was done three times. The average and standard deviation of the quantifications of the DHH1 and the TR signals from the three Western blots are shown.

3.1.5 Summary of the mass spectrometry results of RNA binding proteins

The first four RNA proteins I tested (Puf6, Puf3, RBP29, ZC3H29) showed no polyribosome association, at least not to a detectable extent. For the ZC3H32 project, I tested the polyribosome association for this zinc finger protein as well (see 3.2.2, fig. 34), although it was found with only one unique peptide in the mass spectrometry results of the membrane-bound polyribosomes. ZC3H32 also showed no detectable association with polyribosomes. I later tested DHH1, which was found in the mass spectrometry results of three polyribosome preparations (see table 6). DHH1 was found in the polyribosome fractions to a larger extent than the negative control (see fig. 25), which strongly suggests that it associates with polyribosomes.
Nine other RNA binding proteins that were found in the mass spectrometry results were shown not to be associated with polyribosomes by different people (see table 6). This shows that in the large-scale polyribosome isolation method proteins present in a low amount in the polyribosomes are detected.
The main problem, as can be seen in figures 19-24, is, that there are many abundant proteins, for example trypanothione reductase, which trail down the gradient and contaminate the polyribosome samples.
Nevertheless, the obtained data can still be useful. However, precautions must be taken. A protein found in only one of the samples is probably not associated with polyribosomes unless it is a) specific for one life cycle stage or b) present with a lot of peptides (more than 6 (value for Puf2, which was tested negative)), like Ago1. Also, abundant proteins are more likely to be contaminants then non-abundant proteins (see calculations, 3.1.6).
Out of the five RNA binding proteins, which were found in three of the five samples (all except the procyclic free polyribosomes, which yielded fewer unique peptides than the other three), four were indeed found in the polyribosomes. The only exception was DRBD3 (also called PTB1), which was found not to be associated with polyribosomes by (Fernandez-Moya, Garcia-Perez et al. 2012). However, the results on DRBD3 are inconsistent: In the same study, Fernandez-Moya et al. found ribosomal proteins in eight TAP-purifications of DRBD3. Although ribosomal proteins are often contaminatants in affinity purifications (Ouna, Stewart et al. 2012), Fernandez-Moya et al. did not detect ribosomal contaminations in the TAP purifications of two other proteins (RRP44 and PABP2), suggesting that this interaction is genuine. Why the TAP purification of PABP2, which is polyribosomal associated (Kramer, Bannerman-Chukualim et al. 2013), did not yield ribosomal proteins is another question.
Also, it has been shown that DRBD3 is involved in *trans*-splicing and localizes partially to the nucleus (Stern, Gupta et al. 2009, Fernandez-Moya, Garcia-Perez et al. 2012). Fernandez-Moya et al. use 1% octyl-glucoside to lyse the cells (protocol adapted from (Kramer, Queiroz et al. 2010)). This might have, at least to a certain extent, lysed the nuclei. If this happened, the DRBD3 proteins, which were formerly localized to the

nucleus, would be present in the cleared cell lysate. This in turn would lead to a larger percentage of DRBD3 in the protein fraction of the polysome gradients.
D. Inchaustegui found DRBD3 in the polyribosomes of procyclic cells, but exclusively after crosslinking the cells (D. Inchaustegui, unpublished data). This suggests that DRBD3 associates with polyribosomes, but the association is unstable.
To sum this up, the currently available data on DRBD3 rather suggests that the fraction of this protein that localizes to the cytoplasm associates with polyribosomes. This means that all five proteins, which have been found in all three preparations and have been tested for polyribosome association, are indeed associated with polyribosomes.

Protein name	accession number	Number of unique peptides					association with polyribosomes tested by Western blot
		bs free	bs mb	pc mb	pc free A	pc free B	
AGO1	Tb927.10.10850			21			positive (Djikeng, Shi et al. 2003; Shi, Chamond et al. 2009)
NOT5	Tb927.3.1920	4	9				signal too weak
DHH1	Tb927.10.3990	2	4	6			positive
DRBD3/ PTB1	Tb09.211.0560	2	5	2			negative (Fernandez-Moya, Garcia-Perez et al. 2012), positive (D. Inchaustegui, unpublished data)
DDX60	Tb927.3.2600			8		1	n.d.
MKT1	Tb927.6.4770	3	2	2			positive (Singh, Minia et al. 2014)
PUF2	Tb927.10.12660		6				negative (B. Anand, PhD Thesis)
ALBA4/ ALBA3	Tb927.4.2030	1	2	2	1		positive* (Mani, Guttinger et al. 2011)
RBP42	Tb927.6.4440	3	1	2			positive (Das, Morales et al. 2012)
ZC3H41	Tb11.46.0009			5			n.d.
PUF6	**Tb927.10.11760**		**4**				negative
RPB29	**Tb927.10.13720**		**3**				negative, nuclear
PUF1	Tb927.10.4430		2				negative (Luu, Brems et al. 2006)
PUF3	**Tb927.10.310**		**2**				negative
ZC3H29	**Tb09.211.1130**		**2**				negative
DBP2	Tb927.10.6630		2				n.d.
PARN-3	Tb09.211.4350			2			n.d.
RBP11	Tb927.8.4450	2					n.d.
NOT2	Tb927.6.850	2					n.d.
ZC3H18	Tb927.7.2140		1				n.d.
ZC3H30	Tb927.10.1540		1				signal too weak
ZC3H32	**Tb927.10.5250**		**1**				negative
PBP1	Tb927.8.4540		1				positive (Singh, Minia et al. 2014)
SUB2	Tb927.10.540		1				nuclear (Serpeloni, Moraes et al. 2011)

Table 6: **RNA binding proteins found in the mass spectrometry results**.

bs free: bloodstream free polyribosomes (see fig. 14 C,D,E,F), bs mb: bloodstream membrane-bound polyribosomes(see fig. 14 A+B), pc mb: procyclic membrane-bound polyribosomes (see fig. 15 A+B), pc free A: procyclic free polyribosomes, 2nd mass spectrometry results (see fig. 15, B+C), pc free B: procyclic free polyribosomes, 1st mass spectrometry results (see fig. 11 A, B, E).

Color coding: Red: This protein associates with polyribosomes, blue: This protein is mainly not associated with polyribosomes, green: Results are unclear (see text).

signal too weak: the association with polyribosomes could not be determined, because the Western blot signal from the tagged cell line was too weak.

*: ALBA3 was found to be partially associated with polyribosomes, while ALBA4 is not. However, these two proteins cannot be distinguished by mass spectrometry (Mani, Guttinger et al. 2011).

Proteins written in bold were tested for polyribosome association by myself (see figures 19- 25 or respectively, 3.3.2 for the results on ZC3H32).

3.1.6 RNA binding proteins in polyribosomes

As five of the six RNA binding proteins I tested were found not to be associated with polyribosomes, at least not to a detectable extent, it was questioned whether it is likely to detect an RNA binding protein on the polyribosomes.

Because of this, I made the following calculation:

A bloodstream trypanosome cell contains approximately 20 000 RNAs (Haanstra, Stewart et al. 2008). In comparison, the levels of putative RNA binding proteins are quite high. The are $4x10^5$ RBP10 proteins per cell (PhD Thesis, Martin Wurst), PUF5 proteins are present at less than $5x10^4$ proteins per cell (Jha, Archer et al. 2013) and PUF2 proteins are present at approximately $1.5x10^4$ proteins per cell (PhD Thesis, B.Jha).

For my calculations, I assumed that the normal protein levels of other RNA binding proteins are similar, meaning in a range from $5x10^4$ to $5x10^5$.

I also considered that very abundant proteins, for example trypanothione reductase, tend to trail down the gradient and therefore are also partially found in the polyribosome fractions. Using the quantifications of the trypanothione reductase signal from six Western blots of polyribosome gradients (made with non-crosslinked cells), I calculated that, on average, 2% of the trypanothione reductase protein pool is found on the polyribosome fractions.

In order to prove that a protein is really associated with polyribosomes and not just a contamination, a larger percentage than 2% of this protein should be present in the polyribosomes.

Assuming now that a protein binds to 5% of the RNA, which would be 1000 RNA molecules per cell, and there are $1x10^5$ copies of this protein per cell, only 1% of this protein would be bound to RNA and therefore could be found on the polyribosomes.

This would be nearly impossible to detect by Western blot.

The percentage of protein bound to RNA gets larger if there is less protein per cell, however, as these proteins are not abundant they are hard to detect on a Western blot to start with (see fig. 26, A).

The percentage also increases if a protein has more RNA targets and also if each target RNA is bound by more than one copy of the protein (see fig. 26, B). If six or more copies of a protein bind to each target RNA and these target RNAs are currently being translated, it should be possible to detect this protein in the polyribosomes.

Considering, however, that probably the majority, but not all of the target RNAs are found on the polyribosomes (see fig. 26, C) or bound to their protein binding partner, the percentage is even less than shown in figure 26 A and B.

Regarding these results, in the future, if no antibody is available, only endogenously tagged proteins should be used in order to test polyribosome association. For example, I used exogenously expressed TAP-tagged Puf6 and Puf3 constructs that are transcribed by PolI, which probably lead to higher protein levels. That might have diminished the percentage of protein found on the polyribosomes and thus lead to a false negative result.

In conclusion, it is no problem to detect RNA binding proteins with multiple RNA targets, like translation initiation factors or PABP, in the polyribosomes. However, proteins binding to only a small pool of target RNAs (less than 10%) cannot be shown to be associated with polyribosomes using this method, especially if only one copy of this protein binds to each target RNA.

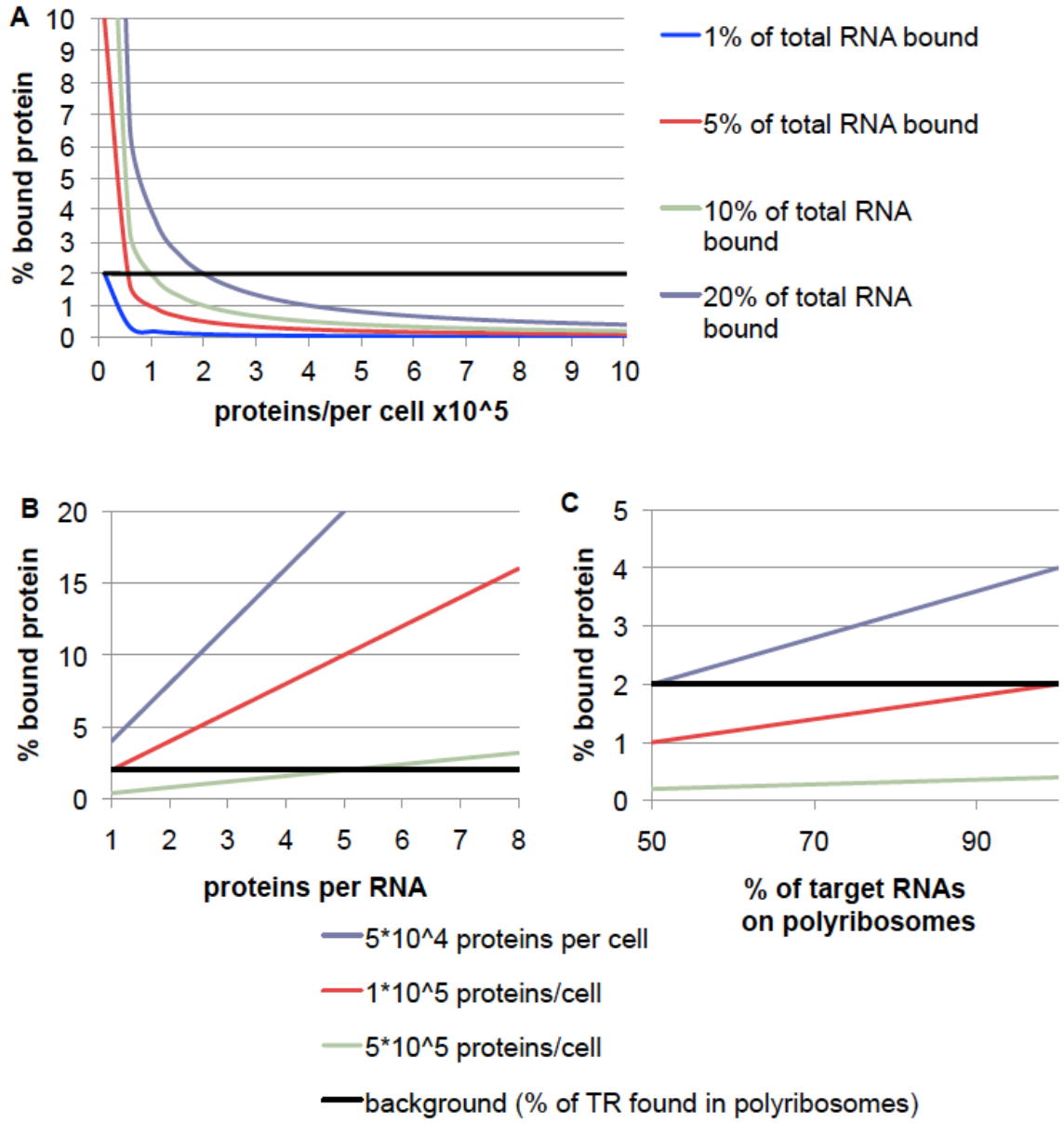

Fig. 26: Diagrams illustrating the possibility to detect an RNA binding protein on the polyribosomes by Western blot

Background: % trypanothione reductase found in polyribosomes. On average, 2% of trypanothione reductase is found in the polyribosomes (fractions after the 80S peak). The data was taken from six Western blots from six different polyribosome gradients (for quantifications see fig. 19 and 20). If the fraction of a protein that associates with the polyribosome is not larger than this background, its polyribosome association probably cannot be detected by Western blotting. A: percentage of protein bound to RNA ("bound protein") plotted against proteins per cell times 10^5. B: percentage of protein bound to RNA plotted against the number of proteins bound to each target RNA. C: percentage of protein bound to RNA plotted against the percentage of the target RNA found on polyribosomes.

3.2 VSG mRNP pull-down

3.2.1 Plan of experiment

The aim of these experiments was to pull down proteins binding to the *VSG* mRNA. For this, it was planned to pull-down the *VSG* mRNP using antibodies binding to the nascent polypeptide. In order to get rid of most of the mature VSG, which would compete with the nascent polypeptide for the antibody, the pull-down would be done with the polyribosome fractions, as the majority of the mature VSG is found in the protein peak. The antibody-bound mRNPs would then be precipitated using protein-A beads. The enrichment of *VSG* mRNPs in the precipitates was checked by Northern blot, however, in the following shown experiment no enrichment of *VSG* mRNA was observed.

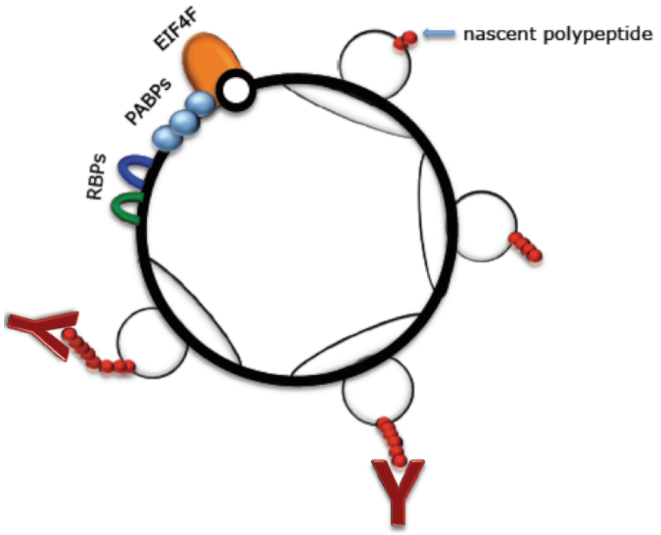

Fig. 27: **Schematic representation of mRNA pull-down.**

3.2.2 VSG222 cell line

For the VSG pull-down experiments, it was planned to create a cell line expressing VSG222 under antibiotic selection. However, the creation of this cell line failed (for plasmid see 2.13.1, table 2 and fig. 9), no clones were obtained.

In order to continue with these experiments, a mainly VSG222 expression cell line was obtained using clonal selection. For this, bs1313 cells were diluted down to 12.5 cells/ml and distributed on a 96 well/plate. 40µl were used per well, resulting into, on average, 0.5 cells/well.

The cells were checked by Western blot, the clone with the strongest signal when probed with the VSG222 antibody was chosen.

In order to prevent RNA degradation from RNAses in the antibody, the antibody was purified by binding to protein-A beads and then eluting it at pH 2.7 (see Materials and Methods 2.10.1).

However, the first mRNP pull-downs did not show an enrichment of VSG222. The yield also did not increase with the double amount of antibody (20µl).

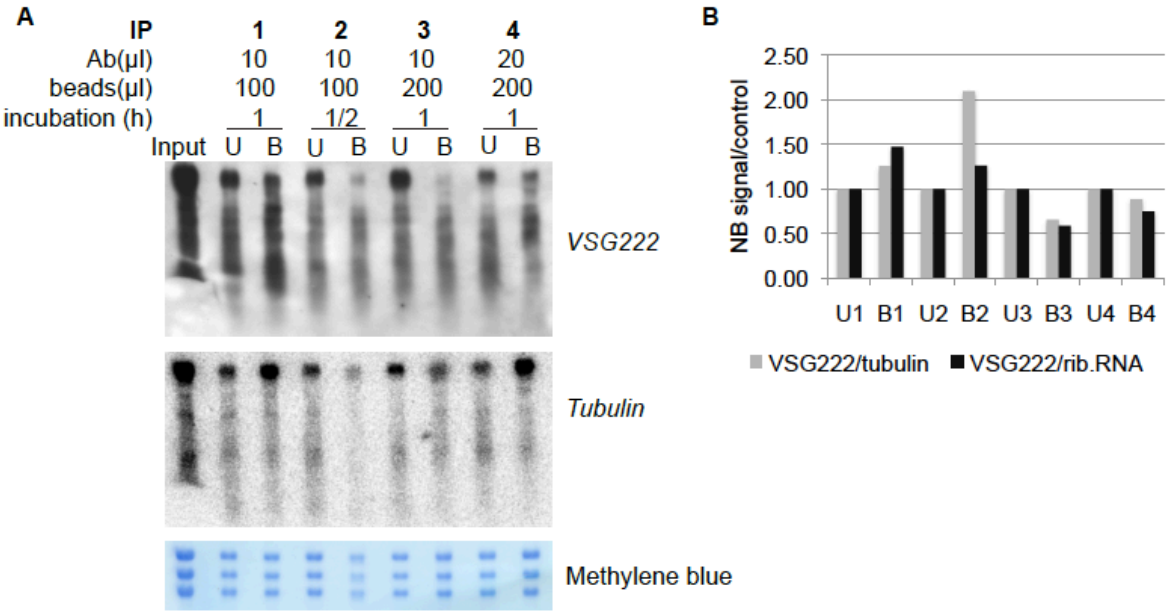

Fig. 28: *VSG222* RNA did not accumulate in the precipitate after the mRNP pull-down.
Four different Immunoprecipitation were made with the polyribosomal fractions of one gradient. Different amounts of antibody (10µl or 20µl) and beads (100µl or 200µl) were used. The incubation time of the Immunoprecipitations was 1hour, with the exception of IP2 (1/2 hour). The total volume of pooled polyribosomes was approximately 2.8ml. 600µl were used for each IP, 300µl were used for the Input sample. For exact protocol, see 2.10.1
A: Northern blot, probed against VSG222 (DIG-labeled probe) and tubulin (^{32}P labeled probe)
Input: Sample from the pooled polyribosome fractions that were used for the Immunoprecipitation. The volume of the Input sample was 300µl, which corresponds to appr. $0.85 \cdot 10^8$ cells.
U: Unbound fractions. 300µl samples were used, which corresponds to appr. $0.85 \cdot 10^8$ cells.
P: Precipitate. Trifast was added to the ProteinA beads after the immunoprecipitation in order to elute the bound RNAs. The samples correspond to appr. $1.7 \cdot 10^8$ cells.
B: quantification of Northern blot shown in A. The VSG signal was divided by tubulin signal (neg. control, grey columns) and the ribosomal RNA signal (from the methylen blue stain, black columns).

3.2.3 VSG118 antibody pull-downs

In order to get a cell line in which the expression of a single VSG was maintained by drug selection, a plasmid from Mark Carrington was used which should express VSG118 under drug control (pHD 3850, for vector map see 2.14, figure 9).
A VSG118 antibody was received from J.Banks.
It was planned to make another VSG118 antibody, but the His-tagged protein was not expressed enough for purification.
A VSG118 peptide antibody was made, but this antibody gave a lot of background on a Western blot. It was also not useful in the immunoprecipitations (see fig. 29 and 30).
The created cell line expressed a VSG that was recognized by the antibody and pulled down by it with high affinity. The pull-down was done with ^{35}S-labeled cells, in order to get rid of the background signal from the antibody (see fig. 29A).
However, the RNA could not be detected with *VSG118* probes, neither radioactive nor non-radioactive probes. Thus, it was concluded that these cell lines did not express VSG118 but are false positives.
I tried to identify the unknown VSG by making first strand cDNA, do a PCR for the 2nd strand using the VSG consensus sequence and then cloning the DNA into the P2T7 blue Plasmid. However, I did not receive any usable clones.
Then I received a VSG118 expressing cell line from Markus Engstler (called VSG118 cells in the following figures). The cell line was used for the mRNP pull-down. However, also no enrichment of *VSG* mRNA was observed after the VSG pull-down (fig. 30 A+B). The pull-down was also not so successful on the protein level (fig. 30 C). A pull-down with ^{35}S-labeled cells was also not successful, but it remains unclear whether this was because of faults in the experiment or whether VSG118 is not pulled down by its antibody. Another change in the IP procedure, in opposite to the first ^{35}S labeling experiment (see fig. 29A) was that the sucrose concentration was adjusted to 30% in order to mimic the sucrose concentration in the polyribosome fractions. Therefore, it might be possible that the pull-down does not work in this sucrose concentration. This would be a huge disadvantage as well.
But it was possible to pull-down at least a part of the VSG protein in an immunoprecipitation with a different buffer, as used by (Schutz, Kieval et al. 1977).
It might be possible to pull down the *VSG* mRNP with these cells, but this method still requires a lot of adjustment in order to work properly.
I tried to transfect these cells once with Mark Carrington's 3850 plasmid, but received no clones. However, if this project would be picked up again, I would recommend to try again to make this cell line, as the VSG118 cells switch quickly (within two weeks) when cultured and then the VSG cannot be detected by Northern blot anymore.

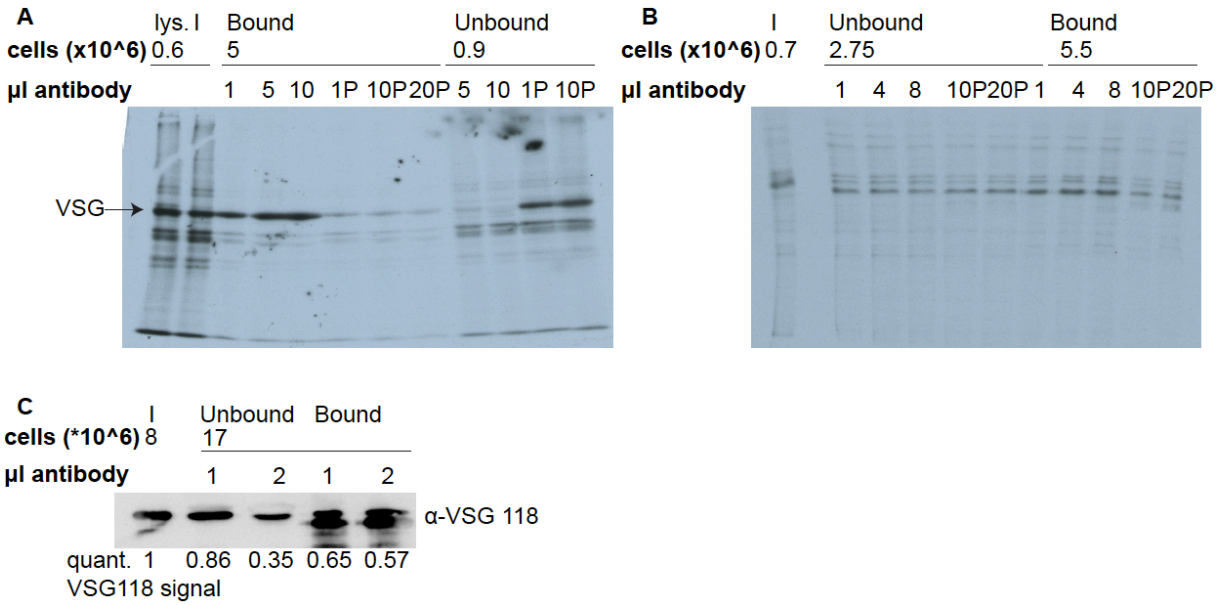

Fig. 29: **Pull-down of VSG protein using the VSG118 antibody and the VSG118 peptide antibody**

A and B: IP-experiments using cells labeled with ^{35}S-methionine labeling. A: pull-down with the bs1313 3850 cell line in polyribosome buffer. 1µl, 5µl and 10µl were used of the VSG118 antibody (labeled 1,5,10), 1µl, 10µl and 20µl were used from the peptide antibody (labeled 1P, 10P and 20P). The antibody was mixed with proteinA beads (100µl). $5 \cdot 10^6$ cells were used per IP. B: Same experiment, done with the VSG118 cell line, in 30% sucrose. 1µl, 4µl and 8µl of the VSG118 antibody were used (labeled 1,4,8), 10µl and 20µl of from the peptide antibody were used (labeled 10P and 20P). $5.5 \cdot 10^6$ cells were used per IP. No enrichment of VSG was observed.
C: Western blot with unlabeled cells. Pull-down with VSG118 cell line with different buffer as used by (Schutz, Kieval et al. 1977). 1µl and 2µl were used of the VSG118 antibody.

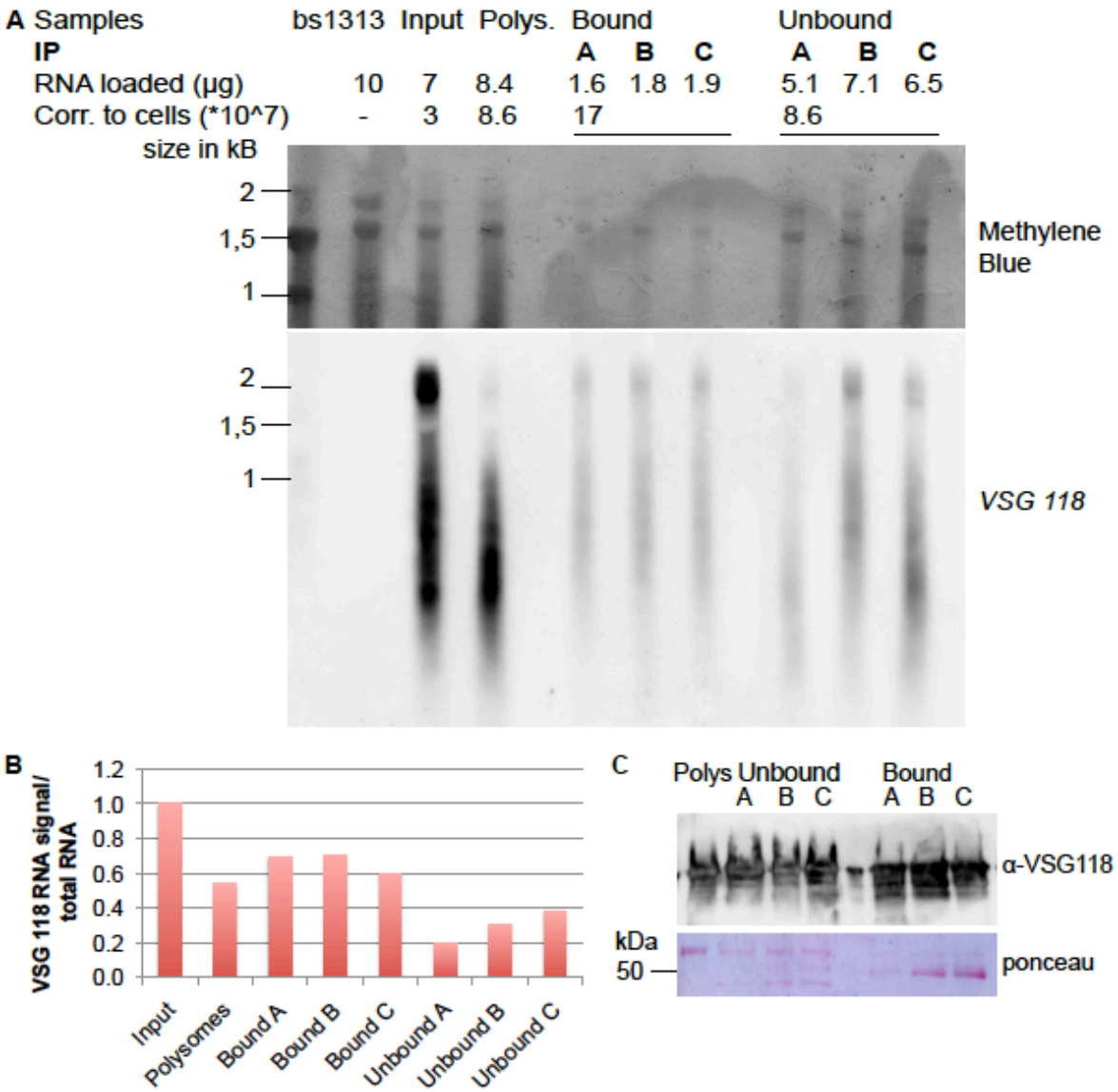

Fig 30: mRNP pull-down with VSG118 cells.

$6 \cdot 10^8$ cells were used for this experiment. A: Northern blot probed against *VSG 118*.

bs 1313: Wild type cells expressing mainly VSG222, Input: cleared lysate, before sucrose gradient centrifugation, Polys: sample of the pooled polyribosome fractions. The remaining polyribosomes were split in three parts and 3 IPs (with 100µl Poly-A beads and different amounts of VSG118 antibody) were made: A: 2,5µl VSG 118 antibody, B: 6,25µl VSG 118 antibody, C: 12,5µl VSG 118 antibody

Corr. to cells: loaded RNA amount corresponds to X · 10^7 cells. 600µl of the pooled polyribosomes were used per IP, this corresponds to $1.7 \cdot 10^8$ cells. 300µl samples were used for the polyribosomes and unbound mRNA samples, this corresponds to $8.6 \cdot 10^7$ cells. U: Unbound fraction, supernatant after the immunoprecipitation. Bound: RNA bound to the beads.

B: quantification of Northern blot: The *VSG118* signal was divided by the total RNA amount loaded on the Northern blot (measured by nanodrop) and normalized to the input.

C: Western blot made from samples from the same IP. 30µl from the pooled polyribosomes and the unbound fractions and 1/20th of the beads was taken as samples (corresponds to appr. $8.5 \cdot 10^6$ cells/lane).

3.3 The role of ZC3H32

3.3.1. Structure and expression

ZC3H32 is a 655 amino acid long zinc finger protein with three CCCH zinc finger domains, two conventional 7-5-3 C3H domains (see fig. 31) and one unconventional 9-5-3 C3H domain (Kramer, Kimblin et al. 2010). These zinc finger domains are conserved among kinetoplastids (*T. b. brucei, T. cruzi, L. major*).

ZC3H32 was found to be a potential binding partner of MKT1 (Singh, Minia et al. 2014) which was suggested by the results of a TAP purification and a yeast two hybrid assay. As shown by (Singh, Minia et al. 2014), ZC3H32 carries the binding motive for MKT1, the HNPY motif, in this case being HTNNPY. This motif is conserved between *T. brucei* and *T. cruzi*, but not from *T. brucei* to *L .major.*

Initially, it was thought that ZC3H32 would stabilize mRNAs with a similar mechanism as the one proposed for ZC3H11 (as described by (Singh, Minia et al. 2014)) see 1.7, fig. 8), namely by binding MKT1, which binds PBP1, which in turn binds the poly-A binding protein, which binds to the poly-A tail and thus protects the RNA from degradation. However, this hypothesis was soon abandoned, as ZC3H32 seems to destabilize mRNAs rather than to stabilize them (see 3.3.8).

The SILAC proteomic analysis by (Urbaniak, Guther et al. 2012) showed that the protein level of ZC3H32 is approximately 17 times higher in the bloodstream form as compared to the procyclic form. The results from (Siegel, Hekstra et al. 2010) indicated that the *ZC3H32* RNA is approximately two fold enriched in the bloodstream form. Sequencing results form our lab (Fadda, Ryten et al. 2014) also show an enrichment of the *ZC3H32* RNA in the bloodstream from (2.5 to 3.9 fold). Northern blot analysis showed that this up-regulation is indeed present (see fig. 32).

Thus, it can be concluded that ZC3H32 is differentially regulated during the life cycle and seems to play a bigger role in the bloodstream form as compared to procyclics.

ZC3H32 was found in the mass spectrometry results from the bloodstream membrane-bound polyribosomes, however, only one unique peptide was found.

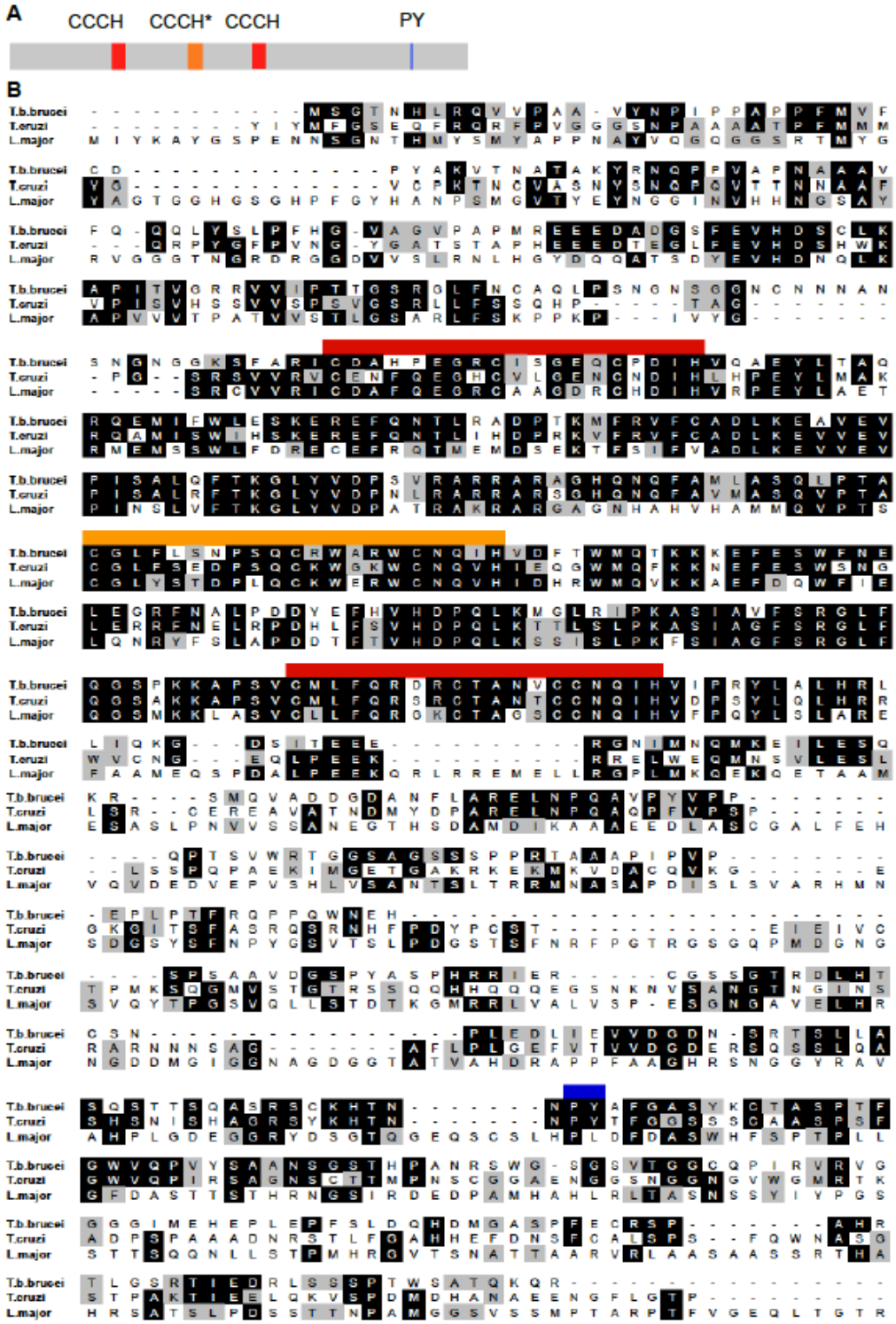

Fig. 31: **Structure of *Tb*ZC3H32 and alignment of its trypanosomtid homologues**

A: Schematic structure of *Tb*ZC3H32, with zinc finger domains as determined by (Kramer, Kimblin et al. 2010). Conventional 7-5-3 zinc finger domains (CCCH) are shown in red, the unconventional 9-5-3 zinc finger domain (CCCH*) is shown in orange. The MKT1 binding motive (HNPY motive) is shown in blue. B: Alignment of ZC3H32 homologues from *T. b. brucei*, strain 427 to *T. cruzi* and *L. major*. Identical amino acid residues are shown in black, similar residues in grey. Zinc finger domains are again shown in red or orange and the HNPY motive in blue. The alignment was done using CLUSTALW

(http://npsa-pbil.ibcp.fr/cgi-bin/npsa_automat.pl?page=/NPSA/npsa_clustalw.html), and the BOXSHADE software (http://mobyle.pasteur.fr/cgi-bin/portal.py#forms::boxshade) and then edited using Microsoft excel.

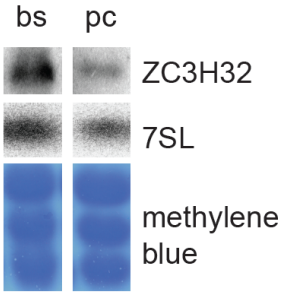

Fig. 32: **ZC3H32 is up-regulated in the bloodstream form**
Comparison of ZC3H32 RNA levels between bloodstream wildtype (bs) and procyclic wildtype (pc). The 7SL RNA, as well as the methylene blue stain, was used as loading control.

3.3.2 Localization of ZC3H32

In order to find out the localization of ZC3H32, cells expressing C-terminally myc-tagged ZC3H32, as well as wild type cells, were analysed by immunofluorescence. A cell line expressing the tethering construct, which is N-terminally tagged with the λN-peptide and C-terminally tagged with two myc-tags, was also analyzed, because this cell line showed a stronger expression of the myc-tagged construct as compared the ZC3H32-myc cell line. This was tested by Western blot.

The myc-tagged constructs were ectopically expressed, under the control of a Tet promoter. The expression was induced 24h before the cells were harvested and fixed to the glass slides.

As can be seen in fig. 32, myc-tagged ZC3H32 localizes to the cytoplasm. As the myc-tagged version of ZC3H32 is functional (see section 3.3.6), this strongly suggests that the untagged protein is cytosolic as well. λN-ZC3H32-myc also localizes to the cytoplasm.

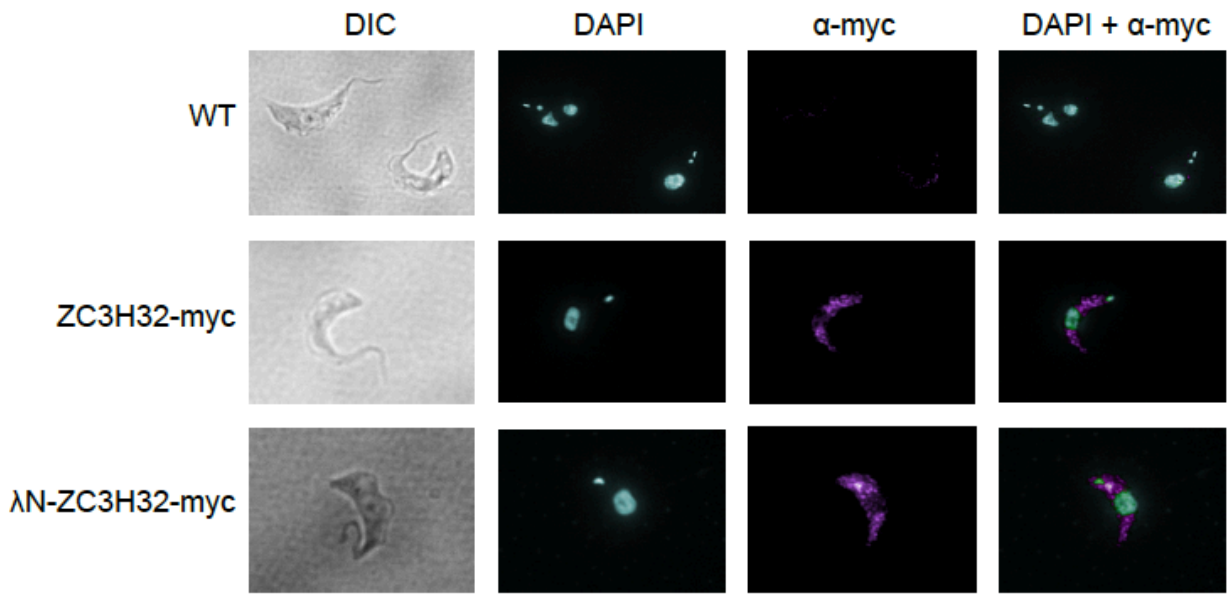

Fig 32: ZC3H32 localizes to the cytoplasm
Immunofluorescence with wild type, ZC3H32-myc, and λN-ZC3H32-myc cells.

ZC3H32 is probably not associated with the polyribosomes. The mass spectrometry results of the large-scale polyribosome preparation suggested it to be in the membrane-bound fraction of the bloodstream polyribosomes (see table 6). However, it was shown by Western blotting (see fig. 34) that only a minor fraction of the V5-tagged version of this protein is found in the polyribosomes, less than compared to a negative control. Also, when the polyribosomes are dissociated by RNAseA treatment, the migration pattern of ZC3H32 on the Western Blot does not change, in opposite to the migration pattern of the ribosomal protein S9 (see fig. 34D and G). Cycloheximide treatment followed by UV-crosslinking prior to harvesting the cells, which should stabilize the RNA-protein interaction, also did not change the pattern.
This strongly suggests that the majority of the ZC3H32 protein is not associated with polyribosomes. However, as calculated in 3.1.6, it might be that a fraction of the ZC3H32 pool is associated with polyribosomes, but this fraction might be too small to be recognized on a Western blot.

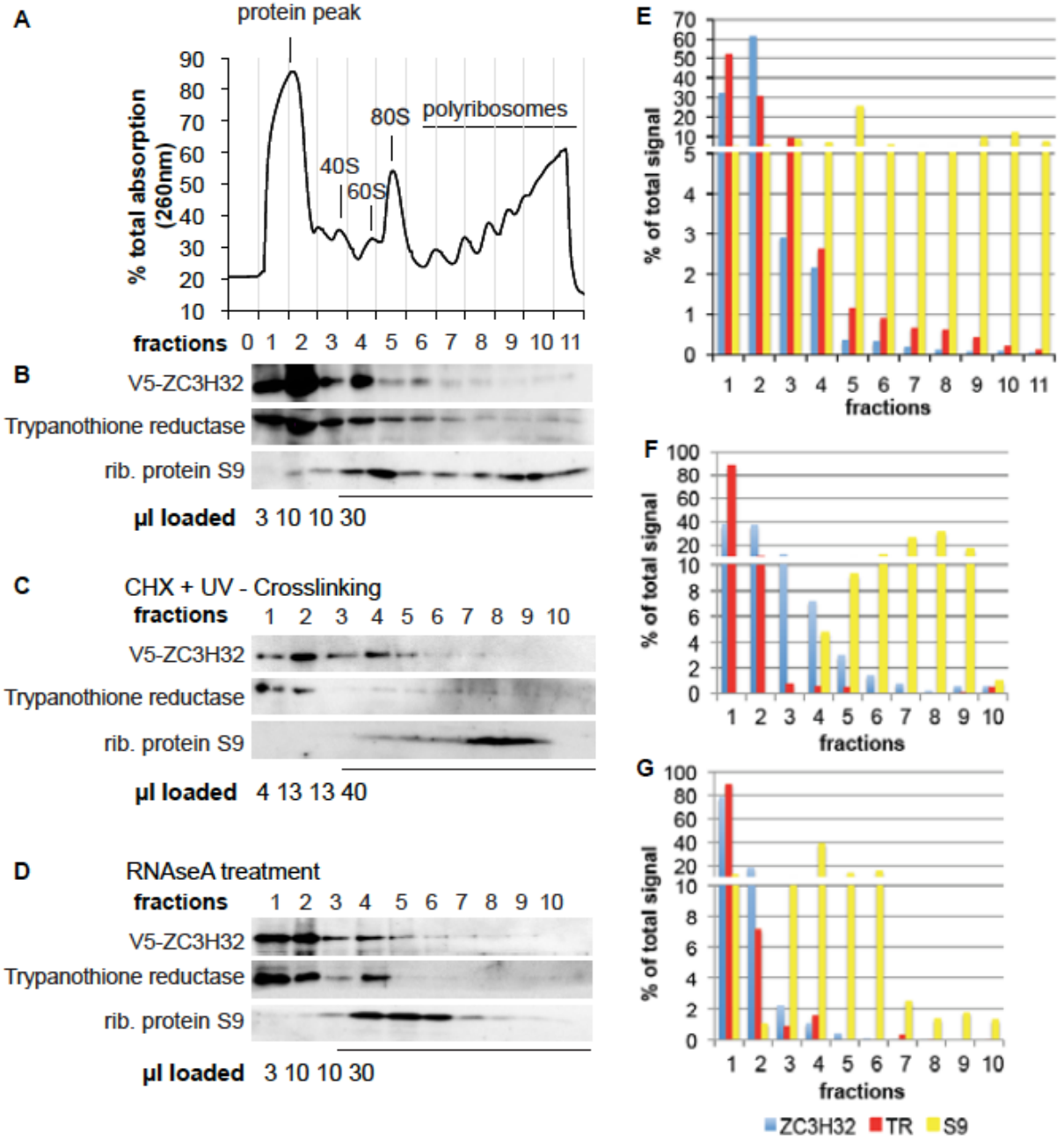

Fig 34: ZC3H32 is mainly not associated with polyribosomes

A: Polyribosome profile of V5-ZC3H32 cells. B: Western Blot made with samples of the fractions from the polyribosome gradient shown in A. 3-10µl was loaded per lane (the total volume of each fraction is approximately 400µl) A smaller amount of sample was loaded from the first three in order to compensate for the large amount of protein present in those. Trypanothione reductase was used as a negative control, the ribosomal protein S9 as a positive control. C: Western Blot with samples from a polyribosome gradient with V5-ZC3H32 cells which were treated with cycloheximide, followed by UV-crosslinking prior to harvesting. When the cells are harvested with UV-crosslinking, more cells are lost than without. Therefore, a larger amount of material was loaded on this blot in comparison to B and D. D: Western Blot with samples from a polyribosome gradient with V5-ZC3H32 cells that were treated with RNAseA after lysis. E, F G: quantifications of Western Blots B, C, D respectively. Percentage calculations take the unequal loading into account.

3.3.3 ZC3H32 interacts with MKT1

A yeast-two-hybrid assay with MKT1, as well as the mass spectrometry results of a TAP purification of MKT1, suggested ZC3H32 as a putative binding partner of MKT1 (Singh, Minia et al. 2014). However, Co-Immunoprecipitation of ZC3H32 (V5 or myc tagged) and YFP-MKT1, showed that only a very small proportion of the ZC3H32-protein pool interacts with MKT1.

This interaction is also observed when the RNA is degraded using RNAseA. This shows that the interaction between ZC3H32 and MKT1 is not dependent on mRNA. It also proves that these two proteins genuinely interact and are not just found on different binding sites of the same target mRNAs.

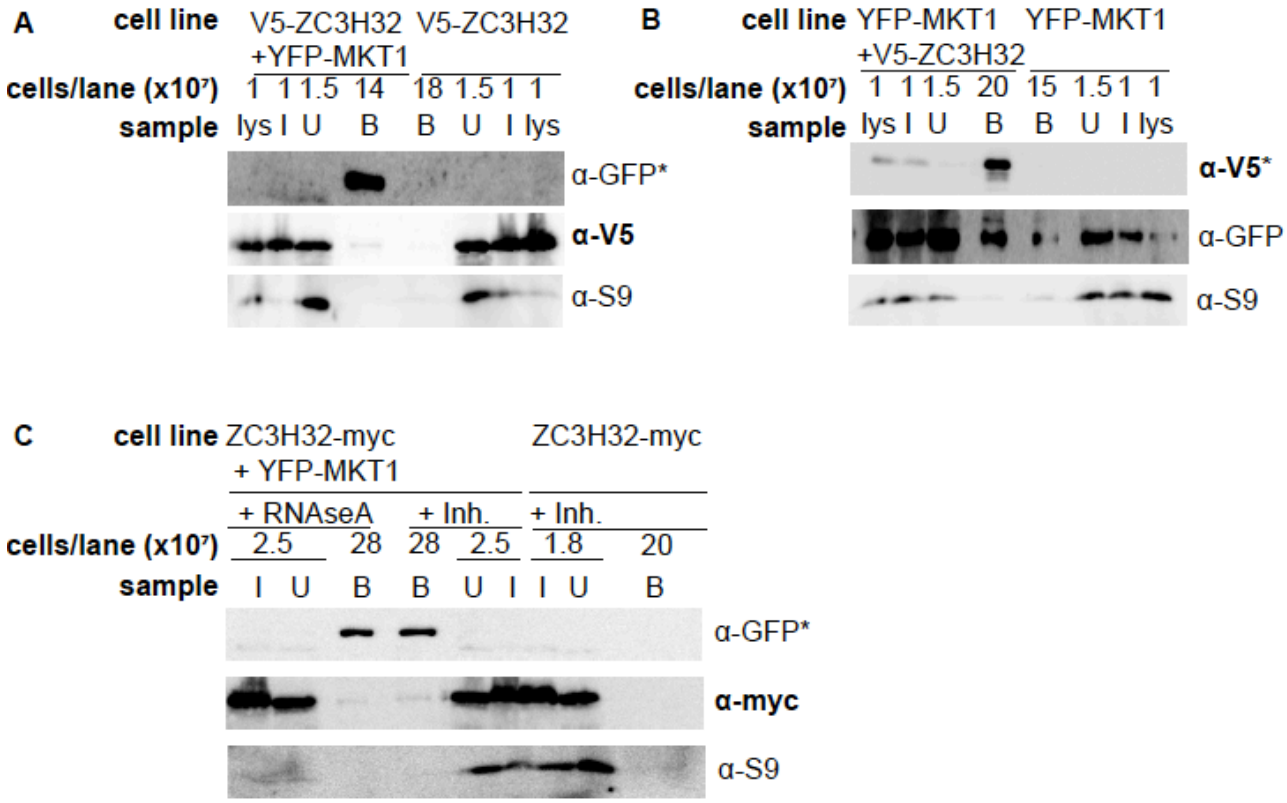

Fig. 35: **ZC3H32 interacts with MKT1, even in the presence of RNAse inhibitor**

* marks the antibody which was used for the precipitation (e.g. α-myc in a pull down with α-myc beads, α-GFP in a pull down with GBP beads). GBP: GFP binding peptide, binds to GFP and YFP. Antibody recognizing the tagged ZC3H32 (either V5 or myc tagged) is written in bold

A: Western blot of affinity purification of YFP-MKT1 and V5-ZC3H32 with GBP-beads (bind to YFP-tag). lys: lysed cells, I: Input (cell lysate cleared by centrifugation), U: unbound fraction, supernatant after IP, B: bound fraction (boiled beads). S9 was used as control. The GFP antibody recognizes the YFP-tag.

B: Western blot of Co-IP of V5-ZC3H32 and YFP-MKT1 with V5-beads. S9 was used as control.

C: Western blot of affinity purification of YFP-MKT1 and V5-ZC3H32 with GBP-beads in the presence of RNAseA (+RNAseA) or RNAse Inhibitor (+Inh)

3.3.4 MKT1 does not interact with the CAF-NOT deadenylation complex component NOT2

NOT2, which is a part of the CAF1-NOT deadenylation complex, was suggested as a binding partner for MKT1 in a yeast-two-hybrid screen (Singh, Minia et al. 2014). Two other components of this complex (CAF40 and NOT1) were co-purified with MKT1 in a TAP purification (Singh, Minia et al. 2014). This suggested an association of MKT1, and thus, possibly, ZC3H32, with the CAF1-NOT deadenylase complex. However, this interaction could not be confirmed by co-immunoprecipitation (see fig. 36).

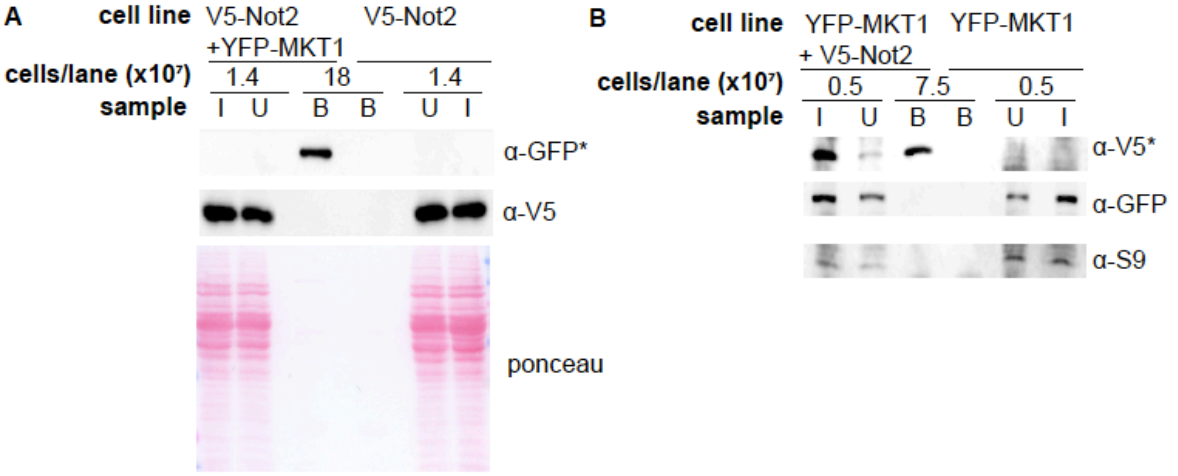

Fig. 36: **MKT1 does not interact with NOT2**

* marks the antibody which was used for the precipitation (e.g. α-myc in a pull down with α-myc beads, α-GFP in a pull down with GBP beads)

A: Western blot of a co-affinity purification with YFP-MKT1 and V5-NOT2 with GBP-beads (GBP binds to the YFP-tag). I: Input (cell lysate cleared by centrifugation), U: Unbound fraction, Supernatant after IP; B: Bound fraction (boiled beads). S9 was used as negative control.

B: Western blot of Co-IP with YFP-MKT1 and V5-Not2 V5-beads. S9 was used as negative control.

3.3.5 ZC3H32 is essential in the bloodstream form

The RNAi screen from Alsford et al. (Alsford, Glover et al. 2005) suggested that ZC3H32 is essential in the bloodstream form, but not in procyclics. In order to test that, ZC3H32 was knocked down in bloodstream and proyclic cells.

Knock-down of ZC3H32 in the bloodstream form lead to a growth defect (see fig. 37, growth curve A and D, Northern blot C and Western blot E). The knock-down was confirmed by Northern blotting (see fig. 37 C).

The decrease of ZC3H32 on the protein level was shown with a Western blot, by inducing RNAi in bloodstream cells expressing endogenously V5-tagged ZC3H32. The protein levels dropped to approximately a tenth of the original level after one day. No protein or RNA samples could be collected for day two and three, as there was almost no cell growth. The protein levels increased on day four, synchronously with the recovery of the cells.

Poly-A+ RNA isolated from the RNAi cell line shown in A and C was sent for high-throughput sequencing (see 3.3.11).

The RNAi in procyclics was not successful (data not shown). Six clones were tested, but none of them showed any significant reduction of the ZC3H32 RNA levels, which are already low in this life cycle stage.

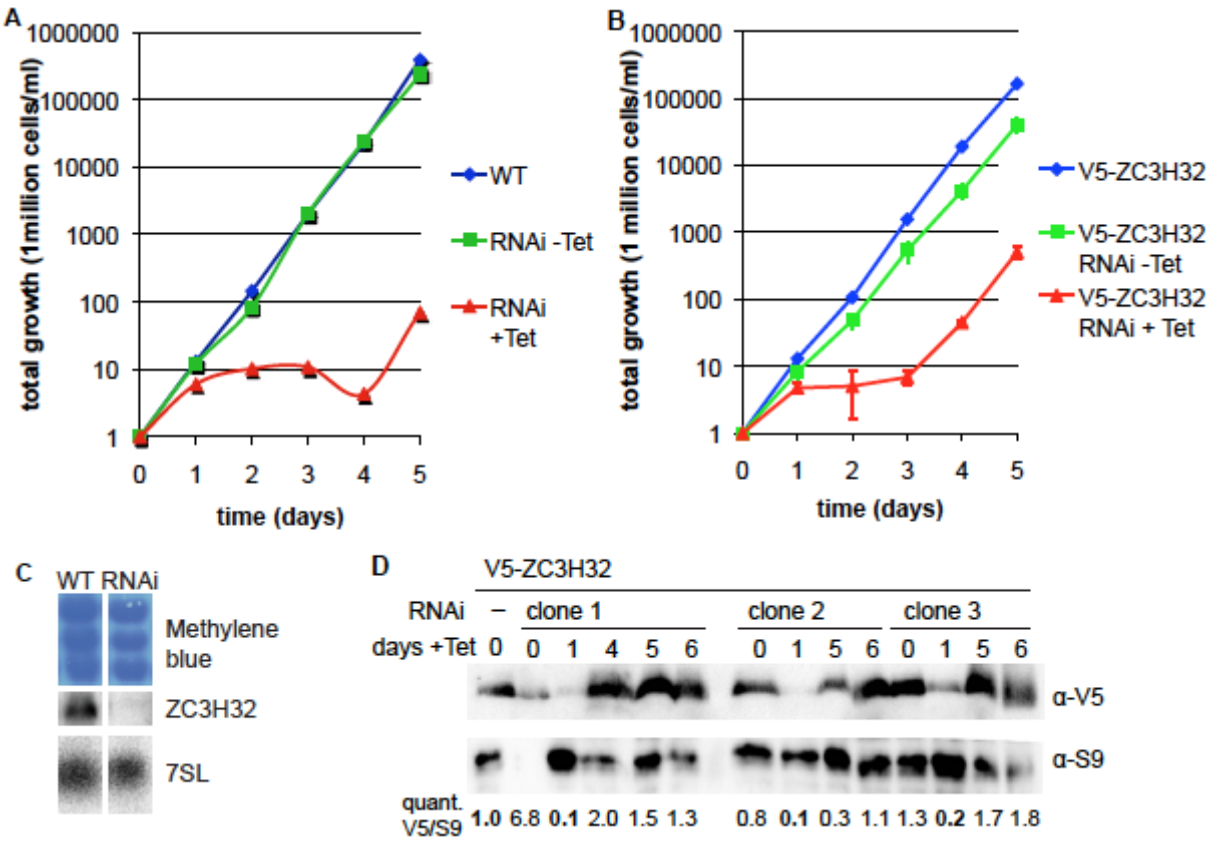

Fig. 37: ZC3H32 is essential in bloodstream form trypanosomes.

A: Cumulative growth curve of bloodstream cells with RNAi against ZC3H32

B: Cumulative growth curve of bloodstream cells with ZC3H32 RNAi expressing V5-ZC3H32. The average and standard deviation of three clones is shown.

C: Northern blot corresponding to growth curve A with samples from wildtype bloodstream cells (WT) and ZC3H32 RNAi cells, induced for 24h (RNAi)

D: Western blot with V5-ZC3H32 cells, with (clone 1-3) and without RNAi (-). Samples were taken before induction, one day after induction (quantification shown in bold) and after the recovery of the cells (4-6 days). The quantification was normalized to the parental cell line (RNAi -).

3.3.6 Knock-out cell lines

In order to test whether the C-terminally myc-tagged ZC3H32 protein, as well as the N-terminally V5-tagged version, were functional, knock-out cell lines were created.
In the cell lines expressing the endogenously expressed V5-ZC3H32, the non-modified copy of the *ZC3H32* gene was knocked out, using a knock-out plasmid carrying a puromycin resistance (plasmids see 2.14). In the cell lines expressing the exogenously expressed ZC3H32-myc, one copy of the gene was knocked out first. Two clones were selected, the expression of the inducible myc-tagged version was induced by adding tetracycline and the cell lines were transfected with the other knock-out vector. The induction was done just prior to the transfection. The clones received from this transfection were maintained in medium containing tetracycline.
It was possible to create both single knock-out V5-ZC3H32 cell lines, as well as double-knock out myc tagged cell lines.
The knock-outs were confirmed by PCR (see fig. 38). Two different sets of primers were used for the confirmation of the knock-outs. One set binds in the ORF of *ZC3H32* (see fig. 38, shown in red). As every cell line possesses either the inducible *ZC3H32-myc*, the endogenous *ZC3H32* or *V5-ZC3H32*, this PCR should be, and was, positive for each genomic DNA sample.
The forward primer of the other set binds in the 5'UTR of *ZC3H32*, the reverse one in the ORF (see fig. 38, shown in black). This PCR yielded no product in the double knock-out cell lines, as these do not possess the endogenous *ZC3H32*.
The V5-ZC3H32 cell line possesses both a non-modified endogenous copy and *V5-ZC3H32*, in which the sequence of the V5-tag, the blasticidin resistance gene, as well as two UTRs, are inserted between the ORF and the 5'UTR. Therefore, for this cell line, the PCR yields two products: A shorter one corresponding to the unmodified *ZC3H32* locus (predicted size: 1109bp), and another, longer PCR product, corresponding to *V5-ZC3H32* (predicted size: 2130bp). For the V5-ZC3H32 single knock-out cell lines, possessing only the tagged endogenous ZC3H32, the PCR yields only the larger product corresponding to the tagged version. Thus, the single knock-out is confirmed.

The fact that it was possible to create both V5-ZC3H32 single knock-out cell lines as well as double knock-out ZC3H32-myc cell lines shows that both tagged versions are, at least partially, functional. The V5 single knock-out cell lines grow a bit slower than the V5-tagged cell line still containing the other ZC3H32 copy (see fig. 39).
The double-knock out cell lines grow well in the presence of tetracycline, which induces the exogenous ZC3H32-myc. Once tetracycline is removed, by spinning down the cells and resuspending them in new media, their growth is arrested (see fig. 39).
This not only shows that the myc-tagged version is functional, but also confirms that ZC3H32 is essential for cell proliferation in the bloodstream form.
After about four days, the cells recover and re-express the myc-tagged protein (Fig. 39, D).

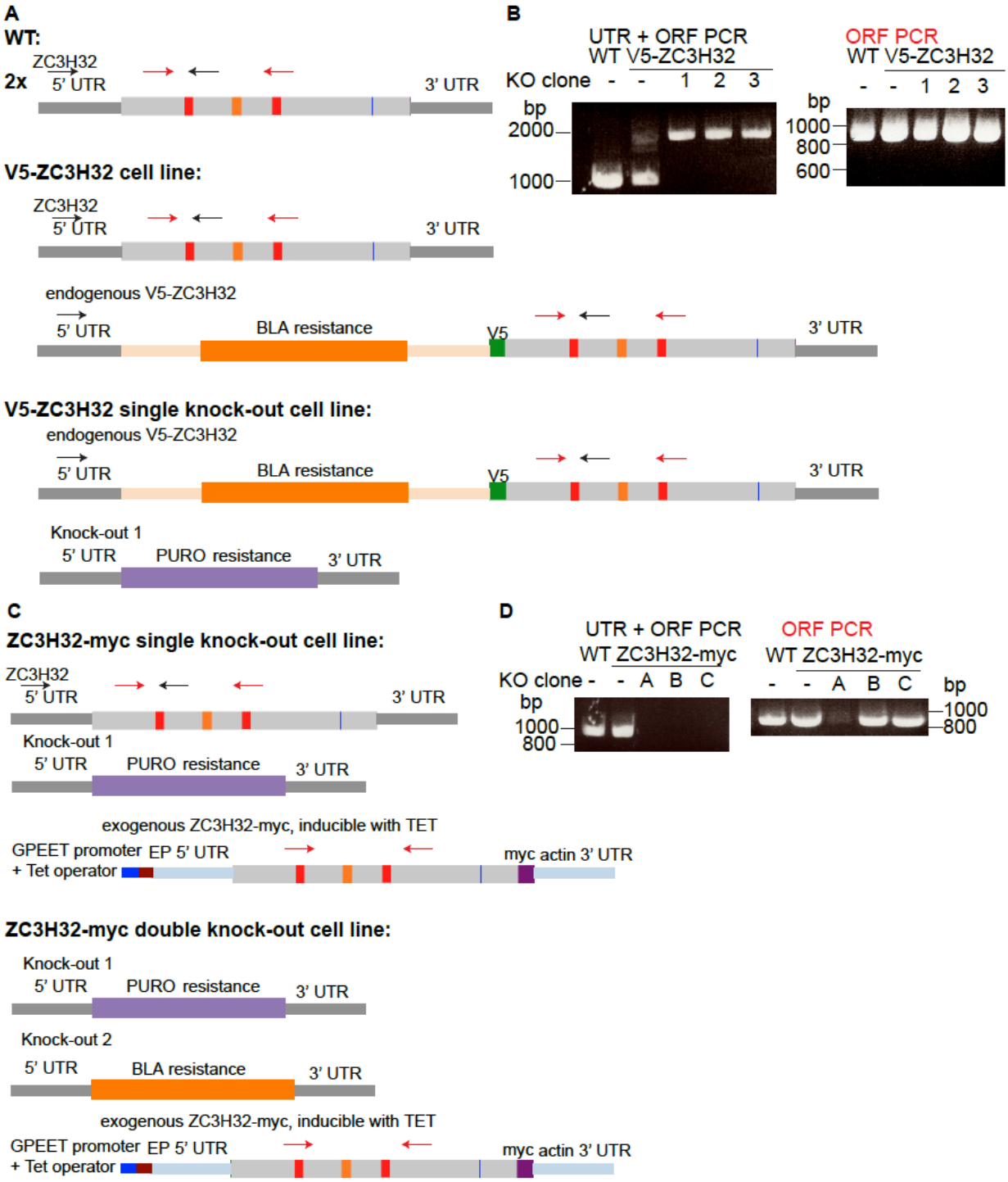

Fig. 38: Verification of single and double knock-out cell lines by PCR

A: Schematic presentation of WT, V5-ZC3H32 and V5-ZC3H32 single knock-out cell lines The UTRs of *ZC3H32* are shown in dark, the ORF is shown in light grey. The zinc finger domains are shown in red (canonical) and orange (non-canonical). The HNPY domain is shown in blue. The blasticidin resistance is shown in orange, the puromycin reistance is shown in purple, the V5-tag is shown in blue. Black arrows: Primer for UTR+ORF PCR Red arrows: primer for ORF PCR. B: PCR results for V5-ZC3H32 cell lines. C: Schematic presentation of ZC3H32-myc cell lines, single and double knock-out. The myc-tag is shown in mauve, the Tet-operator and GPEET promoter in blue and red. D: PCR results for ZC3H32-myc cell lines.

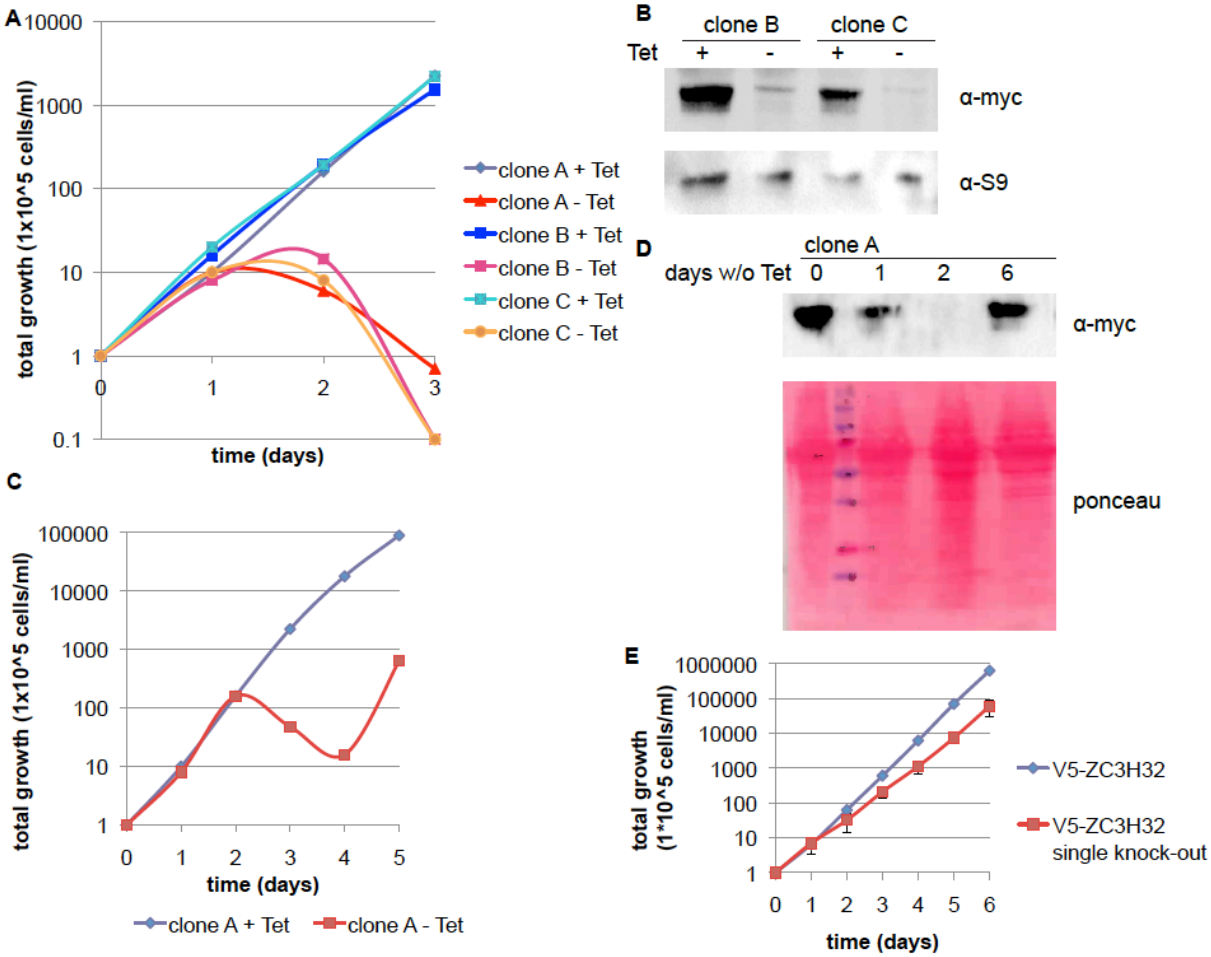

Fig. 39: Growth of ZC3H32 double knock-out cell line and V5-ZC3H32 single knock-out cell line

A: Cumulative growth curve for 3 ZC3H32-myc double knock-out clones for three days, with and without tetracycline.

B: Western Blot with samples from clone B and C, with and without Tet. –Tet samples were collected 24h after Tet removal.

C: Cumulative growth curve for clone A for five days.

D: Western blot with samples from clone A.

E: Growth curve of the V5-ZC3H32 cell line and three V5-ZC3H32 single knock-out cell lines.

3.3.7 ZC3H32-myc expression in procyclics

ZC3H32-myc, which has been shown to be fully functional (see 3.3.6), was expressed in procyclic cells. Northern blotting showed that the RNA levels of the myc-tagged protein were much higher than the RNA levels of endogenous ZC3H32 (see fig. 40B). This was confirmed by high throughput sequencing (3.3.11), which showed a 32-fold higher level of ZC3H32 in procyclic ZC3H32-myc cells as compared to procyclic wild type cells.
Growth curves of two clones, however, show no effect on growth upon ZC3H32-myc induction.
Therefore, it can be concluded that induction of ZC3H32-myc in procyclic cells leads to much higher ZC3H32 levels (overexpression), but this does not seem to impair the trypanosome growth.
As ZC3H32 is down-regulated in procyclics, as compared to the bloodstream form, it was thought that this protein targets RNAs that are differentially regulated between the two life cycle stages. Therefore, exogenous expression of this protein in procyclics should have an effect on these RNA levels. Thus, RNA from a ZC3H32-myc cell line was sent for high-throughput sequencing (see 3.3.11).

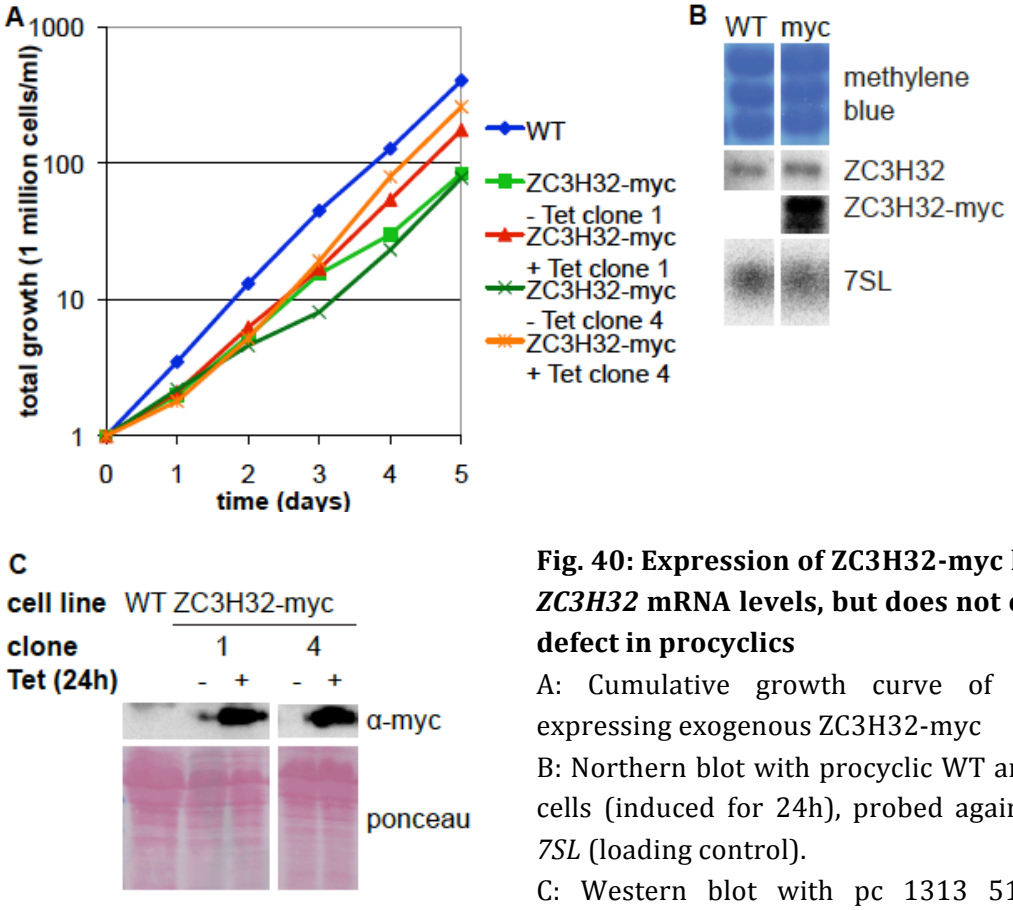

Fig. 40: Expression of ZC3H32-myc leads to higher *ZC3H32* mRNA levels, but does not cause a growth defect in procyclics

A: Cumulative growth curve of procyclic cells expressing exogenous ZC3H32-myc

B: Northern blot with procyclic WT and ZC3H32-myc cells (induced for 24h), probed against *ZC3H32* and *7SL* (loading control).

C: Western blot with pc 1313 514 ("WT") and ZC3H32-myc cells, clone 1 and 4. ZC3H32-myc expression was induced for 24h.

3.3.8 Tethering of the ZC3H32 protein to a reporter RNA leads to its degradation

We wanted to see which effect ZC3H32 has on the mRNAs it interacts with. Therefore, we used an assay in which we tethered the protein to a reporter RNA. Its interaction with MKT1, which was shown to stabilize the reporter RNA in the same assay, suggested that tethering ZC3H32 would stabilize the reporter RNA as well.

For the tethering, a fusion protein was created, containing the lambdaN domain from phage lambda at its N-terminus and two myc-tags at its C-terminus. This protein was expressed ectopically and its expression was induced by adding tetracycline.

The reporter RNA, encoding chloramphenicol-acetyl-transferase (CAT), carries 5 copies of the BoxB sequence in its 3'UTR, to which the lambdaN peptide binds with high affinity. Thus, the fusion protein is tethered to the *CAT* RNA. As a control, a cell line containing the reporter RNA without the BoxB was used. *CAT* RNA levels were measured by Northern blotting, CAT protein levels with an enzymatic assay using ^{14}C-labeled Butyryl-CoA (description see 2.6).

As seen in fig. 41, the tethering of ZC3H32 to the *CAT* RNA leads to both lower CAT protein levels as well as lower *CAT* RNA levels, which was not the effect we expected.

Thus, It can be concluded that tethering of Z3CH32 to a reporter RNA leads to its degradation and thus to lower levels of the encoded protein.

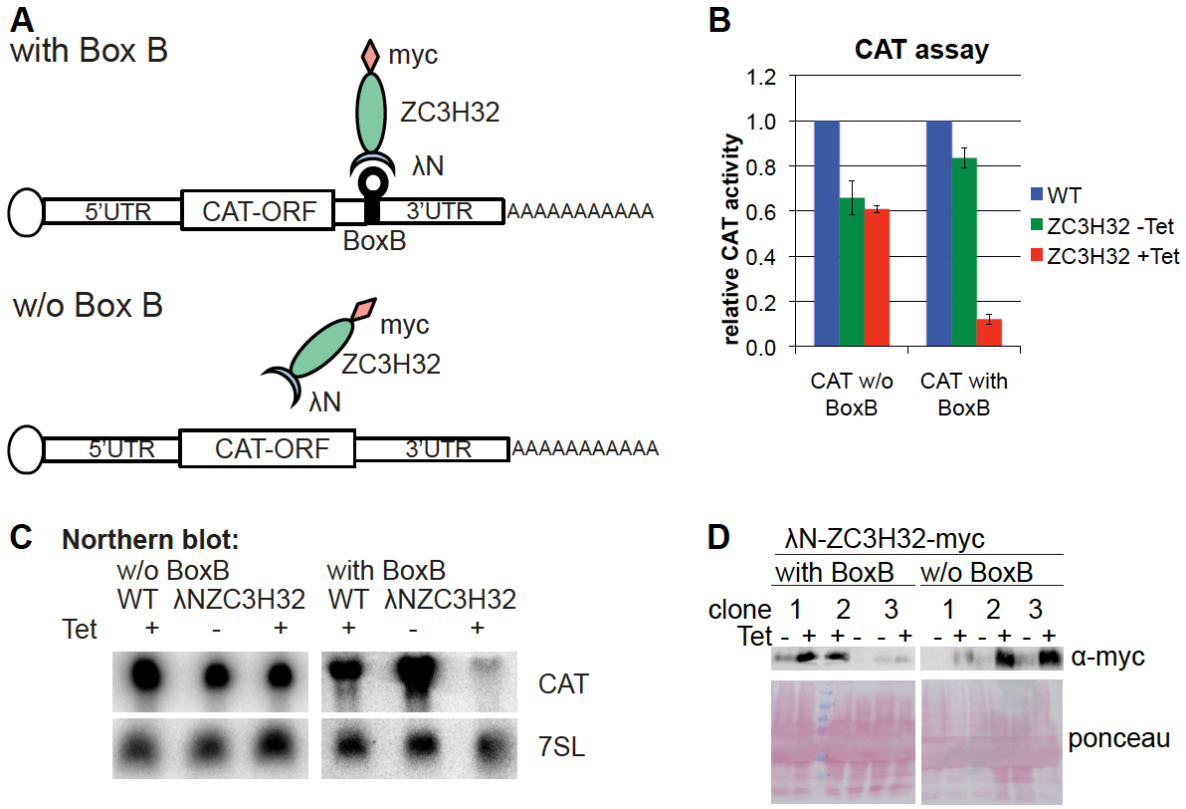

Fig. 41: **Tethering of ZC3H32 leads to the degradation of the *CAT* RNA**

A: schematic graph of the tethering experiment. The experiments were done with three clones each. B: CAT assay results for λN-ZC3H32-myc after an induction of 24 hours. C: Northern blot probed against the *CAT* reporter RNA and *7SL* as control. D: Western blot with λN-ZC3H32-myc clones, from cell lines containing the *CAT* reporter with and without the BoxB copies. λN-ZC3H32-myc expression was checked using the antibody against the myc tag.

In order to see whether the tagging on both ends has an effect on the activity of the fusion protein, another construct was made in which both the myc-tag and the λN-peptide were on the N-terminus. The induction of this fusion protein also led to a decrease in CAT activity.

3.3.9 The C- and the N-terminus of the ZC3H32 protein seem to be responsible for RNA degradation

In order to find out which part of the protein catalyzes the effect, fusion proteins with fragments of the ZC3H32 sequence were made:

Fig. 42: Overview of tethering experiments with ZC3H32 fragments

AA: amino acid.

Numbers below AA: pHd number of plasmid.

*: one clone (instead of three) was tested

**: two clones were tested

n.d.: not determined

Surprisingly, tethering of both the C-terminal (AA 274 - 655) and the N-terminal half (AA 1-274) lead to a decrease in CAT activity. This indicates that ZC3H32 might have two active domains, one in the C-terminus and the other one in the N-terminus. A 145 amino acid long fragment (AA 1-145) of the N-terminus is sufficient to cause a decrease in CAT activity. For the C-terminus, the last 293 Amino acids (AA 362-655) are also

sufficient. Expression of a 174 AA long fragment (AA 362-538), which does not contain the HNPY domain, did not lead to a decrease in CAT activity.
These results indicate that the first 145, as well as the last 293 Amino acids, probably contain the domains of this protein that are active in decreasing RNA levels. They suggest also that the HNPY domain is important for the function of the C-terminal domain.
Tethering of the middle part of the protein (AA 146-538) did not lead to a decrease CAT activity. This part contains the three zinc fingers, which indicates that, for wild type protein, this part might be mainly responsible for the binding to the RNA targets, while the N- and the C-terminus are probably responsible for their degradation.

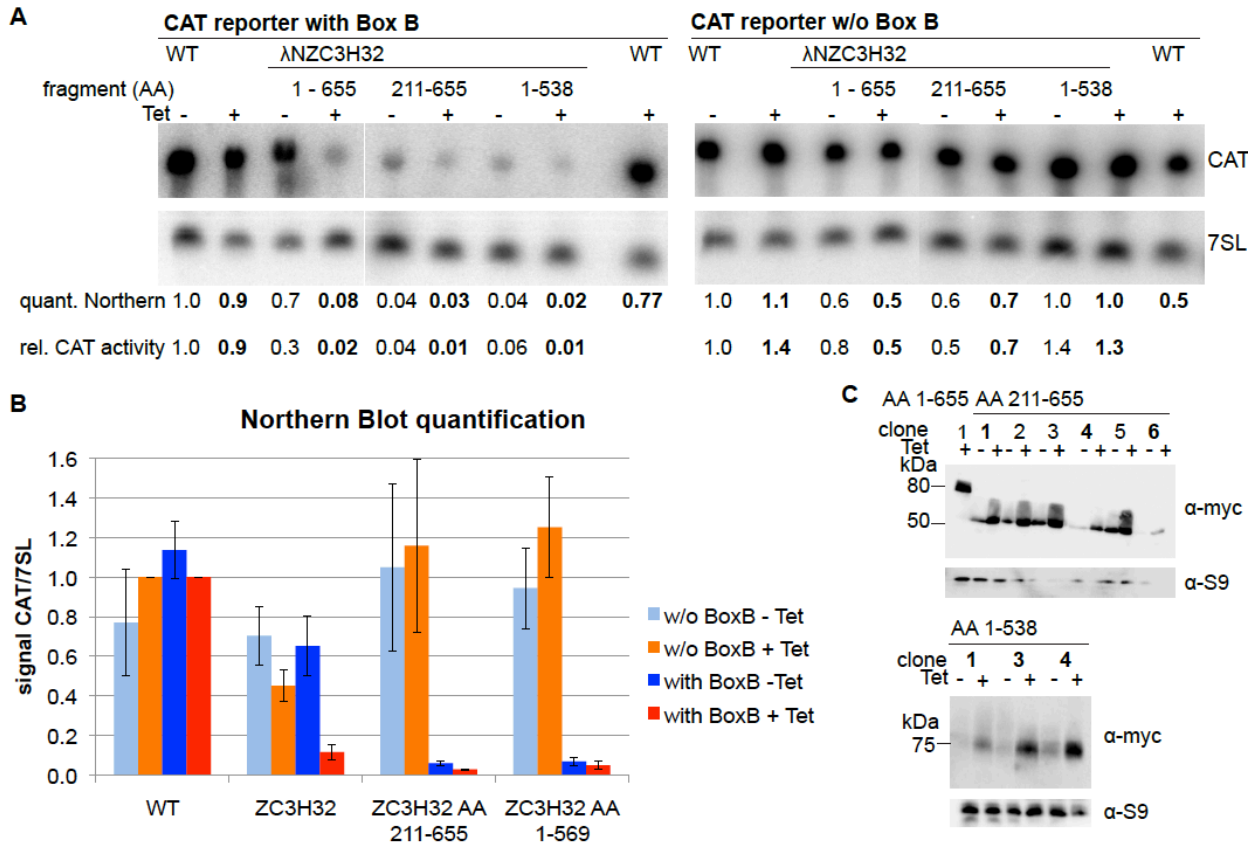

Fig. 43: Tethering of fragments AA211-655 and AA1-538 leads to a decrease in *CAT* RNA levels

The experiments were done in cell lines expressing the CAT reporter with the BoxB and in cell lines expressing the reporter without the BoxB.
A: Northern blot probed against the *CAT* reporter RNA. The *7SL* RNA was used as loading control. The relative CAT activity (determined by CAT assay) is written below the Northern blot quantification. B: Chart showing the quantification of Northern blots. For each construct three clones were used. D: Western Blot of ZC3H32 fragments. The clones shown in bold were used to make the samples for the Northern blots.

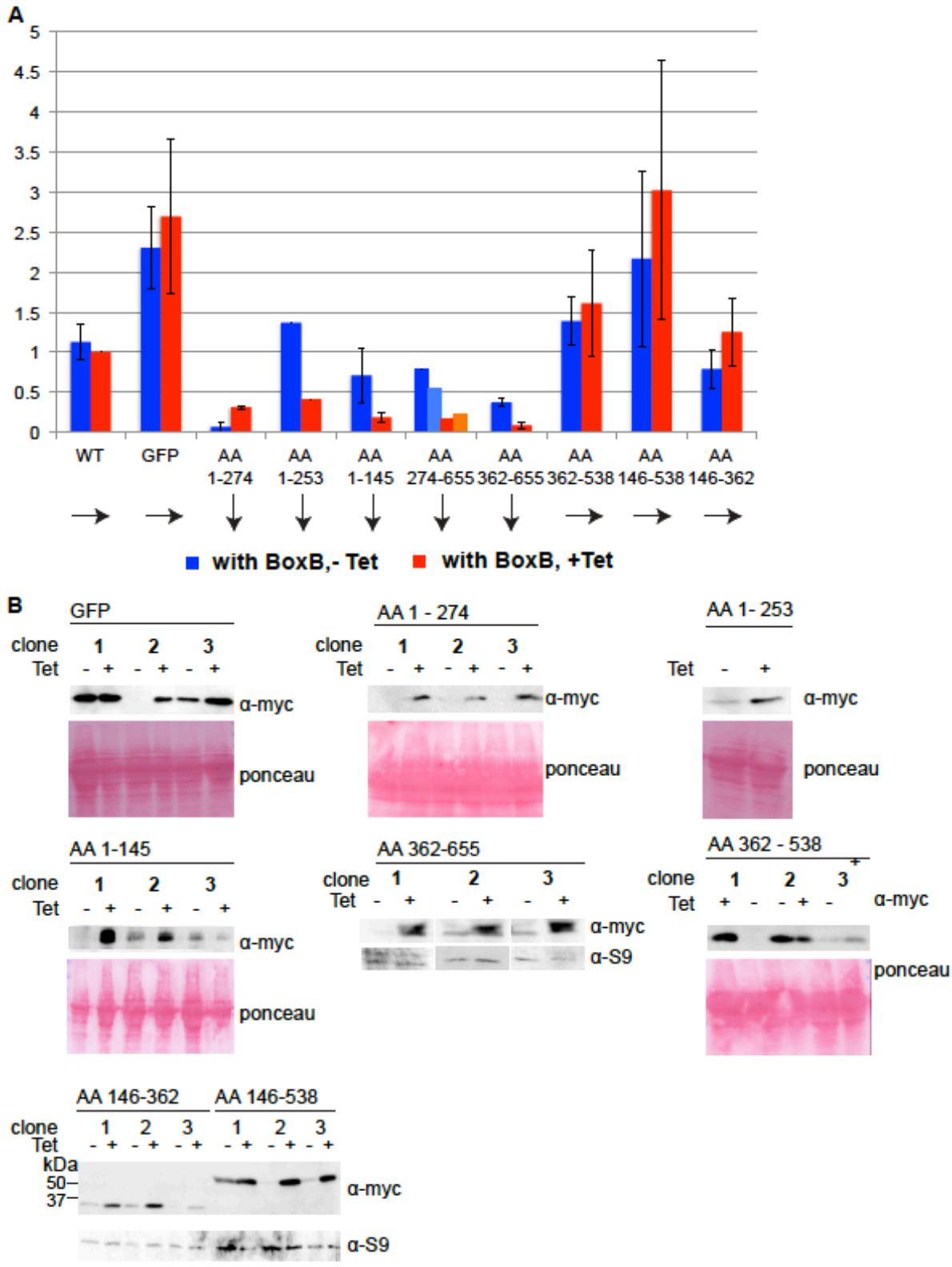

Fig 44: Tethering experiment with GFP (control construct) and ZC3H32 fragments

A: CAT assay results for λN-GFP-myc (control construct) and λN-ZC3H32-myc fragments. Arrows indicate interpretation of results, as shown in figure 42 (down: down-regulation, straight: no effect). The CAT activity was normalized to activity of the WT +Tet sample.

B: Western blots done to check construct expression. The myc-tagged constructs were detected using α-myc. AA: amino acid.

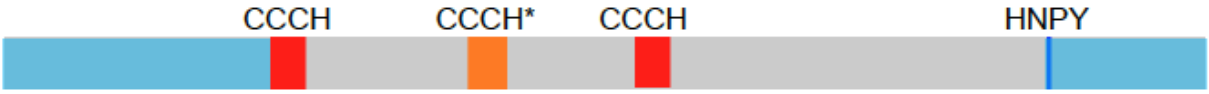

Fig. 45: **Summary of CAT assay results**.
The putative functional domains of ZC3H32, at the C and the N-terminus, are shown in light blue

3.3.10 Tethering of ZC3H32 causes a decrease in *CAT* RNA translation

In order to check whether tethering of the ZC3H32 protein to the *CAT* RNA affects its translation, I tested whether it still co-localized with the polyribosome fractions after the induction of the λN-ZC3H32-myc construct.

Two λN-ZC3H32-myc cell lines were used, one containing the *CAT* reporter RNA with the BoxBs in its 3'UTR and the other containing the *CAT* reporter without the BoxBs (negative control). λN-ZC3H32-myc expression was induced for four hours, this time span being the minimum needed until adequate levels of λN-ZC3H32-myc were detectable on a Western Blot (see fig. 46, F).

RNA was isolated from the cell lysate (Input: $1/10^{th}$ of the total input was used as sample) and from the sucrose gradient fractions and put on a Northern blot, which was probed against *CAT*, *Histone H4* (*HisH4*) and human *β-globin*. *HisH4* was used as control, as its translation should be equal in both cell lines. *In vitro* expressed *β-globin* RNA (made by I. Minia) was added to each RNA sample in order to check the efficiency of the RNA isolation in the different fractions.

As can be seen in fig.46, while the *CAT* RNA without the BoxB localizes to the higher fractions (polyribosomal fractions) of the polyribosome gradient, the *CAT* RNA with the BoxB is found in similar levels in all the fractions. There also seem to be some bands corresponding to shorter *CAT* fragments, which might correspond to degradation products. These fragments are not visible in the Northern blots from the cell line carrying the *CAT* RNA without the BoxB.

These results show that, on average, less ribosomes sit on the *CAT* RNA with the BoxB than on the one without the BoxB. This indicates that, upon tethering of λN-ZC3H32-myc to the *CAT* RNA, its translation decreases. The Northern blots also show that the total *CAT* RNA level is already lower in the BoxB cell line as compared to the negative control, although the construct was only induced for 4 hours.

Quantification of the *CAT* signal of four Northern blots of the BoxB cell line and three Northern blots of the control cell line, followed by the division with signal from the *HisH4* RNA, clearly shows that the *CAT* RNA with the BoxB is more likely to be found in the lower fractions (pre-ribosomal fractions) than the one without the BoxB (see fig.46, G).

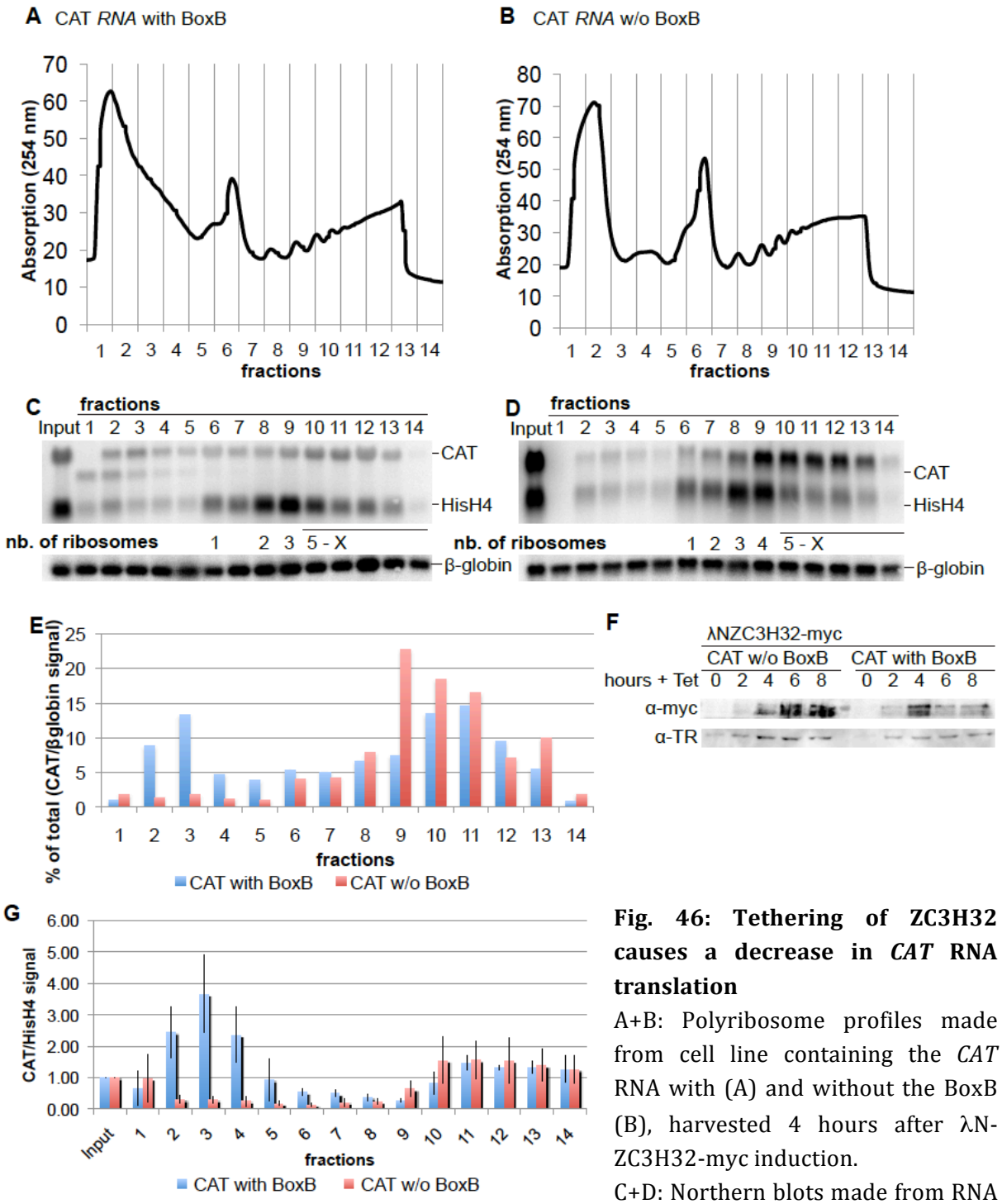

Fig. 46: Tethering of ZC3H32 causes a decrease in *CAT* RNA translation

A+B: Polyribosome profiles made from cell line containing the *CAT* RNA with (A) and without the BoxB (B), harvested 4 hours after λN-ZC3H32-myc induction.

C+D: Northern blots made from RNA isolated from the collected fractions, probed against *CAT, HisH4* and *β-globin*. In vitro synthesized *β-globin* RNA (made by I. Minia) was added to each fraction in order to check the efficiency of each RNA isolation. E: Quantification of Northern blots. The signal from the *CAT* RNA was divided by the signal from the *β-globin* RNA, in order to compensate for differences in RNA isolation efficiency (relative *CAT* signal). Then, the signals from each fraction (without Input) were added up and the percentage of the relative *CAT* signal in each fraction was calculated. F: Western blot made from both cell lines, to check λN-ZC3H32-myc expression after 2,4,6 and 8 hours after induction. Trypanothione reductase was used as loading control. G: Quantification of Northern blots (4 for BoxB cell line, 3 for control cell line) from replicas of the same experiment. The intensity of the *CAT* signal was divided by the *HisH4* signal and normalized to the input.

3.3.11 High-throughput sequencing results

Poly-A+ RNA from bloodstream cells expressing the ZC3H32 RNAi construct and procyclic cells expressing ZC3H32-myc (called procyclic overexpression), made 24 hours after the induction of the cells, was sent for high-throughput sequencing.

From the bloodstream RNAi cell line two different poly-A+ preparations were sent for sequencing. These two replicas yielded quite different results (R = 0.52). This is surprising as the same cell line was used and the cells were induced for the same amount of time (24h). The level of downregulation seemed to be similar, the relative amount of *ZC3H32* RNA, as compared to the wild type, was 0.094 in the first and 0.12 in the second replica. However, it cannot be ruled out that the levels of ZC3H32 protein differed in the two separate preparations. Also, small differences in the poly-A+ RNA or in the cDNA library preparation might have caused a difference in mRNA levels, although the same protocols were used.

Due to the large discrepancy between the two replicas, only those RNAs were labeled as up-regulated, or respectively, down-regulated, which showed an increase/decrease of at least two fold in both preparations and were present on both with at least 10rpm (reads per million).

Comparison of the average results from both bloodstream RNAi replicas with the procyclic overexpression data showed a correlation factor of about zero (R=0.025, see table 7, row 2, only genes which were found with more than 10 rpm in both sequencing results were taken into account). This means that the effect ZC3H32 overexpression has on the mRNA metabolism in procyclics is different from the effect ZC3H32 RNAi has in the bloodstream form. However, the effect was not opposite, meaning that mRNAs which were up-regulated in the bloodstream form upon ZC3H32 RNAi were not down-regulated in the procyclic form and vice versa. One explanation might be that other RNA-binding proteins influence the activity of ZC3H32. These proteins could, for example, prevent ZC3H32 from binding and thus limit its influence in the procyclic form.

Another explanation might be that the mRNA levels in both cell lines are influenced by secondary effects. For example, there seems to be a decrease in RNAs coding for proteins involved in RNA metabolism (see fig. 48). 14 *trans*-acting factors are down-regulated in both the bloodstream RNAi and the procyclic overexpression cell line (e.g. PUF2, ZFP1 and ZC3H29). Therefore, any effect observed might as well be caused by the downregulation of any of these *trans*-acting factors.

Another secondary effect which surely influenced the mRNA levels in the bloodstream RNAi cell line is the stress reponse, as ZC3H32 knock-down causes a growth defect. Exogenous expression of ZC3H32-myc in procyclics does not cause a growth defect (see fig. 40), thus, it is unlikely that the mRNA levels of these cells are influenced by the stress response.

There is a positive correlation between the average of the two sequencing replicas of bloodstream RNAi cell lines and the sequencing result of other RNAi cell lines (MKT1, RRP45, CAF1, PUF2 and CTR9 RNAi (see table 7)).

One possible explanation of the correlation between the MKT1 and the ZC3H32 dataset is that these proteins interact. Also, the *MKT1* mRNA seems to be down-regulated two fold in the ZC3H32 cell lines (see table 7, row 8, column four). If ZC3H32 knock-down causes lower *MKT1* RNA levels, this could influence the levels of the RNA targets of MKT1, thus causing a correlation between the two datasets. This could also explain the correlation between the ZC3H32 dataset and the PUF2 RNAi dataset, as the *PUF2* RNA is down-regulated approximately five fold in the ZC3H32 RNAi cell line. But this is not the case for CAF1 and CTR9, whose mRNAs seem to be only slightly down-regulated in this cell line, and also not for RRP45, whose mRNA is not down-regulated. However, in these cell lines, the *ZC3H32* mRNA levels seem to have decreased. In the RRP45 and CTR1 RNAi cell line even with a factor of 0.1, which is the same degree of decrease as in the ZC3H32 RNAi cell lines. In the CAF1 cell line, the *ZC3H32* mRNA is down-regulated with a factor of 0.3. Thus, for these cell lines the correlation could be caused by the opposite effect; if, for example, the knock-down of RRP45 decreases the level of ZC3H32, this could influence the target mRNAs of ZC3H32 and thus cause a correlation.

Another possible explanation is the negative correlation between the length of the coding sequence and the relative RNA amount in the sequencing results from the ZC3H32 RNAi cell line. This means, that, when ZC3H32 is knocked down, RNAs with long coding sequences are more likely to be less abundant than compared to the wild type. RNAs with short coding sequences, on the other hand, are more likely to show comparatively higher levels.

Thus, short RNAs, which seem to be enriched in the ZC3H32 RNAi cell line, are more likely to be false positives (see table 8, column 15, sequences shown in pink) than longer RNAs.

The same correlation was observed with the majority of the other sequencing datasets (see table 7, column 5).

The only exceptions are the datasets from the procyclic ZC3H32 overexpression cell line and the ZC3H11 RNAi dataset, which show no correlation (0.012 and 0.001), as well as the XRNA RNAi dataset, which shows a positive correlation (0.47).

This correlation with the CDS length might also explain the correlation of the sequencing results between the ZC3H32 cell line and the cell lines showing the same correlation (MKT1, RRP45, CAF1, PUF2 and CTR9 RNAi cell line).

It should be mentioned that, while it would have been more informative to calculate the correlation between the length of the RNA and the relative RNA levels in the respective cell line, this was not possible, as for too many RNAs the length of the UTRs are unknown, and thus the length of the entire RNA cannot be determined with certainty. Therefore, the CDS length was used for the calculation. It is not unlikely that the correlation between the RNA length and the relative RNA levels in the RNAi cell lines might be even higher.

An interesting observation, however, was that there seems to be a positive correlation (0.31) between the relative RNA levels from the ZC3H32 bloodstream RNAi results and the proportions of the RNA levels between procyclics and bloodstream wild type cells

(rpm procyclic WT/rpm bloodstream WT), meaning that if an RNA is up-regulated in the procyclic form, as compared to the bloodstream form, it is more likely to be up-regulated in the ZC3H32 RNAi cell line (see fig. 47, panel F).

	datasets	corr. with ZC3H32 RNAi	rel. RNA levels in ZC3H32 RNAi	rel. ZC3H32 RNA levels	corr. with CDS length
1	pc OE	0.025			0.012
2	XRNA RNAi	-0.12	0.4	-	0.47
3	ZC3H11 RNAi	-0.07	0.5	1.2	0.001
4	CTR9 RNAi	0.43	0.8	0.1	-0.42
5	Puf2 RNAi	0.45	0.2	1.3	-0.51
6	CAF1RNAi	0.46	0.6	0.3	-0.40
7	RRP45 RNAi	0.49	1.4	0.1	-0.37
8	MKT1 RNAi	0.59	0.5	1	-0.38
9	pc WT/bs WT	0.31			-0.17
10	CDS length	-0.42			1

Table 7: Comparison of different sequencing datasets.
The correlation between the relative RNA levels (rpm cell line/ rpm bloodstream WT) of the datasets is shown. Correlations higher than 0.3 are shown in red, correlations lower than -0.3 in blue.
Column 2: datasets used for comparison:
Row 1: Procyclic ZC3H32-myc cell line (pc 1313 514 2332)
Row 2-8: Other bloodstream RNAi cell lines.
Row 9: Correlation between the relative RNA levels in the bloodstream ZC3H32 RNAi cell line and the proportion between procyclic WT and bloodstream WT sequencing results (rpm procyclic WT/rpm bloodstream WT)
Row 10: Correlation between the relative RNA levels in the bloodstream ZC3H32 RNAi cell line and the length of the coding sequence (in base pairs).
Column 3: Correlation coefficient R between the relative RNA levels form the sequencing results from the respective cell line and the average of the datasets of the two sequencing replicas of the ZC3H32 RNAi cell line.
Column 4: Only applicable for RNAi cell lines. Relative RNA level of the respective RNAi target in the ZC3H32 cell line (e.g. MKT1: 0.5, meaning the *MKT1* RNA is down-regulated two fold in the ZC3H32 RNAi cell line). Values below 0.5 are shown in blue.
Column 5: Only applicable for RNAi cell lines. Relative RNA level of *ZC3H32* in the sequencing results from the respective RNAi cell. Values below 0.5 are shown in blue. In the XRNA cell line not enough rpms were obtained for the *ZC3H32* RNA.
Column 6: Correlation (R) between the relative RNA levels of the named dataset and the length of the coding sequence of the respective RNAs.
Data taken from: XRNA: (Manful, Fadda et al. 2011), ZC3H11: (Droll, Minia et al. 2013), CTR9: (Ouna, Nyambega et al. 2012), Puf2: (Jha, Fadda et al. 2014), Caf1 and RRP45: (Fadda, Farber et al. 2013) MKT1: (Singh, Minia et al. 2014), procyclic WT/bloodstream WT: (Fadda, Ryten et al. 2014)

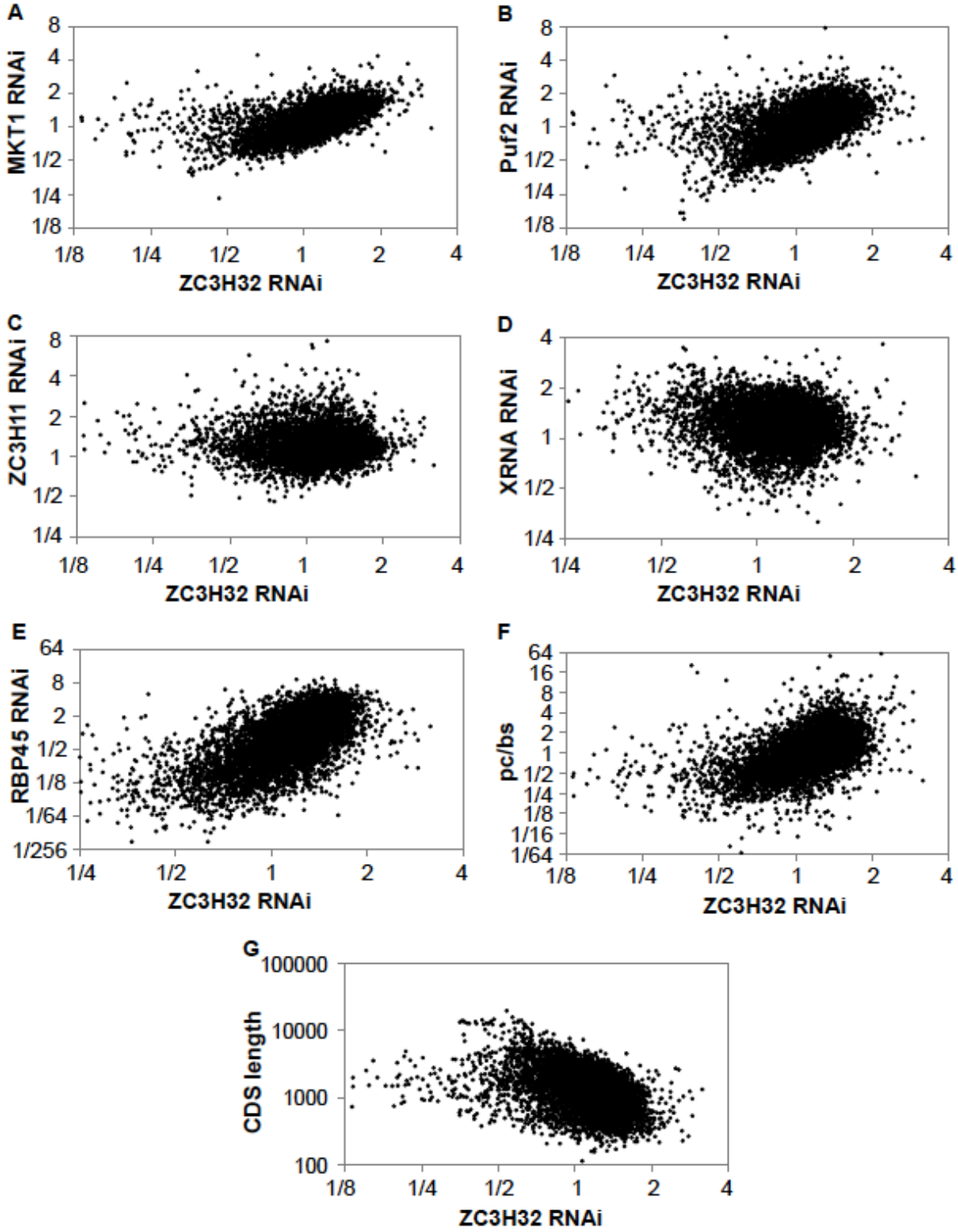

Fig. 47: Comparison of the ZC3H32 sequencing results with other sequencing datasets

Scatter blots for the comparison of sequencing results from the bloodstream ZC3H32 RNAi cell line with other sequencing datasets, the coding sequence length (G) and the proportions of the RNA levels between procyclics and bloodstream wild type cells (rpm procyclic WT/rpm bloodstream WT) (F). A: bloodstream MKT1 RNAi cell line (Singh, Minia et al. 2014) B: bloodstream PUF2 RNAi cell line (Jha, Fadda et al. 2014) C: bloodstream ZC3H11 RNAi cell line (Droll, Minia et al. 2013) D: bloodstream XRNA RNAi cell line (Manful, Fadda et al. 2011) E: bloodstream RRP45 RNAi cell line (Fadda, Farber et al. 2013). F: rpm procyclic WT/ rpm bloodstream WT (Fadda, Ryten et al. 2014) G: coding sequence length

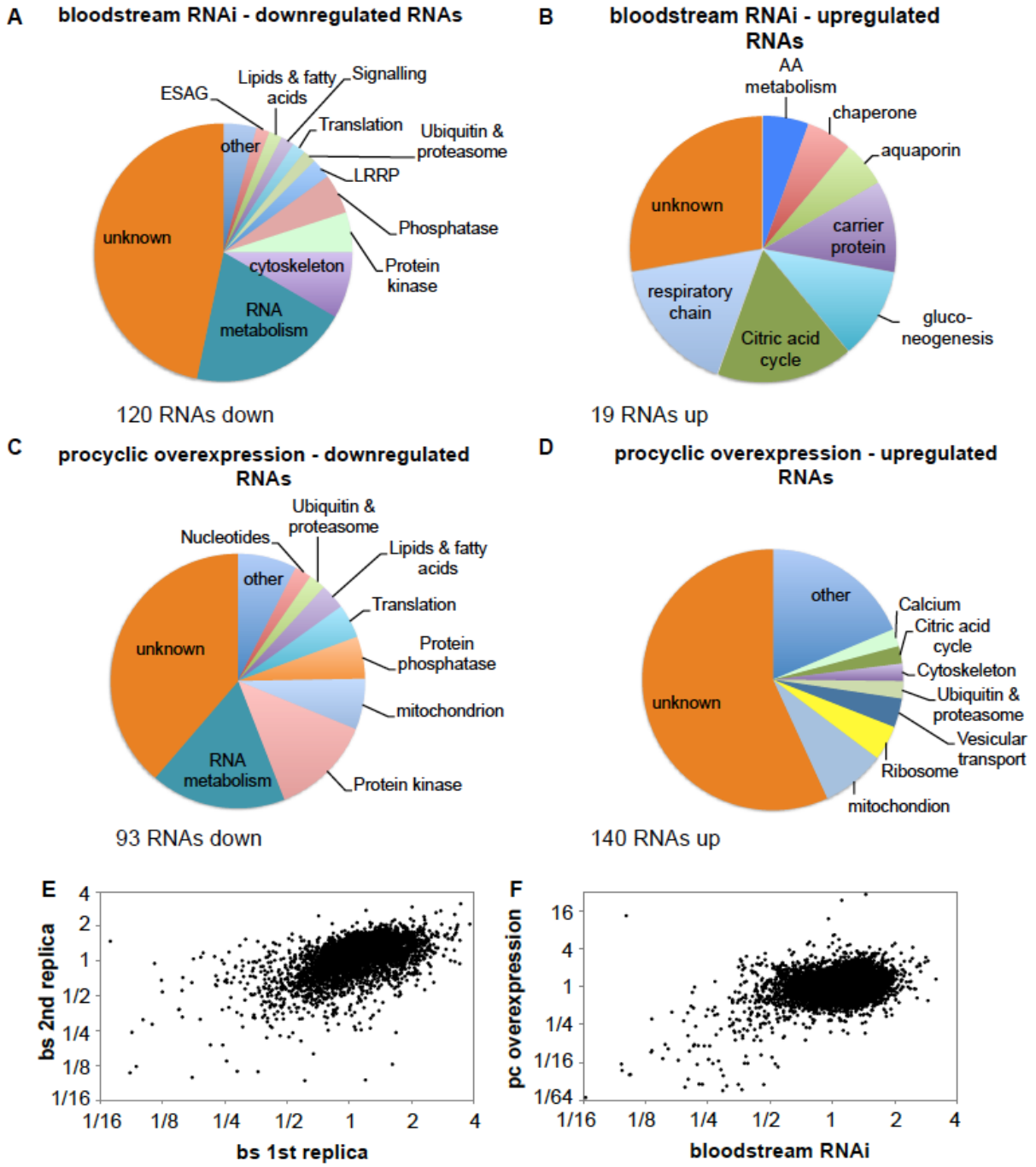

Fig. 48: Overview of RNAseq results

A+B: data from the bloodstream RNAi cell line (combined from both replicas) Up- and down-regulated mRNAs sorted by function. The threshold was a two fold change in comparison to the wild type

C+D: data from the procyclic ZC3H32-myc cell line. E: Scatter blot showing the comparison between the data from bloodstream and procyclic RNAseq F: Scatter blot showing the comparison between the data from the bloodstream replicas.

For entire datasets, see table 8 and suppl. 6.2.

				ZC3H32										
gene	**name**	**pathway**	**location**	**A**	**B**	**NB**	**pc OE**	**pc/ bs**	**MKT**	**ZC3H 11**	**Puf2**	**Caf1**	**RRP45**	**CDS (bp)**
Tb927.3.1790	pyruvate dehydrogenase E1 β-subunit (PDH)	Citric acid cycle	mito*	3.8	2.1	2 ± 0.15	1.3	3.7	1.9	1.3	2.0	0.6	0.2	1047
Tb927.11.6280	pyruvate phosphate dikinase (PPDK)	gluconeo-genesis	glyc.[1]	3.4	2.0	2.1 ± 0.9	-	22.6	1.4	1.8	1.4	0.4	0.4	2742
Tb927.3.2230	Succinyl CoA synth. α-subunit (SCS)	Citric acid cycle	mito*	3.2	2.5	1.2 ± 0.3	1.4	4.4	1.6	1.3	2.9	1.7	2.4	906
Tb927.10.12240	short-chain dehydrogenase, putative	-	mito	2.8	2.1	-	1.8	3.6	1.8	1.2	1.8	1.0	3.6	984
Tb927.11.900	Isocitrate dehydrogenase, putative	Citric acid cycle	mito[2]	2.5	2.5	1.4 ± 0.5	-	1.0	2.2	1.5	0.8	1.2	1.0	1242
Tb927.10.15410	glycosomal malate dehydrogenase (gMDH)	gluconeo-genesis	glyc.[2]	2.3	2.1	2.2 ± 0.5	2.2	31.4	1.4	1.3	1.1	0.3	0.4	972
Tb927.2.5980	heat shock protein 104	Chaperone	cytoplasm	2.3	2.3	-	2.1	1.0	3.7	1.4	0.7	2.2	0.7	2613
Tb927.3.3460	hyp. protein, (SDH5 in T cruzi)	respiratory chain	nn	2.3	2.4	-	1.0	3.7	-	-	-	-	-	1452
Tb927.11.5290	mitochondrial carrier protein, MCP9	carrier protein	mito*	2.1	2.1	0.9	-	1.7	2.4	1.0	1.0	1.2	3.5	849
Tb927.4.2240	hyp. protein	-	nn	2.0	2.0	-	1.9	1.6	1.6	1.4	2.3	2.8	1.0	1173
Tb927.8.5270	hyp. protein	-	nn	2.0	2.0	-	1.8	0.6	1.7	1.2	1.0	1.0	1.3	840
Tb927.4.3520	hyp. protein	-	nn	4.1	2.1	-	5.6	4.1	1.9	1.7	1.5	0.5	0.2	537
Tb927.6.1520	aquaporin 3, putative (AQP1)	-	mem-brane[2]	3.4	3.1	-	0.5	6.3	2.4	1.9	1.9	0.7	0.7	966
Tb927.4.4990	ubiquinol-cytochrome c reductase, putative	respiratory chain	mito[2]	3.3	2.1	-	1.6	9.1	1.7	1.4	1.9	0.4	0.6	216
Tb927.7.3520	mitochondrial pyruvate carrier-like protein	carrier protein	mito*	2.8	2.7	-	1.2	3.6	2.1	1.9	2.3	3.1	1.3	405
Tb927.7.210	proline dehydrogenase	AA	mito[2]	2.6	2.6	-	1.1	7.6	2.8	1.9	3.4	1.3	0.7	1671

		metabolism												
Tb927.11.6700	hyp. protein	-	mito*	2.3	2.0	-	-	1.6	1.7	1.3	1.4	3.3	3.0	399
Tb927.10.3120	cytochrome c oxidase assembly protein	respiratory chain	mito*[2]	2.0	2.2	-	0.6	2.5	1.3	1.3	1.2	0.6	0.8	699
Tb927.10.10000	hyp. protein	-	nn	2.0	2.9	-	1.2	5.9	2.6	2.2	1.8	4.1	0.6	1224

Table 8: RNAs enriched in the bloodstream ZC3H32-RNAi cell line

High throughput sequencing results. RNAs which were up-regulated upon ZC3H32 knock-down in both sequencing datasets (A and B) are shown.
pc OE: results from overexpression in procyclics;
pc/bs: RNA levels in procyclic cells/RNA levels in bloodstream cells, from wild type cells
NB: results from Northern blotting (see fig. 49 and 50)
MKT1, ZC3H11, Puf2, Caf1, RRP45: RNA sequencing results for these mRNAs from of MKT1, ZC3H11, Puf2, Caf1 and RRP45 RNAi cell lines. Data taken from: XRNA: (Manful, Fadda et al. 2011), ZC3H11: (Droll, Minia et al. 2013), CTR9: (Ouna, Nyambega et al. 2012), PUF2: (Jha, Fadda et al. 2014), CAF1 and RRP45: (Fadda, Farber et al. 2013) MKT1: (Singh, Minia et al. 2014), procyclic WT/bloodstream WT: (Fadda, Ryten et al. 2014)
CDS length: coding sequence length. Sequences shorter than the first quartile (801bp) are shown in pink, shorter than the median in dark blue, longer than the median length (1276bp) are shown in dark green and longer than the third quartile (2007bp) are shown in light green.
Localzation: mito: mitochondrion; glyc: glycosome
* mitochondrial localisation predicted by MitoCarta
1: (Cosenza, Bringaud et al. 2002)
2: localization determined by homology

In the bloodstream form, 120 RNAs were down-regulated upon ZC3H32 RNAi induction, while 19 were up-regulated. In the procyclic form, 93 were down- and 140 up-regulated. Up and downregulation was defined by at least a two-fold change in RNA levels as compared for the wild type. For the bloodstream RNAi results, the effect had to be present in both replicas in order to be definded as up/downregulation. Also, RNAs that were shown to be affected in all RNAi cell lines were not defined as up or down-regulated, even if they changed 2 fold in both replicas.

There seem to be more RNA level changes in the procyclic data, however, this is due to two things: for once, this sequencing reaction was done only once. Also, apart from two wild type samples, there was no other sequencing data from procyclics available (that means, from RNAi cell lines or cell lines in which another protein was exogenously expressed), with which to compare this data. Therefore, less data could be discarded; thus there seem to be more targets.

What is surprising is, that, although the tethering experiments indicate that ZC3H32 is destabilizing, more RNAs seem to be down-regulated upon its decrease in the bloodstream form, while more appear to be stabilized upon its exogenous expression in procyclics. But this might be a secondary effect.

What was interesting, however, was, that among the 19 stabilized RNAs (see table 3) in the bloodstream form, 11 encode proteins localizing to the mitochondrion. Of the 12 putative targets, which could be linked to a cellular pathway, 3 were found to be associated with the citric acid cycle (note: one of them is a subunit of pyruvate dehydrogenase, which is not, in fact, part of the citric acid cycle) and three with the respiratory chain.

This might a response to the stress, as the cells are dying they might increase their energy metabolism. But it could also be possible that ZC3H32 down-regulates RNAs encoding mitochondrial proteins in the bloodstream form.

3.3.12 Validation of the high-throughput sequencing results by Northern blotting

The high-throughput sequencing results showed that the majority of the RNAs, which were enriched in the bloodstream ZC3H32 RNAi cell line, encoded proteins found in the mitochondrion and/or involved in energy metabolism. In order to find out whether these targets were indeed down-regulated upon ZC3H32 knock-down, Northern blots were made using both the inducible knock-out cell lines and the RNAi cell line (the same clone which was also used for sequencing).
Six candidate mRNAs were tested: Pyruvate phosphate dikinase (*PPDK*), glycosomal malate dehydrogenase (*gMDH*), isocitrate dehydrogenase (*IDH*), the alpha subunit of succinyl-CoA synthetase (*SCS*), the beta subunit of E1 of pyruvate dehydrogenase (*PDH*) and mitochondrial carrier protein 9 (*MCP9*).
The expected upregulation was not much, as the sequencing results also showed no higher increase than 3.8 fold as compared to the wildtype.
The Northern blots showed that, upon downregulation of ZC3H32, either by inducing RNAi or by stopping the expression of ZC3H32-myc in the double knock-out cell lines, the RNA levels of *SCS, PDH* and *IDH* show a slight increase, however, the results are inconclusive. There was no increase in the RNA levels of *MCP-9* (see fig. 49 and 50, as well as table 8). *gMDH* and *PPDK* were shown to be up-regulated at least two fold in two independent experiments (for *gMDH*, see fig. 49 B and D, for PPDK see fig. 50 A and B). The results of *PDH* also point towards an upregulation, upon knock-down, it was up-regulated 2 folds in the double knock-out cell line and 1.9 fold in the RNAi cell line. Thus, it can be concluded, that ZC3H32 knock-down affects the RNA levels of *gMDH* and *PPDK* and probably *PDH* as well.

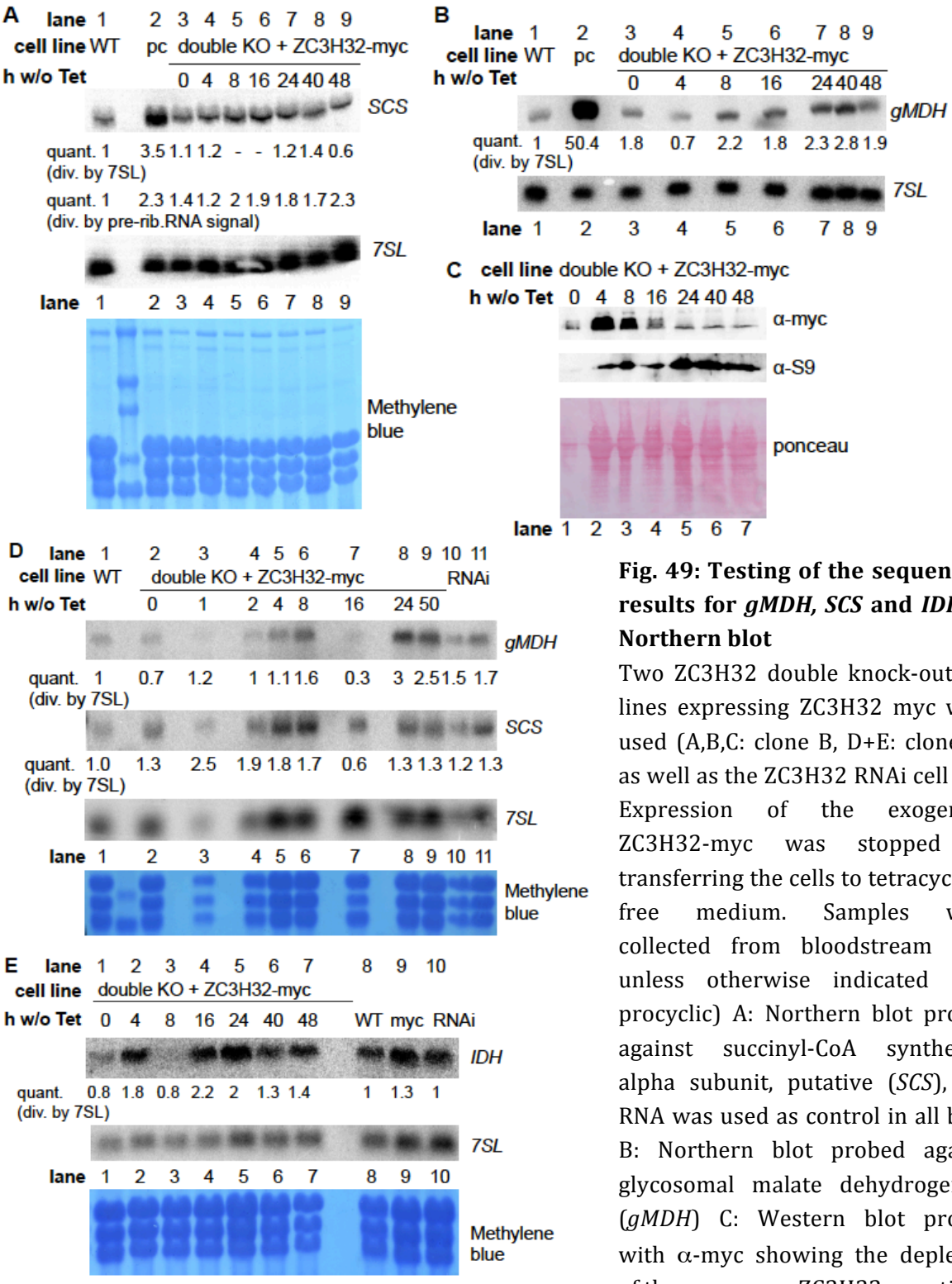

Fig. 49: Testing of the sequencing results for *gMDH, SCS* and *IDH* by Northern blot

Two ZC3H32 double knock-out cell lines expressing ZC3H32 myc were used (A,B,C: clone B, D+E: clone A), as well as the ZC3H32 RNAi cell line. Expression of the exogenous ZC3H32-myc was stopped by transferring the cells to tetracycline-free medium. Samples were collected from bloodstream cells unless otherwise indicated (pc= procyclic) A: Northern blot probed against succinyl-CoA synthetase alpha subunit, putative (*SCS*), *7SL* RNA was used as control in all blots B: Northern blot probed against glycosomal malate dehydrogenase (*gMDH*) C: Western blot probed with α-myc showing the depletion of the exogenous ZC3H32 over time. D: Second Northern blot probed against *SCS* and *gMDH*. RNAi (ZC3H32 RNAi) samples were collected after 24h of induction E: Northern blot probed against isocitrate dehydrogenase, putative (*IDH*). myc: cells expression exogenous ZC3H32-myc (no knock-out). Both myc and RNAi cell lines were induced for 24h.

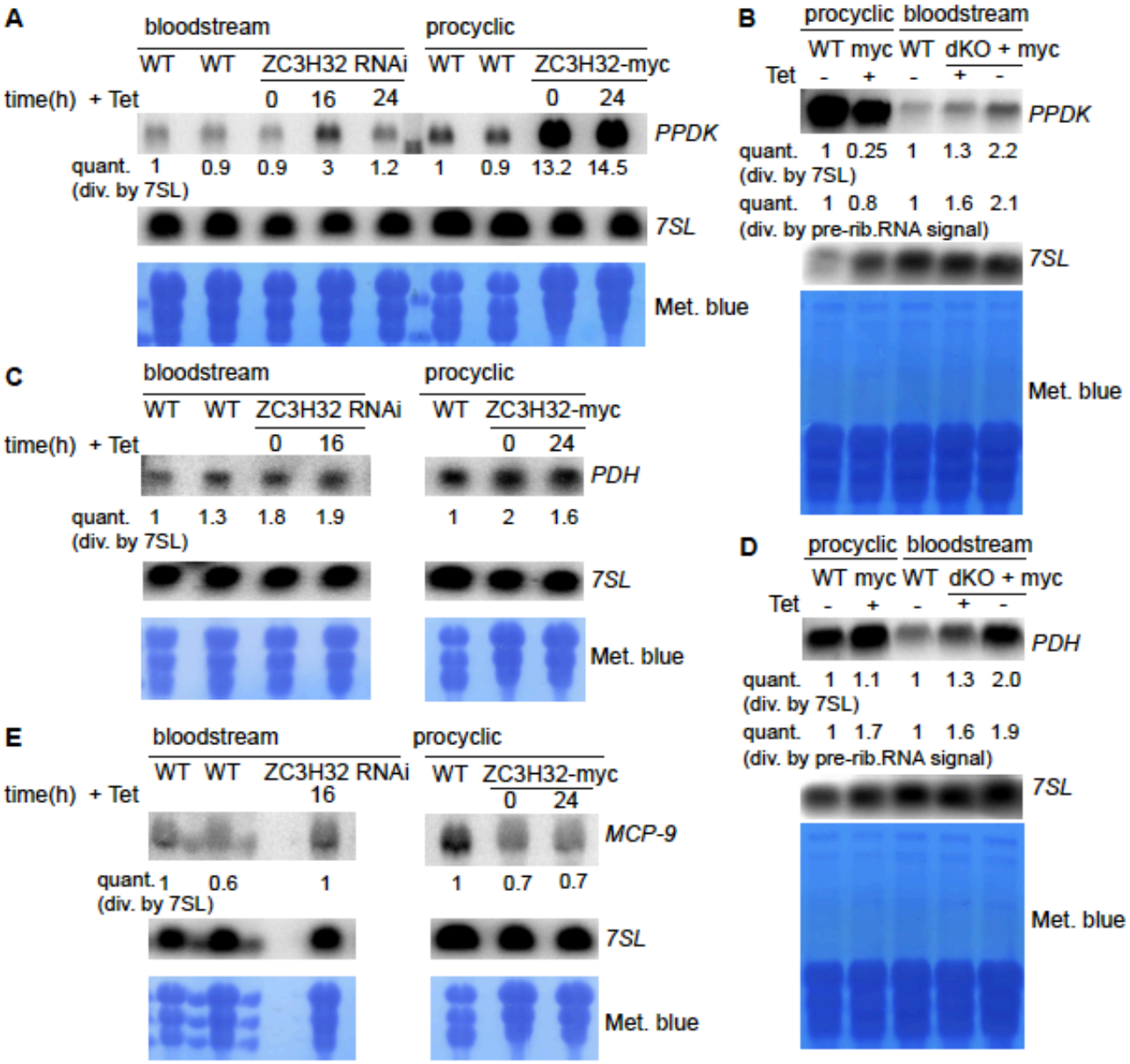

Fig. 50: Testing of the sequencing results for *PPDK, PDH* and *MCP-9* by Northern blot

For these Northerns, RNA samples from different cell lines were used:

bloodstream and procyclic 1313 ("WT"), the ZC3H32 RNAi cell line ("RNAi", see panel A, C and E),

a double knock-out cell line (clone A, labeled "dKO", see panel B, D; clone A was used) and the procyclic ZC3H32-myc cell line (no knock-out of ZC3H32), referred to as "ZC3H32-myc" (A,C,E) and "myc" (B,D).

RNAi was induced by adding tetracycline (**+**Tet), expression of the exogenous ZC3H32-myc was stopped by transferring the cells to tetracycline-free medium (**-**Tet).

7SL RNA was used as control in all blots

A and B: Northern blots probed against pyruvate phosphate dikinase (*PPDK*)

C +D: Northern blot probed against pyruvate dehydrogenase E1 beta subunit, putative (*PDH*)

E: Northern blot probed against mitochondrial carrier protein 9 (*MCP9*)

3.3.13 ZC3H32 and the degradation machinery

As ZC3H32 degrades RNA, it was thought that it interacts with some parts of the trypanosome degradation machinery. I therefore tested several proteins involved in mRNA degragation for an interaction with ZC3H32. I started with members of the CAF-NOT complex, because there were indications that MKT1 interacts with components of this complex: a yeast-two-hybrid screen showed NOT2 as a putative MKT1 binding partner while CAF40 and NOT1 were co-purified with MKT1 in a TAP purification (Singh, Minia et al. 2014). However, I could not detect an interaction between ZC3H32 and any of these proteins (see fig. 51).
I also tested the exoribonuclease XRNA and the exosome component RRP45 (fig. 52A) as well as DHH1 (fig. 52B), which is involved in translation, for an interaction with ZC3H32. XRNA and RRP45 were chosen because they play a role in mRNA degradation and also because specific antibodies were available. DHH1 was tested because it was also found in the TAP purification of MKT1 (Singh, Minia et al. 2014). But as the initial IP did not suggest any interaction (fig. 52), I stopped testing these candidates. However, the interaction between ZC3H32 and these proteins, as well as with the members of the CAF-NOT complex, might be too transient to be observed. Thus, it remains unclear whether ZC3H32 degrades RNA and how it does that.

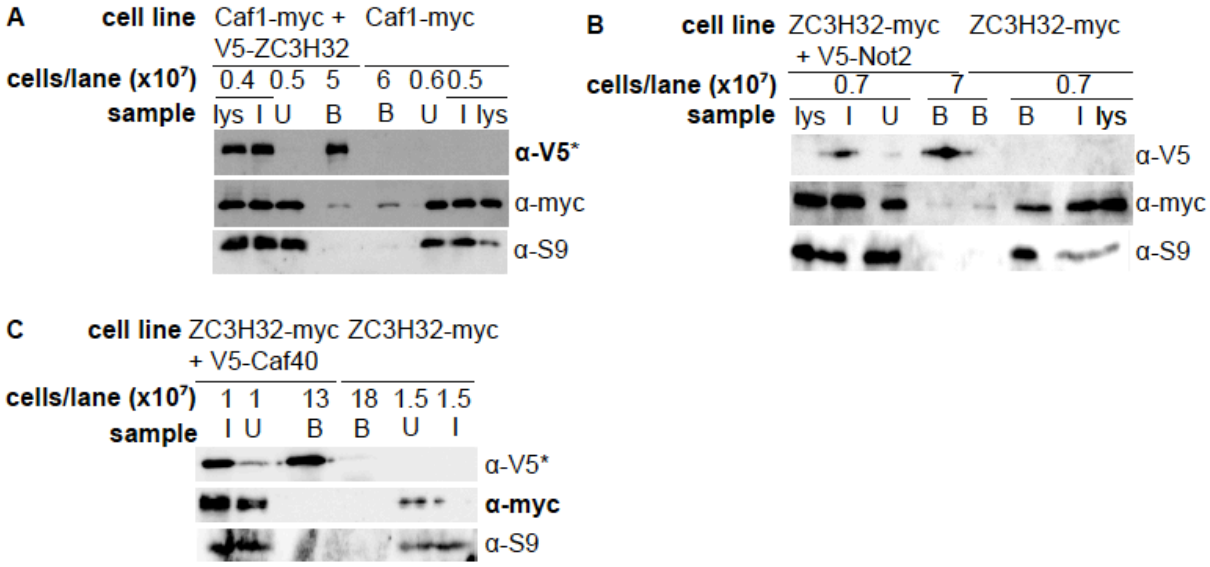

Fig. 51: ZC3H32 does not interact with the CAF1-NOT complex

* marks the antibody which was used for the precipitation (here: α-V5, as α-V5 beads were used for all three IPs)

The antibody recognizing the tagged ZC3H32 (either V5 or myc tagged) is written in bold

A: V5-IP with V5-ZC3H32 and CAF1-myc. S9 was used as control.

B: V5-IP with V5-Not2 and ZC3H32-myc. S9 was used as control.

C: V5-IP with V5-CAF40 and ZC3H32-myc. S9 was used as control.

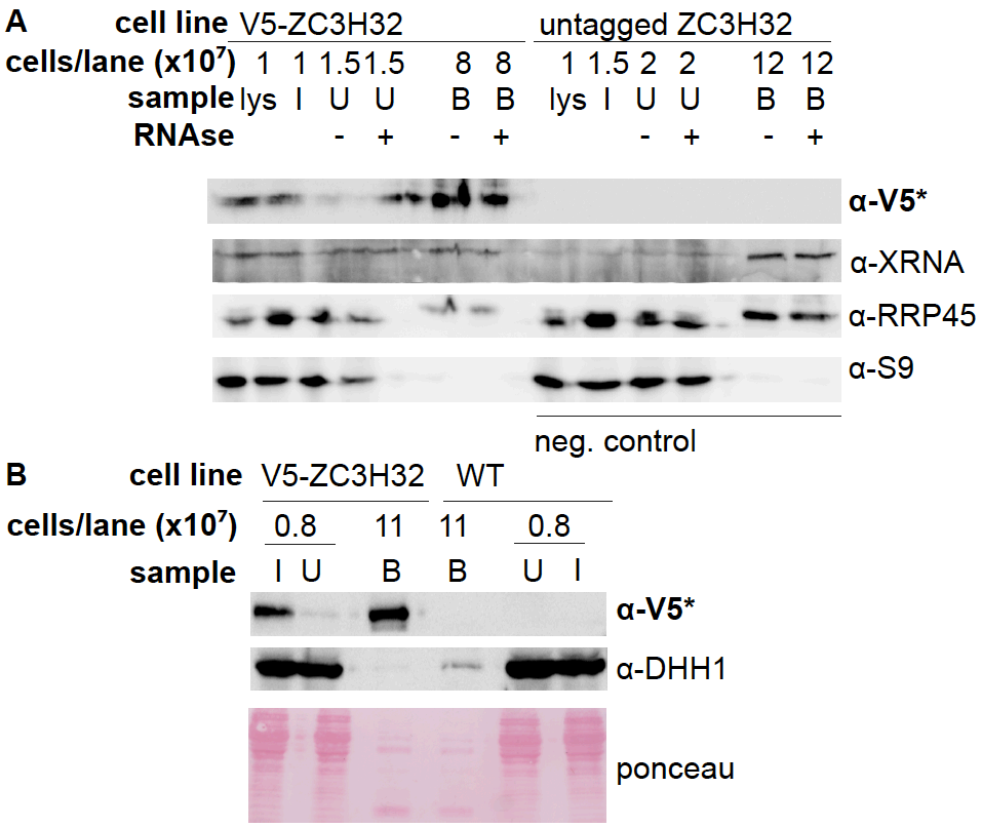

Fig. 52: ZC3H32 does not co-purify RRP45, XRNA and DHH1

* marks the antibody which was used for the precipitation (here: α-V5, as α-V5 beads were used for both IPs)

The antibody recognizing the tagged ZC3H32 (here: α-V5) is written in bold

A: V5-IP with V5-ZC3H32 expressing cells. Cells expressing MKT1-YFP were used as control cell line. ("untagged ZC3H32", Western blot signal for YFP-MKT1 not shown). The Western blot was probed with α-V5, α-XRNA, α-RRP45 and α-S9 (negative control). The IPs were done with and without RNAse.

D: V5-IP with V5-ZC3H32 and WT cells (control cell line). The Western blot was probed with α-DHH1 and α-V5.

3.3.14 Immunoprecipitation of ZC3H32 followed by Mass spectrometry

In order to find interaction partners of ZC3H32, two ZC3H32-myc Immunoprecipitations were done with anti-myc beads, one in the presence of RNAse Inhibitor, the other in the presence of RNAseA. As a control, an IP with a wild type cell line, also in the presence of RNAse Inhibitor, was done.

The beads were boiled in Laemmli buffer and the eluted proteins were sent for comparative mass spectrometry. The control sample was labeled with formaldehyde ("light" labeling), the inhibitor sample with deuterated formaldehyde ("medium") and the RNAse sample was labeled with deuterated and ^{13}C containing formaldehyde ("heavy").

The results are shown in table 9. ZC3H32 was shown to be enriched, as compared to the control, in both preparations, which shows that the pull-down was successful. MKT1 was not enriched, neither were any members of the degradation machinery.

Some putative RNA binding proteins were found, though, for example ZC3H28, DRBD2, ZC3H41 and ZC3H40.

eIF4E-IP and DRBD4 are enriched in both RNAse and Inhibitor preparation, however, only with one unique peptide, which is too little for conformation. eIF4E-IP was tested for interaction by Co-IP (result see fig. 53), but no interaction was seen.

PBP1 is enriched in the Inhibitor sample, however, it only shows one unique peptide as well (see table in suppl. data).

In order to check the mass Spectrometry data, two candidates, DRBD2 and the hypothetical protein Tb927.7.2780, which were both enriched in both the RNAse and the Inhibitor sample, were tested for interaction with ZC3H32. However, the Co-IPs showed that there was no interaction. This finding, combined with the fact that MKT1, which was shown to interact with ZC3H32 both in the presence and absence of RNAseA, was not found to be enriched in neither of the samples, shows, that the mass spectrometry results probably do not show real interaction partners of ZC3H32 and thus cannot be used.

Accession number	Description	Σ# Unique Peptides	RNAse/control Heavy/Light	Inh./control Medium/Light
Tb927.10.5250	ZC3H32	19	300.00	300.00
Tb927.7.2780	**hyp. protein**	**2**	**300.00**	**300.00**
Tb09.211.4540	**DRBD2**	**4**	**300.00**	**300.00**
Tb927.6.4870	S-adenosylmethionine synthetase, putative	3	300.00	300.00
Tb927.6.4480	valyl-tRNA synthetase, putative (ValRS)	4	300.00	300.00
Tb11.01.1170	hyp. protein, unique to Kinetoplastids	5	300.00	300.00
Tb927.4.4060	hyp. protein	2	79.770	300.000
Tb927.10.14140	pyruvate kinase 1 (PYK1)	6	1.000	300.000
Tb927.4.560	Cytoplasmic dynein 2 heavy chain, putative	6	300.00	66.18
Tb927.7.1040	40S rib. protein S16	5	22.88	18.01
Tb927.8.6260	hyp. protein, N-terminal leucine zipper	4	26.71	17.61
Tb09.160.1160	nucleolar protein (NOP86)	5	29.78	15.50
Tb927.4.450	coatomer alpha subunit, putative	3	31.76	13.53
Tb927.4.4310	Nucleoporin (TbNup64)	4	15.26	10.37
Tb927.6.3650	ADP-ribosylation factor, putative	2	14.20	10.29
Tb11.02.4040	protein transport protein Sec31, putative	3	18.12	7.33
Tb11.02.0030	dynein heavy chain, putative	11	37.66	6.74
Tb09.211.4240	phosphoinositide-binding protein, putative	3	11.35	6.51
Tb09.211.1070	ZC3H28	4	11.03	6.04
Tb11.02.3120	malic enzyme	2	1.488	4.961
Tb927.10.5340	40S ribosomal protein S18	6	6.94	4.72
Tb09.211.4780	Nucleoporin (Nup82)	3	15.16	4.38
Tb11.02.1566	VSG-related, putative	5	0.953	3.966
Tb927.10.12710	HSP110	4	33.38	3.34
Tb927.10.14950	ZC3H40	3	17.09	3.34
Tb11.02.4300	hyp. protein	14	300.00	1.86
Tb927.10.10360	microtubule-associated protein, putative	3	4.81	1.83
Tb927.4.2740	hyp. protein	2	7.86	1.82

Tb927.8.1870	Golgi/lysosome glycoprotein 1 (tGLP1)	2	4.84	1.52
Tb11.46.0009	ZC3H41	5	9.33	1.50
Tb11.03.0250	Cyclophilin-type peptidyl-prolyl cis-trans isomerase (CYPA)	7	3.01	1.44
Tb927.10.4570	elongation factor 2	11	5.17	1.43
Tb927.3.3580	lipophosphoglycan biosynthetic protein	2	17.01	1.43
Tb927.10.8230	protein disulfide isomerase, putative	6	3.81	1.36
Tb927.10.2890	enolase	11	3.59	1.27
Tb11.02.1120	adenylosuccinate synthetase, putative	3	5.45	1.24
Tb11.01.7010	hyp. protein (TbKap123)	4	3.57	1.15
Tb09.211.3610	ubiquitin-activating enzyme e1, putative	12	4.99	1.07
Tb11.01.1400	glycyl-tRNA synthetase, putative	2	7.11	1.02
Tb927.4.1300	hyp. protein	4	3.83	0.84
Tb927.3.2960	inosine-adenosine-guanosine-nucleosidehydrolase	2	4.68	0.76
Tb09.211.1620	hyp. protein	6	3.31	0.74
Tb927.3.910	gamma-tubulin	2	78.45	0.16
Tb927.7.1300	protein disulfide isomerase,ERp72-like, putative	2	3.25	0.04

Table 9: Mass spectrometry results from myc-Immunoprecipitation of ZC3H32.

The control sample (boiled beads from the IP done with wild type cells) was labeled with formaldehyde ("light" labeling), the sample of the IP done with the ZC3H32-myc cell line in the presence of RNAse Inhibitor ("Inh.") with deuterated formaldehyde ("medium") and sample of the IP done with the ZC3H32-myc cell line in the presence of RNAseA was labeled with deuterated and ^{13}C containing formaldehyde ("heavy").

Numbers indicate the enrichment of the protein in the respective sample ("Inh."/"medium") or ("RNAse"/"heavy") as compared to the control ("light"). 300 indicates the maximum measurable level. The colour coding indicates the enrichment. red: 300 (maximum); dark orange: 300-20; salmon: 20-10; light orange: 10-5; light yellow: 5-2; white: <2 (not significant or not enriched).

Candidates shown in bold were tested by Co-IP (see fig. 53).

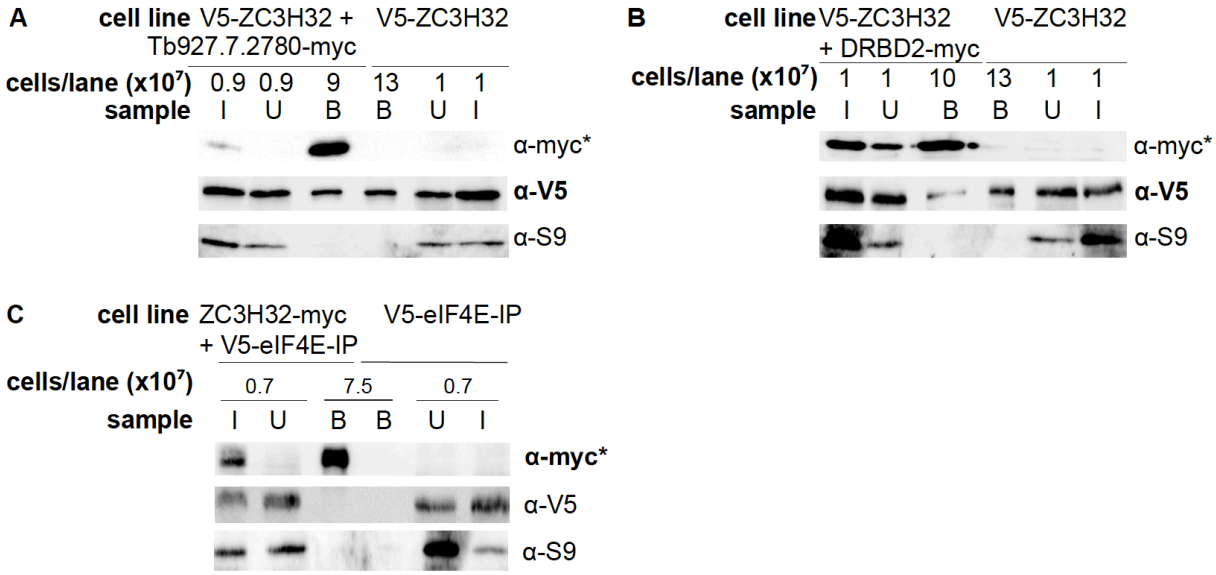

Fig. 53: The mass spectrometry results could not be verified with Co-Immunoprecipiations

* marks the antibody which was used for the precipitation (here: α-myc, α-myc beads were used in all three IPs).

The antibody recognizing the tagged ZC3H32 (which is either V5 or myc-tagged) is written in bold

S9 was used as negative control in all three IPs.

A: myc-IP with *Tb*927.7.2780-myc and V5-ZC3H32.

B: myc-IP with DRBD2-myc and V5-ZC3H32

C: myc-IP with ZC3H32-myc and V5-eIF4E-IP

3.3.15 Testing ZC3H32-RNA interaction by CLIP

In order to test whether ZC3H32 binds directly to RNA, a CLIP (Crosslinking Immunoprecipitation) was done using ZC3H32-myc cells, wild type cells as negative control and UBP-1-myc cells as positive control. For this experiment, the cells were crosslinked twice with UV-light (Stratalinker, 4000), then harvested and stored in liquid nitrogen. The cells were lysed in a buffer containing 0.5% IP-40. Then, the RNA that was not bound to any protein, was digested with RNAseT1. The Immunoprecipitation was done using myc-beads. After the IP, the RNA in the precipitates was labelled with γATP and the RNA-protein complexes were separated on a NuPAGE Bis-TRIS gel. The gel was then exposed using a Phosphoimager film (see fig. 54 A and C).

On the gel of the first CLIP experiment, a huge band was seen for the positive control at approximately 50kDa. UBP1 has a size of 24.3kDa (plus appr. 2kDa for the myc-tag), however, as this is an RNA-protein complex, it is expected to run higher. The same was observed in the CLIP experiments done by B. Jha (Jha, Fadda et al. 2014).

A faint band was seen at 100kDa in the ZC3H32-precipitate. This could possibly be the band for the RNA-protein complex, as ZC3H32 has a size of 72 kDa, and a difference between the molecular weight of the protein and the protein-RNA complex of appr. 25kDa was also observed for UBP-1. However, the same band was also observed in the positive control, meaning that it is probably a contamination.

The experiment was repeated twice, however, in both repetitions no band was observed in the ZC3H32 precipitate.

These experiments show that, if ZC3H32 interacts directly with the RNA, this interaction might be too transient to be observed using this method. Another possibility is that the RNA binding site might be too small to offer protection against RNAseT1.

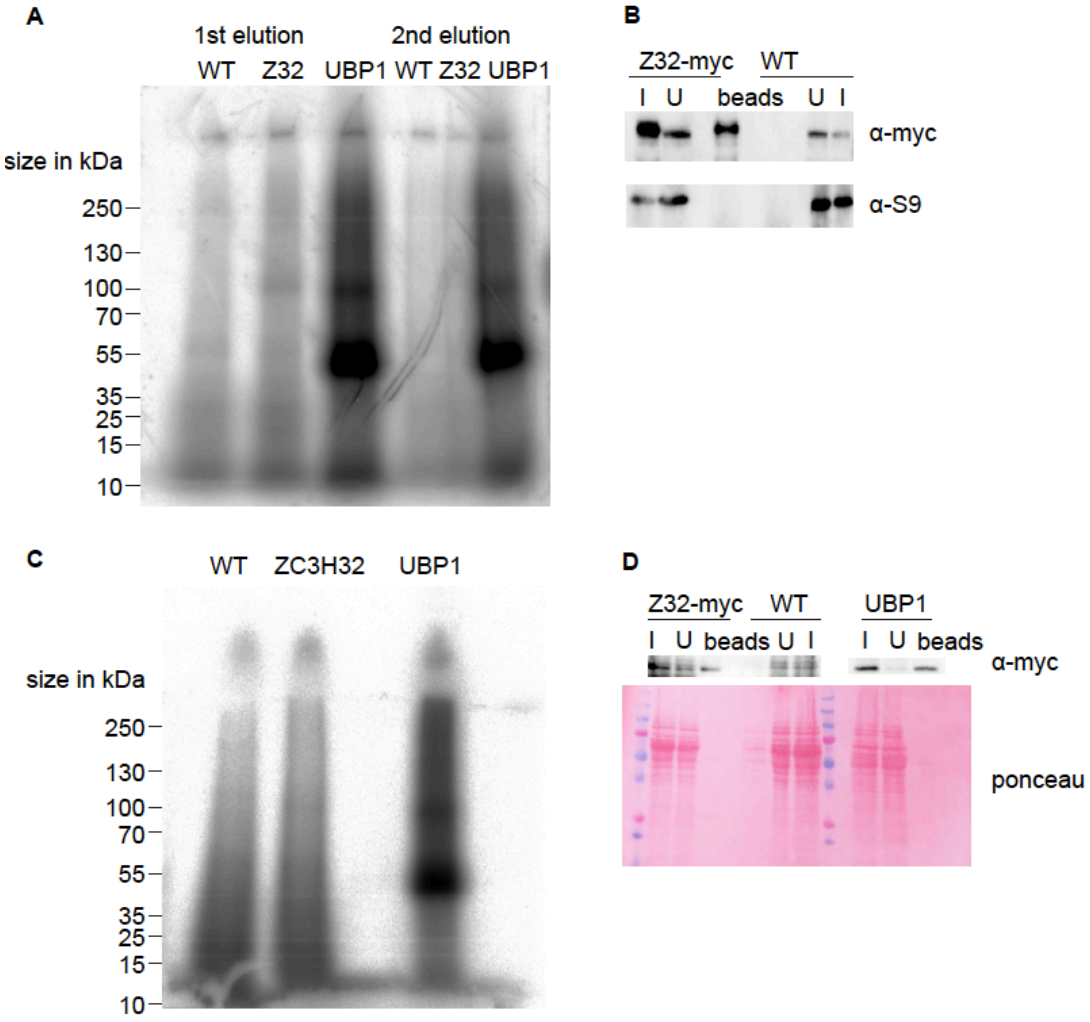

Fig 54: ZC3H32-RNA interaction cannot be detected using iCLIP

A: 1st CLIP experiment, NuPAGE gel with γATP labeled RNA. B: Western blot with samples from 1st CLIP. I: Input, U: unbound, beads: protein bound to the beads. ZC3H32 was pulled down using myc-beads. C and D: 2nd CLIP experiment, NuPAGE gel and Western blot

4. Discussion

4.1 Mass Spectrometry of free and membrane bound polyribosomes

In order to determine the function of a putative RNA binding protein, polyribosome association is an important indication, especially if the candidate protein is supposed to be stabilizing its target RNAs. However, sucrose gradient centrifugation, followed by fractionation, has one big disadvantage: abundant proteins, like trypanothione reductase, trail down the gradient, which leads to false positives. This fact makes it difficult to determine whether an RNA binding protein really associates with polyribosomes, especially if this protein is abundant and/or has only a few RNA targets. Non-abundant proteins might not be visible on a Western blot or detectable by mass spectrometry.

Therefore, in order to test on a large scale which of the putative RNA binding proteins in *T. brucei* genuinely bind to RNA, other methods might be better. One alternative method would be a precipitation with oligo-dT beads.

Also, it is very likely that the majority of RNA binding proteins is present in abundance, as it is the case for PABP (Gorlach, Burd et al. 1994). This is a problem when polyribosome association is tested by Western blot. Because, if a protein is present with $1x10^5$ copies/cell and would bind 5% of the cells total mRNA, only 1% of the total protein pool would be bound to RNA, while 99% would be unbound and thus not associated with polyribosomes (for calculation see 3.1.6).

Also, an RNA binding protein's association with its target RNAs could be transient, especially if its role destabilizing. This might be the case for ZC3H32 or PUF2. A transient interaction would lead to a larger percentage of unbound protein and decrease the chance to proof a polyribosome association.

Therefore, sucrose gradient centrifugation, whether followed by mass spectrometry or Western blotting, is still more suitable to determine the polyribosome association of more common RNA regulators, like PABP, DHH1 and MKT1, than of more specific RNA binding proteins.

Another problem is that the mass spectrometry data contains not only false positives, but also false negatives. For example, the translation initiation factor eIF4G3 was not found in the mass spectrometry results of the bloodstream free polyribosomes, while eIF4G4 was not found in the results of the membrane-bound polyribosomes. However, Western blots from different gradients showed that these two proteins are present in both free and membrane-bound polyribosomes to the same extent (see figure 17).

However, the obtained data gives an indication whether a protein is associated with polyribosomes or not. If the candidate protein in question is not very abundant but still found in the mass spectrometry results the polyribosome association is likely to be genuine.

Also, a protein found in more than one of the mass spectrometry results is very likely to be a candidate: the five RNA binding proteins that were present in three of the five mass spectrometry data sets were all proven to be polyribosome associated. For DRBD3, however, crosslinking the cells is necessary in order to detect this protein in the polyribosomes.
Thus, the data is still useful, especially in combination with the data obtained by other screens, e.g. the tethering screen developed by E. Erben. This screen gives an indication whether a protein is stabilizing or destabilizing mRNAs.
If an RNA binding protein is found in my mass spectrometry results and is identified as stabilizing by the tethering screen, this information would strongly suggest that the protein is associated with polyribosomes and stabilizes its targets.

4.2 VSG mRNP pull down

I tried to isolating the VSG mRNP by first isolation polyribosomes and then pulling down the mRNP via the nascent polypeptide using Protein A beads and a VSG antibody. However, this did not work, the VSG mRNA was not enriched on the beads.
If this method is repeated, the first thing needed is a cell line that expresses a certain VSG variant under drug control. This can be achieved with the Mark Carrington vector 3850 (pHD 2606) or a completely new construct. Otherwise, the efficiency of the pull-down cannot be tested by Northern blot, which makes it impossible to adjust the pull-down conditions. However, there are several problems that remain: the procedure remains lengthy, which can lead to RNA binding proteins falling of the *VSG* RNA. This could be prevented, or at least, decreased, by UV-crosslinking.
A more important problem is the mature VSG protein. As already mentioned, abundant proteins trail down the gradient, VSG being no exception. The mature VSG can block the antibody and thus prevent the nascent polypeptide from binding. It is not unlikely that the mature protein binds the antibody with higher affinity than the nascent polypeptide. While it is surely possible to get rid of some of the mature VSG, e.g. by adding GLP-transaminases to the cells prior to lysis, it is unlikely that all of the mature VSG can be removed from the IP. This would increase the amount of antibodies and poly-A beads needed for the IP, which in turn would lead to a higher background.
The high background is another problem: while it is possible to decrease the background, e.g. by blocking the beads and washing the IP stringently, a negative control is still necessary in order to sort out proteins that bind unspecifically to the beads. Especially if quantitative mass spectrometry is chosen for protein identification, an appropriate negative control is crucial.
Empty beads are not suitable, as this would not sort out proteins binding unspecifically to the VSG antibody. It might be possible to use another antibody as a control, e.g. anti-tubulin. However, this would pull down tubulin mRNPs and that would be a completely different IP, with completely different results.

Using a cell line expressing another VSG, e.g. a VSG222 cell line for the VSG118 pull down, is also not an option, as it is likely that an antibody against one VSG binds another VSG variant as well.
Therefore, it should be considered to use a different approach before working on adjusting this method. An alternative would be the method developed by D. Inchaustegui, in which the 3'UTR of the protein of interest is cloned behind the *CAT* ORF, which carries three tags, with eight streptavidin binding peptides each, on its N-terminus.
In order to get rid of the mature protein, the immunoprecipitation is done with the polyribosomal fractions, using anti-streptavidin beads, which bind to the nascent polypeptide. As the streptavidin binding peptides are on the N-terminus, they are translated first and thus it is assured that the nascent polypeptide can bind to the streptavidin beads.
It has already been shown that a 97nt long sequence at the 3' end of the *VSG* mRNA (containing the last 10 codons of the *VSG* ORF and the 3'UTR) can stabilize a reporter RNA in the bloodstream form (Berberof, Vanhamme et al. 1995). A conserved 8mer and a conserved 14mer have shown to be important for the stage-specific regulation.
Knowing this, two constructs could be made: One construct containing the entire sequence and a control construct, which does not contain the 14mer and the 8mer.
The first construct should be stabilized in the bloodstream form and destabilized in the procyclic form, while, according to the result of (Berberof, Vanhamme et al. 1995) the second one should show no stage-specific regulation. A CAT assay can be used to verify that.
This approach would have several advantages over the method I tried to develop:
For once, this method is already developed and has been applied successfully by D. Inchaustegui.
Secondly, with deleting the conserved regions, a suitable control construct can be made. If this does not work, a control construct without the streptavidin tags can be made.
Thirdly, the CAT construct is inducible. This means, if the expression is not leaky, the cells can be harvested a few hours after induction, which would mean lower levels of the mature protein. A CAT assay can be used to determine how long it takes for the protein to be induced. A Northern blot of the polyribosomes can determine when the CAT RNA is translated. Thus, the ideal harvest time can be determined, at which the CAT RNA is already being translated, while there is still a low level of CAT protein. But even if the expression of the CAT construct were leaky the levels of the mature protein would still be lower than the levels of mature VSG.
Thus, this method would probably be a better approach in order to find proteins binding to the VSG 3'UTR.

4.3 The role of ZC3H32

4.3.1 ZC3H32 is a putative destabilizing C3H zinc finger protein

Tethering of ZC3H32 to a reporter RNA leads to the RNA's degradation. This suggests that ZC3H32 destabilizes its targets.

Tethering of different ZC3H32 fragments showed that the first 145, as well as the last 293 amino acids are sufficient to decrease the levels of the CAT reporter. This suggests that at least one of these domains is responsible for the RNA degrading activity. The putative MKT1 binding motif, the HNPY motif, which is found at position 538 (117 amino acids away from the C-terminus), seems to be necessary for the activity of the C-terminal fragment. This indicates that MKT1 plays a role in the activity of ZC3H32.

The middle part of the protein shows no activity in the tethering screen. As this part contains the three zinc fingers, it is very likely that it is responsible for the binding to the RNA targets, while either the N- or the C-terminal part (or both) are responsible for the target's degradation.

Tethering of λN-ZC3H32-myc also decreased the translation of the *CAT* RNA: After induction of λN-ZC3H32-myc, the *CAT* RNA with the BoxB, which the λN-ZC3H32-myc fusion protein binds to, tended localize to the lower polyribosomal fractions, as well as the pre-ribosomal fractions. *CAT* RNA without the BoxB, on the other hand, was mostly found in the high polyribosome fraction. Thus, when ZC3H32 is tethered to the *CAT* RNA, the *CAT* RNA is bound by fewer ribosomes. This indicates that, if ZC3H32 interacts with an mRNA, this mRNA is translated less.

These results suggest that ZC3H32 might degrade RNA by relocating it from the polyribosomes, which subsequently leads to its degradation.

4.3.2 Putative ZC3H32 mRNA targets

High-throughput sequencing revealed 20 RNAs that are up-regulated upon ZC3H32 knock-down (see 3.3.11). As ZC3H32 is very likely a destabilizing RNA binding proteins these mRNAs are putative ZC3H32 targets.

The majority of these mRNAs show stage-specific regulation, 15 out of these 20 are up-regulated in the procyclic form (Fadda, Ryten et al. 2014), while 3 more of them are slightly up-regulated (less than two fold but more than 1.5 fold). This upregulation was confirmed for five proteins (see fig. 48 and 49).

Opposite to these 20 mRNAs, the RNA levels of ZC3H32 are up-regulated in the bloodstream form, suggesting that this protein is enriched in this life cycle stage (see 3.3.1). ZC3H32 is essential for the survival of the bloodstream form of *Trypanosoma brucei*, which was shown by both RNAi and knock-out studies (3.5 and 3.6), while an RNAi screen indicated that this protein is not essential in procyclics (Alsford, Glover et al. 2005).

ZC3H32 is up-regulated and essential in the bloodstream form, while its putative targets are down-regulated in this life cycle stage. Also, the tethering screen shows that ZC3H32 can induce a reporter RNA's degradation (see 3.3.8 – 3.3.10). Together, these results suggest that ZC3H32 might be involved in the degradation of procyclic specific proteins.
Moreover, 12 of the putative targets are involved in energy metabolism. Ten of them are found in the mitochondrion, two in the glycosomes. These proteins include enzymes of the TCA cycle as well as components of the respiratory chain, two pathways that are not active in the bloodstream form trypanosome. The glycosomal proteins (pyruvate phosphate dikinase and glycosomal malate dehydrogenase) are involved in glyconeogenesis and their protein levels are also down-regulated in the bloodstream form (Urbaniak, Guther et al. 2012), which is not surprising considering the high glucose level of the mammalian bloodstream.
Out of the six tested candidates, five showed upregulation in upon ZC3H32 reduction (either by RNAi or by stopping the expression of ZC3H32-myc in the double knock-out cell line).
However, high-throughput sequencing of RNAi cell lines has shown to have some drawbacks. For once, it remains unclear whether the observed upregulation is caused directly by ZC3H32, as many RNA binding proteins, for example PUF2, MKT1 and XRNA, are down-regulated upon ZC3H32 RNAi induction. Thus, the stabilization of the target proteins could be caused by the absence of any of these proteins.
Another problem, which has already been described in (Jha, Fadda et al. 2014), is that the high-throughput sequencing results of many RNAi cell lines (PUF2, MKT1, RRP45, CTR9, CAF1 and ZC3H32) show a bias towards RNAs with short coding sequences. This means that RNAs with short coding sequences are more likely to be up-regulated, as compared to the wild type, than RNAs with long coding sequences.
This might be due to an effect on transcription, because, if transcription were slowed down, long RNAs would be more strongly affected than short ones, leading to lower levels of long RNAs (Jha, Fadda et al. 2014).
The correlation (0.42) between the ZC3H32 sequencing result and the CDS length clearly shows that this effect also influences the ZC3H32 sequencing result. However, out of the 20 up-regulated RNAs only 4 have a short open reading frame (meaning coding sequences that are shorter than the coding sequences of three quarters of the sequenced mRNAs). Also, two of them are not up-regulated in any of the other sequencing results (one encodes cytochrome c oxidase assembly protein and the other one a hypothetical protein), which does not suggest an unspecific upregulation, despite their short length. The other two, however, are up-regulated in other data sets as well and are probably false positives.
Another problem is the stress response, as some RNAs could simply be up-regulated because the cell is stressed. The samples were collected after 24 hours of induction. After this time, the growth of the cells has already been arrested. However, in order to see when this effect occurs, RNA was collected at earlier timepoints as well and the

levels of three candidates were tested by Northern blotting (see 3.3.12, fig. 48). While the RNA of glycosomal malate dehydrogenase (*gMDH*) was up-regulated after eight hours, the RNA levels of isocitrate dehydrogenase (*IDH*) and succinyl-CoA synthetase (*SCS*) were already up-regulated after four and, respectively, two hours. This indicates that these RNAs are not up-regulated because the cell is stressed. Also, although the high-throughput sequencing results show that the mRNA of pyruvate dehydrogenase (*PDH)* seems to be up-regulated upon PUF2 knock-down, *IDH* seems to be up-regulated in the MKT1 RNAi cell line and *SCS* is up-regulated in both the PUF2 and RRP45 RNAi cell line, none of the tested RNAs a generally up-regulated in RNAi cell lines.

Whether the stabilization of these RNAs is caused by a direct interaction with ZC3H32 or by an indirect effect is unclear. It was not possible to show whether ZC3H32 interacts with RNA by CLIP (see 3.3.14, fig. 52), probably because this RNA destabilizes its targets. Thus, any interaction would be rather short. This makes it very hard to determine a direct interaction. Another problem is that the RNA levels of the putative candidate genes in the bloodstream forms are rather low. I made an Immunoprecipitation with UV-crosslinked ZC3H32-myc cells and myc-beads, followed by Northern and Western blotting. While the Western blot showed that the IP worked well, the candidate RNAs (*PPDK, PDH* and *gMDH*) could not be detected in the pellet and also the signals from the input and the supernatant were not very strong (results not shown), suggesting that this approach is not very likely to succeed.

Another possibility would be to repeat the sequencing of the procyclic ZC3H32-myc cell line, in which ZC3H32 is overexpressed. The main advantage of this cell line is that it shows no growth defect. Also, the sequencing results did not correlate with the length of the coding sequence, showing that this side effect is irrelevant in this case.

The problem is that the overexpression in procyclic cells did not cause an opposite effect as compared to the ZC3H32 knock-down in the bloodstream form: While the results did not correlate, they are also not opposite (R is approximately 0). Also, only one of the putative ZC3H32 targets seemed to be destabilized upon ZC3H32 overexpression in procyclics. As already mentioned, ZC3H32 overexpression does not cause a growth defect in procyclics. Together, these results suggest that the influence of ZC3H32 is limited in the procyclic form. This might be caused by the presence other *trans*-acting factors in this life cycle stage, which prevent ZC3H32 from binding. It is also possible that ZC3H32 needs one or more other proteins to function, which might not be present in this life cycle stage.

Thus, a repetition of the high-throughput sequencing of the procyclic overexpression cell line might only give limited information about the role of this protein in the bloodstream form.

Another approach to further characterize the effect of ZC3H32 on these proteins would be to test whether their translation is affected by ZC3H32 knock-down. This could be done by inducing the RNAi cell line for a short time, make a polyribosome profile and check whether the translation of the candidate RNAs increases as compared to a wild

type cell line. The induction time should just be long enough to ensure a significant decrease in ZC3H32 protein levels but also not too long, so that the cells are still be growing. The same experiment can also be done using the double knock-out cell line, this would have the advantage that each result would be verified using a completely different cell line. What is more, this would rule out any side effect caused by unspecific RNAi targets.
While this would still not prove beyond doubt that an interaction with ZC3H32 causes the stabilization of these candidate RNAs, this experiment might at least support the results of the tethering assay, which showed that ZC3H32 can lower the translational efficiency of a reporter RNA.
It is also possible to do high-throughput sequencing of the low ribosomal fractions (monosomes and up to 4 ribosomes) and the high polyribosomal fractions using the RNAi or the knock-out cell lines. This would show which RNAs are translated with low efficiency (low ribosomal fractions) and which one with a high efficiency (high ribosomal fractions). Comparison with a the sequencing results from the same fractions made using wild type cells would then tell us for which mRNAs the translation efficiency changes upon ZC3H32 knock-down.

4.3.3 Interaction partners of ZC3H32

It was already suggested by a yeast-two hybrid screen, as well as a TAP-purification, that ZC3H32 interacts with MKT1 (Singh, Minia et al. 2014). This interaction was confirmed by Co-Immunprecipitation (see 3.3.4, fig. 34). However, only a small fraction of the ZC3H32 pool seems to interact with MKT1. A Co-IP in the presence of RNAseA showed that this interaction is not dependent on RNA binding. This also shows that ZC3H32 and MKT1 really interact and not just bind to different binding sites of the same mRNAs.
An interaction between ZC3H32 and members of the degradation machinery (CAF40, XRNA, RRP45, NOT2, CAF1) could not be confirmed. A yeast-two-hybrid screen suggested that MKT1 interacts with NOT2, a member of the CAF-NOT deadenylase complex (Singh, Minia et al. 2014). This interaction could not be confirmed by co-immunoprecipitation as well. A possible reason might be that these interactions are too transient to be observed by these methods.
Thus, it stays unclear how ZC3H32 degrades its target RNAs.
There are two methods that can be used to determine ZC3H32's interaction partners. One would be a yeast-two-hybrid screen. This method has the disadvantage that it has a high rate of false positives. Another possibility is a pull-down followed by mass spectrometry. This was already tried (see 3.3.14) but without success. One possible reason is that the quantitative mass spectrometry failed. Maybe too much material was given for the analysis and only very abundant proteins were detected. Another possible reason might have been that the myc-tag purification was only a one-step purification. Thus, the background might have been too high. If this experiment is repeated, a two-step purification, using a TAP-tag for example, might be better.

Once the interaction partners are known, it might be possible to deduct a possible mechanism for this RNA binding protein.

5. References

Alsford, S., L. Glover and D. Horn (2005). "Multiplex analysis of RNA interference defects in Trypanosoma brucei." Mol Biochem Parasitol **139**(1): 129-132.

Archer, S. K., V. D. Luu, R. A. de Queiroz, S. Brems and C. Clayton (2009). "Trypanosoma brucei PUF9 regulates mRNAs for proteins involved in replicative processes over the cell cycle." PLoS Pathog **5**(8): e1000565.

Benz, C., J. Mulindwa, B. Ouna and C. Clayton (2011). "The Trypanosoma brucei zinc finger protein ZC3H18 is involved in differentiation." Mol Biochem Parasitol **177**(2): 148-151.

Berberof, M., A. Pays and E. Pays (1991). "A similar gene is shared by both the variant surface glycoprotein and procyclin gene transcription units of *Trypanosoma brucei*." Mol. Cell. Biol. **11**: 1473-1479.

Berberof, M., L. Vanhamme, P. Tebabi, A. Pays, D. Jefferies, S. Welburn and E. Pays (1995). "The 3'-terminal region of the mRNAs for VSG and procyclin can confer stage specificity to gene expression in *T. brucei*." EMBO J. **14**(12): 2925-2934.

Blackshear, P. J., W. S. Lai, E. A. Kennington, G. Brewer, G. M. Wilson, X. Guan and P. Zhou (2003). "Characteristics of the interaction of a synthetic human tristetraprolin tandem zinc finger peptide with AU-rich element-containing RNA substrates." J Biol Chem **278**(22): 19947-19955.

Boothroyd, J. C. and G. A. M. Cross (1982). "Transcripts coding for variant surface glycoproteins of Trypanosoma brucei have a short, identical exon at their 5,Ä≤ end." Gene **20**(2): 281-289.

Brecht, M. and M. Parsons (1998). "Changes in polysome profiles accompany trypanosome development." Mol Biochem Parasitol **97**(1-2): 189-198.

Brems, S., D. L. Guilbride, D. Gundlesdodjir-Planck, C. Busold, V. D. Luu, M. Schanne, J. Hoheisel and C. Clayton (2005). "The transcriptomes of Trypanosoma brucei Lister 427 and TREU927 bloodstream and procyclic trypomastigotes." Mol Biochem Parasitol **139**(2): 163-172.

Brooks, S. A. and P. J. Blackshear (2013). "Tristetraprolin (TTP): interactions with mRNA and proteins, and current thoughts on mechanisms of action." Biochim Biophys Acta **1829**(6-7): 666-679.

Campbell, D. A., K. Kubo, C. G. Clark and J. C. Boothroyd (1987). "Precise identification of cleavage sites involved in the unusual processing of trypanosome ribosomal RNA." J Mol Biol **196**(1): 113-124.

Caro, F., N. Bercovich, C. Atorrasagasti, M. J. Levin and M. P. Vazquez (2006). "Trypanosoma cruzi: analysis of the complete PUF RNA-binding protein family." Exp Parasitol **113**(2): 112-124.

Chaudhuri, M., W. Ajayi, S. Temple and G. C. Hill (1995). "Identification and partial purification of a stage-specific 33 kDa mitochondrial protein as the alternative oxidase of the Trypanosoma brucei brucei bloodstream trypomastigotes." J Eukaryot Microbiol **42**(5): 467-472.

Clarkson, A. B. J., E. J. Bienen, G. Pollakis and R. W. Grady (1989). "Respiration of bloodstream forms of the parasite Trypanosoma brucei brucei is dependent on a plant-like alternative oxidase." J. Biol. Chem. **264**: 17770-17776.

Clayton, C. (2013). "The regulation of trypanosome gene expression by RNA-binding proteins." PLoS Pathog **9**(11): e1003680.

Clery, A., M. Blatter and F. H. Allain (2008). "RNA recognition motifs: boring? Not quite." Curr Opin Struct Biol **18**(3): 290-298.
Coller, J. and R. Parker (2005). "General translational repression by activators of mRNA decapping." Cell **122**(6): 875-886.
Coller, J. M., M. Tucker, U. Sheth, M. A. Valencia-Sanchez and R. Parker (2001). "The DEAD box helicase, Dhh1p, functions in mRNA decapping and interacts with both the decapping and deadenylase complexes." RNA **7**(12): 1717-1727.
Cosenza, L. W., F. Bringaud, T. Baltz and F. M. Vellieux (2002). "The 3.0 A resolution crystal structure of glycosomal pyruvate phosphate dikinase from Trypanosoma brucei." J Mol Biol **318**(5): 1417-1432.
Cross, G. A., R. A. Klein and D. J. Linstead (1975). "Utilization of amino acids by Trypanosoma brucei in culture: L-threonine as a precursor for acetate." Parasitology **71**(2): 311-326.
Das, A., R. Morales, M. Banday, S. Garcia, L. Hao, G. A. Cross, A. M. Estevez and V. Bellofatto (2012). "The essential polysome-associated RNA-binding protein RBP42 targets mRNAs involved in Trypanosoma brucei energy metabolism." RNA **18**(11): 1968-1983.
De Lange, T. and P. Borst (1982). "Genomic environment of the expression-linked extra copies of genes for surface antigens of Trypanosoma brucei resembles the end of a chromosome." Nature **299**(5882): 451-453.
Droll, D., I. Minia, A. Fadda, A. Singh, M. Stewart, R. Queiroz and C. Clayton (2013). "Post-transcriptional regulation of the trypanosome heat shock response by a zinc finger protein." PLoS Pathog **9**(4): e1003286.
Ehlers, B., J. Czichos and P. Overath (1987). "RNA turnover in *Trypanosoma brucei*." Mol. Cell. Biol. **7**: 1242-1249.
Estevez, A. M., T. Kempf and C. Clayton (2001). "The exosome of Trypanosoma brucei." EMBO J **20**(14): 3831-3839.
Estevez, A. M., B. Lehner, C. M. Sanderson, T. Ruppert and C. Clayton (2003). "The roles of intersubunit interactions in exosome stability." J Biol Chem **278**(37): 34943-34951.
Evans, D. A. and R. C. Brown (1972). "The utilization of glucose and proline by culture forms of *Trypanosoma brucei*." J. Protozool. **19**(4): 686-690.
Fadda, A., V. Farber, D. Droll and C. Clayton (2013). "The roles of 3'-exoribonucleases and the exosome in trypanosome mRNA degradation." RNA **19**(7): 937-947.
Fadda, A., M. Ryten, D. Droll, V. Färber, F. Rojas, J. R. Haanstra, B. M. Bakker, K. Matthews and C. Clayton (2014). "Transcriptome-wide analysis of mRNA decay suggests explanations for complex degradation kinetics." Nucleic Acids Res **submitted**.
Fang, J. and D. S. Beattie (2002). "Novel FMN-containing rotenone-insensitive NADH dehydrogenase from Trypanosoma brucei mitochondria: isolation and characterization." Biochemistry **41**(9): 3065-3072.
Fang, J. and D. S. Beattie (2003). "Alternative oxidase present in procyclic Trypanosoma brucei may act to lower the mitochondrial production of superoxide." Arch Biochem Biophys **414**(2): 294-302.
Fenn, K. and K. R. Matthews (2007). "The cell biology of Trypanosoma brucei differentiation." Curr Opin Microbiol **10**(6): 539-546.
Fernandez-Moya, S. M. and A. M. Estevez (2010). "Posttranscriptional control and the role of RNA-binding proteins in gene regulation in trypanosomatid protozoan parasites." Wiley Interdiscip Rev RNA **1**(1): 34-46.

Fernandez-Moya, S. M., A. Garcia-Perez, S. Kramer, M. Carrington and A. M. Estevez (2012). "Alterations in DRBD3 ribonucleoprotein complexes in response to stress in Trypanosoma brucei." PLoS One **7**(11): e48870.
Figueiredo, L. M. and G. A. Cross (2010). "Nucleosomes are depleted at the VSG expression site transcribed by RNA polymerase I in African trypanosomes." Eukaryot Cell **9**(1): 148-154.
Fischer, N. and K. Weis (2002). "The DEAD box protein Dhh1 stimulates the decapping enzyme Dcp1." EMBO J **21**(11): 2788-2797.
Flynn, I. W. and I. B. Bowman (1973). "The metabolism of carbohydrate by pleomorphic African trypanosomes." Comp Biochem Physiol B **45**(1): 25-42.
Freire, E. R., R. Dhalia, D. M. Moura, T. D. da Costa Lima, R. P. Lima, C. R. Reis, K. Hughes, R. C. Figueiredo, N. Standart, M. Carrington and O. P. de Melo Neto (2011). "The four trypanosomatid eIF4E homologues fall into two separate groups, with distinct features in primary sequence and biological properties." Mol Biochem Parasitol **176**(1): 25-36.
Frydman, J., E. Nimmesgern, K. Ohtsuka and F. U. Hartl (1994). "Folding of nascent polypeptide chains in a high molecular mass assembly with molecular chaperones." Nature **370**(6485): 111-117.
Furger, A., N. Schürch, U. Kurath and I. Roditi (1997). "Elements in the 3' untranslated region of procyclin mRNA regulate expression in insect forms of *Trypanosoma brucei* by modulating RNA stability and translation." Mol. Cell. Biol. **17**: 4372-4380.
Gibson, W., L. Peacock, V. Ferris, K. Williams and M. Bailey (2008). "The use of yellow fluorescent hybrids to indicate mating in Trypanosoma brucei." Parasites & Vectors **1**(1): 4.
Gilinger, G. and V. Bellofatto (2001). "Trypanosome spliced leader RNA genes contain the first identified RNA polymerase II gene promoter in these organisms." Nucleic Acids Res. **29**: 1556-1564.
Gorlach, M., C. G. Burd and G. Dreyfuss (1994). "The mRNA poly(A)-binding protein: localization, abundance, and RNA-binding specificity." Exp Cell Res **211**(2): 400-407.
Gruszynski, A. E., F. J. van Deursen, M. C. Albareda, A. Best, K. Chaudhary, L. J. Cliffe, L. del Rio, J. D. Dunn, L. Ellis, K. J. Evans, J. M. Figueiredo, N. A. Malmquist, Y. Omosun, J. B. Palenchar, S. Prickett, G. A. Punkosdy, G. van Dooren, Q. Wang, A. K. Menon, K. R. Matthews and J. D. Bangs (2006). "Regulation of surface coat exchange by differentiating African trypanosomes." Mol Biochem Parasitol **147**(2): 211-223.
Haanstra, J. R., M. Stewart, V. D. Luu, A. van Tuijl, H. V. Westerhoff, C. Clayton and B. M. Bakker (2008). "Control and regulation of gene expression: quantitative analysis of the expression of phosphoglycerate kinase in bloodstream form Trypanosoma brucei." J Biol Chem **283**(5): 2495-2507.
Hafner, M., M. Landthaler, L. Burger, M. Khorshid, J. Hausser, P. Berninger, A. Rothballer, M. Ascano, Jr., A. C. Jungkamp, M. Munschauer, A. Ulrich, G. S. Wardle, S. Dewell, M. Zavolan and T. Tuschl (2010). "Transcriptome-wide identification of RNA-binding protein and microRNA target sites by PAR-CLIP." Cell **141**(1): 129-141.
Hafner, M., M. Landthaler, L. Burger, M. Khorshid, J. Hausser, P. Berninger, A. Rothballer, M. Ascano, A. C. Jungkamp, M. Munschauer, A. Ulrich, G. S. Wardle, S. Dewell, M. Zavolan and T. Tuschl (2010). "PAR-CliP--a method to identify transcriptome-wide the binding sites of RNA binding proteins." J Vis Exp(41).
Hall, J. P., H. Wang and J. D. Barry (2013). "Mosaic VSGs and the scale of Trypanosoma brucei antigenic variation." PLoS Pathog **9**(7): e1003502.

Hanas, J., G. Linden and K. Stuart (1975). "Mitochondrial and cytoplasmic ribosomes and their activity in blood and culture form Trypanosoma brucei." J Cell Biol **65**(1): 103-111.
Hannaert, V., F. Bringaud, F. R. Opperdoes and P. A. M. Michels (2003). "Evolution of energy metabolism and its compartmentation in Kinetoplastida." Kinetoplastid Biology and Disease **2**: 11.
Hannaert, V. and P. A. Michels (1994). "Structure, function, and biogenesis of glycosomes in kinetoplastida." J Bioenerg Biomembr **26**(2): 205-212.
Hartmann, C., C. Benz, S. Brems, L. Ellis, V. D. Luu, M. Stewart, I. D'Orso, C. Busold, K. Fellenberg, A. C. Frasch, M. Carrington, J. Hoheisel and C. E. Clayton (2007). "Small trypanosome RNA-binding proteins TbUBP1 and TbUBP2 influence expression of F-box protein mRNAs in bloodstream trypanosomes." Eukaryot Cell **6**(11): 1964-1978.
Hehl, A., E. Vassella, R. Braun and I. Roditi (1994). "A conserved stem-loop structure in the 3' untranslated region of procyclin mRNAs regulates expression in *Trypanosoma brucei*." Proc. Natl. Acad. Sci. USA **91**: 370-374.
Hendriks, E. F. and K. R. Matthews (2005). "Disruption of the developmental programme of Trypanosoma brucei by genetic ablation of TbZFP1, a differentiation-enriched CCCH protein." Mol Microbiol **57**(3): 706-716.
Hendriks, E. F., D. R. Robinson, M. Hinkins and K. R. Matthews (2001). "A novel CCCH protein which modulates differentiation of Trypanosoma brucei to its procyclic form." EMBO J. **20**: 6700-6711.
Horn, D. and R. McCulloch (2010). "Molecular mechanisms underlying the control of antigenic variation in African trypanosomes." Curr Opin Microbiol **13**(6): 700-705.
Hotz, H.-R., C. Hartmann, K. Huober, M. Hug and C. E. Clayton (1997). "Mechanisms of developmental regulation in *Trypanosoma brucei*: A polypyrimidine tract in the 3'-untranslated region of a trypanosome surface protein mRNA affects RNA abundance and translation." Nucl. Acids Res. **25**: 3017-3025.
Hudson, B. P., M. A. Martinez-Yamout, H. J. Dyson and P. E. Wright (2004). "Recognition of the mRNA AU-rich element by the zinc finger domain of TIS11d." Nat Struct Mol Biol **11**(3): 257-264.
Hug, M., H. R. Hotz, C. Hartmann and C. E. Clayton (1994). "Hierarchies of RNA processing signals in a trypanosome surface antigen mRNA precursor." Mol. Cell. Biol. **14**: 7428-7435.
Janzen, C. J., F. van Deursen, H. Shi, G. A. Cross, K. R. Matthews and E. Ullu (2006). "Expression site silencing and life-cycle progression appear normal in Argonaute1-deficient Trypanosoma brucei." Mol Biochem Parasitol **149**(1): 102-107.
Jensen, B. C., D. Sivam, C. T. Kifer, P. J. Myler and M. Parsons (2009). "Widespread variation in transcript abundance within and across developmental stages of Trypanosoma brucei." BMC Genomics **10**: 482.
Jha, B. A., S. K. Archer and C. E. Clayton (2013). "The Trypanosome Pumilio Domain Protein PUF5." PLoS ONE **8**(10): e77371.
Jha, B. A., A. Fadda, C. Mercé, E. Mugo, D. Droll and C. Clayton (2014). "Depletion of the trypanosome pumilio domain protein PUF2 or mRNA decay enzymes causes transcriptome changes related to coding region length." Eukaryot Cell **doi:10.1128/EC.00018-14**.
Kabani, S., K. Fenn, A. Ross, A. Ivens, T. K. Smith, P. Ghazal and K. Matthews (2009). "Genome-wide expression profiling of in vivo-derived bloodstream parasite stages and dynamic

analysis of mRNA alterations during synchronous differentiation in Trypanosoma brucei." BMC Genomics **10**: 427.
Kedersha, N. L., M. Gupta, W. Li, I. Miller and P. Anderson (1999). "RNA-binding proteins TIA-1 and TIAR link the phosphorylation of eIF-2 alpha to the assembly of mammalian stress granules." J Cell Biol **147**(7): 1431-1442.
Keene, J. D. (2007). "RNA regulons: coordination of post-transcriptional events." Nat Rev Genet **8**(7): 533-543.
Keene, J. D. and S. A. Tenenbaum (2002). "Eukaryotic mRNPs may represent posttranscriptional operons." Mol Cell **9**(6): 1161-1167.
Kelly, S., J. Reed, S. Kramer, L. Ellis, H. Webb, J. Sunter, J. Salje, N. Marinsek, K. Gull, B. Wickstead and M. Carrington (2007). "Functional genomics in Trypanosoma brucei: a collection of vectors for the expression of tagged proteins from endogenous and ectopic gene loci." Mol Biochem Parasitol **154**(1): 103-109.
Kerscher, S. J. (2000). "Diversity and origin of alternative NADH:ubiquinone oxidoreductases." Biochim Biophys Acta **1459**(2-3): 274-283.
Kindler, S., H. Wang, D. Richter and H. Tiedge (2005). "RNA transport and local control of translation." Annu Rev Cell Dev Biol **21**: 223-245.
Kramer, S. (2012). "Developmental regulation of gene expression in the absence of transcriptional control: the case of kinetoplastids." Mol Biochem Parasitol **181**(2): 61-72.
Kramer, S., B. Bannerman-Chukualim, L. Ellis, E. A. Boulden, S. Kelly, M. C. Field and M. Carrington (2013). "Differential localization of the two T. brucei poly(A) binding proteins to the nucleus and RNP granules suggests binding to distinct mRNA pools." PLoS One **8**(1): e54004.
Kramer, S. and M. Carrington (2011). "Trans-acting proteins regulating mRNA maturation, stability and translation in trypanosomatids." Trends Parasitol **27**(1): 23-30.
Kramer, S., N. Kimblin and M. Carrington (2010). "Genome-wide in silico screen for CCCH-type zinc finger proteins of Trypanosoma brucei, Trypanosoma cruzi and Leishmania major." BMC Genomics **11**(1): 283.
Kramer, S., R. Queiroz, L. Ellis, J. D. Hoheisel, C. Clayton and M. Carrington (2010). "The RNA helicase DHH1 is central to the correct expression of many developmentally regulated mRNAs in trypanosomes." J Cell Sci **123**(Pt 5): 699-711.
Kulkarni, M., S. Ozgur and G. Stoecklin (2010). "On track with P-bodies." Biochem Soc Trans **38**(Pt 1): 242-251.
Lai, W. S., E. Carballo, J. R. Strum, E. A. Kennington, R. S. Phillips and P. J. Blackshear (1999). "Evidence that tristetraprolin binds to AU-rich elements and promotes the deadenylation and destabilization of tumor necrosis factor alpha mRNA." Mol Cell Biol **19**(6): 4311-4323.
Lamont, G. S., R. S. Tucker and G. A. Cross (1986). "Analysis of antigen switching rates in Trypanosoma brucei." Parasitology **92 (Pt 2)**: 355-367.
Lamour, N., L. Rivière, V. Coustou, G. H. Coombs, M. P. Barrett and F. Bringaud (2005). "Proline Metabolism in Procyclic Trypanosoma brucei Is Down-regulated in the Presence of Glucose." Journal of Biological Chemistry **280**(12): 11902-11910.
Lang, B. D., A.-m. Li, H. D. Black-Brewster and J. L. Fridovich-Keil (2001). "The brefeldin A resistance protein Bfr1p is a component of polyribosome-associated mRNP complexes in yeast." Nucleic Acids Research **29**(12): 2567-2574.

Li, C. H., H. Irmer, D. Gudjonsdottir-Planck, S. Freese, H. Salm, S. Haile, A. M. Estevez and C. Clayton (2006). "Roles of a Trypanosoma brucei 5'->3' exoribonuclease homolog in mRNA degradation." RNA **12**(12): 2171-2186.
Ling, A. S., J. R. Trotter and E. F. Hendriks (2011). "A zinc finger protein, TbZC3H20, stabilizes two developmentally regulated mRNAs in trypanosomes." J Biol Chem **286**(23): 20152-20162.
Manful, T., A. Fadda and C. Clayton (2011). "The role of the 5'-3' exoribonuclease XRNA in transcriptome-wide mRNA degradation." RNA **17**(11): 2039-2047.
Mani, J., A. Guttinger, B. Schimanski, M. Heller, A. Acosta-Serrano, P. Pescher, G. Spath and I. Roditi (2011). "Alba-domain proteins of Trypanosoma brucei are cytoplasmic RNA-binding proteins that interact with the translation machinery." PLoS One **6**(7): e22463.
Marcello, L. and J. D. Barry (2007). "Analysis of the VSG gene silent archive in Trypanosoma brucei reveals that mosaic gene expression is prominent in antigenic variation and is favored by archive substructure." Genome Res **17**(9): 1344-1352.
Mayho, M., K. Fenn, P. Craddy, S. Crosthwaite and K. Matthews (2006). "Post-transcriptional control of nuclear-encoded cytochrome oxidase subunits in Trypanosoma brucei: evidence for genome-wide conservation of life-cycle stage-specific regulatory elements." Nucleic Acids Res **34**(18): 5312-5324.
Mazet, M., P. Morand, M. Biran, G. Bouyssou, P. Courtois, S. Daulouede, Y. Millerioux, J. M. Franconi, P. Vincendeau, P. Moreau and F. Bringaud (2013). "Revisiting the Central Metabolism of the Bloodstream Forms of Trypanosoma brucei: Production of Acetate in the Mitochondrion Is Essential for Parasite Viability." PLoS Negl Trop Dis **7**(12): e2587.
Michel, S. L., A. L. Guerrerio and J. M. Berg (2003). "Selective RNA binding by a single CCCH zinc-binding domain from Nup475 (Tristetraprolin)." Biochemistry **42**(16): 4626-4630.
Millerioux, Y., C. Ebikeme, M. Biran, P. Morand, G. Bouyssou, I. M. Vincent, M. Mazet, L. Riviere, J. M. Franconi, R. J. Burchmore, P. Moreau, M. P. Barrett and F. Bringaud (2013). "The threonine degradation pathway of the Trypanosoma brucei procyclic form: the main carbon source for lipid biosynthesis is under metabolic control." Mol Microbiol **90**(1): 114-129.
Najafabadi, H. S., Z. Lu, C. MacPherson, V. Mehta, V. Adoue, T. Pastinen and R. Salavati (2013). "Global identification of conserved post-transcriptional regulatory programs in trypanosomatids." Nucleic Acids Res **41**(18): 8591-8600.
Navarro, M. and K. Gull (2001). "A pol I transcriptional body associated with VSG mono-allelic expression in Trypanosoma brucei." Nature **414**(6865): 759-763.
Ouna, B. A., B. Nyambega, T. Manful, C. Helbig, M. Males, A. Fadda and C. Clayton (2012). "Depletion of trypanosome CTR9 leads to gene expression defects." PLoS One **7**(4): e34256.
Ouna, B. A., M. Stewart, C. Helbig and C. Clayton (2012). "The Trypanosoma brucei CCCH zinc finger proteins ZC3H12 and ZC3H13." Mol Biochem Parasitol **183**(2): 184-188.
Paterou, A., P. Walrad, P. Craddy, K. Fenn and K. Matthews (2006). "Identification and stage-specific association with the translational apparatus of TbZFP3, a CCCH protein that promotes trypanosome life-cycle development." J Biol Chem **281**(51): 39002-39013.
Peacock, L., M. Bailey, M. Carrington and W. Gibson (2013). "Meiosis and Haploid Gametes in the Pathogen Trypanosoma brucei." Curr Biol.
Pereira, M. M., A. M. Malvezzi, L. M. Nascimento, T. D. Lima, V. S. Alves, M. L. Palma, E. R. Freire, D. M. Moura, C. R. Reis and O. P. de Melo Neto (2013). "The eIF4E subunits of two distinct trypanosomatid eIF4F complexes are subjected to differential post-translational

modifications associated to distinct growth phases in culture." Mol Biochem Parasitol **190**(2): 82-86.

Queiroz, R., C. Benz, K. Fellenberg, J. D. Hoheisel and C. Clayton (2009). "Transcriptome analysis of differentiating trypanosomes reveals the existence of multiple post-transcriptional regulons." BMC Genomics **10**: 495.

Regmi, S., K. G. Rothberg, J. G. Hubbard and L. Ruben (2008). "The RACK1 signal anchor protein from Trypanosoma brucei associates with eukaryotic elongation factor 1A: a role for translational control in cytokinesis." Molecular Microbiology **70**(3): 724-745.

Riviere, L., P. Moreau, S. Allmann, M. Hahn, M. Biran, N. Plazolles, J. M. Franconi, M. Boshart and F. Bringaud (2009). "Acetate produced in the mitochondrion is the essential precursor for lipid biosynthesis in procyclic trypanosomes." Proc Natl Acad Sci U S A **106**(31): 12694-12699.

Robertson, M. (1912). "Notes on the Polymorphism of Trypanosoma gambiense in the Blood and Its Relation to the Exogenous Cycle in Glossina palpalis." Proceedings of the Royal Society of London. Series B, Containing Papers of a Biological Character **85**(582): 527-539.

Robinson, N. P., N. Burman, S. E. Melville and J. D. Barry (1999). "Predominance of duplicative VSG gene conversion in antigenic variation in African trypanosomes." Mol Cell Biol **19**(9): 5839-5846.

Rudenko, G. (2011). "African trypanosomes: the genome and adaptations for immune evasion." Essays Biochem **51**: 47-62.

Rudenko, G., D. Bishop, K. Gottesdiener and L. H. Van der Ploeg (1989). "Alpha-amanitin resistant transcription of protein coding genes in insect and bloodstream form Trypanosoma brucei." EMBO J **8**(13): 4259-4263.

Sandler, H., J. Kreth, H. T. Timmers and G. Stoecklin (2011). "Not1 mediates recruitment of the deadenylase Caf1 to mRNAs targeted for degradation by tristetraprolin." Nucleic Acids Res **39**(10): 4373-4386.

Sanduja, S., F. F. Blanco and D. A. Dixon (2011). "The roles of TTP and BRF proteins in regulated mRNA decay." Wiley Interdiscip Rev RNA **2**(1): 42-57.

Sather, S. and N. Agabian (1985). "A 5' spliced leader is added in trans to both alpha- and beta-tubulin transcripts in Trypanosoma brucei." Proc Natl Acad Sci U S A **82**(17): 5695-5699.

Schumann Burkard, G., P. Jutzi and I. Roditi (2011). "Genome-wide RNAi screens in bloodstream form trypanosomes identify drug transporters." Mol Biochem Parasitol **175**(1): 91-94.

Schürch, N., A. Furger, U. Kurath and I. Roditi (1997). "Contribution of the procyclin 3' untranslated region and coding region to the regulation of expression in bloodstream forms of *Trypanosoma brucei*." Mol. Biochem. Parasit. **89**: 109-121.

Schutz, G., S. Kieval, B. Groner, A. E. Sippel, D. Kurtz and P. Feigelson (1977). "Isolation of specific messenger RNA by adsorption of polysomes to matrix-bound antibody." Nucleic Acids Res **4**(1): 71-84.

Schwede, A., L. Ellis, J. Luther, M. Carrington, G. Stoecklin and C. Clayton (2008). "A role for Caf1 in mRNA deadenylation and decay in trypanosomes and human cells." Nucleic Acids Res **36**(10): 3374-3388.

Schwede, A., T. Manful, B. A. Jha, C. Helbig, N. Bercovich, M. Stewart and C. Clayton (2009). "The role of deadenylation in the degradation of unstable mRNAs in trypanosomes." Nucleic Acids Res **37**(16): 5511-5528.

Sharova, L. V., A. A. Sharov, T. Nedorezov, Y. Piao, N. Shaik and M. S. Ko (2009). "Database for mRNA half-life of 19 977 genes obtained by DNA microarray analysis of pluripotent and differentiating mouse embryonic stem cells." DNA Res **16**(1): 45-58.

Siegel, T. N., D. R. Hekstra, X. Wang, S. Dewell and G. A. Cross (2010). "Genome-wide analysis of mRNA abundance in two life-cycle stages of Trypanosoma brucei and identification of splicing and polyadenylation sites." Nucleic Acids Res **38**(15): 4946-4957.

Singh, A., I. Minia, D. Droll, A. Fadda, C. Clayton and E. Erben (2014). "Trypanosome MKT1 and the RNA-binding protein ZC3H11: interactions and potential roles in post-transcriptional regulatory networks." Nucleic Acids Res.

Sogin, M. L., J. H. Gunderson, H. J. Elwood, R. A. Alonso and D. A. Peattie (1989). "Phylogenetic meaning of the kingdom concept: an unusual ribosomal RNA from *Giardia lamblia*." Science **243**: 75-77.

Spriggs, K. A., M. Stoneley, M. Bushell and A. E. Willis (2008). "Re-programming of translation following cell stress allows IRES-mediated translation to predominate." Biol Cell **100**(1): 27-38.

Stern, M. Z., S. K. Gupta, M. Salmon-Divon, T. Haham, O. Barda, S. Levi, C. Wachtel, T. W. Nilsen and S. Michaeli (2009). "Multiple roles for polypyrimidine tract binding (PTB) proteins in trypanosome RNA metabolism." RNA **15**(4): 648-665.

Sweet, T., C. Kovalak and J. Coller (2012). "The DEAD-box protein Dhh1 promotes decapping by slowing ribosome movement." PLoS Biol **10**(6): e1001342.

t Hoen, P. A., M. Hirsch, E. J. de Meijer, R. X. de Menezes, G. J. van Ommen and J. T. den Dunnen (2011). "mRNA degradation controls differentiation state-dependent differences in transcript and splice variant abundance." Nucleic Acids Res **39**(2): 556-566.

Tschudi, C., H. Shi, J. B. Franklin and E. Ullu (2012). "Small interfering RNA-producing loci in the ancient parasitic eukaryote Trypanosoma brucei." BMC Genomics **13**: 427.

Turner, C. M. and J. D. Barry (1989). "High frequency of antigenic variation in Trypanosoma brucei rhodesiense infections." Parasitology **99 Pt 1**: 67-75.

Ule, J., K. Jensen, A. Mele and R. B. Darnell (2005). "CLIP: a method for identifying protein-RNA interaction sites in living cells." Methods **37**(4): 376-386.

Urbaniak, M. D., M. L. Guther and M. A. Ferguson (2012). "Comparative SILAC proteomic analysis of Trypanosoma brucei bloodstream and procyclic lifecycle stages." PLoS ONE **7**(5): e36619.

Utter, C. J., S. A. Garcia, J. Milone and V. Bellofatto (2011). "PolyA-specific ribonuclease (PARN-1) function in stage-specific mRNA turnover in Trypanosoma brucei." Eukaryot Cell **10**(9): 1230-1240.

Van der Ploeg, L. H., A. W. Cornelissen, J. D. Barry and P. Borst (1984). "Chromosomes of kinetoplastida." EMBO J **3**(13): 3109-3115.

van Deursen, F. J., D. J. Thornton and K. R. Matthews (2003). "A reproducible protocol for analysis of the proteome of Trypanosoma brucei by 2-dimensional gel electrophoresis." Mol Biochem Parasitol **128**(1): 107-110.

van Hellemond, J. J., F. R. Opperdoes and A. G. Tielens (2005). "The extraordinary mitochondrion and unusual citric acid cycle in Trypanosoma brucei." Biochem Soc Trans **33**(Pt 5): 967-971.

van Weelden, S. W., B. Fast, A. Vogt, P. van der Meer, J. Saas, J. J. van Hellemond, A. G. Tielens and M. Boshart (2003). "Procyclic Trypanosoma brucei do not use Krebs cycle activity for energy generation." J Biol Chem. **278**: 12854-12863.

van Weelden, S. W., J. J. van Hellemond, F. R. Opperdoes and A. G. Tielens (2005). "New functions for parts of the Krebs cycle in procyclic Trypanosoma brucei, a cycle not operating as a cycle." J Biol Chem **280**(13): 12451-12460.

Vanhamme, L., M. Berberof, D. Le Ray and E. Pays (1995). "Stimuli of differentiation regulate RNA elongation in the transcription units for the major stage-specific antigens of *Trypanosoma brucei*." Nucleic Acids Res. **23**(11): 1862-1869.

Vasquez, J. J., C. C. Hon, J. T. Vanselow, A. Schlosser and T. N. Siegel (2014). "Comparative ribosome profiling reveals extensive translational complexity in different Trypanosoma brucei life cycle stages." Nucleic Acids Res.

Vassella, E., R. Braun and I. Roditi (1994). "Control of polyadenylation and alternative splicing of transcripts from adjacent genes in a procyclin expression site: a dual role for polypyrimidine tracts in trypanosomes?" Nucleic Acids Res. **22**: 1359-1364.

Vickerman, K. (1985). "Developmental cycles and biology of pathogenic trypanosomes." Br Med Bull **41**(2): 105-114.

Walrad, P., A. Paterou, A. Acosta-Serrano and K. R. Matthews (2009). "Differential trypanosome surface coat regulation by a CCCH protein that co-associates with procyclin mRNA cis-elements." PLoS Pathog **5**(2): e1000317.

Walrad, P. B., P. Capewell, K. Fenn and K. R. Matthews (2012). "The post-transcriptional trans-acting regulator, TbZFP3, co-ordinates transmission-stage enriched mRNAs in Trypanosoma brucei." Nucleic Acids Res **40**(7): 2869-2883.

Wang, D., Y. Guo, C. Wu, G. Yang, Y. Li and C. Zheng (2008). "Genome-wide analysis of CCCH zinc finger family in Arabidopsis and rice." BMC Genomics **9**: 44.

Wang, X., J. McLachlan, P. D. Zamore and T. M. Hall (2002). "Modular recognition of RNA by a human pumilio-homology domain." Cell **110**(4): 501-512.

Weiden, M., Y. N. Osheim, A. L. Beyer and L. H. Van der Ploeg (1991). "Chromosome structure: DNA nucleotide sequence elements of a subset of the minichromosomes of the protozoan Trypanosoma brucei." Mol Cell Biol **11**(8): 3823-3834.

Wickens, M., D. S. Bernstein, J. Kimble and R. Parker (2002). "A PUF family portrait: 3'UTR regulation as a way of life." Trends Genet **18**(3): 150-157.

Worthington, M. T., J. W. Pelo, M. A. Sachedina, J. L. Applegate, K. O. Arseneau and T. T. Pizarro (2002). "RNA binding properties of the AU-rich element-binding recombinant Nup475/TIS11/tristetraprolin protein." J Biol Chem **277**(50): 48558-48564.

Yang, E., E. van Nimwegen, M. Zavolan, N. Rajewsky, M. Schroeder, M. Magnasco and J. E. Darnell, Jr. (2003). "Decay rates of human mRNAs: correlation with functional characteristics and sequence attributes." Genome Res **13**(8): 1863-1872.

Zinoviev, A., Y. Akum, T. Yahav and M. Shapira (2012). "Gene duplication in trypanosomatids: Two DED1 paralogs are functionally redundant and differentially expressed during the life cycle." Molecular and Biochemical Parasitology **185**(2): 127-136.

Zinoviev, A., M. Leger, G. Wagner and M. Shapira (2011). "A novel 4E-interacting protein in Leishmania is involved in stage-specific translation pathways." Nucleic Acids Research **39**(19): 8404-8415.

Zinoviev, A. and M. Shapira (2012). "Evolutionary conservation and diversification of the translation initiation apparatus in trypanosomatids." Comp Funct Genomics **2012**: 813718.

6. Supplemental data

6.1. Mass spectrometry results

			Unique peptides					found in 1st MS results?		
			2nd mass spec bs		2nd mass spec pc		total	pc		bs
Protein name	Accession numbers	function	free	mb	free	mb		free	mb	free
S-adenosylhomocysteine hydrolase	Tb11.01.1350	AA meta-bolism	5		17	1	23	1		
heat shock protein HSP70	Tb927.10.12710	CHAP	8		23		31			1
heat shock protein HSP70	Tb927.7.710	CHAP	4	5	12		21			
chaperone protein DNAj	Tb927.2.5160	CHAP	4	7	2		13			
lipid metabolisim putative prefoldin	Tb11.52.0006	CHAP		11			11			
heat shock protein HSP78	Tb927.2.3030	CHAP		4	4		8			
heat shock protein HSP84	Tb11.02.0250	CHAP		5	2		7			1
similarity to p23 (Hsp90 co-chaperone)	Tb09.211.1690	CHAP	2	2			4			1
chaperone protein DNAj	Tb11.01.8480	CHAP		4			4			
heat shock protein HSP100	Tb927.2.5980	CHAP		4			4			
chaperone protein DNA	Tb927.10.6610	CHAP		2			2			
heat shock protein HSP70	Tb09.211.1390	CHAP		2			2			
heat shock protein HSP70	Tb09.160.3090	CHAP		2			2			
chaperone protein DNAj	Tb11.03.0110	CHAP		1			1			
heat shock protein binding, DnaJ	Tb927.10.14740	CHAP		1			1			
heat shock protein HSP20	Tb927.7.4290	CHAP		1			1			
syntaxin	Tb09.160.2420	CHAP		1			1			
co-chaperone GrpE	Tb927.6.2170	CHAP	1				1			
stress-induced protein sti1	Tb927.5.2940	CHAP	1				1			
heat shock protein HSP70	Tb11.01.3110	CHAP	27	23	35	11	96			
heat shock protein HSP90	Tb927.10.10890	CHAP	19	13	26	4	62			
protein disulfide isomerase	Tb927.10.8230	CHAP	12	5	5	1	23			
histone H2B	Tb927.10.10460	Chromatin	6	3	6	5	20			
histone H4	Tb927.5.4170	Chromatin	4	4	4	4	16			
2-oxoglutarate dehydrogenase E2	Tb11.01.3550	TCA	4	3	10	2	19			
no domains FL-CYSK-MEMB	Tb11.02.0210	CYSKEL	14	12			26			
C-terminal motor kinesin	Tb927.10.14890	CYSKEL	7	15			22			
Ca-dependent membrane targeting domain	Tb927.4.2080	CYSKEL		16			16			
stomatin-like protein	Tb927.5.520	CYSKEL	2	13			15			
paraflagellar rod component	Tb11.01.5100	CYSKEL	4	10			14			
putative leucine rich repeat, outer arm dynein light chain 1 domain	Tb11.01.8770	CYSKEL		1	11	1	13			
flagellar calcium-binding protein, calflagin	Tb927.8.5460	CYSKEL	1	12			13			
microtubule-associated protein 2	Tb10.v4.0052	CYSKEL	8	5			13			
actin A	Tb09.211.0620	CYSKEL	5	5			10			
microtubule TRAF3 and DISC1 binding protein,	Tb927.10.450	CYSKEL	3	7			10			
cytoskeleton-associated protein CAP5.5	Tb927.4.3950	CYSKEL			8	2	10			
intraflagellar transport protein IFT81	Tb927.10.2640	CYSKEL		10			10			
flagellar transport protein	Tb927.3.1110	CYSKEL	2	6			8			
paraflagellar rod component	Tb927.8.6660	CYSKEL	2	6			8			
intraflagellar transport protein-like protein	Tb927.7.3370	CYSKEL	4	3			7			
73 kDa paraflagellar rod protein,PFR1	Tb927.3.4290	CYSKEL	3	1	2		6			
intraflagellar transport complex B protein 46 Ce	Tb927.6.3100	CYSKEL	2	4			6			
Cytoskeletal protein with EF hand	Tb927.7.3440	CYSKEL	2	2			4			
dynein light intermediate chain D1bLIC	Tb11.01.8570	CYSKEL	2	2			4			
kinesin	Tb927.8.4950	CYSKEL			4		4			
microtubule-associated protein	Tb927.10.10280	CYSKEL			4		4			
intraflagellar transport protein IFT52	Tb927.10.14980	CYSKEL	1	2			3			
flagellum-adhesion glycoprotein	Tb927.8.4060	CYSKEL		3			3			
trypanosoma specific. plasma membrane and cytoskeleton. no	Tb927.3.1010	CYSKEL		3			3			

domains										
flagellar attachment zone protein	Tb927.4.3740	CYSKEL			3		3			
kinesin	Tb927.8.2630	CYSKEL		2			2			
paraflagellar rod protein	Tb11.01.6740	CYSKEL		2			2			
intraflagellar transport protein IFT55/IFT57	Tb927.10.11310	CYSKEL	2				2			
intraflagellar transport protein, Member of IFT complex A	Tb09.160.5670	CYSKEL			2		2			
69 kDa paraflagellar rod protein,PFR2	Tb927.8.4970	CYSKEL		1			1			
BILBO1 flagellar protein essential for flagellar pocket biogenesis	Tb11.01.3960	CYSKEL		1			1			
homology to vacuolar proteins	Tb927.10.14320	CYSKEL		1			1			
Cytoskel. Fraction, flagellum	Tb927.8.6920	CYSKEL		1			1			
intraflagellar transport protein IFT88	Tb11.55.0006	CYSKEL		1			1			
MORN repeat-containing protein,flagellar component	Tb927.6.4670	CYSKEL		1			1			
Prefoldin domain, spectrin repeat, CYSK proteome	Tb927.4.5340	CYSKEL		1			1			
dynein heavy chain	Tb927.10.5350	CYSKEL	1				1			
beta tubulin	Tb927.1.2330	CYSKEL	20	26	23	11	80			
alpha tubulin	Tb927.1.2340	CYSKEL	18	20	18	7	63			
delta-1-pyrroline-5-carboxylate dehydrogenase	Tb927.10.3210	ENZ	15		19	4	38			
aminopeptidase, putative,metallo-peptidase, Clan MA(E) Family M1	Tb11.02.1070	ENZ			23		23			
Five SET domains - protein lysyl methyltransferase?	Tb09.211.1620	ENZ			21		21			
calpain-like cysteine peptidase	Tb927.8.8330	ENZ	4	13			17			
carboxypeptidase	Tb11.02.0100	ENZ	2		14		16			
lipophosphoglycan biosynthetic protein, HSP90	Tb927.3.3580	ENZ	3	9	2		14			
cytosolic leucyl aminopeptidase	Tb927.8.3060	ENZ	5		9		14			
aspartyl aminopeptidase	Tb927.3.3410	ENZ	5		8		13			
prolyl oligopeptidase, putative,serine peptidase clan SC, family S9A	Tb927.10.8020	ENZ			13		13			
dihydrolipoamide acetyltransferase E2 subunit	Tb927.10.7570	ENZ	4		8		12			
acidic phosphatase	Tb927.5.630	ENZ	6	5			11			
phosphoglycerate kinase	Tb927.1.710	ENZ			11		11			
tryparedoxin peroxidase	Tb09.160.4250	ENZ	3		5	2	10			
tryparedoxin peroxidase	Tb09.160.4280	ENZ	5	5			10			
cytosolic malate dehydrogenas	Tb11.01.3040	ENZ	3	2	4		9			
nucleoside hydrolase	Tb927.7.4570	ENZ	3	1	5		9			
cystathione gamma lyase	Tb09.211.3330	ENZ			8		8	1		
trypanothione reductase	Tb927.10.10390	ENZ	1		8		9			
arginine kinase	Tb09.160.4590	ENZ			9		9			
thimet oligopeptidase A, putative,metallo- peptidase,	Tb927.7.190	ENZ			9		9			
3-ketoacyl-CoA thiolase	Tb927.8.2540	ENZ		2	6		8			
thioredoxin-like, lipocalin domain, cyskel flag proteome	Tb11.01.1170	ENZ		6	2		8			
aminopeptidase, putative,metallo-peptidase, Clan MF	Tb11.02.0070	ENZ	4		4		8			
cytosolic nonspecific dipeptidase	Tb927.10.12260	ENZ			8		8			
transketolase	Tb927.8.6170	ENZ			6		6	1	1	
L-threonine 3-dehydrogenase	Tb927.6.2790	ENZ			7		7			
hydroxymethylglutaryl-CoA synthase activity	Tb927.8.6110	ENZ	1		5		6			
oligopeptidase b,serine peptidase, clan SC, family S9A-like protein	Tb11.52.0003	ENZ			6		6			
peptidase, putative,metallo-peptidase	Tb927.8.7020	ENZ			6		6			
arginine kinase	Tb09.160.4570	ENZ	4	1			5			
protein phosphatase 2C	Tb11.03.0390	ENZ	3	2			5			
thioredoxin	Tb927.4.2450	ENZ	1	4			5			
mitogen-activated protein kinase	Tb927.8.3770	ENZ		5			5			
orotidine-5-phosphate decarboxylase	Tb927.5.3810	ENZ		5			5			
arginine N-methyltransferase	Tb927.10.3560	ENZ			5		5			
carnitine O-palmitoyltransferase II	Tb927.3.3900	ENZ			5		5			
N-acetyltransferase subunit Nat1	Tb927.10.5670	ENZ			5		5			
S-adenosylmethionine synthetase	Tb927.6.4840	ENZ			5		5			
protease regulatory ATPase subunit 4	Tb927.10.3520	ENZ	2	2			4			
adenylyl cyclase	Tb927.4.4470	ENZ		4			4			

protein kinase	Tb927.10.5140	ENZ		4			4			
phosphoinositide-binding protein	Tb09.211.4240	ENZ		4			4			
phospholipase A1	Tb927.1.4830	ENZ		4			4			
creatinase, endopeptidase, histone chaperone, SPT6/FACT subunit	Tb927.3.5620	ENZ			4		4			
threonine synthase	Tb927.7.4390	ENZ			4		4			
guanosine monophosphate reductase	Tb927.5.2080	ENZ			2		2	1	1	
calpain-like cysteine peptidase	Tb927.7.4060	ENZ	1	2			3			
6-phosphogluconate dehydrogenase	Tb09.211.3180	ENZ	1		2		3			
carbonic anhydrase-like protein	Tb11.01.0290	ENZ		3			3			
protein kinase	Tb927.10.14780	ENZ		3			3			
D-alanine aminotransferase	Tb927.1.3950	ENZ	3				3			
tryparedoxin peroxidase	Tb927.8.1990	ENZ	3				3			
aminopeptidase P, putative,metallo-peptidase, Clan MG, Family M24	Tb09.211.4330	ENZ			3		3			
aminopeptidase P1, putative,metallo-peptidase, Clan MG, Family M24	Tb927.3.2090	ENZ			3		3			
aminopeptidase, putative,metallo-peptidase, Clan MG, Family M24	Tb927.10.14790	ENZ			3		3			
phosphoacetylglucosamine mutase	Tb927.8.980	ENZ			3		3			
protein kinase	Tb927.10.5930	ENZ			3		3			
pseudouridine synthase, Cbf5p	Tb927.10.170	ENZ			3		3			
trypanothione synthetase	Tb927.2.4370	ENZ			3		3			
3-oxo-5-alpha-steroid 4-dehydrogenase	Tb927.3.1840	ENZ		2			2			
calpain-like protein fragment	Tb927.1.2230	ENZ		2			2			
calpain-like protein fragment	Tb927.1.2260	ENZ		2			2			
cysteine peptidase precursor	Tb927.6.1000	ENZ		2			2			
glycogen synthase kinase 3	Tb927.10.13780	ENZ		2			2			
Methyltransferase type 11 putative	Tb927.7.6890	ENZ		2			2			
methylthioadenosine phosphorylase	Tb927.7.7040	ENZ	2				2			
peptidylprolyl isomerase-like protein	Tb927.10.16100	ENZ	2				2			
serine carboxypeptidase III precursor	Tb927.10.1040	ENZ		2			2			
serine/threonine-protein kinase	Tb927.3.2440	ENZ		2			2			
uridine phosphorylase	Tb927.8.4430	ENZ	2				2			
aminopeptidase, putative,metallo-peptidase, Clan MA(E) Family M1	Tb927.3.4750	ENZ			2		2			
arginine N-methyltransferase	Tb927.1.4690	ENZ			2		2			
cystathionine beta-synthase	Tb11.02.5400	ENZ			2		2			
guanine deaminase	Tb927.5.4560	ENZ			2		2			
peptidase t, putative,aminotripeptidase	Tb927.7.6270	ENZ			2		2			
phosphoribosylpyrophosphate synthetase	Tb927.5.2960	ENZ			2		2			
prostaglandin f synthase	Tb11.02.2310	ENZ			2		2			
Putative phosphatase, DUF domain	Tb927.7.5210	ENZ			2		2			
ribonucleoside-diphosphate reductase large chain	Tb11.02.5720	ENZ			2		2			
metacaspase MCA4	Tb927.10.2440	ENZ		1			1			
phosphatic acid phsophatasetype-2 like domain	Tb927.8.480	ENZ		1			1			
branched-chain amino acid aminotransferase	Tb927.2.4590	ENZ	1				1			
lysine decarboxylase	Tb927.5.1460	ENZ	1				1			
metalloprotease, FtsH homologue	Tb11.01.6360	ENZ	1				1			
Peptidase M24	Tb11.02.1670	ENZ	1				1			
fructose-bisphosphate aldolase, glycosomal	Tb927.10.5620	Glucose & glycerol	27	22	5	3	57	1		
enolase	Tb927.10.2890	Glucose & glycerol	17	12	22	1	52	1		
hexokinase	Tb927.10.2010	Glucose & glycerol	16	17	8	2	43			
ATP-dependent phosphofructokinase	Tb927.3.3270	Glucose & glycerol	13	6	4		23	1	1	1
glycerol kinase, glycosomal	Tb09.211.3540	Glucose & glycerol	3	6	9	4	22	1	1	
glycerol-3-phosphate dehydrogenase [NAD], glycosomal	Tb927.8.3530	Glucose & glycerol	3	4	7	4	18	1	1	
pyruvate phosphate dikinase	Tb11.02.4150	GLYC			23	8	31			
glyceraldehyde 3-phosphate dehydrogenase, glycosomal	Tb927.6.4280	GLYC	4	10			14			
PEX14	Tb927.10.240	GLYC	2	12			14			
phosphoenolpyruvate carboxykinase, glycosomal	Tb927.2.4210	GLYC			7	3	10	1	1	

phosphoglycerate kinase PGKC	Tb927.1.700	GLYC	3	8			11			
glucose-6-phosphate isomerase, glycosomal	Tb927.1.3830	GLYC	9	1			10			
glyceraldehyde 3-phosphate dehydrogenase, cytosolic	Tb927.10.6880	GLYC	4		4		8			
PEX12	Tb927.10.15850	GLYC		8			8			
Gim5B protein,glycosomal membrane protein	Tb09.211.2740	GLYC	2	2			4			
malate dehydrogenase, glycosomal	Tb927.10.15410	GLYC			2	2	4			
PEX11	Tb11.01.3370	GLYC		4			4			
PEX3	Tb927.3.2410	GLYC		3			3			
2,3-bisphosphoglycerate-independent phosphoglycerate mutase	Tb927.10.7930	GLYC			3		3			
triosephosphate isomerase	Tb11.02.3210	GLYC		2			2			
75 kDa invariant surface glycoprotein	Tb927.5.360	MEMB	18	4			22			
glycosylphosphatidylinositol-specific phospholipase C	Tb927.2.6000	MEMB	2	3			5			
transmembrane domain protein	Tb927.5.309b	MEMB	2	2			4			
75 kDa invariant surface glycoprotein	Tb927.5.390	MEMB	4				4			
Signal pep. secrete/ER.	Tb927.10.11140	MEMB		4			4			
64 kDa invariant surface glycoprotein	Tb927.5.1410	MEMB		2			2			
antigenic protein, putative	Tb927.4.2070	MEMB		2			2			
2 transmembrane domains,homology to ABC transporter	Tb927.7.470	MEMB	2				2			
N-myristoyltransferase	Tb927.10.14240	MEMB			2		2			
FG-GAP repeat protein	Tb927.7.6460	MEMB		1			1			
membrane-bound acid phosphatase 1 precursor	Tb11.01.4701	MEMB	1				1			
64 kDa invariant surface glycoprotein	Tb927.2.3270	MEMB	1				1			
64 kDa invariant surface glycoprotein	Tb927.2.3320	MEMB	1				1			
Signal peptide, 4 TM domains	Tb927.4.2530	MEMB		1			1			
heat shock 70 kDa protein, mitochondrial precursor	Tb927.6.3740	MITOS	17	14	22	3	56			
homologue to slingshot, isoforms of drosophila localised to putative mitochondrial RNA binding complex 1	Tb927.7.2570	MITOS	3	5	2		10	1		
2-oxoglutarate dehydrogenase E1 component	Tb11.01.1740	MITOS			36	1	37			
2-oxoglutarate dehydrogenase E1 componen	Tb11.47.0004	MITOS			27		27			
chaperonin Hsp60, mitochondrial	Tb927.10.6400	MITOS	6	3	15		24			
adenylosuccinate synthetase	Tb11.02.1120	MITOS	13	2	8		23			
pyruvate dehydrogenase E1 alpha subunit	Tb927.10.12700	MITOS	7	1	12		20			
pyruvate kinase 1	Tb927.10.14140	MITOS	9	1	8		18			
pyruvate dehydrogenase E1 beta subunit	Tb927.3.1790	MITOS	7		7		14	1	1	
succinyl-coA:3-ketoacid-coenzyme A transferase, mitochondrial	Tb11.02.0290	MITOS	1		13		14			
dihydrolipoyl dehydrogenase	Tb11.01.8470	MITOS			14		14			
malic enzyme	Tb11.02.3120	MITOS			11	1	12			
ABC transporter domain, predicted ATPase, locates to mithcondrial RNA binding complex 1	Tb927.3.1590	MITOS	2		9		11			
aconitase	Tb927.10.14000	MITOS			9		9			
kinetoplast DNA-associated protein	Tb11.01.8090	MITOS	5	2			7			
succinyl-CoA ligase [GDP-forming] beta-chain	Tb927.10.7410	MITOS			7		7			
fumarate hydratase, class I	Tb927.3.4500	MITOS			6		6			
NADH-dependent fumarate reductase	Tb927.5.940	MITOS			6		6			
glycerol-3-phosphate dehydrogenase (FAD-dependent), mitochondrial	Tb11.02.5280	MITOS	2	3			5			
2-amino-3-ketobutyrate coenzyme A ligase, putative,glycine acetyltransferase	Tb927.8.6060	MITOS			5		5			
malic enzyme	Tb11.02.3130	MITOS			5		5			
glutamine synthetase	Tb927.7.4970	MITOS			3		3	1		
adenylosuccinate lyase	Tb09.160.5560	MITOS			4		4			
succinyl-CoA synthetase alpha subunit	Tb927.3.2230	MITOS			4		4			
mitochondrial processing peptidase, beta subunit	Tb927.5.1060	MITOS			2		2	1	1	
3,2-trans-enoyl-CoA isomerase, mitochondrial precursor	Tb927.4.4910	MITOS		3			3			
Mitochondrial TBRGG1 oligo-U binding	Tb927.6.2230	MITOS		3			3			

protein										
Ribosome binding factor A signature. Processing of 16S rRNA? similar to ring finger protein 127 [Gallus gallus]	Tb09.211.1240	MITOS		3			3			
glutamine hydrolysing carbomoyl phosphate synthase	Tb927.5.3800	MITOS			3		3			
Assoc with F0F1 ATP synthase, essential for ATP synthesis	Tb927.10.520	MITOS	1	1			2			
mit. Membrane protein	Tb11.02.5660	MITOS		2			2			
universal minicircle sequence binding protein (UMSBP)	Tb927.10.6060	MITOS		2			2			
glutamate dehydrogenase	Tb09.160.4310	MITOS			2		2			
1-acyl-sn-glycerol-3-phosphate acyltransferase protein	Tb11.01.6800	MITOS		1			1			
importin alpha subunit, putative	Tb927.6.2640	NUC	4	5	4		13			
nucleosome assembly protein, putative	Tb927.10.15180	NUC	4	4	3		11			
TbKap123 transport factor (importin)	Tb11.01.7010	NUC		8	3		11			
splicing factor TSR1	Tb927.8.900	NUC	2	5			7	1		
predicted nuclear, no domains	Tb11.01.6790	NUC		8			8			
prohibitin	Tb10.v4.0045	NUC	3	2			5			
proliferative cell nuclear antigen (PCNA)	Tb09.160.3710	NUC	3		2		5			
replication factor C, subunit 1	Tb11.02.3360	NUC		5			5			
DNA topoisomerase type IB small subunit	Tb09.160.5070	NUC	2	2			4			
histone H2A	Tb927.7.2820	NUC	1		3		4			
ruvB-like DNA helicase	Tb927.4.1270	NUC			4		4			
ruvB-like DNA helicase	Tb927.4.2000	NUC			4		4			
histone H3	Tb927.1.2430	NUC	1		2		3			
double-strand-break repair protein rad21	Tb927.7.6900	NUC		3			3			
GTP-binding nuclear protein rtb2	Tb927.3.1120	NUC		3			3			
replication Factor A 28 kDa subunit	Tb927.5.1700	NUC		3			3			
SH3 domain protein, conserved	Tb927.10.14720	NUC		3			3			
homology to tRNA ligase and zinc finger proteins	Tb927.8.2080	NUC		2			2			
replication factor C, subunit 2	Tb927.6.3890	NUC		2			2			
replication factor C, subunit 3	Tb09.211.3310	NUC		2			2			
Nuclease and TUDOR domains =staphylococcal nuclease domain protein of H. sapiens	Tb11.01.5780	NUC			2		2			
prohibitin 1	Tb927.8.4810	NUC			2		2			
spliceosome-associated protein, putative	Tb927.6.2000	NUC		1			1			
transcription elongation factor s-II	Tb927.2.3580	NUC		1			1			
TTAGGG binding factor.	Tb927.10.12850	NUC		1			1			
DNA-directed RNA polymerase, alpha subunit	Tb927.10.15370	NUC	1				1			
nucleolar RNA binding protein, snoRNA binding domain	Tb09.160.3820	nucleolus	8		8		16	1		
nucleolar GTP-binding protein 1	Tb11.02.0620	nucleolus	3		6		9	1		
fibrillarin	Tb927.10.7500	nucleolus	5	2	2		9			
S-adenosyl-methonine-dependent methyl transferase	Tb927.4.3840	nucleolus			7		7			
homologies to Ribosomal RNA large subunit methyltransferase L of pseudomonas	Tb927.2.2230	nucleolus	2	2			4			
ribosome biogenesis protein	Tb927.7.270	nucleolus	3	1			4			
nucleolar RNA-binding protein, truncated	Tb927.8.740	nucleolus			2		2	1		
snoRNP protein GAR1	Tb927.4.470	nucleolus	2	1			3			
ENP1, rRNA processing protein	Tb927.6.1900	nucleolus		3			3			
U3 small nucleolar ribonucleoprotein protein MPP10	Tb927.3.3590	nucleolus		2			2			
fibrillarin	Tb927.10.14750	nucleolus	2				2			
rRNA processing protein EBP2	Tb09.244.2790	nucleolus	1				1			
inosine-5'-monophosphate dehydrogenase	Tb927.10.16120	nucleotide	5	8	3	2	18			
nucleoside diphosphate kinase	Tb11.01.7800	nucleotide	3	1	2	1	7			
Nucleoporin NUP98	Tb927.3.3180	NUP		4			4			
Nucleoporin NUP64	Tb927.4.4310	NUP		2			2			
NUP-1 protein	Tb927.2.4230	NUP		2			2			
ATP synthase F1, beta subunit	Tb927.3.1380	Ox. phosphorylation	12	6	15	7	40	1	1	
ATP synthase F1, alpha subunit	Tb927.7.7420	Ox.	6	2	11	3	22	1		

		phosphorylation								
aminopeptidase, putative,metallo-peptidase, Clan M	Tb11.02.4440	Protease/peptidase	10		18	2	30	1		1
calpain-like cysteine peptidase	Tb927.1.2100	Protease/peptidase	1		25	2	28	1		
40S ribosomal protein L14	Tb11.01.3020	Ribosome	7	8	6		21			
60S ribosomal protein L36	Tb09.244.2725	Ribosome	8	7			15	1		1
40S ribosomal protein S25	Tb927.10.2840	Ribosome	5	6			11			
40S ribosomal protein S21	Tb11.02.4360	Ribosome	3	3	3		9			
60S ribosomal protein L32	Tb927.10.270	Ribosome	3	6			9			
60S ribosomal protein L31	Tb09.211.3270	Ribosome	3	3			6			
60S acidic ribosomal protein P2	Tb927.6.5120	Ribosome	4				4			1
40S ribosomal protein S30	Tb927.6.2100	Ribosome	2	1			3			
40S ribosomal protein S15	Tb927.7.2340	Ribosome	2				2			1
60S acidic ribosomal protein	Tb927.5.1820	Ribosome	2				2			
60S ribosomal protein L38	Tb09.160.0815	Ribosome		1			1			
60S ribosomal protein L39	Tb927.8.5260	Ribosome		1			1			
60S Ribosomal protein L1	Tb927.10.8200	Ribosome	1				1			
60S ribosomal protein L4	Tb927.3.5050	Ribosome	21	20	23	8	72	1	1	1
60S ribosomal protein L3	Tb927.4.1790	Ribosome	22	17	22	9	70	1	1	1
40S ribosomal protein S4	Tb11.02.1085	Ribosome	19	15	18	12	64			
40S ribosomal protein S3A	Tb927.10.3940	Ribosome	18	19	14	11	62			
60S acidic ribosomal subunit	Tb11.46.0001	Ribosome	17	15	19	8	59	1	1	
60S ribosomal protein L13	Tb927.3.3310	Ribosome	14	17	9	4	44	1	1	1
60S ribosomal protein L7a	Tb927.8.1330	Ribosome	13	13	13	6	45			
60S ribosomal protein L5	Tb09.244.2730	Ribosome	16	10	12	6	44			
60S ribosomal protein L10	Tb09.211.0110	Ribosome	11	13	11	7	42			
40S ribosomal protein S3	Tb09.160.4450	Ribosome	11	13	10	6	40	1	1	1
60S ribosomal protein L2 L8	Tb11.01.7960	Ribosome	13	12	10	5	40			
60S ribosomal protein L7	Tb927.7.1730	Ribosome	12	10	10	6	38			1
40S ribosomal protein S18	Tb927.10.5330	Ribosome	12	15	6	4	37			
40S ribosomal protein S2	Tb927.10.14600	Ribosome	11	13	7	6	37			
60S ribosomal protein L21e	Tb11.50.0005	Ribosome	8	12	9	5	34			
60S ribosomal protein L23a, or L25	Tb927.7.5170	Ribosome	10	11	8	5	34			
60S ribosomal protein L10a	Tb11.01.1470	Ribosome	8	12	7	5	32	1		1
60S ribosomal protein L13a	Tb927.4.3550	Ribosome	7	10	8	6	31	1	1	1
60S ribosomal protein L6	Tb927.10.11390	Ribosome	8	11	8	5	32			
40S ribosomal protein S7	Tb09.160.2550	Ribosome	8	9	6	7	30	1		1
60S ribosomal protein L19	Tb927.7.5000	Ribosome	9	10	6	4	29	1	1	1
60S ribosomal protein L23	Tb09.211.2630	Ribosome	9	9	6	5	29	1		1
40S ribosomal protein S16	Tb927.7.1040	Ribosome	8	10	8	4	30			
40S ribosomal protein SA	Tb11.01.2560	Ribosome	8	9	8	5	30			
60S ribosomal protein L35a	Tb927.4.2180	Ribosome	7	7	8	5	27	1	1	1
40S ribosomal protein S6	Tb927.10.190	Ribosome	12	11	4	1	28			
60S ribosomal protein L27	Tb11.01.7535	Ribosome	7	8	7	6	28			
60S ribosomal protein L18	Tb11.01.5720	Ribosome	6	8	8	3	25	1		1
40S ribosomal protein S13	Tb927.10.15120	Ribosome	7	11	5	3	26			
40S ribosomal protein S17	Tb11.01.3675	Ribosome	8	9	5	4	26			
40S ribosomal protein S5	Tb11.02.4170	Ribosome	8	8	4	4	24	1	1	1
40S ribosomal protein S6	Tb09.244.2630	Ribosome	3	3	11	7	24	1		1
40S ribosomal protein S8	Tb927.8.6150	Ribosome	6	7	6	5	24	1	1	1
40S ribosomal protein S9	Tb927.10.5610	Ribosome	6	7	7	5	25			
40S ribosomal protein S19	Tb927.4.1860	Ribosome	7	8	4	4	23	1		1
60S ribosomal protein L28	Tb11.02.4050	Ribosome	6	8	5	4	23			
60S ribosomal protein L30	Tb927.10.4110	Ribosome	7	7	6	3	23			
60S ribosomal protein L9	Tb927.10.1100	Ribosome	5	5	8	5	23			
60S ribosomal protein L17	Tb11.02.2430	Ribosome	5	7	6	4	22			
40S ribosomal protein S10	Tb927.10.5360	Ribosome	6	7	3	4	20	1		
40S ribosomal protein S11	Tb927.10.560	Ribosome	4	5	5	6	20			
60S ribosomal protein L11	Tb09.160.5580	Ribosome	5	5	5	2	17	1		
60S ribosomal protein L18	Tb11.02.1840	Ribosome	5	6	4	3	18			
60S ribosomal protein L44	Tb11.02.0740	Ribosome	6	8	3	1	18			
40S ribosomal protein S14	Tb927.6.4980	Ribosome	4	5	4	3	16	1	1	1
40S ribosomal protein S15A	Tb11.02.4000	Ribosome	4	5	4	4	17			1
40S ribosomal protein S26	Tb11.01.0355	Ribosome	4	5	3	3	15	1	1	1
40S ribosomal protein S27	Tb11.01.1475	Ribosome	4	4	4	3	15	1	1	1
40S ribosomal protein S24E	Tb927.10.7330	Ribosome	5	6	3	2	16			
60S ribosomal protein L27a	Tb09.211.2650	Ribosome	5	5	2	2	14	1	1	1
40S ribosomal protein S12	Tb927.10.8430	Ribosome	3	4	4	2	13			
40S ribosomal protein S23	Tb927.10.1080	Ribosome	5	3	3	2	13			
60S ribosomal protein L12	Tb09.211.4550	Ribosome	5	3	2	3	13			

60S ribosomal protein L15	Tb927.6.5040	Ribosome	3	2	4	2	11	1		1
60S ribosomal protein L29	Tb11.01.1790	Ribosome	3	4	2	2	11	1	1	1
60S ribosomal protein L26	Tb09.211.4850	Ribosome	2	4	3	3	12			
60S ribosomal protein L37a	Tb927.10.220	Ribosome	3	5	2	1	11			
40S ribosomal protein S33	Tb927.7.230	Ribosome	3	4	2	1	10			
60S ribosomal protein L24	Tb927.10.5460	Ribosome	1	4	3	2	10			
60S ribosomal protein L35	Tb09.160.0700	Ribosome	3	4	2	1	10			
60S acidic ribosomal protein	Tb09.160.4200	Ribosome	3	2	2	2	9			
60S ribosomal proteins L38	Tb927.10.3280	Ribosome	2	4	2	1	9			
40S ribosomal protein S27+ ubiquitin	Tb927.10.5030	Ribosome	2	3	2	1	8			
60S ribosomal protein L22	Tb11.01.1920	Ribosome	2	3	2	1	8			
60S ribosomal protein L34	Tb11.01.1480	Ribosome	2	2	2	2	8			
60S ribosomal protein L37	Tb09.211.0865	Ribosome	2	2	2	1	7			
AGO1	Tb927.10.10850	RNA			21		21			1
NOT5	Tb927.3.1920	RNA	4	9			13			
DHH1	Tb927.10.3990	RNA	2	4	6		12			
DRBD3 (PTB1)	Tb09.211.0560	RNA	2	5	2		9			
DDX60	Tb927.3.2600	RNA			8		8	1		
Dbp2	Tb927.8.1510	RNA	3	4			7			
RBP42	Tb927.6.4440	RNA	3	1	2		6			
PUF2	Tb927.10.12660	RNA		6			6			
ZC3H41	Tb11.46.0009	RNA			5		5			
PUF6	Tb927.10.11760	RNA		4			4			
RPB29	Tb927.10.13720	RNA		3			3			
Dbp2/HEL64	Tb927.10.6630	RNA		2			2			
PUF1	Tb927.10.4430	RNA		2			2			
PUF3	Tb927.10.310	RNA		2			2			
ZC3H29	Tb09.211.1130	RNA		2			2			
NOT2	Tb927.6.850	RNA	2				2			
RBP11	Tb927.8.4450	RNA	2				2			
PUF10	Tb11.02.4570	RNA			2		2			
SUB2	Tb927.10.540	RNA		1			1			
PBP1	Tb927.8.4540	RNA		1			1			
ZC3H18	Tb927.7.2140	RNA		1			1			
ZC3H30	Tb927.10.1540	RNA		1			1			
ZC3H32	Tb927.10.5250	RNA		1			1			
MEX67	Tb11.22.0004	RNA		2			2			
ALBA4/ ALBA3	Tb927.4.2030	RNA	1	2	2	1	6			
MKT1	Tb927.6.4770	RNA	3	2	2		7			
PARN-3	Tb09.211.4350	RNA			2		2			
LA protein	Tb927.10.2370	RNA, putative	2		2		4			
cytoplasmic RNA-binding protein or Prp46p splicing factor	Tb09.160.5620	RNA, putative	1	2			3			
CCCH zinc finger PS50103, up slightly in PC.	Tb11.02.1470	RNA, putative		2			2			
hypothetical protein, conserved has two RBDs	Tb11.01.5680	RNA, putative	2				2			
P-loop nucloside phosphate hydrolase, PH domain-like	Tb927.3.2490	RNA, putative			2		2			
NRBD2	Tb11.01.5590	r/tRNA processing	12	11	12	6	41	1		1
NOP86	Tb09.160.1160	r/tRNA processing	5	25	9	2	41			
nucleolar protein, NOP5 domain	Tb927.8.3750	r/tRNA processing	3	1	11		15	1		1
T-complex protein 1, theta subunit	Tb927.10.8190	TRANS	2		17		19	1		
T-complex protein 1, alpha subunit	Tb11.01.8510	TRANS			18		18	1		
T-complex protein 1, delta subunit	Tb927.10.1060	TRANS			17	2	19			
T-complex protein 1 gamma subunit	Tb927.8.3150	TRANS		2	17		19			
T-complex protein 1, beta subunit	Tb11.42.0003	TRANS			16		16	1		
T-complex protein 1, epsilon subunit	Tb11.01.5860	TRANS			15		15	1		
T-complex protein 1, zeta subunit	Tb11.02.0750	TRANS	1		14		15			
T-complex protein 1, eta subunit	Tb09.211.2570	TRANS			11		11	1		
Dbp1	Tb927.10.14550	TRANS	3	9	3		15			
Ded1	Tb09.211.3510	TRANS		9	5		14			
EIF3a	Tb927.7.6090	TRANS	8		16		24			
EIF4G3	Tb927.8.4820	TRANS	14		5		19	1		
EIF4A1	Tb09.160.3270	TRANS	6	6	8		20			1
EIF3c	Tb927.10.8270	TRANS	1		13		14			
Bfr1, polysome component. loc in ER of Sc. Interacts RF1, AP3. 2x higher in BF	Tb927.10.14150	TRANS	3	6			9			

EIF5	Tb927.10.2770	TRANS		5	4		9			
EIF3 7 eukaryotic translation initiation factor 3 subunit 7	Tb927.6.4370	TRANS			7		7			
EIF eukaryotic translation initiation factor	Tb11.01.3420	TRANS			6		6			
EIF3b	Tb927.5.2570	TRANS			6		6			
eIF3L	Tb927.10.4640	TRANS			6		6			
ERF1 eukaryotic release factor 1	Tb11.22.0012	TRANS		1	4		5			
EF1 beta	Tb927.4.3570	TRANS	2		3		5			
EIF3g	Tb927.4.1930	TRANS	5				5			
EIF3 eukaryotic translation initiation factor 3	Tb11.01.1370	TRANS			5		5			
EIF4E3	Tb11.01.3630	TRANS	1	3			4			
EIF4G4	Tb11.01.2330	TRANS		3			3			
GTP-binding protein RBG1 (yeast)	Tb927.10.6800	TRANS		3			3			
EIF2 gamma eukaryotic translation initiation factor 2 gamma	Tb11.01.4830	TRANS			3		3			
ERF3 eukaryotic release factor 3	Tb11.02.4030	TRANS			3		3			
elongation factor Tu	Tb927.10.13360	TRANS			2		2			
elongation initiation factor 2 alpha subunit	Tb927.3.2900	TRANS			2		2			
IF2	Tb927.2.3780	TRANS			2		2			
EIF3c	Tb927.10.8290	TRANS	1				1			
PABP2	Tb09.211.2150	TRANS	28	21	24	6	79	1	1	1
PABP1	Tb09.211.0930	TRANS	24	11	25	4	64	1	1	1
EF2	Tb927.10.4560	TRANS	10		45	8	63			
TbRACK1, associated with ribosomes	Tb11.01.3170	TRANS	15	14	15	8	52	1	1	1
EF1 alpha	Tb927.10.2100	TRANS	9	10	9		28	1		
EF1 gamma	Tb11.01.4660	TRANS	4	1	10	2	17	1		
EIF4E4	Tb927.6.1870	TRANS	10	3	2		15	1		1
threonyl-tRNA synthetase	Tb927.5.1090	tRNAsynth			17		17			
glycyl-tRNA synthetase	Tb11.01.1400	tRNAsynth	2		13		15			
seryl-tRNA synthetase	Tb11.02.5020	tRNAsynth	4		8	1	13			
isoleucyl-tRNA synthetase	Tb927.10.9190	tRNAsynth			13		13			
cysteinyl-tRNA synthetase	Tb927.6.950	tRNAsynth			12		12			
lysyl-tRNA synthetase	Tb927.8.1600	tRNAsynth	6		5		11			
leucyl-tRNA synthetase	Tb11.02.1210	tRNAsynth			9		9			
arginyl-tRNA synthetase, putative	Tb11.46.0008	tRNAsynth			8		8			
valyl-tRNA synthetase, putative	Tb927.6.4480	tRNAsynth			8		8			
phenylalanyl-tRNA synthetase (beta subunit)	Tb11.22.0005	tRNAsynth	3		3		6			
glutamyl-tRNA synthetase	Tb927.6.4590	tRNAsynth			6		6			
tyrosyl-tRNA synthetase	Tb927.7.2400	tRNAsynth		5			5			
asparaginyl-tRNA synthetase	Tb927.4.2310	tRNAsynth			3		3			
glutaminyl-tRNA synthetase	Tb09.160.3730	tRNAsynth			3		3			
methionyl-tRNA synthetase	Tb927.10.1500	tRNAsynth			3		3			
tyrosyl-tRNA synthetase	Tb927.7.3620	tRNAsynth			3		3			
alanyl-tRNA synthetase	Tb927.6.700	tRNAsynth			2		2			
aspartyl-tRNA synthetase	Tb927.6.1880	tRNAsynth			2		2			
proteasome regulatory non-ATPase subunit 11	Tb927.10.2980	Ubi	3	1			4			
polyubiquitin	Tb11.01.1680	Ubi			2		2	1	1	
proteasome beta 6 subunit,20S proteasome beta 6 subunit	Tb927.7.4790	Ubi	2	1			3			
proteasome regulatory non-ATPase subunit 8	Tb927.10.14530	Ubi	2	1			3			
proteasome regulatory ATPase subunit 3	Tb927.6.1090	Ubi		1	2		3			
proteasome beta-1 subunit	Tb927.6.1260	Ubi	1		2		3			
ubiquitin-like protein	Tb11.02.1600	Ubi		3			3			
proteasome regulatory non-ATPase subunit 6	Tb927.2.2440	Ubi			3		3			
proteasome regulatory ATPase subunit 5	Tb927.7.2550	Ubi		2			2			
proteasome regulatory non-ATP-ase subunit 10	Tb927.8.570	Ubi		2			2			
ubiquitin-conjugating enzyme e2	Tb11.01.5790	Ubi		2			2			
proteasome alpha 2 subunit	Tb927.10.290	Ubi	2				2			1
proteasome regulatory non-ATP-ase subunit 2	Tb11.01.0960	Ubi			2		2			
ubiquitin-conjugating enzyme	Tb927.7.6960	Ubi		1			1			
proteasome alpha 3 subunit	Tb927.7.4420	Ubi	1				1			
proteasome alpha 5 subunit, 20S	Tb927.10.230	Ubi	1				1			

proteasome										
V-type ATPase, A subunit	Tb927.4.1080	VAC		3	5		8			
vacuolar ATP synthase subunit d	Tb927.10.3760	VAC		5			5			
vacuolar ATP synthase subunit c	Tb927.10.14040	VAC		2			2			
vacuolar ATP synthase, subunit C or D	Tb927.5.550	VAC		2			2			
vacuolar ATP synthase subunit b	Tb11.01.3560	VAC			2		2			
vacuolar protein sorting-associated protein 4	Tb927.3.3280	VAC		1			1			
vacuolar proton translocating ATPase subunit A	Tb927.5.1300	VAC		1			1			
Golgi/lysosome glycoprotein 1	Tb927.8.1870	VES	6	6			12			
adaptin complex 1 subunit, beta-adaptin	Tb927.10.8040	VES	3	8			11			
clathrin heavy chain	Tb927.10.6050	VES		3	5		8			
Sec13, putative,cytosolic coat protein,	Tb927.10.14180	VES	3	4			7			
ADP-ribosylation factor-like protein 3A	Tb927.3.3450	VES	1	3			4			
lysosomal/endosomal membrane protein p67	Tb927.5.1810	VES	1	3			4			
major sperm protein or PapD domain. PM-FLAG-CYSK proteomes,	Tb11.01.4810	VES		4			4			
SNF7 protein transport	Tb11.18.0015	VES		4			4			
ERV46, membrane fusions, Cop11 vesicles	Tb11.02.5080	VES	2	1			3			
Translocon-associated protein alpha	Tb927.7.2190	VES	1	2			3			1
vesicle-associated membrane protein, putative	Tb927.5.3560	VES	1	2			3			
ADP-ribosylation factor, putative	Tb09.211.4460	VES		3			3			
clathrin coat assembly protein	Tb11.02.2410	VES		3			3			
endoplasmic reticulum oxidoreductin	Tb927.8.4890	VES		3			3			
GPI transamidase GPI16	Tb927.4.1920	VES		3			3			
GPI transamidase TTA1	Tb11.01.7400	VES		3			3			
RAB1	Tb927.8.890	VES		3			3			
translocon-associated protein beta	Tb927.6.4500	VES		3			3			
vesicle protein SN7 family protein.	Tb11.01.1390	VES		3			3			
calreticulin, putative	Tb927.4.5010	VES	3				3			
GRAM domain Glucosyltransferases	Tb09.160.5200	VES	3				3			
ADP-ribosylation factor-like protein	Tb09.160.5300	VES		2			2			
GPI inositol deacylase precursor	Tb927.10.4780	VES		2			2			
GPI-anchor transamidase subunit 8 (GPI8)	Tb927.10.13860	VES		2			2			
Rab-like 5, small G protein	Tb11.01.8590	VES		2			2			
ras-like small GTPase, evidence=traceable author statement	Tb11.02.0240	VES		2			2			
ras-related protein rab-5,small GTPase, putative	Tb927.10.12960	VES		2			2			
small GTP-binding protein Rab11,Rab11A	Tb927.8.4330	VES		2			2			
small GTP-binding protein, putative;evidence=traceable author statement	Tb927.3.5550	VES		2			2			
translocon-associated protein gamma 4 transmembrane domains	Tb927.7.4470	VES		2			2			
SRP68	Tb927.4.1850	VES	2				2			
RAB GDP dissociation inhibitor alpha	Tb927.3.4680	VES			2		2			
ADP-ribosylation factor GTPase activating protein	Tb09.244.2540	VES		1			1			
COP protein	Tb09.244.2760	VES		1			1			
low homology to syntaxin	Tb11.01.1960	VES		1			1			
SNF7-related domain	Tb09.211.1770	VES		1			1			
14-3-3-like protein	Tb11.01.1290	VES	1				1			
glucose-regulated protein 78, putative,luminal binding protein 1 (BiP)	Tb11.02.5450	VES	26	34	15	5	80			
dynamin, putative,vacuolar sortin protein 1	Tb927.3.4720	VES	12	8	12		32	1		1
Valosin-comtaiing protein homologue, transitional ER	Tb927.10.5770	VES	1	2	15	1	19			
VSG	Tb08.27P2.220	VSG	7	6			13			
VSG	Tb927.5.4820	VSG	1	1	2	1	5			
VSG	Tb927.1.05	VSG	2	1			3			
VSG	Tb09.v4.0136	VSG		2			2			
VSG	Tb10.v4.0241	VSG		1			1			
VSG	Tb05.5K5.540	VSG	1				1			
low homology to EIF-3.H of C. elegans,	Tb927.8.1170		1		2		3			

none in yeast										
C2 calcium/lipid-binding region, CaLB,	Tb927.7.3550		22	25	9		56			
prefoldin domain, Spectrin repeat low homologies, CYSK proteome	Tb927.8.6980			26			26			
hypothetical, mRNA up in BS	Tb927.7.2650		12	11			23			1
ubiquitin-activating enzyme e1	Tb09.211.3610				13		13			
hypothetical protein, no matches in yeast or human	Tb927.4.1300				11		11	1		
FtsJ cell division protein, putative	Tb927.2.4550		6	2	2		10			
brucei-congo speciific. no domains	Tb927.10.2930		1	9			10			
low homology to RNA helicase of toxoplasma gondii, trypanosoma-specific	Tb927.3.3300			10			10			
WD40 domains, nuclear? slightly up BS, medium homology to plectin	Tb927.10.840			10			10			
orthologues have ARM repeat	Tb927.7.2240		4	5			9			
FY-rich domain IPR003889	Tb927.7.1060		2	5			7			
hypothetical protein	Tb927.1.4310			7			7			
down in stat phase. no matches	Tb927.10.14700		3	3			6			
low homology to coiled-cooil proteins and hook proteins (cytoskeletal linkers)	Tb11.02.4300		4	2			6			
hypothetical protein	Tb927.8.1960			3	3		6			
homology (medium) to cox4 neighbour, predicted mito. UPF0172 family	Tb927.8.1570			6			6			
hypothetical protein	Tb927.6.1470		3	2			5			
low homology to a CPSF-like protein but no domains, possibly nuclear	Tb927.4.3540		1	4			5			
hypothetical protein	Tb11.39.0004		5				5			
orthologues have SMAD/FHA domain, no homologies found	Tb09.211.4170		5				5			
telomere repeat dimerization domain	Tb927.7.2170				5		5			
hypothetical protein,clow homology to syntaxin of giardia lamdia	Tb927.4.3060		2	2			4			
no domains, no clear location	Tb11.02.0010		1	3			4			
no homologies, possibly nuclear	Tb927.3.5370		1	3			4			
nuclear?	Tb09.211.1150		1	3			4			
homology to imilar to NSP5beta3beta [Gallus gallus]. And other DNA binding proteins	Tb927.10.5450			4			4			
hypothetical protein	Tb11.47.0020			4			4			
hypothetical protein	Tb927.1.4280			4			4			
low homology to dynactin	Tb927.5.2500			4			4			
low homology to WD-repeat protein, putative [Toxoplasma gondii]	Tb927.10.5870			4			4			
homologies to hypotheticasl proteins	Tb927.6.5070		4				4			
predicted WD40 repeat	Tb11.02.4620				2		2	1		
homology to hyp. Proteins, none in yeast	Tb927.8.1500		1	2			3			
LisH dimerisation motif orthologue	Tb09.211.1800		1	2			3			
homology to zinc finger proteins (low)	Tb927.8.2260			3			3			
hypothetical protein	Tb927.10.15250			3			3			
hypothetical protein	Tb927.2.2940			3			3			
Proteophosphoglycan	Tb927.10.5880			3			3			
Trypanosoma-specific no matches	Tb927.7.5030			3			3			
Up in BS. no domains	Tb927.10.13790			3			3			
up in PC. no matches.	Tb11.01.2550			3			3			
low homology to 26S proteasome domain	Tb927.3.1680		3				3			
ARF-like 2 binding protein BART	Tb927.10.5810		3				3			1
cAMP-specific phosphodiesterase PDEB2	Tb09.160.3630				3		3			
hypothetical protein, conserved	Tb11.02.2520				3		3			
major vault protein	Tb927.10.6310				3		3			
major vault protein	Tb927.5.4460				3		3			
ubiquitin-activating enzyme e1	Tb927.8.2640				3		3			
3 transmembrane regions	Tb09.211.1050			2			2			
brucei-specific, higher in BS, no matches	Tb11.02.0350			2			2			
C3H4 zinc finger	Tb927.10.12940			2			2			
C3H4 zinc finger	Tb927.10.6380			2			2			
GTP binding protein	Tb927.2.5060				2		2			
homology to a porin of toxoplasma gondii	Tb927.2.2510			2			2			
hypothetical protein	Tb927.10.3780			2			2			
low homologies, no domains	Tb927.5.3190			2			2			

low homology to mitochondrial phenylalanyl-tRNA synthetase [Schizosaccharomyces pombe]	Tb927.7.5240			2			2			
low homology to phosphatidylserinsynthase	Tb927.4.2170			2			2			
low homology to toxoplasma gondii zinc finger proteins,	Tb11.01.4400			2			2			
LysM domain (peptidoglycan binding). trypanosoma-specific	Tb927.5.3460			2			2			
no clear location, no domains, no hits	Tb11.01.1090			2			2			
Trypanosoma-specific, SSF52047 RNI-like	Tb09.211.0160			2			2			
hypothetical protein,	Tb11.50.0001		2				2			
low homology to heat shock protein SSC1, mitochondrial precursor [Candida albicans WO-1]	Tb927.10.8940		2				2			
low homology to d tRNA methyltransferase of s: cerevisiae	Tb927.10.15760		2				2			
small homology to ATP-dependent DNA helicase II subunit 1	Tb927.2.3800		2				2			
major vault protein	Tb927.10.1990				2		2			
Ribosome recycling factor domain	Tb927.7.2640				2		2			
Breast cancer type I susceptibility protein domain	Tb09.211.1310			1			1			
CS domain, HCP-like domain, medium homology to sel-1 homolog 2 precursor [Mus musculus]	Tb11.01.3290			1			1			
homology to kintoun isoform 2 [Homo sapiens]	Tb927.10.12860			1			1			
homology to nuclear factor of activated T-cells 5 isoform a [Homo sapiens]	Tb09.211.0200			1			1			
homology to RhoGAP domain-containing protein	Tb927.10.4070			1			1			
homology to UBX domain-containing protein 7 [Homo sapiens]	Tb927.3.5320			1			1			
Hypothetical conserved in trypanosoma, Leish match not syntenic	Tb927.10.12670			1			1			
hypothetical protein	Tb09.160.0400			1			1			
hypothetical protein	Tb11.02.4290			1			1			
hypothetical protein	Tb927.10.3810			1			1			
hypothetical protein, conserved	Tb927.10.16110			1			1			
low homology to dynactin, only brucei, BS specific.	Tb927.4.1230			1			1			
mannose-specific lectin, putative	Tb11.02.1680			1			1			
no domains	Tb11.01.4570			1			1			
no domains, low homology to proteasome beta 10 subunit proprotein [Homo sapiens]	Tb11.01.4890			1			1			
SAP domain (helix-loop-helix)	Tb927.10.4440			1			1			
signal anchor sequence, transmembrane domain	Tb11.01.2460			1			1			
signal anchor, low homology to actin regulating protein Neurabin2	Tb927.8.7720			1			1			
signal peptide low homology to zinc finger transcription factor TRPS1 [Mus musculus]	Tb927.3.3820			1			1			
signal peptide, no homologies	Tb927.5.1990			1			1			
Tetratricopeptide repeat domain	Tb927.6.4800			1			1			
low homology to CAP-Gly domain-containing linker protein 1 isoform b (H.Sapiens)	Tb09.211.2700		1				1			
no homologues	Tb11.01.6835		1				1			
replication factor C subunit 4 [Plasmodium vivax SaI-1] low homology	Tb11.02.4120		1				1			
		Total	1507	1859	2123	423				

6.2 High-throughput RNA sequencing results

6.2.1 mRNAs down-regulated in the bloodstream ZC3H32 RNAi cell line (as compared to WT)

gene	name	class	ZC3H32_1 /WT	ZC3H32_2 /WT
Tb927.11.16720	cyclin 6,mitotic cyclin (CYC6)	Cell cycle	0.32	0.44
Tb927.11.2490	kinesin, putative,Unc104-like kinesin, putative	Cytoskeleton	0.49	0.47
Tb927.6.3150	Hydin,flagellar component	Cytoskeleton	0.48	0.32
Tb927.4.870	dynein heavy chain, putative	Cytoskeleton	0.40	0.30
Tb927.2.5270	dynein heavy chain, putative	Cytoskeleton	0.48	0.42
Tb927.11.11220	dynein heavy chain, putative	Cytoskeleton	0.42	0.38
Tb927.11.8160	dynein heavy chain, putative	Cytoskeleton	0.49	0.38
Tb927.11.2430	dynein heavy chain, putative (DHC1b) or DYNC2H2	Cytoskeleton	0.48	0.36
Tb927.8.3250	dynein heavy chain, putative	Cytoskeleton	0.42	0.27
Tb927.3.930	dynein heavy chain, putative	Cytoskeleton	0.46	0.23
Tb927.11.3250	dynein heavy chain, putative	Cytoskeleton	0.50	0.19
Tb927.9.13610	helicase, putative	DNA helicase	0.39	0.48
Tb927.1.5080	ESAG9, putative	ESAG	0.50	0.15
Tb927.6.2850	ESAG8-associated protein, putative (PIE8)	ESAG	0.29	0.11
Tb927.7.2420	glycogen synthase kinase-3 alpha, putative	Glycan synthesis & metabolism	0.07	0.35
Tb927.10.4050	serine palmitoyltransferase, putative	Lipids & fatty acids	0.26	0.40
Tb927.2.3080	fatty acid desaturase, putative,oleate desaturase, putative	Lipids & fatty acids	0.45	0.48
Tb927.1.3320	leucine-rich repeat protein (LRRP)	LRRP	0.35	0.41
Tb927.2.1380	leucine-rich repeat protein (LRRP)	LRRP	0.04	0.22
Tb927.3.1490	leucine-rich repeat protein (LRRP)	LRRP	0.40	0.42
Tb927.11.6890	DNA repair and recombination helicase protein PIF1	Mitochondrial DNA	0.12	0.48
Tb927.9.14600	iron/ascorbate oxidoreductase family protein, putative	Mitochondrial pathway	0.00	0.48
Tb927.5.3620	dual specificity phosphatase, putative	Phosphatase	0.15	0.38
Tb927.7.7160	dual specificity phosphatase, putative	Phosphatase	0.38	0.49
Tb927.2.4280	dual specificity phosphatase, putative	Phosphatase	0.31	0.46
Tb927.11.7010	protein kinase, putative	Protein kinase	0.21	0.49
Tb927.6.2030	protein kinase, putative	Protein kinase	0.04	0.43
Tb927.8.870	serine/threonine kinase, putative,protein kinase, putative	Protein kinase	0.31	0.27
Tb927.7.6310	polo-like protein kinase,protein kinase (PLK)	Protein kinase	0.41	0.40
Tb927.9.6560	protein kinase, putative	Protein kinase	0.43	0.34
Tb927.11.4610	protein kinase A regulatory subunit (PKA-R)	Protein kinase	0.34	0.18
Tb927.10.14270	TFIIF-stimulated CTD phosphatase, putative	Protein phosphatase	0.15	0.34
Tb927.6.640	kinetoplastid-specific phospho-protein phosphatase, putative	Protein phosphatase	0.11	0.28
Tb927.5.4380	kinetoplastid-specific phospho-protein phosphatase, putative	Protein phosphatase	0.48	0.44
Tb927.10.12760	ZC3H36	RNA binding	0.11	0.39
Tb927.10.5150	ZC3H31	RNA binding	0.11	0.42
Tb927.8.6650	DRBD12	RNA binding	0.13	0.21
Tb927.7.5380	RNA-binding protein, putative, RBD	RNA binding	0.09	0.37
Tb927.10.12780	ZC3H37	RNA binding	0.39	0.37
Tb927.11.16550	ZC3H46	RNA binding	0.08	0.27
Tb927.10.12800	ZC3H38	RNA binding	0.44	0.31
Tb927.6.3480	DRBD5	RNA binding	0.36	0.11
Tb927.6.3490	ZFP1	RNA binding	0.03	0.17
Tb927.6.820	PUF4	RNA binding	0.06	0.43
Tb927.9.9520	ZC3H29	RNA binding	0.38	0.45
Tb927.10.5250	ZC3H32	RNA binding	0.09	0.12
Tb927.7.2140	ZC3H18	RNA binding	0.42	0.43
Tb927.10.11760	PUF6	RNA binding	0.39	0.45
Tb927.10.12660	PUF2	RNA binding	0.06	0.25
Tb927.3.3940	DRBD11	RNA binding	0.09	0.11
Tb927.1.2600	PUF9	RNA binding	0.06	0.33
Tb927.8.710	DRBD17	RNA binding	0.24	0.19
Tb927.8.4540	PBP1	RNA degradation	0.24	0.38
Tb927.7.4900	5'-3' exonuclease XRNA, putative,exoribonuclease 1, putative (XRNA)	RNA degradation	0.43	0.35
Tb927.10.1510	NOT complex subunit NOT1	RNA degradation	0.39	0.34
Tb927.2.3880	heterogeneous nuclear ribonucleoprotein H/F, putative +	RNA processing	0.17	0.10
Tb927.8.900	splicing factor TSR1 (TSR1)	RNA processing	0.29	0.36
Tb927.2.3580	transcription elongation factor s-II, putative (TFIIS2-1)	RNA synthesis II	0.42	0.27
Tb927.1.1930	TbTOR4 = TOR-like 2	Signalling	0.40	0.32
Tb927.2.2260	PIK-related	Signalling	0.38	0.33

Tb927.10.14550	ATP-dependent DEAD/H RNA helicase, DED1-1	Translation	0.06	0.14
Tb927.9.12510	ATP-dependent DEAD/H RNA helicase, DED1-2	Translation	0.49	0.35
Tb927.5.2400	ubiquitin carboxyl-terminal hydrolase, putative	Ubiquitin & proteasome	0.38	0.42
Tb927.8.1590	ubiquitin-protein ligase, putative (upl3)	Ubiquitin & proteasome	0.35	0.34
Tb927.10.3410	hypothetical protein		0.02	0.25
Tb927.6.1790	hypothetical protein		0.02	0.49
Tb927.9.4130	hypothetical protein, conserved		0.04	0.48
Tb927.7.2090	hypothetical protein, conserved		0.14	0.37
Tb927.5.2480	hypothetical protein, conserved		0.38	0.43
Tb927.10.480	hypothetical protein, conserved		0.23	0.16
Tb927.9.9370	hypothetical protein, conserved		0.36	0.22
Tb927.6.3880	hypothetical protein, conserved		0.47	0.40
Tb927.10.12650	hypothetical protein, conserved		0.02	0.25
Tb927.2.3090	hypothetical protein, conserved		0.47	0.48
Tb927.1.1470	hypothetical protein, conserved		0.34	0.33
Tb927.6.690	hypothetical protein, conserved		0.05	0.38
Tb927.5.2360	hypothetical protein, conserved		0.26	0.48
Tb927.10.11630	hypothetical protein, conserved		0.30	0.34
Tb927.11.16820	hypothetical protein, conserved		0.39	0.37
Tb927.4.710	hypothetical protein, conserved		0.23	0.26
Tb927.11.4620	hypothetical protein, conserved		0.39	0.13
Tb927.8.7820	hypothetical protein, conserved		0.02	0.47
Tb927.5.2010	hypothetical protein		0.46	0.41
Tb927.2.2340	hypothetical protein, conserved		0.21	0.29
Tb927.10.3400	hypothetical protein, conserved		0.03	0.20
Tb927.11.15160	hypothetical protein, conserved		0.49	0.43
Tb927.5.2620	hypothetical protein, conserved		0.27	0.48
Tb927.4.1910	hypothetical protein, conserved		0.06	0.24
Tb927.11.6600	hypothetical protein, conserved		0.02	0.46
Tb927.8.3820	hypothetical protein, conserved		0.42	0.41
Tb927.7.3970	hypothetical protein, conserved		0.16	0.33
Tb927.1.1500	hypothetical protein, conserved		0.06	0.23
Tb927.8.910	hypothetical protein, conserved		0.04	0.11
Tb927.2.2770	hypothetical protein, conserved		0.43	0.41
Tb927.11.2860	hypothetical protein, conserved		0.08	0.48
Tb927.5.3290	hypothetical protein, conserved		0.40	0.50
Tb927.11.14220	hypothetical protein, conserved		0.07	0.14
Tb927.7.5340	hypothetical protein, conserved		0.21	0.19
Tb927.10.9330	hypothetical protein, conserved		0.41	0.45
Tb927.5.2000	hypothetical protein		0.35	0.32
Tb927.8.7850	hypothetical protein, conserved		0.48	0.42
Tb927.8.5110	hypothetical protein, conserved		0.09	0.24
Tb927.8.1290	hypothetical protein, conserved		0.10	0.31
Tb927.9.7520	hypothetical protein, conserved		0.30	0.42
Tb927.9.4080	hypothetical protein, conserved		0.05	0.46
Tb927.11.6860	hypothetical protein		0.27	0.35
Tb927.8.880	hypothetical protein		0.15	0.38
Tb927.9.15290	hypothetical protein, conserved		0.46	0.45
Tb927.7.6690	hypothetical protein		0.19	0.31
Tb927.3.4270	hypothetical protein, conserved		0.42	0.50
Tb927.4.4580	hypothetical protein, conserved		0.45	0.37
Tb927.6.620	hypothetical protein, conserved		0.46	0.47
Tb927.10.15730	hypothetical protein, conserved		0.48	0.35
Tb927.11.6440	hypothetical protein, conserved, often in TAP MS		0.37	0.31
Tb927.8.5580	hypothetical protein, conserved		0.40	0.44
Tb927.1.880	hypothetical protein, conserved		0.44	0.42
Tb927.10.7230	hypothetical protein, conserved		0.49	0.47
Tb927.1.4310	hypothetical protein, conserved		0.26	0.14
Tb927.9.1750	hypothetical protein, conserved		0.36	0.36
Tb927.7.3550	hypothetical protein, conserved		0.40	0.22

6.2.2 mRNAs up-regulated in the procyclic ZC3H32-myc cell line (as compared to WT)

Gene ID	Annotation	Class	ZC3H32-myc
Tb927.8.6060	2-amino-3-ketobutyrate coenzyme A ligase, putative	Amino acid metabolism	2.14
Tb927.11.2230	carnitine O-acetyltransferase, putative (CAT)	Amino acid metabolism	2.63
Tb927.10.11970	kynurenine aminotransferase, putative	Amino acid metabolism	4.46
Tb927.11.6680	amino acid permease/transporter, putative	Amino acid transporter	2.70
Tb927.11.9790	calmodulin, putative	Calcium	2.13

Tb927.4.3330	hyp. protein	Calcium	2.20
Tb927.10.370	calcineurin B subunit, putative	Calcium	2.55
Tb927.6.5020	cyclin 7, putative,CYC2-like cyclin, putative (CYC7)	Cell cycle	3.31
Tb927.11.5710	chaperone protein DNAj, putative	Chaperone	2.00
Tb927.2.5980	heat shock protein 104 (HSP104)	Chaperone	2.06
Tb927.10.15600	FKBP-type peptidyl-prolyl cis-trans isomerase, putative	Chaperone	2.12
Tb927.7.1320	10 kDa heat shock protein, putative (HSP10)	Chaperone	2.87
Tb927.6.3850	chaperone protein DNAj, putative	Chaperone	2.90
Tb927.3.4500	fumarate hydratase, class I (FHc)	Citric acid cycle	2.30
Tb927.11.900	isocitrate dehydrogenase, putative (IDH)	Citric acid cycle	2.90
Tb927.10.14000	aconitase (ACO)	Citric acid cycle	3.37
Tb927.10.13430	citrate synthase, putative	Citric acid cycle	6.59
Tb927.11.4660	kinesin family member 6, putative (Kif13-2)	Cytoskeleton	2.02
Tb927.4.870	dynein heavy chain, putative	Cytoskeleton	2.03
Tb927.10.4690	dynein light chain, putative	Cytoskeleton	2.06
Tb927.10.1110	kinesin, putative	Cytoskeleton	2.11
Tb927.8.4840	kinesin, putative	Cytoskeleton	2.13
Tb927.11.11220	dynein heavy chain, putative	Cytoskeleton	2.14
Tb927.10.13330	paraflagellar rod protein PFC20	Cytoskeleton	2.16
Tb927.2.3660	paraflagellar rod protein PFC10	Cytoskeleton	2.19
Tb927.11.2430	dynein heavy chain, putative (DHC1b) or DYNC2H2	Cytoskeleton	2.19
Tb927.2.5270	dynein heavy chain, putative	Cytoskeleton	2.34
Tb927.3.930	dynein heavy chain, putative	Cytoskeleton	2.52
Tb927.11.3250	dynein heavy chain, putative	Cytoskeleton	2.54
Tb927.8.3250	dynein heavy chain, putative	Cytoskeleton	2.69
Tb927.11.8160	dynein heavy chain, putative	Cytoskeleton	2.88
Tb927.11.320	unspecified product	Cytoskeleton	2.90
Tb927.11.16310	myosin, putative,myosin heavy chain, putative	Cytoskeleton_Actin	2.03
Tb927.10.10600	ARP2/3 complex 16kDa subunit, putative	Cytoskeleton_Actin	2.32
Tb927.2.2900	ARP2/3 complex subunit, putative	Cytoskeleton_Actin	2.50
Tb927.5.3760	meiotic recombination protein spo11, putative	DNA synthesis, modification, repair	2.01
Tb927.10.5490	hyp. protein,predicted HORMA domain protein	DNA synthesis, modification, repair	2.10
Tb927.2.5190	hyp. protein	DNA synthesis, modification, repair	2.37
Tb927.8.2210	pteridine reductase (PTR1)	Folate	2.21
Tb927.1.2820	pteridine transporter, putative	Folate	2.70
Tb927.8.3530	glycerol-3-phosphate dehydrogenase [NAD], glycosomal	Glucose & glycerol	2.19
Tb927.10.4780	GPI inositol deacylase precursor (GPIdeAc)	GPI anchors & metabolism	2.07
Tb927.3.2610	GPI inositol deacylase 2 (GPIdeAc2)	GPI anchors & metabolism	2.08
Tb927.11.580	lipid-like atypical dual specificity phosphatase, putative	Lipids & fatty acids	2.06
Tb927.10.690	palmitoyl acyltransferase 3, putative	Lipids & fatty acids	2.56
Tb927.1.4490	acetyltransferase, putative	Lipids & fatty acids	3.48
Tb927.8.480	phosphatidic acid phosphatase protein, putative	Lipids & fatty acids	23.26
Tb927.5.1830	lysosomal/endosomal membrane protein p67 (p67)	Lysosome	2.20
Tb927.10.3760	vacuolar ATP synthase subunit d, putative	Lysosome	2.39
Tb927.4.1400	vacuolar transport protein 4A, putative	Lysosome	2.41
Tb927.11.10740	vacuolar sorting-associated protein-like, putative	Lysosome	2.61
Tb927.11.1470	65 kDa invariant surface glycoprotein (ISG65)	Membrane protein	2.17
Tb927.9.11640	hyp. protein, predicted GPI anchor	Membrane protein	2.67
Tb927.9.7830	mitochondrial tRNA import complex, putative	Mitochondrial biogenesis	4.17
Tb927.10.8950	kinetoplast DNA-associated protein, putative	Mitochondrial DNA	2.15
Tb927.11.11800	DNA repair and recombination helicase protein PIF3	Mitochondrial DNA	2.37
Tb927.11.14790	DNA repair and recombination helicase protein PIF4	Mitochondrial DNA	3.44
Tb927.11.15550	NADH-cytochrome b5 reductase, putative (B5R)	Mitochondrial electron transport	2.07
Tb927.11.6640	cytochrome b5, putative (CYB5)	Mitochondrial electron transport	4.83
Tb927.9.12500	hyp. protein	Mitochondrial membrane	2.12
Tb927.7.3590	Complex II subunit, putative	Mitochondrial pathway	2.04
Tb927.3.2180	Mitochondrial ATP synthase subunit, putative	Mitochondrial pathway	2.08
Tb927.10.5050	Mitochondrial ATP synthase epsilon subunit, putative	Mitochondrial pathway	2.13
Tb927.9.13580	hyp. protein	Mitochondrial pathway	2.17
Tb927.2.3610	Mitochondrial ATP synthase subunit, putative	Mitochondrial pathway	2.42
Tb927.5.510	hyp. protein	Mitochondrial pathway	2.75
Tb927.11.9800	serine peptidase, Clan SP, family S59, putative Nucleoporin	Nucleo-cytoplasmic transport	2.05
Tb927.5.1360	nucleoside 2-deoxyribosyltransferase (NDRT)	Nucleotides	2.42
Tb927.7.1790	Adenine phosphoribosyltransferase, putative	Nucleotides-Purines	2.58
Tb927.3.590	adenosine transporter, putative	Nucleotides-Purines	5.56
Tb927.8.4430	uridine phosphorylase;with=PDB:3BJE	Nucleotides-Pyrimidines	2.94
Tb927.11.14600	procyclin-associated gene 2-like protein, putative	PAG	4.23
Tb927.11.11740	membrane-bound acid phosphatase, putative	Phosphatase	2.27
Tb927.11.7320	dual specificity phopshatase, putative	Phosphatase	2.38
Tb927.10.3490	kinetoplastid-specific dual specificity phosphatase, putative	Phosphatase	2.39
Tb927.4.2670	pyroglutamyl-peptidase I (PGP), putative,cysteine peptidase	Protease or peptidase	2.03

Tb927.10.14300	protein kinase, putative,serine/threonine protein kinase, putative	Protein kinase	2.18
Tb927.11.11110	protein kinase, putative,serine/threonine kinase, putative	Protein kinase	2.73
Tb927.9.1500	protein kinase, putative	Protein kinase	2.86
Tb927.11.4990	kinetoplastid-specific phospho-protein phosphatase, putative	Protein phosphatase	2.43
Tb927.9.6090	PTP1-interacting protein, 39 kDa PIP39	Protein phosphatase	3.71
Tb927.3.5090	tryparedoxin, putative	Redox pathways	2.44
Tb927.11.1370	glutaredoxin, putative	Redox pathways	2.53
Tb927.11.3230	60S ribosomal protein L44	Ribosome	2.35
Tb927.10.3380	60S acidic ribosomal protein P2	Ribosome	2.38
Tb927.10.4120	60S ribosomal protein L30	Ribosome	2.60
Tb927.9.15210	60S ribosomal protein L36	Ribosome	2.94
Tb927.5.1820	60S acidic ribosomal protein	Ribosome	3.35
Tb927.11.5850	RBP38	RNA binding	2.27
Tb927.6.4050	ZC3H14	RNA binding	2.30
Tb927.7.4730	PUF5	RNA binding	2.38
Tb927.9.4560	RBP32	RNA binding	4.66
Tb927.10.5250	ZC3H32	RNA binding	13.29
Tb927.10.2220	piwi-like protein 1	RNA degradation	2.49
Tb927.10.16140	Adenylate/guanylate cyclase, putative	Signalling	2.10
Tb927.10.12170	RAB-interacting protein, putative	Signalling	2.24
Tb927.2.2260	PIK-related	Signalling	3.00
Tb927.7.5230	lanosterol synthase	Sterols	2.05
Tb927.8.2480	3-oxo-5-alpha-steroid 4-dehydrogenase-like, putative	Sterols	2.20
Tb927.4.4080	C-5 sterol desaturase, putative	Sterols	2.24
Tb927.11.9700	nascent polypeptide associated complex alpha subunit, putative	Translation	2.55
Tb927.4.2710	ubiquitin-conjugating enzyme e2, putative	Ubiquitin & proteasome	2.16
Tb927.11.12340	predicted Zinc finger, C3HC4 type (RING finger) protein	Ubiquitin & proteasome	2.44
Tb927.11.13940	ubiquitin-conjugating enzyme e2, putative	Ubiquitin & proteasome	2.92
Tb927.8.3660	protein transport protein Sec23 (SEC23.1)	Vesicular transport	2.06
Tb927.11.10270	golgi SNARE protein-like, putative	Vesicular transport	2.07
Tb927.2.5120	vesicle-associated membrane protein, in Tc vacuolar proteome	Vesicular transport	2.11
Tb927.9.10010	Sec63 homologue, chaperone protein DNAj	Vesicular transport	2.17
Tb927.9.14080	vesicle-associated membrane protein, putative	Vesicular transport	2.18
Tb927.8.7050	mu-adaptin 4, adaptor complex AP-4 medium subunit, putative	Vesicular transport	2.21
Tb927.7.3160	dynein heavy chain, cytosolic, putative	Vesicular transport	2.22
Tb927.11.14240	hyp. protein	Vesicular transport	2.24
Tb927.11.5490	synaptojanin (N-terminal domain), putative	Vesicular transport	2.35
Tb927.7.6440	hyp. protein	Vesicular transport	2.37
Tb927.9.12870	hyp. protein	Vesicular transport	2.61
Tb927.10.580	hyp. protein		2.01
Tb927.2.5970	hyp. protein		2.01
Tb927.11.13630	hyp. protein		2.01
Tb927.7.1700	hyp. protein		2.01
Tb927.9.12390	hyp. protein		2.01
Tb927.4.4890	hyp. protein		2.02
Tb927.7.5830	hyp. protein		2.02
Tb927.8.7480	hyp. protein		2.02
Tb927.8.5590	hyp. protein		2.02
Tb927.11.14540	hyp. protein		2.03
Tb927.10.7830	hyp. protein		2.03
Tb927.10.4140	hyp. protein		2.04
Tb927.7.5510	hyp. protein		2.04
Tb927.4.1260	hyp. protein		2.05
Tb927.11.8900	hyp. protein		2.05
Tb927.11.520	hyp. protein		2.05
Tb927.11.12620	hyp. protein		2.05
Tb927.3.4480	hyp. protein		2.05
Tb927.3.1550	hyp. protein		2.06
Tb927.11.5620	hyp. protein		2.06
Tb927.11.16330	hyp. protein		2.06
Tb927.8.2110	hyp. protein		2.06
Tb927.11.7090	hyp. protein		2.06
Tb927.5.1590	hyp. protein		2.07
Tb927.7.7190	hyp. protein		2.07
Tb927.11.5640	hyp. protein		2.07
Tb927.3.4870	hyp. protein		2.07
Tb927.10.7000	hyp. protein		2.08
Tb927.1.1300	hyp. protein		2.09
Tb927.10.9690	hyp. protein,predicted C2 domain protein		2.11
Tb927.8.5050	hyp. protein		2.11
Tb927.8.4340	hyp. protein		2.11

Tb927.3.3600	hyp. protein		2.12
Tb927.7.4750	hyp. protein		2.12
Tb927.5.3260	hyp. protein		2.12
Tb927.8.7990	hyp. protein		2.13
Tb927.11.15610	hyp. protein		2.13
Tb927.11.5660	hyp. protein		2.13
Tb927.7.4230	hyp. protein		2.13
Tb927.3.2380	hyp. protein		2.14
Tb927.8.3390	hyp. protein		2.14
Tb927.11.2190	hyp. protein		2.15
Tb927.8.5160	hyp. protein		2.16
Tb927.3.2360	hyp. protein		2.18
Tb927.2.1790	hyp. protein		2.18
Tb927.2.4680	hyp. protein		2.18
Tb927.11.6100	hyp. protein		2.18
Tb927.4.1830	hyp. protein		2.19
Tb927.7.490	hyp. protein		2.19
Tb927.11.2930	hyp. protein		2.19
Tb927.9.1750	hyp. protein		2.19
Tb927.10.11060	hyp. protein		2.20
Tb927.3.1870	hyp. protein		2.20
Tb927.8.5550	hyp. protein		2.20
Tb927.9.10360	hyp. protein		2.20
Tb927.7.3130	hyp. protein		2.21
Tb927.10.15730	hyp. protein		2.22
Tb927.8.1700	hyp. protein		2.22
Tb927.9.12950	hyp. protein		2.23
Tb927.4.2570	hyp. protein		2.24
Tb927.6.2870	hyp. protein		2.24
Tb927.10.9270	hyp. protein		2.24
Tb927.8.5190	hyp. protein		2.24
Tb927.8.5870	hyp. protein		2.26
Tb927.5.1290	hyp. protein		2.27
Tb927.9.1360	hyp. protein		2.27
Tb927.8.5580	hyp. protein		2.28
Tb927.11.12840	hyp. protein		2.28
Tb927.11.5790	hyp. protein		2.28
Tb927.10.1810	hyp. protein		2.29
Tb927.3.5390	hyp. protein		2.29
Tb927.8.2190	hyp. protein		2.31
Tb927.5.1220	hyp. protein		2.32
Tb927.11.4510	hyp. protein		2.32
Tb927.4.1390	hyp. protein		2.33
Tb927.4.2380	sarcoplasmic reticulum glycoprotein, putative		2.34
Tb927.7.3600	hyp. protein		2.34
Tb927.7.3530	hyp. protein		2.34
Tb927.3.650	hyp. protein		2.35
Tb927.8.7550	hyp. protein		2.36
Tb927.8.1970	hyp. protein		2.36
Tb927.9.13070	hyp. protein,predicted heat shock factor binding protein		2.37
Tb927.5.3790	hyp. protein		2.37
Tb927.9.10160	hyp. protein		2.37
Tb927.10.1650	hyp. protein		2.38
Tb927.11.1170	hyp. protein		2.38
Tb927.10.4660	hyp. protein		2.38
Tb927.1.1040	hyp. protein		2.38
Tb927.3.5080	hyp. protein		2.39
Tb927.9.7040	hyp. protein		2.39
Tb927.3.1260	hyp. protein		2.40
Tb927.10.2850	hyp. protein		2.40
Tb927.10.3530	hyp. protein		2.41
Tb927.4.370	hyp. protein		2.41
Tb927.8.6890	hyp. protein		2.42
Tb927.1.1880	hyp. protein		2.42
Tb927.8.5270	hyp. protein		2.43
Tb927.11.390	hyp. protein		2.44
Tb927.10.12080	hyp. protein		2.45
Tb927.8.5850	hyp. protein		2.45
Tb927.11.15410	hyp. protein		2.48
Tb927.1.780	hyp. protein		2.48
Tb927.9.8330	hyp. protein		2.49

Tb927.10.2340	hyp. protein		2.49
Tb927.1.1640	hyp. protein		2.50
Tb927.4.520	hyp. protein		2.51
Tb927.3.2460	hyp. protein		2.51
Tb927.8.5320	hyp. protein		2.52
Tb927.5.2350	hyp. protein		2.53
Tb927.2.3340	hyp. protein		2.53
Tb927.4.2420	hyp. protein		2.54
Tb927.8.3990	hyp. protein		2.54
Tb927.4.3520	hyp. protein		2.54
Tb927.11.12990	hyp. protein		2.56
Tb927.11.5540	hyp. protein		2.57
Tb927.11.3460	hyp. protein		2.57
Tb927.10.2820	hyp. protein		2.58
Tb927.7.860	hyp. protein		2.58
Tb927.9.9810	hyp. protein		2.58
Tb927.10.6560	hyp. protein		2.59
Tb927.11.7550	hyp. protein		2.61
Tb927.10.14450	hyp. protein		2.62
Tb927.4.3340	hyp. protein		2.63
Tb927.7.7000	hyp. protein		2.66
Tb927.10.2920	hyp. protein		2.68
Tb927.10.2400	hyp. protein		2.69
Tb927.9.3750	hyp. protein		2.70
Tb927.8.5900	hyp. protein		2.70
Tb927.11.15510	hyp. protein		2.72
Tb927.10.1300	hyp. protein		2.79
Tb927.4.3500	hyp. protein		2.80
Tb927.11.1330	hyp. protein		2.83
Tb927.3.2940	hyp. protein		2.84
Tb927.10.440	hyp. protein		2.84
Tb927.11.15670	hyp. protein		2.88
Tb927.10.14350	hyp. protein		2.94
Tb927.9.8320	hyp. protein		2.97
Tb927.4.4320	divalent cation tolerance protein, putative		3.02
Tb927.7.3660	hyp. protein		3.04
Tb927.10.14370	hyp. protein		3.10
Tb927.9.4550	hyp. protein		3.10
Tb927.11.9120	hyp. protein		3.12
Tb927.8.6100	hyp. protein		3.16
Tb927.11.16260	hyp. protein		3.17
Tb927.10.9300	adiponectin receptor protein 1		3.20
Tb927.3.2920	hyp. protein		3.28
Tb927.9.12740	hyp. protein		3.29
Tb927.11.13610	hyp. protein		3.29
Tb927.11.9860	hyp. protein		3.31
Tb927.10.10770	hyp. protein		3.34
Tb927.4.4390	hyp. protein		3.35
Tb927.9.10510	hyp. protein		3.36
Tb927.11.15660	hyp. protein		3.37
Tb927.4.390	hyp. protein		3.38
Tb927.10.9510	hyp. protein		3.40
Tb927.10.2970	hyp. protein		3.42
Tb927.10.300	hyp. protein		3.43
Tb927.4.500	hyp. protein		3.43
Tb927.4.4780	hyp. protein		3.47
Tb927.5.4020	hyp. protein		3.63
Tb927.9.8030	hyp. protein		3.64
Tb927.9.8760	hyp. protein		3.78
Tb927.4.3480	hyp. protein		3.89
Tb927.10.780	hyp. protein		4.14
Tb927.11.5720	hyp. protein		4.20
Tb927.9.10930	hyp. protein		4.41
Tb927.11.2460	hyp. protein		4.47
Tb927.9.15690	hyp. protein		4.61
Tb927.10.3360	hyp. protein		4.90
Tb927.11.15200	hyp. protein		5.08
Tb927.7.2180	hyp. protein		6.45
Tb927.9.11910	hyp. protein		11.84
Tb927.9.15350	hyp. protein		28.87
Tb927.9.15100	hyp. protein		237.48

6.2.3 mRNAs down-regulated in the procyclic ZC3H32-myc cell line (as compared to WT)

Gene ID	Annotation	Class	ZC3H32 - myc
Tb927.8.6340	CYC2-like cyclin, putative (CYC10)	Cell cycle	0.14
Tb927.9.10950	chaperone protein DNAj, putative	Chaperone	0.22
Tb927.10.2620	HSP20 cold-shock domain (p23-like)	Chaperone	0.35
Tb927.10.12380	chaperone protein DNAj, putative	Chaperone	0.48
Tb927.10.2290	chaperone protein DNAj, endoplasmatic reticulum	Chaperone	0.49
Tb927.3.3490	high mobility group protein, putative (TDP1)	Chromatin	0.41
Tb927.11.2690	succinyl-coA:3-ketoacid-coenzyme A transferase, putative	Citric acid cycle	0.35
Tb927.10.2560	mitochondrial malate dehydrogenase (mMDH)	Citric acid cycle	0.38
Tb927.10.5960	engulfment and cell motility domain 2, putative	cytoskeleton	0.35
Tb927.11.12180	kinesin, putative	Cytoskeleton	0.41
Tb927.10.2640	intraflagellar transport protein IFT81, putative	Cytoskeleton	0.45
Tb927.7.3000	kinesin, putative	Cytoskeleton	0.45
Tb927.10.12490	kinesin, putative	Cytoskeleton	0.47
Tb927.10.450	hyp. protein	Cytoskeleton	0.47
Tb927.11.7820	endonuclease/exonuclease/phosphatase, putative	DNA synthesis, modification, repair	0.04
Tb927.4.1330	DNA topoisomerase IB, large subunit	DNA synthesis, modification, repair	0.42
Tb927.9.14120	hyp. protein, phosphatase domain	enzyme	0.31
Tb927.7.5450	lipin, putative	Enzyme	0.41
Tb927.8.3970	oxidoreductase, putative	Enzyme	0.43
Tb927.5.2650	L-galactonolactone oxidase (GAL/ALO)	Enzyme	0.43
Tb927.10.9560	oxidoreductase, putative	Enzyme	0.48
Tb927.7.1930	nucleoside diphosphatase, putative5	Enzyme	0.49
Tb927.10.2020	hexokinase (HK2)	Glucose & glycerol	0.18
Tb927.7.2420	glycogen synthase kinase-3 alpha, putative	Glycan synthesis & metabolism	0.07
Tb927.10.2570	lysosomal alpha-mannosidase precursor, putative	Glycan synthesis & metabolism	0.37
Tb927.5.2760	UDP-Gal or UDP-GlcNAc-dependent glycosyltransferase, putative	Glycan synthesis & metabolism	0.44
Tb927.10.12290	UDP-Gal or UDP-GlcNAc-dependent glycosyltransferase, putative	Glycan synthesis & metabolism	0.45
Tb927.6.1140	dolichyl-P-Man:GDP-Man5GlcNAc2-PP-dolichyl alpha-1,2-mannosyltransferase, putative	Glycan synthesis & metabolism	0.49
Tb927.9.15460	calcium motive p-type ATPase, putative	Ion channel or pump	0.50
Tb927.10.4050	serine palmitoyltransferase, putative	Lipids & fatty acids	0.25
Tb927.11.3350	phospholipid-transporting ATPase 1-like protein, putative	Lipids & fatty acids	0.31
Tb927.2.3080	fatty acid desaturase, putative,oleate desaturase, putative	Lipids & fatty acids	0.46
Tb927.6.3550	phospholipid-translocating P-type ATPase (flippase), putative	Lipids & fatty acids	0.47
Tb927.10.8900	Choline phosphotransferase	Lipids & fatty acids	0.47
Tb927.10.2410	MSP-C, putative	Membrane protein	0.40
Tb927.11.15040	chaperonin HSP60, mitochondrial precursor	Mitochondrial biogenesis	0.46
Tb927.6.4090	chaperonin HSP60, mitochondrial precursor	Mitochondrial biogenesis	0.48
Tb927.1.4010	TbPRI2, primase 2, kDNA replication	Mitochondrial DNA	0.26
Tb927.11.6890	DNA repair and recombination helicase protein PIF1	Mitochondrial DNA	0.36
Tb927.1.3800	hyp. protein	Mitochondrial membrane	0.39
Tb927.5.520	stomatin-like protein, putative	Mitochondrial pathway	0.37
Tb927.7.7080	mitochondrial glycoprotein-like protein	Mitochondrial pathway	0.49
Tb927.10.10830	RGG2, MRB complex component	Mitochondrial RNA	0.29
Tb927.6.2140	Mitochondrial RNA binding complex I component, putative	Mitochondrial RNA	0.36
Tb927.3.1820	mitochondrial RNA binding complex 1 subunit	Mitochondrial RNA	0.40
Tb927.9.13780	Mitchondrial SSU ribosomal protein	Mitochondrial translation	0.06
Tb927.6.4080	Mitchondrial LSU ribosomal protein	Mitochondrial translation	0.37
Tb927.9.14050	Mitchondrial LSU ribosomal protein	Mitochondrial translation	0.49
Tb927.11.3380	Ran-binding protein 1, putative	Nucleo-cytoplasmic transport	0.40
Tb927.6.1970	nuclear cap binding protein, putative (CBC20)	Nucleo-cytoplasmic transport	0.45
Tb927.6.4740	importin-alpha re-exporter protein, putative	Nucleo-cytoplasmic transport	0.46
Tb927.6.2640	importin alpha subunit, putative (TbKap60)	Nucleo-cytoplasmic transport	0.46
Tb927.10.2530	adenylate kinase, putative	Nucleotides-Purines	0.29
Tb927.6.220	purine nucleoside transporter (TbNT9)	Nucleotides-Purines	0.37
Tb927.9.7470	purine nucleoside transporter (TbNT10)	Nucleotides-Purines	0.43
Tb927.11.3650	adenylosuccinate synthetase, putative	Nucleotides-Purines	0.43
Tb927.10.16120	inosine-5'-monophosphate dehydrogenase,IMP dehydrogenase	Nucleotides-Purines	0.49
Tb927.7.4570	inosine-guanine nucleoside hydrolase (IG-NH)	Nucleotides-Purines	0.49
Tb927.10.10810	adenosine deaminase-like protein	Nucleotides-Purines	0.49
Tb927.5.3620	kinetoplastid-specific dual specificity phosphatase, putative	Phosphatase	0.34
Tb927.6.4540	HMG-CoA reductase	Prenylation	0.47
Tb927.6.400	peptidase M20/M25/M40, putative	Protease or peptidase	0.35
Tb927.10.9600	protein kinase, putativ	Protein kinase	0.03

Tb927.6.2030	protein kinase, putative	Protein kinase	0.03
Tb927.11.16790	mitogen-activated protein kinase (ECK1)	Protein kinase	0.05
Tb927.3.1630	casein kinase 1, putative (CK1)	Protein kinase	0.08
Tb927.2.1820	protein kinase, putative	Protein kinase	0.14
Tb927.8.870	serine/threonine kinase, putative,protein kinase, putative	Protein kinase	0.21
Tb927.11.14070	protein kinase, putative	Protein kinase	0.22
Tb927.7.6220	protein kinase, putative	Protein kinase	0.26
Tb927.1.1380	serine/threonine protein phosphatase 2A reg. subunit, putative	Protein kinase	0.26
Tb927.7.6680	protein kinase, putative	Protein kinase	0.27
Tb927.11.7010	protein kinase, putative	Protein kinase	0.30
Tb927.2.4200	protein kinase, putative	Protein kinase	0.30
Tb927.7.3650	protein kinase, putative	Protein kinase	0.31
Tb927.10.10870	protein kinase, putative	Protein kinase	0.35
Tb927.2.2720	protein kinase, putative	Protein kinase	0.38
Tb927.7.5770	Nuclear Dbf2-related kinase (PK53)	Protein kinase	0.39
Tb927.11.4610	protein kinase A regulatory subunit (PKA-R)	Protein kinase	0.41
Tb927.10.3340	protein kinase, putative	Protein kinase	0.42
Tb927.10.10350	protein kinase, putative	Protein kinase	0.42
Tb927.6.4970	serine/arginine-rich protein specific kinase SRPK, putative	Protein kinase	0.48
Tb927.10.15020	protein kinase, putative	Protein kinase	0.49
Tb927.6.640	kinetoplastid-specific phospho-protein phosphatase, putative	Protein phosphatase	0.09
Tb927.10.14270	TFIIF-stimulated CTD phosphatase, putative	Protein phosphatase	0.11
Tb927.6.1800	protein phosphatase 2C, putative	Protein phosphatase	0.20
Tb927.10.8050	TFIIF-stimulated CTD phosphatase, putative	Protein phosphatase	0.27
Tb927.7.4020	protein phosphatase 2C, putative	Protein phosphatase	0.35
Tb927.4.3680	protein phosphatase 2C, putative	Protein phosphatase	0.48
Tb927.6.2050	ribosome biogenesis regulatory protein (RRS1), putative	Ribosome	0.46
Tb927.11.530	RBP3	RNA binding	0.03
Tb927.6.820	PUF4	RNA binding	0.03
Tb927.6.3490	ZFP1	RNA binding	0.04
Tb927.10.12660	PUF2	RNA binding	0.07
Tb927.11.8470	ZC3H45	RNA binding	0.08
Tb927.8.2780	RBP10	RNA binding	0.11
Tb927.10.5150	ZC3H31	RNA binding	0.12
Tb927.11.16550	ZC3H46	RNA binding	0.12
Tb927.3.1910	hyp. protein	RNA binding	0.14
Tb927.3.5250	ZC3H8	RNA binding	0.16
Tb927.1.2600	PUF9	RNA binding	0.17
Tb927.4.4230	RBP31	RNA binding	0.17
Tb927.7.3730	RBP26	RNA binding	0.17
Tb927.7.5380	RNA-binding protein, putative, RBD	RNA binding	0.23
Tb927.10.14930	ZC3H39	RNA binding	0.25
Tb927.10.12330	ZC3H34	RNA binding	0.30
Tb927.9.9520	ZC3H29	RNA binding	0.35
Tb927.8.6650	DRBD12	RNA binding	0.39
Tb927.5.760	cell cycle sequence binding phosphoprotein (RBP33), CSBP2	RNA binding	0.40
Tb927.9.13280	DRBD10	RNA binding	0.40
Tb927.3.3670	TRRM3	RNA binding	0.42
Tb927.10.12760	ZC3H36	RNA binding	0.43
Tb927.9.13990	DRBD2	RNA binding	0.44
Tb927.8.710	DRBD17	RNA binding	0.46
Tb927.5.810	ZC3H11	RNA binding	0.49
Tb927.3.1030	RPB28	RNA binding	0.49
Tb927.6.600	NOT complex subunit CAF1 deadenylase	RNA degradation	0.15
Tb927.6.4770	MKT1	RNA degradation	0.26
Tb927.11.550	SCD6	RNA degradation	0.30
Tb927.8.900	splicing factor TSR1 (TSR1)	RNA processing	0.30
Tb927.2.3880	heterogeneous nuclear ribonucleoprotein H/F, putative (HNRNPH)	RNA processing	0.30
Tb927.2.4710	TRRM1	RNA processing	0.33
Tb927.6.2700	small nuclear ribonucleoprotein Sm-E	RNA processing	0.37
Tb927.2.5240	PRP19-like protein, putative (TbPRP19)	RNA processing	0.48
Tb927.3.3590	U3 small nucleolar ribonucleoprotein protein MPP10, putative	RNA processing	0.48
Tb927.3.3160	poly(A) polymerase,polynucleotide adenylyltransferase (PAP)	RNA processing	0.49
Tb927.11.10420	DNA-directed RNA polymerase, putative (RPA12)	RNA synthesis I	0.47
Tb927.2.3580	transcription elongation factor s-II, putative (TFIIS2-1)	RNA synthesis II	0.39
Tb927.4.470	snoRNP protein GAR1, putative	rRNA-tRNA processing	0.22
Tb927.11.3070	hyp. protein	rRNA-tRNA processing	0.45
Tb927.8.2500	ribosomal RNA methyltransferase, putative	rRNA-tRNA processing	0.48
Tb927.10.7190	D-tyrosyl-tRNA deacylase, putative	rRNA-tRNA processing	0.49
Tb927.10.14550	ATP-dependent DEAD/H RNA helicase, DED1-1	Translation	0.05
Tb927.5.1490	eukaryotic initiation factor 4G, eIF4G1	translation	0.19

Tb927.9.11050	4E-interacting protein, putative	Translation	0.34
Tb927.6.3870	SGN1	Translation	0.37
Tb927.11.2260	eukaryotic translation initiation factor 4e, eIF4E1	Translation	0.46
Tb927.9.12510	ATP-dependent DEAD/H RNA helicase, DED1-2	Translation	0.46
Tb927.5.2570	translation initiation factor, putative (EIF3B)	Translation	0.48
Tb927.6.700	alanyl-tRNA synthetase, putative	Translation tRNA	0.43
Tb927.6.2060	histidyl-tRNA synthetase	Translation tRNA	0.45
Tb927.6.4590	glutamyl-tRNA synthetase, putative	Translation tRNA	0.45
Tb927.5.2430	membrane transporter protein, putative	Transporter	0.18
Tb927.2.5410	ABC transporter, putative. multidrug resistance protein	Transporter	0.44
Tb927.5.2400	ubiquitin carboxyl-terminal hydrolase, putative	Ubiquitin & proteasome	0.25
Tb927.9.13430	ubiquitin carboxyl-terminal hydrolase, putative	Ubiquitin & proteasome	0.34
Tb927.6.1260	proteasome beta-1 subunit, putative (TbPSB1)	Ubiquitin & proteasome	0.48
Tb927.6.440	haptoglobin-hemoglobin receptor (HpHbR)	Vesicular transport	0.19
Tb927.8.4770	small GTP-binding protein Rab18 (TbRAB18)	Vesicular transport	0.29
Tb927.6.4670	MORN repeat-containing protein,flagellar component (TbMORN1)	Vesicular transport	0.33
Tb927.6.3650	ADP-ribosylation factor, putative	Vesicular transport	0.38
Tb927.5.2660	hyp. protein	Vesicular transport	0.45
Tb927.10.6230	hyp. protein,MORN repeat containing protein	Vesicular transport	0.49
Tb927.6.350	hyp. protein	Zinc finger	0.29
Tb927.8.910	hyp. protein		0.02
Tb927.11.2820	hyp. protein		0.02
Tb927.11.16780	hyp. protein		0.02
Tb927.6.690	hyp. protein		0.03
Tb927.10.15310	hyp. protein		0.03
Tb927.8.7820	hyp. protein		0.03
Tb927.10.3400	hyp. protein		0.04
Tb927.6.2520	hyp. protein		0.05
Tb927.11.6600	hyp. protein		0.06
Tb927.11.14220	hyp. protein		0.06
Tb927.10.9610	hyp. protein		0.06
Tb927.4.4520	hyp. protein		0.06
Tb927.11.3720	hyp. protein		0.06
Tb927.11.2860	hyp. protein		0.07
Tb927.9.4080	hyp. protein		0.07
Tb927.8.4200	hyp. protein		0.07
Tb927.7.6300	hyp. protein		0.07
Tb927.4.1910	hyp. protein		0.09
Tb927.1.1500	hyp. protein		0.10
Tb927.8.5110	hyp. protein		0.10
Tb927.7.3970	hyp. protein		0.11
Tb927.2.2340	hyp. protein		0.11
Tb927.10.9630	hyp. protein		0.14
Tb927.6.3880	hyp. protein		0.15
Tb927.7.6340	hyp. protein		0.16
Tb927.5.2620	hyp. protein		0.19
Tb927.11.16820	hyp. protein		0.19
Tb927.6.860	hyp. protein		0.20
Tb927.4.1010	hyp. protein		0.20
Tb927.3.4590	hyp. protein		0.21
Tb927.5.2360	hyp. protein		0.21
Tb927.4.1000	hyp. protein		0.22
Tb927.10.11630	hyp. protein		0.23
Tb927.5.2390	hyp. protein		0.25
Tb927.10.15040	hyp. protein		0.26
Tb927.11.12690	hyp. protein		0.26
Tb927.10.8730	hyp. protein		0.26
Tb927.6.2160	hyp. protein		0.27
Tb927.5.2300	formin, putative		0.28
Tb927.3.600	hyp. protein		0.28
Tb927.7.5340	hyp. protein		0.28
Tb927.10.2580	hyp. protein		0.29
Tb927.10.12430	hyp. protein		0.29
Tb927.11.2870	hyp. protein		0.29
Tb927.9.7520	hyp. protein		0.29
Tb927.6.2530	hyp. protein		0.29
Tb927.11.11880	hyp. protein		0.30
Tb927.3.3060	hyp. protein		0.30
Tb927.8.7290	hyp. protein		0.31
Tb927.10.12060	hyp. protein		0.32
Tb927.11.13110	hyp. protein		0.32

Tb927.4.3970	hyp. protein		0.33
Tb927.10.12270	hyp. protein		0.33
Tb927.10.12390	hyp. protein		0.34
Tb927.6.2090	hyp. protein		0.34
Tb927.7.4680	hyp. protein		0.34
Tb927.7.5270	hyp. protein		0.34
Tb927.9.9370	hyp. protein		0.35
Tb927.10.2460	hyp. protein		0.35
Tb927.1.4020	hyp. protein		0.36
Tb927.2.3090	hyp. protein		0.37
Tb927.7.6700	hyp. protein		0.37
Tb927.10.2700	hyp. protein,predicted WD40 repeat protein		0.37
Tb927.8.1270	hyp. protein		0.38
Tb927.5.2730	hyp. protein		0.38
Tb927.10.14940	hyp. protein		0.38
Tb927.7.6210	hyp. protein		0.38
Tb927.5.2530	hyp. protein		0.38
Tb927.8.1290	hyp. protein		0.38
Tb927.11.12540	hyp. protein		0.38
Tb927.6.2120	hyp. protein		0.38
Tb927.1.1470	hyp. protein		0.39
Tb927.11.3300	hyp. protein		0.39
Tb927.6.4380	hyp. protein		0.40
Tb927.11.11760	hyp. protein		0.40
Tb927.10.12410	hyp. protein		0.40
Tb927.6.4320	hyp. protein		0.40
Tb927.5.2500	hyp. protein		0.40
Tb927.4.1900	hyp. protein		0.41
Tb927.8.1150	hyp. protein		0.41
Tb927.3.1010	hyp. protein		0.41
Tb927.5.2310	hyp. protein		0.41
Tb927.7.4720	hyp. protein		0.41
Tb927.6.4520	hyp. protein		0.41
Tb927.5.2520	hyp. protein		0.42
Tb927.5.2630	hyp. protein		0.42
Tb927.5.2640	hyp. protein		0.42
Tb927.6.410	hyp. protein		0.42
Tb927.11.5810	hyp. protein		0.43
Tb927.10.1560	hyp. protein		0.43
Tb927.10.5730	hyp. protein		0.43
Tb927.7.3380	hyp. protein		0.43
Tb927.1.740	hyp. protein		0.43
Tb927.9.13320	hyp. protein		0.43
Tb927.6.4360	hyp. protein		0.43
Tb927.5.4100	hyp. protein		0.43
Tb927.5.2670	hyp. protein		0.44
Tb927.8.5670	hyp. protein		0.44
Tb927.6.2620	hyp. protein		0.44
Tb927.11.12300	hyp. protein		0.44
Tb927.5.600	hyp. protein		0.44
Tb927.6.3700	hyp. protein		0.44
Tb927.7.4780	hyp. protein		0.44
Tb927.6.3180	hyp. protein		0.44
Tb927.6.1470	hyp. protein		0.44
Tb927.1.4680	hyp. protein		0.44
Tb927.5.840	hyp. protein		0.45
Tb927.11.780	hyp. protein		0.45
Tb927.1.4710	hyp. protein		0.45
Tb927.5.2600	hyp. protein		0.46
Tb927.3.2780	hyp. protein		0.46
Tb927.5.1260	hyp. protein		0.46
Tb927.11.13570	hyp. protein		0.46
Tb927.11.16450	hyp. protein		0.46
Tb927.5.2320	hyp. protein		0.46
Tb927.6.1830	hyp. protein		0.46
Tb927.10.11600	hyp. protein		0.46
Tb927.5.2770	hyp. protein		0.46
Tb927.1.2210	hyp. protein		0.47
Tb927.2.3420	hyp. protein		0.47
Tb927.7.6690	hyp. protein		0.47
Tb927.4.2160	hyp. protein		0.47

Tb927.10.5090	hyp. protein		0.47
Tb927.10.2930	hyp. protein		0.47
Tb927.1.2750	hyp. protein		0.47
Tb927.8.6670	hyp. protein		0.47
Tb927.3.3260	hyp. protein		0.47
Tb927.2.3400	hyp. protein, copurified with splicing complex		0.47
Tb927.10.7720	hyp. protein		0.48
Tb927.9.13460	hyp. protein		0.48
Tb927.6.3710	hyp. protein		0.48
Tb927.7.2450	hyp. protein		0.48
Tb927.8.2600	hyp. protein		0.48
Tb927.5.2110	hyp. protein		0.48
Tb927.11.1690	hyp. protein		0.48
Tb927.11.5200	hyp. protein		0.48
Tb927.8.1320	hyp. protein		0.48
Tb927.10.14150	hyp. protein		0.48
Tb927.6.630	hyp. protein		0.49
Tb927.4.710	hyp. protein		0.49
Tb927.7.4440	hyp. protein		0.49
Tb927.8.5300	hyp. protein		0.49
Tb927.7.180	hyp. protein		0.49
Tb927.5.2440	hyp. protein		0.49
Tb927.10.8640	hyp. protein		0.49
Tb927.11.12720	hyp. protein		0.49
Tb927.8.4310	hyp. protein		0.49
Tb927.11.12940	hyp. protein		0.49
Tb927.11.820	hyp. protein		0.49
Tb927.8.3950	hyp. protein		0.49
Tb927.10.3330	hyp. protein		0.49
Tb927.1.1700	hyp. protein		0.49
Tb927.5.2840	hyp. protein		0.49
Tb927.5.770	hyp. protein		0.49
Tb927.10.13800	hyp. protein		0.50
Tb927.11.1420	hyp. protein		0.50
Tb927.10.4790	hyp. protein		0.50
Tb927.10.14330	hyp. protein		0.50
Tb927.7.1360	hyp. protein		0.50